C1INH HALF-LIFE EXTENSION AND AAT SELECTIVITY FOR KALLIKREIN

TOWARDS NOVEL IMPROVED ANTI-KALLIKREIN AGENTS: EXTENDING THE CIRCULATORY HALF-LIFE OF C1INH AND IDENTIFYING NOVEL VARIANTS OF AAT M358R WITH ENHANCED ANTI-KALLIKREIN SELECTIVITY

By SANGAVI SIVANANTHAN, B.Sc, M.Sc

A Thesis Submitted to the School of Graduate Studies in Partial Fulfillment of the Requirements for the Degree, Doctor of Philosophy

DOCTOR OF PHILOSPHY (2025)

Medical Sciences

McMaster University

Hamilton, Ontario

TITLE: Towards novel improved anti-kallikrein agents: Extending the circulatory half-life of C1INH and identifying novel variants of AAT M358R with enhanced anti-kallikrein selectivity

AUTHOR: Sangavi Sivananthan, B.Sc, M.Sc (McMaster University)

SUPERVISOR: Dr. William P. Sheffield

NUMBER OF PAGES: xxx, 269

Lay Abstract

Hereditary Angioedema (HAE) is a rare genetic disorder that causes painful and potentially life-threatening swelling, triggered by excessive activity of bradykinin. Current treatments, such as C1-esterase inhibitor (C1INH), are effective but have a short half-life in the bloodstream, requiring frequent dosing. The goal of my research was: (i) to extend the circulatory half-life of C1INH through protein fusion, (ii) and to identify new variants of alpha-1 antitrypsin M358R (AAT M358R) that more selectively target kallikrein. By combining molecular engineering with biochemical testing, I generated modified proteins with properties that support their potential as next generation therapeutic candidates. This work contributes to the early-stage development of more durable and targeted treatments for HAE. In the long term, such advancements may lay the groundwork for improved quality of care for patients with rare disorders, and demonstrate how protein design can address unmet needs in medicine.

Abstract

Hereditary Angioedema (HAE) is a rare disorder characterized by recurrent and severe swelling caused by excessive activation of bradykinin due to unregulated plasma kallikrein (Pka). Current therapies, including plasma derived or recombinant C1-esterase inhibitor (C1INH), aim to suppress Pka activity but are limited by short circulatory half-lives, necessitating frequent dosing. Additionally, while the engineered serpin Alpha1-antitrypsin M358R (AAT M358R) can inhibit Pka, it lacks sufficient selectivity, raising concerns about off-target effects on other proteases. This thesis addresses these challenges through three complementary approaches. First, I engineered C1INH-mouse serum albumin (MSA) fusion proteins to prolong *in vivo* half-life. I found that N-terminal MSA fusions preserved C1INH function and significantly extended circulatory persistence in mice, with orientation-dependent effects on SDS stability and activity. Second, using T7 phage display, I screened AAT M358R libraries mutated at key positions within the reactive center loop (RCL). Third, I performed rational loop-swapping experiments between AAT M358R and C1INH to explore whether segments of the C1INH RCL could improve Pka selectivity. Both the second and third projects identified novel sequence motifs that enhanced reactivity toward Pka, uncovering previously uncharacterized RCL combinations with potential therapeutic relevance. Together, these studies contribute new insights into therapeutic serpin engineering. The half-life extension work highlights the potential of albumin fusions to improve pharmacokinetics without

compromising activity. The AAT M358R variant screening uncovers previously uncharacterized RCL sequences that promote Pka selectivity, expanding the known sequence space for functional serpin design. Overall, this thesis advances the development of improved biologics for HAE and provides a framework for engineering more selective, long-acting protease inhibitors for future therapeutic applications.

Acknowledgements

It is hard to believe I have finally reached the point of writing this section, something I have daydreamed about during countless failed experiments, late night writing sprints, and existential crises in the lab. This thesis would not have been possible without the support, patience, and sometimes heroic interventions of the people (and animals) around me.

First and foremost, I would like to thank my supervisor, Dr. William P. Sheffield. Thank you for your unwavering guidance, your honest and constructive feedback, and for giving me the space to grow (even when it took a few extra days… or months). Your high standards pushed me to think critically, ask better questions, and take pride in my work.

I am also deeply grateful to my committee members, Dr. Collin Kretz and Dr. Patricia Liaw, for their time, thoughtful feedback, and invaluable perspectives throughout this process. Your challenging questions and insightful suggestions helped me see my work in new ways, strengthened my thesis, and pushed me to grow as a scientist. Thank you for your patience, encouragement, and for helping me keep my work (and myself) on track.

To my past and present lab mates (Negin, Tatiana, and Tyler) thank you for being my academic support group, my built-in therapy circle, and my emergency snack suppliers. Your support, laughter, and shared suffering made this journey not just tolerable, but often hilarious. A massive thank you to Varsha for being the true MVP. Every time an experiment does not work (which was

often), you somehow pulled off a miracle and rescued the day. I do not know how you do it…are you secretly three PhDs in a lab coat? You have kept me sane, and more importantly, you have kept my experiments alive. To Ghofran, I came into this program looking for academic growth but left with a best friend; you made the worst days survivable and the best days even brighter. From our caffeine-fueled planning sessions to our spontaneous life talks between Western blots, I could not have asked for a better person to share this journey with.

To my dog, Enzo, you may not have pipetted a single microliter or written a single word, but you have been there through it all. Thank you for being my emotional support sponge, my study buddy, and my fluffy reminder that life exists outside the lab. You have listened to me rehearse presentations and watched me cry into my keyboard. If anyone else knows as much about kallikrein inhibition as I do, it is probably you. Truly, a good boy and a silent co-author.

To my parents (Sivananthan and Ranjithamalar), my brother (Shaaranhan), and my cousin (Sarmista) thank you for your endless patience, encouragement, and unconditional love. Thank you for always believing in me (even when I was not quite sure what I was doing) and for pretending to understand my science, even when I was using words that sounded made up. Your faith in me never wavered, even when I considered quitting to become a dog walker or full-time nap enthusiast.

To my partner (Vesaken) thank you for your infinite patience, unwavering encouragement, and unconditional love. You were always there through the

highs and lows, offering me perspective, reminding me why I started, and making sure I never lost sight of the bigger picture. Your belief in me, even when I doubted myself, meant more than words can ever express. I couldn't have done this without you.

To my friends (Afsa, Kishara, Harrani, and Sweta), thank you for never making me feel guilty when I disappeared into the thesis-writing void, and for pulling me out of it when I needed a break. Whether it was a meme, a walk, or a last-minute venting session, your support carried me through the hardest moments and made the triumphs even sweeter.

This thesis is not just a culmination of years of research, it is a symbol of all the people (and pets) who lifted me up, made me laugh, and believed in me even on the days I did not believe in myself. Thank you, all of you. We did it.

Table of Contents

CHAPTER 1 - INTRODUCTION 1

1. The Kallikrein-Kinin System/Contact Pathway 2

1.1. Coagulation Pathway and their Intersection with the Kallikrein-Kinin System 2

1.2. The Kallikrein-Kinin system 5

1.3. The Key Elements of Plasma Kallikrein 7

1.3.1. The Differences and Similarities between Pka and FXIa 9

1.3.2. The Similarities and Differences between Plasma Kallikrein and Tissue Kallikrein 10

2. Hereditary Angioedema 13

2.1. The Prevalence, Pathology, and Genetics of HAE 13

2.2. The Diagnosis and Tests Available for HAE 16

2.3. 2.3 Types of Treatments Available for HAE 18

2.3.1. Prophylactic Treatments to Prevent HAE 18

2.3.2. Acute Treatments for HAE 22

2.3.2.1. Half-Life Extension Technology 24

3. Serpins 28

3.1. The Key Structural Features of Serpins 30

3.2. The Mechanism of Serpins 33

3.3. Serpin Clearance 34

3.3.1. Overview of LRP1 mechanism 35

3.3.2. LRP1-independent Clearance and Catabolism of Native Plasma Proteins 36

4. Introduction to C1-esterase Inhibitor 38

4.1. The Structure of C1INH 39

4.2. C1INH Involvement in Multiple Pathways 41

4.3. C1INH Expressed Across Multiple Platforms 44

5. Introduction to Alpha-1 Antitrypsin 46

5.1. Structural Features of AAT 46

5.2. Mutational Studies Done on AAT M358R 49

5.3. Implementing Phage Display with AAT M358R 50

5.4. Implementing RCL Loop Exchange with AAT 53

5.5. AAT Expressed in Multiple Systems 55

6. Rationale, Hypothesis and Objectives 57

CHAPTER 2: Prolonging the circulatory half-life of C1 esterase inhibitor via albumin fusion 59

1. Abstract 60

2. Introduction 61

3. Methods 63

3.1. Expression and Purification of H_6-trC1INH(MGS), H_6-MSA, and H_6-trC1INH(MGS)-MSA Fusion Protein in *P. pastoris* 63

3.2. Protease Inhibition Assays with H_6-trC1INH(MGS) and H_6-trC1INH(MGS)-MSA 65

3.3. Electrophoretic Analysis of H_6-trC1INH(MGS) and Pka Interaction 66
3.4. Detection of C1INH Binding to Kallikrein by Modified ELISA 66
3.5. *In vivo* Clearance and Protein Detection in Mice 67
3.6. Statistical Analysis and Significance Testing 70
4. Results 70
4.1. Novel Recombinant Proteins 70
4.2. Characterization of Fused and Unfused Truncated, Non-glycosylated C1INH Proteins 73
4.3. *In vivo* Clearance of Recombinant Proteins 77
4.4. Pharmacokinetic Analysis 80
5. Discussion 82
6. References 87
7. Supporting Information 91
CHAPTER 3: N-terminal fusion of albumin enhances the plasma residency time of C1-esterase inhibitor 103
1. Abstract 104
2. Introduction 105
3. Methods 107
3.1. Expression and Purification of H_6-MSA-trC1INH(MGS) in *Pichia pastoris* 107
3.2. Protease Inhibition Assays with H_6-MSA-trC1INH(MGS) 108

3.3. Electrophoretic Analysis of H_6-MSA-trC1INH(MGS) and Pka Interaction 109
3.4. *In vivo* Clearance and Protein Detection in Mice 110
3.5. Statistical Analysis and Significance Testing 111
4. Results 111
4.1. Expression and Purification of H_6-MSA-trC1INH(MGS) 111
4.2. Characterization of H_6-MSA-trC1INH(MGS) compared to Chapter 2 113
4.3. Further Extension of Plasma Half-life with H_6-MSA-trC1INH(MGS) 115
5. Discussion 117
6. References 123
CHAPTER 4: Enhancement of plasma kallikrein specificity of antitrypsin variants identified by phage display and partial reversion 127
1. Abstract 128
2. Introduction 129
3. Methods 131
3.1. Materials 131
3.2. DNA Manipulation 132
3.3. Biopanning of Phage Display Libraries 132
3.4. Deep Sequencing 133
3.5. GST Expression and Purification 134
3.6. Protease Inhibition Assays with AAT M358R Variants 134

3.7. Plasma Clotting Tests 135
3.8. Electrophoretic Analysis of AAT M358R Variants with Pka/FXIa Interactions 136
3.9. Protein Modeling 136
3.10. Statistical Analysis and Significance Testing 137
4. Results 137
4.1. Phage Display of AAT M358R P7-P3' and Characterization of 7-QLIPS-3 and 2-VRRAY-3' 137
4.2. Characterization of Revertants and Combinatorial Mutagenesis of Selected Variants 142
4.3. Molecular Modeling suggests Correlation between the Distance and Activity 149
5. Discussion 153
6. Conclusion 159
7. List of Abbreviations 160
8. Declarations 163
9. References 164
10. List of Additional Files 168
CHAPTER 5: Substitution of reactive centre loop residues from C1 esterase inhibitor increases the inhibitory specificity of Alpha-1 Antitrypsin for plasma kallikrein 174
1. Abstract 175

2. Introduction 176

3. Materials and Methods 180

3.1. Reagents and Materials 180

3.2. DNA Manipulations 180

3.3. Expression and Purification of GST-fusion Constructs 182

3.4. Protease Inhibition Assays for AAT M358R Variants 183

3.5. Electrophoretic Analysis of AAT M358R Variants and Protease Complex Formation 184

3.6. Intrinsic Fluorescence of AAT M358R and AC (10-3/4') 184

3.7. Protein Modeling of AAT M358R Variants and Protease Complexes 185

3.8. Statistical Analysis and Evaluation of Testing 185

4. Results 186

4.1. Characterization of Maximal AAT M358R-C1INH Loop Exchanged Variants 186

4.2. Characterization of additional AAT M358R-C1INH Loop Exchanged Variants 190

4.3. Inhibition of Thrombin, Factor Xa, and Factor XIIa by Selected Variants 192

4.4. Intrinsic Fluorescence of AAT M358R and AC (10-3/4') 193

4.5. Molecular Modeling of AAT M358R and Variant encounter Complexes with Pka and FXIa 194

5. Discussion 197

6. References 205

7. Supplementary Information 209

8. Highlights 217

CHAPTER 6 - DISCUSSION 218

1. Overall Context and Contributions to Knowledge 218

2. Potential Therapeutic Implications 219

3. Albumin Fusion 222

4. Mutagenic Strategies 223

5. Comparisons to Ecallantide and Lanadelumab 227

6. Challenges and Limitations 228

7. Future Experiments 240

8. Genetic therapies for HAE 241

CHAPTER 7 - REFERENCES 247

List of Figures

INTRODUCTION

- Figure 1: Schematic diagram of kallikrein-kinin system 4
- Figure 2: Excessive swelling in Hereditary Angioedema 15
- Figure 3: Serpin mechanism pathway with kallikrein 32

CHAPTER 2

- Figure 1: C1-esterase inhibitor (C1INH) recombinant proteins 72
- Figure 2: Complex characterization of C1INH recombinant proteins 76
- Figure 3: Protein clearance of H_6-trC1INH(MGS), H_6-trC1INH(MGS)-MSA, and H_6-MSA 79

CHAPTER 3

- Figure 1: Schematic diagram of C1INH recombinant proteins 112
- Figure 2: Complex characterization of C1INH proteins 115
- Figure 3: Protein clearance of H_6-trC1INH(MGS)-MSA, H_6-MSA-trC1INH(MGS), and H_6-MSA. 117

CHAPTER 4

- Figure 1: Schematic representation of the native AAT M358R and selected AAT M358R variants at positions P7-P3' 138
- Figure 2: Electrophoretic profile of reactions of AAT M358R, 7-QLIPS-3, and 2-VRRAY-3' with Pka or FXIa 141
- Figure 3: Schematic diagrams of reversion mutations and combination of selective AAT M358R mutants 142

- Figure 4: Electrophoretic profile of reactions of revertants and combination variant with Pka and FXIa 148
- Figure 5: Molecular models of Pka and FXIa encounter complex to AAT M358R variants 152
- Supplementary Figure 1. Immunoblot of 7-FLIAI-3 with or without protease reaction 169
- Supplemental Figure 2. Diluted APTT Assay 170

CHAPTER 5

- Figure 1: Structural Representation of AAT M358R and C1INH RCL Positions. 187
- Figure 2: Electrophoretic profile of reactions of AAT M358R and AC (10-3) with Pka or FXIa. 189
- Figure 3: Electrophoretic profile of reactions of AC (10-3/4') and AC (10-4) with Pka or FXIa. 192
- Figure 4: Modeling of Pka and AAT M358R and AC variant encounter complexes. 195
- Supplemental Figure S1A. DNA sequence of synthetic DNA fragment (gene block) encoding 3' sector of open reading frame (ORF) encoding AC (10-4'/d2). 210

- Supplemental Figure S1B. Amino acid sequence of full GST-AC (10-4'/d2) fusion protein ORF designed for expression using plasmid pGEX-AC AC (10-4'/d2). 211
- Supplemental Figure S1C. Synthetic DNA sequences (gene blocks) 212
- Supplemental Figure S2. Electrophoretic profile of reactions of AAT M358R, AC (10-3), AC (10-4'), and AC (10-4'/d2), with Pka or FXIa. 213
- Supplemental Figure S3. Electrophoretic profile of reactions of additional revertant variants with Pka or FXIa. 214
- Supplemental Figure S4. Electrophoretic profiles of reactions of selected variants with thrombin or FXIIa. 215
- Supplemental Figure S5. Intrinsic fluorescence profiles of AAT M358R and AC (10-3/4'). 216

DISCUSSION

- Figure 1: Summary of ways to improve HAE therapeutics 245

List of Tables

CHAPTER 2

- Table 1: Pharmacokinetic characterization of activity of C1INH recombinant proteins 75
- Table 2: H_6-trC1INH(MGS), H_6-trC1INH(MGS)-MSA, H_6-MSA pharmacokinetic analysis of clearance 81
- S1 Appendix (1) Protein sequences and lengths 91
- S1 Appendix (2) All data from Table 1 95
- S1 Appendix (3) All data from Figure 2B 96
- S1 Appendix (4) All data from Figure 3A, 3B, 3C, and 3D 96
- S1 Appendix (5) All data from Figure 3E 97
- S1 Appendix (6) All data from Table 2 97
- S1 Appendix (7) All data relating to effect of sex or weight on terminal half-life, by protein 98
- S1 Appendix (8) All data relating to mouse weight 99

CHAPTER 3

- Table 1: Pharmacokinetic characterization of activity of C1INH proteins 113

CHAPTER 4

- Table 1: Kinetic characterization of protease inhibition by AAT M358R, 7-QLIPS-3, and 2-VRRAY-3' 140

- Table 2: Kinetic characterization of back mutants and combinatorial mutagenesis 145
- Table 3: Modeled distances between alpha carbon of R358 and S195 hydroxyl side chain in AAT M358R and variant encounter complexes 150
- Supplemental Table 1. Kinetic characterization of 7-FLIAI-3 168
- Supplemental Table 2. Raw data for all quantitative results of the study 171

CHAPTER 5

- Table 1: Aligned reactive centre loop sequences of C1INH, AAT M358R, and initial constructs 181
- Table 2: Amino acid configuration of AAT M358R constructs showing stepwise reversion from AC (10-4') to AC (10-8). 182
- Table 3: Kinetic parameters of inhibition of Pka or FXIa by AAT M358R and initial constructs. 188
- Table 4: Kinetic parameters of inhibition of Pka or FXIa by AAT M358R and constructs produced to study stepwise reversion from AC (10-3/2'-4') to AC (10-8). 191
- Table 5: Kinetic parameters of inhibition of thrombin, FXa, or FXIIa by AAT M358R, AC (10-3/3'-4'), and AC (10-3/4'). 193

- Table 6: Modeled distances (Å) between alpha carbon of R358 in AAT M358R and S195 hydroxyl side chain of protease in AAT M358 R: protease encounter complexes in AAT M358R and variant encounter complexes, and number of intramolecular modeled hydrogen bonds in the AAT M358R or variant RCL residues or intermolecular modeled hydrogen bonds between the AAT M358R or variant RCL and Pka or FXIa. 197

List of Abbreviations and Symbols

2-PRRAY-3′	Alpha-1 Antitrypsin M358R, S359R, I360A, P361Y
2-PRSAY-3′	Alpha-1 Antitrypsin M358R, I360A, P361Y
2-PRSIY-3′	Alpha-1 Antitrypsin M358R, P361Y
2-QLIPSVRRAY-3′	Alpha-1 Antitrypsin F352Q, E354I, A355P, I356S, P357V, M358R, S359R, I360A, P361Y
2-VRRAY-3′	Alpha-1 Antitrypsin P357V, M358R, S359R, I360A, P361Y
7-FLEAS-3	Alpha-1 Antitrypsin I356S, M358R
7-FLEPS-3	Alpha-1 Antitrypsin A355P, I356S, M358R
7-FLIAI-3	Alpha-1 Antitrypsin E354I, M358R
7-FLIPS-3	Alpha-1 Antitrypsin E354I, A355P, I356S, M358R
7-QLIPS-3	Alpha-1 Antitrypsin F352Q, E354I, A355P, I356S, M358R
AAT	Alpha-1 antitrypsin
AATD	Alpha-1 antitrypsin deficiency
AAT M358R	Alpha-1 antitrypsin with substitution at position 358 from methionine to arginine
AC (10-3)	Alpha-1 Antitrypsin P10-P3 exchanged with C1-esterase inhibitor P10-P3
AC (10-3/2′-4′)	Alpha-1 Antitrypsin P10-P3 and P2′-P4′ exchanged with C1-esterase inhibitor P10-P3 and P2′-P4′

AC (10-3/3′-4′)	Alpha-1 Antitrypsin P10-P3 and P3′-P4′ exchanged with C1-esterase inhibitor P10-P3 and P3′-P4′
AC (10-3/4′)	Alpha-1 Antitrypsin P10-P3 and P4′ exchanged with C1-esterase inhibitor P10-P3 and P4′
AC (10-4)	Alpha-1 Antitrypsin P10-P4 exchanged with C1-esterase inhibitor P10-P4
AC (10-4′)	Alpha-1 Antitrypsin P10-P4′ exchanged with C1-esterase inhibitor P10-P4′; no change in Alpha-1 Antitrypsin P2
AC (10-4′/d2)	Alpha-1 Antitrypsin P10-P4′ exchanged with C1-esterase inhibitor P10-P4′; deletion of Alpha-1 Antitrypsin P2
AC (10-5)	Alpha-1 Antitrypsin P10-P5 exchanged with C1-esterase inhibitor P10-P5
AC (10-6)	Alpha-1 Antitrypsin P10-P6 exchanged with C1-esterase inhibitor P10-P6
AC (10-7)	Alpha-1 Antitrypsin P10-P7 exchanged with C1-esterase inhibitor P10-P7
AC (10-8)	Alpha-1 Antitrypsin P10-P8 exchanged with C1-esterase inhibitor P10-P8
AOX1	Alcohol oxidase 1
aPC	Activated Protein C

AR	Alanine-arginine
ASGPR	Asialoglycoprotein receptor
AUC	Area under the curve
B1R	Bradykinin receptor 1
B2R	Bradykinin receptor 2
BK	Bradykinin
Bp	Base pair
BSA	Bovine serum albumin
C1INH	C1-esterase inhibitor
C1s	Complement component 1s
Cas9	CRISPR-associated protein 9
CHO	Chinese hamster ovaries
COPD	Chronic Obstructive Pulmonary Disease
CRISPR	Clustered Regularly Interspaced Short Palindromic Repeats
Da	Daltons
E.coli	*Escherichia coli*
EHL	Extended half-life
ELISA	Enzyme-Linked Immunosorbent Assay
ER	Endoplasmic reticulum
FcRn	Neonatal Fc receptor
FIX	Factor IX

FIXa	Activated Factor IX
FVII	Factor VII
FVIIIa	Activated Factor VIII
FX	Factor X
FXa	Activated FX
FXI	Factor XI
FXIa	Activated FXI
FXII	Factor XII
FXIIa	Activated FXII
GST	Glutathione S-transferase
H_6-MSA	Hexahistidine-tagged to N-terminus of mouse serum albumin
H_6-MSA-trC1INH(MGS)	Hexahistidine-tagged to N-terminus of mouse serum albumin, mouse serum albumin fused to N-terminus of truncated C1-esterase with mutated glycosylation sites
H_6-trC1INH(MGS)	Hexahistidine-tagged to N-terminus of truncated C1-esterase with mutated glycosylation sites
H_6-trC1INH(MGS)-MSA	Hexahistidine-tagged to N-terminus of truncated C1-esterase with mutated glycosylation sites, C1-esterase with mutated glycosylation sites fused to N-terminus of mouse serum albumin

HAE	Hereditary Angioedema
HCII	Heparin cofactor II
HMWK	High molecular weight kininogen
HRP	Horseradish peroxidase
HSA	Human serum albumin
IIa	Thrombin
IPTG	Isopropyl β-D-1-thiogalactopyranoside
IV	Intravenous
k_2	Second order rate constat
kDa	Kilodaltons
KKS	Kallikrein-kinin system
KLK	Kallikrein-related peptidases
KPI	Kunitz protease inhibitor
LB	Luria Broth
LB-amp	Luria Broth with ampicillin
LMWK	Low molecular weight kininogen
LPS	Lipopolysaccharides
LRP1	Low-density lipoprotein receptor-related protein 1
LTB4	Leukotriene B4
M	Molar
$M^{-1}s^{-1}$	Moles per liter per second
M9LB	M9 salts in Luria broth

mg	Milligram
MGS	Mutated glycosylation sites
min	Minute
ml	Millilitre
mM	Millimolar
MSA	Mouse serum albumin
NE	Neutrophil elastase
ng	Nanogram
Ni-NTA	Nickel Nitrilotriacetic acid
nM	Nanomolar
P1-P1′	Cleavage site
PBS	Phosphate-buffered saline
PBST	Phosphate-buffered saline with Tween-20
pdAAT	Plasma derived Alpha-1 antitrypsin
pdC1INH	Plasma derived C1-esterase inhibitor
PEG	Polyethylene glycol
pfu	Plaque-forming unit
PI	Isoelectric point
PK	Prekallikrein
Pka	Plasma kallikrein
P. pastoris	*Pichia pastoris*
PRCP	Prolylcarboxypeptidase

PSA	Polysialic acid
rC1INH	Recombinant C1-esterase inhibitor
RCL	Reactive centre loop
rpm	Revolutions per minute
RR	Arginine-Arginine
s	Second
Serpin	Serine protease inhibitor
SD	Standard deviation
SDS	Sodium Dodecyl Sulfate
SDS-PAGE	Sodium Dodecyl Sulfate-Polyacrylamide Gel Electrophoresis
SI	Stoichiometry of Inhibition
S-2222	Chromogenic substrate for activated Factor X
S-2238	Chromogenic substrate for thrombin
S-2302	Chromogenic substrate for plasma kallikrein
S-2366	Chromogenic substrate for activated Factor XI
TF	Tissue factor
TFPI	Tissue Factor Pathway Inhibitor
TIF	Tagged image file
TMB	3,3',5,5'-tetramethylbenzidine
TNF-α	Tumor Necrosis Factor alpha
tPA	Tissue-type plasminogen activator

U/kg	Unit per kilogram
v/v	Volume by volume
w/v	Weight by volume
Å	Angstrom
°C	Degree in Celsius
Δ	Deletion
µg	Microgram
µl	Microlitre
µM	Micromolar
µmol/L	Micromole per litre
%	Percentage
±	Plus or minus
′	Prime

Declaration of Academic Achievements

This thesis is submitted in partial fulfillment of the requirements for the degree of Doctor of Philosophy in the Medical Sciences Graduate Program at McMaster University. It is presented in sandwich thesis format and includes, under the supervision of Dr. William P. Sheffield in the Department of Pathology and Molecular Medicine, original research conducted between November 2021 to April 2025 by Sangavi Sivananthan, with contributions and assistance as follows. In Chapter 2 and Chapter 3, Negin Tehrani assisted with mouse blood collection for pharmacokinetic analyses. In Chapter 4, Tyler Seto performed phage display and contributed a subset of constructs involving one portion of the reactive center loop (RCL), specifically for the P7-P3 portion. In Chapter 5, Ameer Shah initiated the project with full-length RCL substitutions, while Ammaar Baig contributed constructs targeting the C-terminal segment of the RCL. For all constructs in Chapters 4 and 5, Sangavi Sivananthan repeated and replicated all kinetic experiments contemporaneously. Throughout all projects, Varsha Bhakta provided consistent technical assistance and troubleshooting support to all lab members.

CHAPTER 1 - INTRODUCTION

Balance is a critical concept in biology, at both macroscopic and microscopic levels. Homeostasis is the balanced state in which an organism can maintain itself in a healthy internal dynamic equilibrium in the face of changes in its external environment (Libretti and Puckett 2025). It is maintained by thousands of control systems that detect and oppose changes in physiological and biochemical setpoints. In mammals, fluid balance between the circulatory system and the tissues is an important homeostatic system mediated by the kallikrein-kinin system (KKS) (Wisniewski, Gangnus, and Burckhardt 2024). This system comprises two largely independent subsystems mediating kinin generation by tissue or plasma kallikreins (Proud and Kaplan 1988; Rhaleb, Yang, and Carretero 2011). Plasma kallikrein (Pka) is regulated by a circulating inhibitor of the serine protease inhibitor (serpin) superfamily called C1-esterase inhibitor (C1INH) (Ravindran et al. 2004). C1INH deficiency causes Hereditary Angioedema (HAE), a disease characterized by episodic swelling due to fluid imbalance (Azmy, Brooks, and Hsu 2020). HAE can be treated acutely during episodes, or prophylactically to prevent episodes. Existing HAE treatments are limited either by inflexibility between acute or prophylactic modes or by cost, providing an unmet clinical need for new treatment agents (Valerieva et al. 2021).

In this thesis, novel recombinant proteins inhibiting Pka were generated and characterized. First, recombinant C1INH was simplified by truncation and glycosylation site removal, and its *in vivo* clearance was slowed by fusion to

serum albumin. Secondly, another serpin, Alpha-1 antitrypsin (AAT) was selected for optimal Pka inhibition using phage display of hypervariable AAT protein libraries and biopanning with Pka. Thirdly, an alternative way of optimizing AAT for Pka inhibition was explored by full or partial substitution of the reactive centre loop (RCL) of C1INH for that of AAT in novel AAT proteins. In the following sections, the KKS system, its links to hemostasis and coagulation, HAE, and the serpins C1INH and AAT are described in detail.

1. The Kallikrein-Kinin System/Contact Pathway

Contact pathway plays a crucial role in coagulation, inflammation, and innate immunity (Long et al. 2016; Wu 2015). This pathway serves as a first-line defense mechanism, linking vascular injury to thrombotic and inflammatory responses. Although traditionally associated with coagulation, the contact pathway is now recognized for its broader physiological roles, including pathogen defense, fibrinolysis, and regulation of vascular permeability. Dysregulation of this pathway, particularly through excessive Pka activity, can lead to pathological conditions such as HAE.

1.1. Coagulation Pathway and their Intersection with the Kallikrein-Kinin System

The coagulation cascade is classically divided into two pathways, the extrinsic and intrinsic pathways, both of which converge to a common pathway for the formation of thrombin, a key enzyme that converts fibrinogen to fibrin and stabilizes the blood clot (Chaudhry, Usama, and Babiker 2025). The extrinsic pathway is initiated upon vascular injury, when tissue factor (TF) is exposed to

circulating Factor VII (FVII). The TF-activated FVII complex activates Factor X (FX) directly or through Factor IX (FIX), leading to thrombin generation (Park and Park 2024). This pathway serves as the primary trigger for hemostasis, rapidly initiating clot formation at sites of vessel damage (Park and Park 2024). In contrast, the intrinsic pathway is initiated in plasma upon exposure to negatively charged surfaces such as polyphosphates, nucleic acids, or collagen (Grover and Mackman 2019). This leads to the autoactivation of Factor XII (FXII) into activated FXIIa (FXIIa), which then activates prekallikrein (PK) into Pka and Factor XI (FXI) into activated FXI (FXIa) (Figure 1). FXIa subsequently activates FIX, with its cofactor activated Factor VIII (FVIIIa), activates FX, converging with the extrinsic pathway at the level of the common pathway (Grover and Mackman 2019). The KKS, responsible for bradykinin (BK) generation, intersects with the intrinsic pathway in multiple ways. Pka can further promote FXII activation and cleave high molecular weight kininogen (HMWK) resulting in the release of BK, a potent vasodilator that increases vascular permeability (Motta, Juliano, and Chagas 2023). As shown in Figure 1, this links the KKS directly to inflammatory signaling, independent of coagulation. Interestingly, FXIIa can also activate components of the fibrinolytic system, such as plasminogen, and interact with the complement system, further embedding the contact system within broader immune and vascular responses (Thangaraj et al. 2020; Bekassy et al. 2022; Konings et al. 2015). Although the extrinsic pathway operates independently of the KKS, the crosstalk between coagulation,

fibrinolysis, complement activation, and the KKS underscores a main role of the contact system as a central node connecting hemostasis, inflammation, and innate immunity.

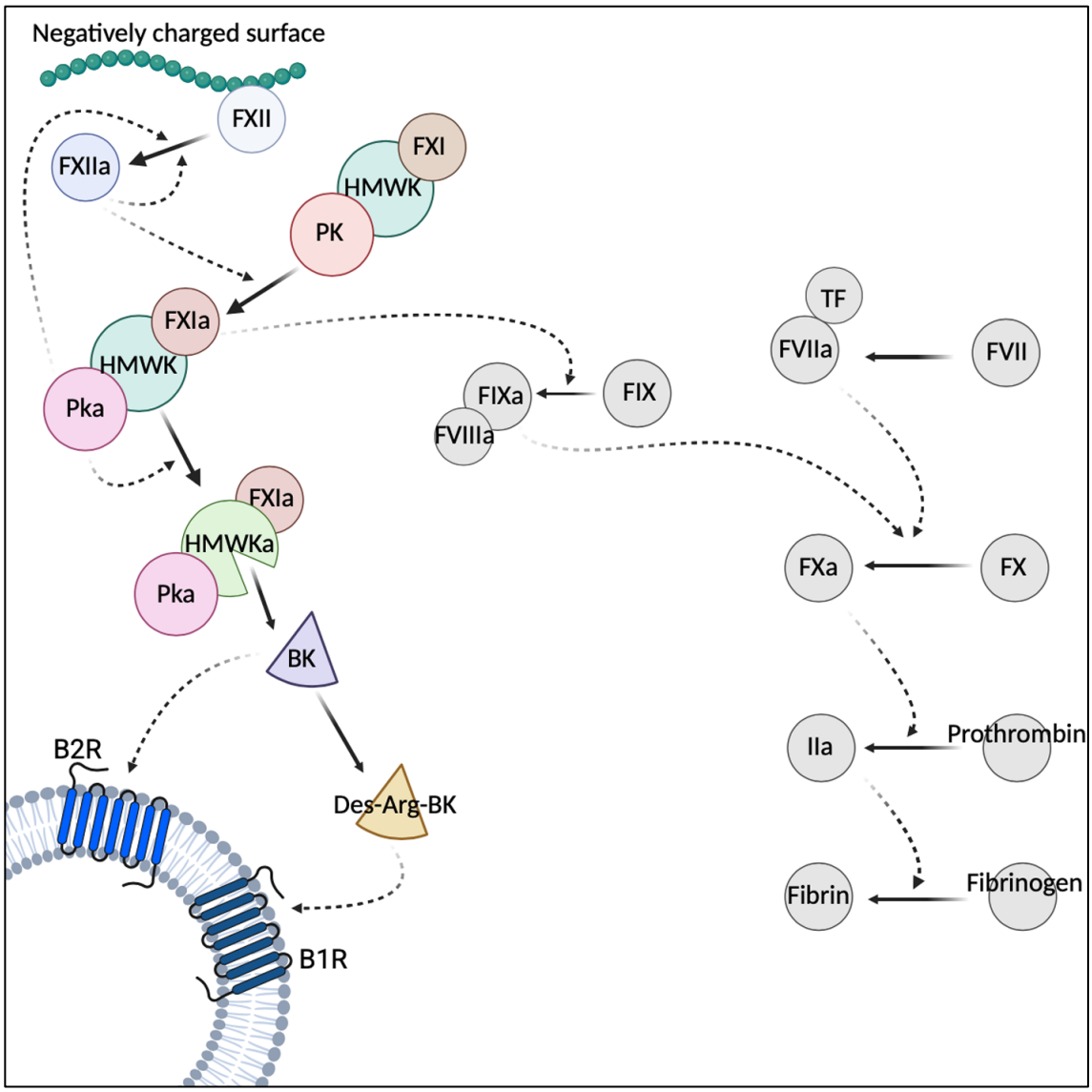

Figure 1: Schematic diagram of kallikrein-kinin system. Upon autoactivation of FXII on negatively charged surfaces, a downstream cascade is activated to release bradykinin. Bradykinin interacts with bradykinin B2 receptor, and Des-

Arg-BK interacts with bradykinin B1 receptor to increase vascular permeability. Both FXIIa and FXIa contribute to the intrinsic pathway of coagulation, eventually leading to fibrinogen conversion to fibrin and clot formation. The KKS system is in colour while the coagulation pathway is shaded grey.

1.2. The Kallikrein-Kinin system

The KKS is part of the intrinsic pathway of the coagulation cascade that is activated when plasma proteins interact with negatively charged surfaces. These can be physiological, such as polyphosphates released from platelets or misfolded proteins, or non-physiological, such as artificial biomaterials or glass surfaces (Wu 2015; Schmaier and McCrae 2007). This interaction triggers the autoactivation of FXII into FXIIa, a serine protease that exists in two functionally distinct forms: α-FXIIa and β-FXIIa. The full-length α-FXIIa drives coagulation by activating FXI, PK, and plasminogen, whereas the truncated β-FXIIa, generated through cleavage by Pka, exhibits greater enzymatic activity toward PK, amplifying the KKS while having little effect on clot formation (Tankersley and Finlayson 1984; Schmaier and McCrae 2007).

PK does not circulate freely in plasma; instead, it is non-covalently bound to HMWK in a 1:1 ratio, forming a complex that localizes PK to sites of activation on endothelial cells (Tait and Fujikawa 1987; Pixley et al. 2011). HMWK acts as a molecular scaffold, bringing PK into proximity with FXII for activation into Pka. Similarly, FXI circulates in plasma bound to HMWK, ensuring its recruitment into the contact pathway when FXIIa is generated. This association is essential for the

interplay between the KKS and the intrinsic coagulation cascade, as FXIIa cleaves FXI into FXIa, further propagating the clotting response (Mohammed et al. 2018). In parallel, Pka itself is a key amplifier of this pathway. Once generated, Pka further activates FXII, shifting the system towards a feed-forward loop. Pka also cleaves single-chain HMWK into activated two-chain form, releasing BK, a potent vasoactive peptide that triggers vasodilation, increased vascular permeability, and recruitment of inflammatory cells, contributing to both normal physiological processes and pathological conditions (Bekassy et al. 2022).

BK signaling is tightly regulated through two G-protein-coupled receptors: the bradykinin B2 receptor (B2R), which is constitutively expressed on endothelial cells and mediates acute inflammatory responses, and the bradykinin B1 receptor (B1R), which is inducible and upregulated under conditions of chronic inflammation, tissue injury, or cytokine stimulation (Leeb-Lundberg et al. 2005). The cleavage of HMWK by Pka primarily generates BK, which preferentially binds to B2R, triggering rapid vasodilation, vascular permeability, and pain sensitization. However, in chronic inflammatory conditions or tissue damage, lysyl-bradykinin (des-Arg9-bradykinin) is formed through the action of carboxypeptidases and preferentially binds to B1R, sustaining prolonged vascular leakage and immune cell recruitment (Leeb-Lundberg et al. 2005).

The KKS is regulated by multiple inhibitors to prevent excessive BK production and uncontrolled inflammation. C1INH is the primary regulator, inhibiting both FXIIa and Pka to maintain homeostasis (Miyata and Horiuchi

2023). Deficiencies in C1INH, as seen in HAE, lead to unchecked Pka activity and excessive BK release, resulting in recurrent episodes of severe swelling (Busse and Kaplan 2022).

1.3. The Key Elements of Plasma Kallikrein

Pka is a 638-amino acid serine protease with a molecular weight of 71.4 kDa that plays a central role in the contact pathway, fibrinolysis, and inflammatory responses (Colman et al. 1985). It is encoded by *KLKB1*, located on chromosome 4q35, and is primarily synthesized in the liver before being secreted into the circulation as its inactive precursor, PK (Bryant & Shariat-Madar, 2009). Pka consists of a trypsin-like serine protease domain and an N-terminal heavy chain comprising four apple domains (A1–A4). These apple domains are structurally characterized by three conserved disulfide bridges and are essential for mediating protein-protein and protein-carbohydrate interactions (Li et al. 2019). They enable PK to bind to HMWK (via domain 6), FXII, and negatively charged surfaces, localizing it to the site of activation (Colman and Schmaier 1997). The trypsin domain contains the classic catalytic triad (His57, Asp102, Ser195), responsible for its proteolytic activity (Pavlopoulou et al. 2010).

Unlike its active counterpart, PK lacks a functional catalytic site due to the improper orientation of its catalytic triad and an incomplete oxyanion hole. Activation occurs through FXIIa, which cleaves PK at Arg371-Val372, generating Pka. Upon activation, Pka undergoes a conformational shift that brings the catalytic residues into alignment (His57 abstracting a proton from Ser195 priming for nucleophilic attack; Asp102 stabilizing His57; Ser195 acting as a nucleophile)

and formation of the oxyanion hole (Gly163 and Ser195) that stabilizes the tetrahedral transition state of substrate cleavage, facilitating efficient proteolysis (Scheiner, Kleier, and Lipscomb 1975; Pathak et al. 2013). Apart from FXIIa, prolylcarboxypeptidase (PRCP) is another important physiological activator of PK. PRCP is an angiotensinase that cleaves PK independently of FXIIa, playing a role in BK generation under pathological conditions (Shariat-Madar, Mahdi, and Schmaier 2004; Shariat-Madar and Schmaier 2004).

Pka selectively cleaves peptidyl bonds at Arg/X and Lys/X sites, including Lys380-Arg381 and Arg389-Ser390 bonds in human HMWK (Zhang et al. 2017). Beyond its primary function in BK release, Pka also amplifies its own activation by cleaving α-FXIIa into β-FXIIa at Arg334-Asn335 and Arg343-Leu344, splitting the heavy chain from light chain. β-FXIIa is a more potent activator of PK than α-FXIIa, since it reduces its procoagulant activity, reinforcing Pka's primary role in inflammation rather than clotting (de Maat, Clark, et al. 2019). Pka also participates in cleaving plasminogen to plasmin and participates in surface-dependent activation of coagulation, fibrinolysis, and inflammatory responses (Kolte and Shariat-Madar 2016; Kearney et al. 2021; Kluft et al. 1979). Recent findings also suggest that Pka may contribute to the activation of FIX (Kearney et al. 2021). Lastly, Pka can bind to heparan sulfate proteoglycans on endothelial cells, where positively charged residues in its apple domains mediate weak electrostatic interactions with negatively charged sulfate groups (Motta and

Tersariol 2017). This surface attachment may assist in kallikrein localization at sites of vascular injury or inflammation.

To prevent excessive BK production and uncontrolled inflammation, Pka is tightly regulated by multiple inhibitors. C1INH is the primary physiological inhibitor of both FXIIa and Pka, forming irreversible covalent complexes to suppress kallikrein-mediated amplification of the system (Ivanov et al. 2019). In addition to C1INH, α_2-macroglobulin functions as a broad-spectrum protease inhibitor, trapping Pka within a steric cage and preventing further substrate cleavage (Lagrange et al. 2022). Furthermore, antithrombin, a well-known inhibitor of coagulation proteases, can also inhibit Pka, albeit with lower efficiency (Olson, Sheffer, and Francis 1993).

1.3.1. The Differences and Similarities between Pka and FXIa

PK and FXI are homologous serine proteases that play distinct but interconnected roles in coagulation, inflammation, and fibrinolysis. Despite their structural and functional similarities, they exhibit significant differences in activation, substrate specificity, physiological roles, and regulation.

Both are synthesized in the liver as zymogens and circulate in plasma. They are structurally similar, with PK and FXI sharing ~58% sequence identity and a conserved N-terminal region containing four apple domains followed by a C-terminal trypsin-like catalytic domain (Chung et al. 1986; McMullen, Fujikawa, and Davie 1991). However, FXI exists as a disulfide-linked homodimer, whereas PK remains monomeric. The homodimeric nature of FXI

enhances its ability to bind platelet surfaces via glycoprotein Ib, a function absent in PK (Baglia et al. 2002).

Both proteases require activation to exert their enzymatic functions, and FXIIa is their primary activator. However, they differ in cleavage sites and activation mechanisms. FXIIa cleaves PK at Arg371-Val372, resulting in a monomeric, two-chain Pka (Xie et al. 2020). In contrast, FXI is cleaved at Arg369-Ile370, generating FXIa (Mohammed et al. 2018). The catalytic domains of Pka and FXIa share ~81% sequence similarity, including a conserved catalytic triad essential for protease function, oxyanion hole stabilizing residues, substrate specificity pocket (Asp189; confers specificity for substrates with basic residues at the P1 position) (Fujikawa et al. 1986; Dennis, Herzka, and Lazarus 1995). Despite these similarities, their substrate preferences diverge significantly. Pka preferentially cleaves FXII, HMWK, and plasminogen (as mentioned above). Conversely, FXIa primarily cleaves FIX at Arg145-Ala146 and Arg180-Val181, activating it into activated FIX (FIXa), which is crucial for thrombin generation and clot formation (Schmidt and Bajaj 2003).

The regulation of these proteases is somewhat similar. Pka is primarily inhibited by C1INH and α_2-macroglobulin (as mentioned below). FXIa is also strongly inhibited by C1INH, along with AAT, α_2-antiplasmin, antithrombin III, which has minor roles in its regulation (Knauer et al. 2000).

1.3.2. The Similarities and Differences between Plasma Kallikrein and Tissue Kallikrein

Tissue kallikrein and kallikrein-related peptides (KLK) are a family of 15 proteases named KLK1-KLK15 that are expressed in various tissues (Kalinska et al. 2016). Pka and KLK are serine proteases that share functional similarities in kinin generation but differ significantly in structure, activation mechanisms, substrate specificity, and physiological roles.

Although Pka belongs to the trypsin-like serine protease family, different types of KLK can belong to either trypsin-like serine protease family, chymotrypsin-like serine protease family, or dual (Kalinska et al. 2016; Koumandou and Scorilas 2013). Pka and KLK1 contribute to KKS by generating kinins that regulate blood pressure, vascular permeability, and inflammation. However, despite these similarities, they have evolved distinct mechanisms of action and regulatory pathways. One of the key structural differences between Pka and KLK is their domain organization and genetic origins. Pka is synthesized as PK, circulates as a monomer bound to HMWK in the bloodstream, and contains four apple domains which mediate interactions with HMWK and other plasma proteins, implicated in coagulation, fibrinolysis, and inflammation. In contrast, KLK is a single-domain serine protease without the apple domains, making it structurally more similar to classical trypsin-like proteases (Koumandou and Scorilas 2013). Moreover, while Pka is encoded by the *KLKB1* gene on chromosome 4q35, KLK is encoded by *KLK* located on chromosome 19q13, which contains 15 paralogous kallikreins with diverse tissue-specific functions (Yousef et al. 2003).

The activation mechanisms of Pka and KLK also differ significantly. PK requires FXIIa or PRCP for activation, but KLK is synthesized as a zymogen with an N-terminal propeptide, which must be cleaved by specific proteases such as cathepsins or trypsin-like enzymes to become active (Kalinska et al. 2016). Pka activation occurs exclusively in the bloodstream, while KLK is predominantly active in interstitial fluids, glandular secretions, and tissues, such as the kidney, salivary glands, pancreas, and vasculature (Kalinska et al. 2016). Functionally, both enzymes generate kinins but from different precursors. Pka cleaves HMWK, releasing BK, to mediate vasodilation, increased vascular permeability, and pain sensation. In contrast, one of the paralogous kallikreins, KLK1, cleaves low-molecular-weight kininogen (LMWK), releasing lys-bradykinin (kallidin), which is later converted to bradykinin by aminopeptidases (Koumandou and Scorilas 2013). Since LMWK is present in tissues rather than plasma, KLK1-mediated kinin release plays a more localized role in renal blood flow regulation, neuroprotection, and cardiovascular homeostasis (Koumandou and Scorilas 2013).

The regulation of Pka and KLK is also distinct. Pka is tightly controlled by C1INH and α_2-macroglobulin. In contrast, KLK is regulated by tissue-specific inhibitors such as canonical Kazal-type inhibitors and kallistatin, but lacks a direct inhibitory relationship with C1INH (Kalinska et al. 2016; Chao et al. 1996).

2. Hereditary Angioedema

HAE is a rare, potentially life-threatening disorder marked by unpredictable, recurrent episodes of swelling in various tissues (Landerman et al. 1962; Donaldson and Evans 1963). Unlike allergic angioedema, HAE does not typically present with urticaria, which often complicates its early recognition and diagnosis (Zingale et al. 2006). Patients usually experience their first attacks during childhood or adolescence, with symptoms that can range from mild discomfort to severe, debilitating episodes. The clinical manifestations vary significantly among individuals, with some patients suffering infrequent attacks while others experience recurrent episodes that substantially impair quality of life (Azmy, Brooks, and Hsu 2020).

Triggers for HAE attacks are diverse and may include physical or emotional stress, minor trauma, or hormonal fluctuations, although episodes can also occur spontaneously. This variability not only underscores the diagnostic challenges but also emphasizes the need for heightened clinical awareness. Despite significant advances in understanding its molecular and genetic basis, HAE remains underdiagnosed, and delays in treatment can have serious consequences (Azmy, Brooks, and Hsu 2020).

2.1. The Prevalence, Pathology, and Genetics of HAE

HAE is classically inherited in an autosomal dominant pattern, with approximately 25% of cases resulting from *de novo* mutations (Eidelman 2010). The underlying pathophysiology of HAE is directly related to the dysregulation of KKS, either classified as type 1 or type 2 HAE. The prevalence of HAE ranges

from 1 in 50,000 to 1 in 100,000 individuals, with type 1 being the most common form, accounting for 85% of cases (Cicardi and Agostoni 1996). Nearly half of HAE patients report experiencing 6-12 attacks per year (Zanichelli et al. 2011). Central to the pathogenesis of HAE types 1 and 2 is the *SERPING1* gene, located on chromosome 11q12–q13.1. Over 400 distinct mutations in *SERPING1* have been reported, encompassing missense, nonsense, frameshift, and splice-site alterations (Drouet et al. 2022). Type 1 is characterized by reduced C1INH antigen levels and reduced functional levels, while type 2 is characterized by normal antigenic levels of C1INH but impaired functionality (Davis 1988). This leads to unchecked activation of the contact pathway and an overproduction of BK (Figure 2). This excess BK is responsible for the localized edema observed during attacks, particularly in the subcutaneous tissues, gastrointestinal tract, and upper airways, where swelling can rapidly progress to airway obstruction and become life-threatening. Work from several laboratories conclusively demonstrated that the primary biological mediator of swelling in C1INH deficiency is the release of BK through the contact pathway. For instance, BK levels show a distinct elevation during attacks rather than between attacks, and this elevation is consistently higher in affected limbs compared to unaffected limbs in the same patient during episodes (Nussberger et al. 1998; Nussberger et al. 1999). The observed swelling results from increased vascular permeability rather than alterations in hydrostatic or oncotic pressure. The mechanism through which BK

induces vascular permeability involves its direct effect on endothelial cells via B2R.

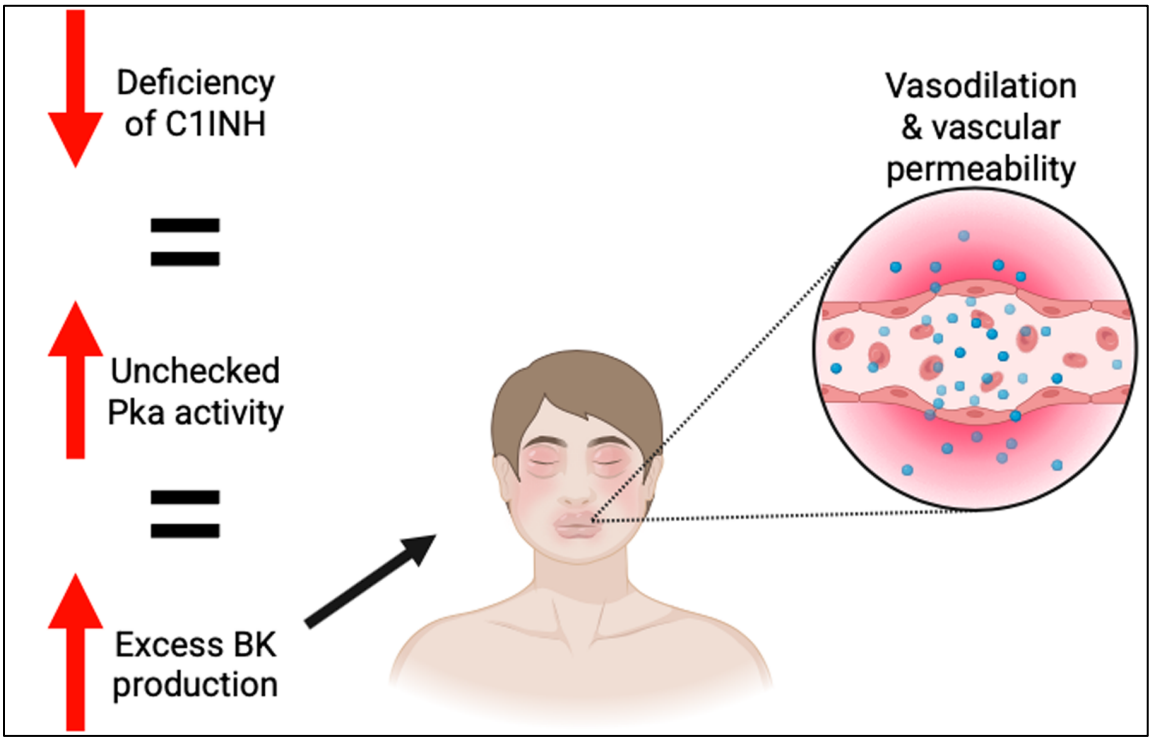

Figure 2: Excessive swelling in Hereditary Angioedema. Type 1 or type 2 HAE (deficiency in antigenic or functional levels of C1INH), resulting in an increased Pka activity due to lower inhibition of Pka, is illustrated schematically. This imbalance results in excessive BK production, resulting in vasodilation and vascular permeability.

There is another type, type 3, which is characterized by normal C1INH antigen and functional levels but associated with genetic lesion in FXII, HMWK, plasminogen, myoferlin, or angiopoietin-1 genes (Bork et al. 2000; Wilkerson and

Moellman 2022; Binkley and Davis 2000). FXII have been implicated in an estrogen-dependent form of HAE that is often more prevalent among females (Sinnathamby et al. 2023). Although these cases are less common, they contribute to the genetic heterogeneity of HAE and may exhibit variable clinical phenotypes. This genetic complexity, combined with the influence of environmental factors and potential modifier genes, helps explain the broad spectrum of disease severity and the unpredictability of attack frequency among patients (Drouet et al. 2022).

2.2. The Diagnosis and Tests Available for HAE

In patients with suspected HAE, diagnosis begins with a thorough clinical evaluation that considers the patient's history of recurrent, non-urticarial swelling episodes and any family history of similar symptoms (Sinnathamby et al. 2023). Although the clinical presentation is often distinctive, laboratory testing is essential for confirmation and to distinguish HAE from other forms of angioedema. Although many individuals experience their first symptoms during childhood or adolescence, most commonly between 10-20 years, the definitive diagnosis is often delayed, with some patients not being correctly diagnosed until decades later (Sinnathamby et al. 2023; Eidelman 2010).

Biochemical assays are the cornerstone of HAE diagnosis for type 1 and type 2. Patients typically exhibit a characteristic complement profile with decreased levels of C4 along with abnormalities in C1INH levels and function (Sinnathamby et al. 2023; Eidelman 2010). Measurement of C1INH antigen levels, usually performed by nephelometry, alongside functional assays using

chromogenic substrates, provides a reliable assessment of the protein's inhibitory capacity (Charest-Morin et al. 2018). However, because C4 levels can occasionally be normal between attacks, reliance solely on these markers may be insufficient, necessitating more in-depth analysis (Eidelman 2010). For types 1 and 2 HAE, measurement of C1INH antigen and functional activity is crucial. Most affected individuals exhibit C1INH antigen and functional levels that are reduced to less than 40% of normal to be clinically diagnosed; 41–67% of normal is regarded as an equivocal range, where results should be interpreted with caution and correlated with clinical findings; and >68% of normal is generally considered within the normal range (Ren et al. 2023; Busse et al. 2021).

Genetic testing has become an invaluable tool in the diagnosis and management of HAE. Techniques such as Sanger sequencing and multiplex ligation-dependent probe amplification are routinely employed to identify point mutations, small insertions or deletions, and larger genomic rearrangements in *SERPING1* (Rozevska et al. 2024; Gosswein et al. 2008; Sheikh et al. 2023). The identification of specific mutations not only aids in confirming the diagnosis but also has potential prognostic value, as emerging evidence suggests that certain mutations may correlate with disease severity and frequency of attacks. Beyond the analysis of *SERPING1*, cases of HAE with normal C1INH levels require a broader genetic workup. In these instances, screening for mutations in genes such as FXII, plasminogen, HMWK, myoferlin, and angiopoietin-1, is essential. Advancements in next-generation sequencing technologies now facilitate a more

comprehensive interrogation of the genomic landscape associated with HAE, allowing clinicians to capture a wider array of genetic alterations that may contribute to the phenotype (Veronez et al. 2021).

2.3. Types of Treatments Available for HAE

The current therapeutic landscape for HAE is characterized by a dual approach, aiming to both prevent attacks and manage them effectively when they occur. Existing treatments can be broadly classified into two categories: prophylactic and acute therapies. Prophylactic treatments are intended to reduce the frequency and severity of HAE attacks, thereby enhancing quality of life and preventing potentially life-threatening episodes, such as those involving upper airway swelling. In contrast, acute treatments are administered at the onset of symptoms to rapidly control the progression of an attack, particularly during emergencies (Sinnathamby et al. 2023).

Despite significant advances in HAE management over recent decades, each treatment modality is accompanied by its own set of limitations. Prophylactic strategies, while effective in many patients, often require regular dosing, can be expensive, and may exhibit variable efficacy among individuals. Similarly, acute treatments, although crucial for preventing severe outcomes, can be constrained by factors such as the narrow therapeutic window for administration, potential adverse effects, and issues related to accessibility during emergencies.

2.3.1. Prophylactic Treatments to Prevent HAE

Prophylactic therapy in HAE aims to reduce the frequency and severity of attacks, thereby mitigating life-threatening complications and improving quality of

life. Current agents can be broadly grouped into plasma-derived C1INH (pdC1INH) concentrates, monoclonal antibodies, and oral kallikrein inhibitors. Each class works through distinct mechanisms, with unique benefits and limitations.

Historically, pdC1INH concentrates such as the commercial products Cinryze™ and Haegarda™ have been the cornerstone of HAE prophylaxis. Cinryze™, for example, functions as a replacement therapy by restoring deficient levels of C1INH in children, adults and adolescents (Sinnathamby et al. 2023; Eidelman 2010; Valerieva and Longhurst 2022). This re-establishes control over the KKS and prevents the excessive production of BK. Its efficacy in reducing attack frequency and severity is well documented; however, its intravenous (IV) administration every 3 to 4 days at a dose of 1000 units can be inconvenient. Repeated IV administration may lead to damaged veins and loss of access, and although indwelling ports may be placed, there is an increased risk for infection (Sinnathamby et al. 2023; Eidelman 2010; Valerieva and Longhurst 2022). Cinryze™ has a plasma half-life of approximately 56 hours, necessitating frequent infusions to maintain therapeutic levels (Lunn, Santos, and Craig 2010). In contrast, Haegarda™ offers an improved administration profile by optimizing for subcutaneous injection. Although also given every 3–4 days, it does not involve the side effects of repeated IV administration (Sinnathamby et al. 2023). Featuring an extended half-life of 69 hours, Haegarda™ allows for less frequent dosing and often permits self-administration (Agboola et al. 2019; Pawaskar et al.

2018). Despite these advantages, both agents share inherent challenges related to cost, supply limitations, and the potential for injection site reactions.

In recent years, engineered recombinant antibody drugs have expanded prophylactic options for HAE. Monoclonal antibodies such as Lanadelumab and Gardacimab have been approved for HAE prophylaxis (Fijen and Levi 2022; Wang et al. 2020). Lanadelumab, a fully human monoclonal antibody, administered to people of 12 years of age or older at a dosage of 300mg, binds and blocks the active site of Pka, thereby preventing the cascade that leads to excessive BK production (Busse and Kaplan 2022). With a long half-life of 14 days that permits dosing every 2-4 weeks via subcutaneous injection, Lanadelumab has proven highly effective in reducing both the number and severity of HAE attacks (Busse and Kaplan 2022; Wang et al. 2020). Similarly, Gardacimab employs a comparable mechanism to inhibit FXIIa, with early clinical data suggesting efficacy and safety profiles akin to those of Lanadelumab (Reshef et al. 2025). Nonetheless, these agents are not without drawbacks; their high cost and potential for injection site reactions can limit accessibility and long-term adherence (Shah et al. 2023). Moreover, as Gardacimab is a relatively newer entrant to the therapeutic arena, its long-term safety profile is still being established.

Complementing these injectable therapies is the oral kallikrein inhibitor Berotralstat, which offers an entirely different approach (Busse and Kaplan 2022). By directly inhibiting Pka, Berotralstat reduces the generation of BK and provides

continuous prophylactic coverage through once-daily dosing of 150mg makes it a convenient option, particularly for patients seeking to avoid injections or infusions. It has a half-life of 93 hours and reaches a steady state levels in 6-12 days (Busse and Kaplan 2022). The oral route enhances convenience and may improve adherence compared to injectable regimens. However, gastrointestinal side effects and the need for ongoing evaluation of its long-term safety and efficacy remain areas of active investigation (Busse and Kaplan 2022).

Prior to the advent of targeted biologic therapies, attenuated androgens, such as Danazol, were widely used as prophylactic agents for HAE administered at 50-200mg. These synthetic derivatives of testosterone function by increasing hepatic production of C1INH, thereby partially restoring regulatory control over the contact pathway for type 1 HAE. However, their plasma half-life of 7-12 hours necessitates daily dosing to maintain efficacy (Guo et al. 2022). While effective in reducing attack frequency, attenuated androgens carry significant risks, including hepatotoxicity, weight gain, virilization in female patients, menstrual irregularities, growth retardation, and long-term cardiovascular concerns (Sinnathamby et al. 2023; Eidelman 2010; Prematta, Prematta, and Craig 2008). Due to these adverse effects, they are generally reserved for patients who lack access to newer therapies or for those in regions where biologics are prohibitively expensive.

Another class of prophylactic therapy includes antifibrinolytics, such as tranexamic acid and epsilon-aminocaproic acid. These agents function by

inhibiting plasmin, thereby reducing fibrinolysis, which in turn decreases the downstream activation of the contact pathway and kallikrein (Ritchie 2003). Antifibrinolytics have demonstrated some efficacy in reducing attack frequency, administered at 500 mg 2-3x daily, particularly in milder cases of HAE, with a 2-hour half-life (Sinnathamby et al. 2023). However, their effect is considerably weaker compared to C1INH based therapies or kallikrein inhibitors (Busse et al. 2021). These agents are rarely used as first-line prophylactic therapy but may be considered in patients who cannot tolerate or access biologic therapies. Additionally, long-term use carries risks of thrombosis, particularly in patients with underlying risk factors (Sinnathamby et al. 2023).

2.3.2. Acute Treatments for HAE

Acute treatment for HAE is essential for rapidly controlling swelling episodes, particularly those affecting the airway, gastrointestinal tract, or extremities. Unlike prophylactic therapies, which aim to reduce attack frequency, acute treatments are administered on demand at the first signs of an attack to prevent progression and alleviate symptoms (Sinnathamby et al. 2023). Current on-demand therapies target key components of the contact pathway, including C1INH replacement therapy, bradykinin receptor antagonists, and kallikrein inhibitors. The four main agents used in acute HAE management are Berinert™, Ruconest™, Icatibant™, and Ecallantide, each with distinct mechanisms, efficacy, half-lives, and limitations (Valerieva and Longhurst 2022).

C1INH replacement therapy remains one of the most direct approaches to treating acute HAE attacks by restoring the deficient regulatory protein.

Berinert™, a pdC1INH, functions by replenishing C1INH levels, thereby inhibiting Pka and FXIIa to prevent excessive BK production. Administered intravenously at a dose of 20 U/kg to adults, Berinert™ provides rapid symptom relief, with most patients experiencing improvement within 30 minutes (Bernstein et al. 2010; Valerieva and Longhurst 2022). Its half-life of approximately 30 hours is significantly longer than that of recombinant C1INH, reducing the likelihood of attack recurrence (Bernstein et al. 2010). However, as a plasma-derived product, Berinert™ is subject to supply limitations and requires IV administration, which may be less convenient for self-treatment. In contrast, Ruconest™, the only recombinant C1INH available for clinical use, offers a non-plasma alternative by being produced in transgenic rabbit milk (Cruz 2015). Similar to Berinert™, Ruconest™ functions by inhibiting Pka and FXIIa, preventing the overproduction of BK. However, Ruconest™ has a much shorter half-life of approximately 2 hours, requiring higher doses (50 U/kg IV) for adults and adolescence to achieve comparable efficacy (Zubareva et al. 2021). While Ruconest™ eliminates concerns related to human donor dependency, its short half-life increases the risk of symptom recurrence, and its recombinant nature poses a risk of immunogenicity in some patients (Cruz 2015).

Beyond C1INH replacement, acute therapy can also target BK signaling directly. Icatibant™, a selective B2R antagonist, competitively inhibits BK binding to endothelial cells, thereby preventing the increased vascular permeability that leads to swelling (Dubois and Cohen 2010). Unlike C1INH replacement

therapies, Icatibant™ is administered as a 30mg subcutaneous injection for patients 18 years or older, allowing for easier self-treatment (Eidelman 2010; Valerieva and Longhurst 2022). With a half-life of 1.5 hours and a duration of action extending 6 hours, Icatibant™ provides symptom relief less than hour, though some patients may require repeat dosing (Eidelman 2010; Leach et al. 2015). One of its major advantages is its efficacy across all HAE subtypes, including type 3 HAE (Boccon-Gibod and Bouillet 2012). However, up to 97% of patients experience mild to moderate injection site reactions, which, while non-serious, can cause discomfort (Boccon-Gibod and Bouillet 2012).

Another approach to acute HAE treatment involves direct inhibition of Pka, preventing excessive BK production at its source. Ecallantide, a recombinant Pka inhibitor, blocks the cleavage of HMWK into BK, effectively stopping the cascade (Valerieva and Longhurst 2022). Administered 30mg subcutaneous injections to patients 12 years or older, Ecallantide has a half-life of approximately 2 hours, providing rapid symptom control (Farkas and Varga 2011; Sinnathamby et al. 2023). While it offers an effective alternative for acute HAE attacks, 3.5% of patients experience hypersensitivity reactions, including anaphylaxis, necessitating administration under medical supervision (Craig et al. 2015). This safety concern limits Ecallantide's use in self-treatment settings and requires patients to receive the drug in a clinical facility where anaphylaxis management is available.

2.3.2.1. Half-Life Extension Technology

A major limitation of current HAE therapies is their short half-life, necessitating frequent injections for effective prophylaxis. This pharmacokinetic constraint increases the treatment burden on patients and highlights the need for half-life extension (EHL) strategies to improve therapeutic longevity. Extending the half-life of biologics allows for less frequent dosing, improving patient adherence and reducing healthcare costs (Ar, Balkan, and Kavakli 2019). Several EHL technologies have been developed, primarily focusing on reducing renal clearance and enhancing recycling via neonatal Fc receptors (FcRn) (Ar, Balkan, and Kavakli 2019).

As mentioned below, renal clearance is particularly relevant for small proteins and peptides that fall below the renal filtration threshold of ~60 kDa (Jia et al. 2009). Therapeutic proteins with molecular weights below this threshold are rapidly filtered by the kidneys, resulting in short half-lives. Strategies to reduce renal clearance include increasing molecular size via pegylation, fusion to large carrier proteins (e.g., albumin or IgG Fc), or binding to endogenous albumin through albumin-binding domains (Zaman et al. 2019; Ar, Balkan, and Kavakli 2019). Among these, serum albumin fusion and Fc fusion technologies have shown promise in prolonging the circulatory half-life of therapeutic proteins by recycling via FcRn. FcRn-mediated recycling is a mechanism in which IgG and albumin are endocytosed by cells and rescued from lysosomal degradation by binding to FcRn simultaneously in a noncooperative manner at low pH, allowing it

to be recycled back into circulation (Sleep, Cameron, and Evans 2013; Ar, Balkan, and Kavakli 2019).

IgG and albumin are the two most abundant soluble proteins in the body, making up over 80% of the total plasma protein pool (Andersen et al. 2014). While albumin serves as a versatile transporter for various small molecules, helps maintain colloidal osmotic pressure, and plays a role in blood pH buffering, IgG functions as the primary antibody class responsible for immune defense against pathogens (Andersen et al. 2014; Culica et al. 2021; Miller and Jedrzejczak 2001). Due to both being recycled through the FcRn, they exhibit exceptionally long half-lives of 19 days, whereas most other circulating proteins are degraded within a few days or less (Andersen et al. 2014; Guo et al. 2016). While both approaches enhance pharmacokinetics, albumin offers several advantages over Fc fusion that make it a more suitable candidate for extending the half-life. First, albumin fusion typically results in a smaller final construct compared to Fc fusion, which improves tissue penetration and diffusion (Chuang et al. 2021). Additionally, Fc-fusion proteins can also interact with Fc gamma receptors on immune cells, potentially leading to unintended immune responses, whereas albumin follows a more predictable catabolic profile as it lacks those components (Qureshi et al. 2017). Immunogenicity is also a concern, as Fc-fusion proteins may retain residual effector functions and develop autoantibodies directed against the Fc fusion, whereas albumin is a naturally occurring, safe, stable, and

non-immunogenic protein, reducing the risk of adverse immune responses (Chuang et al. 2021; Liu 2018).

Various mammalian albumins have been explored for EHL applications, including human serum albumin (HSA) and murine serum albumin (MSA) (Guo et al., 2016). Fusing therapeutic proteins to albumin can significantly extend their half-life, as has been demonstrated in several approved biologics. One notable example is Albuleukin, a fusion protein comprising recombinant human interleukin-2 (rIL-2) and HSA. In preclinical studies involving murine models, Albuleukin demonstrated a plasma half-life ranging from 6-8 hours, a significant increase compared to the 19–57 minutes observed with rIL-2 alone. This extension in half-life correlated with enhanced anti-tumor efficacy without an associated increase in mortality (Melder et al. 2005). Another example involves the fusion of the Kunitz protease inhibitor (KPI) domain of protease nexin-2 to HSA, aiming to improve its therapeutic potential as an antithrombotic agent. The KPI-HSA fusion protein exhibited an 8-fold increase in mean terminal half-life compared to KPI alone. Importantly, this modification did not impair the inhibitor's antithrombotic properties; instead, it expanded its therapeutic window by reducing rapid *in vivo* clearance (Sheffield, Eltringham-Smith, and Bhakta 2018). Furthermore, in a pivotal study, researchers evaluated the safety and efficacy of a recombinant fusion protein linking coagulation FIX with HSA (rIX-FP) in patients with hemophilia B. The study demonstrated that rIX-FP has a mean terminal half-life of 102 hours, which is approximately 4.3 times longer than that of previous

FIX treatments. This extended half-life allowed for less frequent dosing schedules, with patients maintaining adequate FIX activity levels on weekly or bi-weekly prophylactic regimens (Santagostino et al. 2016). In contrast, Sheffield et al. (2004), investigated the pharmacokinetics of a genetically engineered fusion protein combining murine FIX with MSA (MFUST). In murine models, the area under the clearance curve for MFUST was reduced compared to control, and the terminal half-life did not significantly differ among the variants tested. These findings suggest that, despite the increased molecular size due to albumin fusion, the clearance behavior of the fusion protein more closely resembled that of FIX than albumin, implying that FIX-specific interactions influencing clearance were preserved (Sheffield et al. 2004). These discrepancies may be attributed to species-specific differences in albumin and FIX metabolism, as well as variations in study design and fusion protein constructs.

To date, EHL strategies have not yet been described for C1INH in peer-reviewed literature.

3. Serpins

Serpins are a superfamily of proteins that play essential roles in regulating proteolytic processes across multiple physiological processes, including coagulation, fibrinolysis, and inflammation (Yaron et al. 2021; Grover and Mackman 2022; Heit et al. 2013). With over 1,500 members identified across species, serpins are highly conserved and structurally similar despite their wide functional diversity (Irving et al. 2000; Law et al. 2006; Rawlings, Tolle, and

Barrett 2004). In humans alone, at least 37 serpins have been characterized, with functions ranging from controlling blood clotting to modulating immune responses (Sanrattana, Maas, and de Maat 2019; Vidalino et al. 2009). Serpins are classified into distinct clades (A-I) based on sequence homology and function (Silverman et al. 2001). Most members act extracellularly to regulate proteolytic cascades, such as antithrombin (*SERPINC1*) in coagulation and AAT (*SERPINA1*) in inflammation, while others function intracellularly, such as the *SERPINB* family, which primarily protects the cell interior from inappropriate protease activity. Interestingly, some serpins have evolved non-inhibitory roles, acting as molecular chaperones or structural proteins, such as HSP47 in collagen folding and ovalbumin in egg storage (Law et al. 2006). Additionally, some bacteria and viruses encode serpins to subvert host immune defenses, highlighting their evolutionary importance in host-pathogen interactions (Varkoly et al. 2023; Abbas et al. 2022). Native serpins are in a metastable state in which they exist in a conformation that is not their most stable state, but rather a kinetically trapped folding intermediate allowing them to undergo a conformational change for their function (Law et al. 2006; Khan et al. 2011; Im et al. 2002). Serpins act as irreversible "suicide-substrate inhibitors", forming a stable covalent complex with their target proteases through a profound conformational rearrangement. This mechanism ensures rapid inhibition but also results in the clearance of both the serpin and the inhibited protease from circulation (Huntington, Read, and Carrell 2000). While this metastability is

essential for their function, it also makes serpins particularly prone to misfolding and polymerization, leading to serpinopathies which is a group of diseases caused by serpin dysfunction (Carrell and Lomas 1997; Law et al. 2006). These include AAT deficiency (AATD), which causes lung and liver disease due to the polymerization of mutant *SERPINA1*; and HAE, caused by a deficiency or dysfunction of C1INH gene (*SERPING1*), leading to excessive complement activation and bradykinin-mediated swelling (Brantly et al. 2020; Davis 1988). Other serpin mutations can lead to thrombophilia, neurodegenerative diseases, and certain cancers, underscoring their clinical significance (Sanchez-Navarro et al. 2021). The widespread conservation and physiological importance of serpins highlight their evolutionary adaptability. Serpins are among the oldest protease inhibitors, dating back to early metazoans, and have undergone functional diversification across species (Irving et al. 2000). This evolutionary plasticity has enabled them to acquire specialized roles, making them key regulators of proteolytic homeostasis.

3.1. The Key Structural Features of Serpins

Serpins consist of a conserved tertiary structure composed of 3 β-sheets (A, B, and C) and 8–9 α-helices (Elliott et al. 1996). Their inhibitory mechanism involves the RCL, a flexible, surface-exposed loop that acts as a bait for target proteases. The RCL extends from β-sheet A and is partially stabilized by interactions with nearby loops, allowing it to remain flexible while still positioned for protease binding (Whisstock and Bottomley 2006). The RCL sequence strongly influences protease specificity, with key residue positions conventionally

designated using Schechter and Berger nomenclature: N-terminal residues of the cleavage site (P1-P1') are designated P2, P3…P15, while C-terminal residues are designated P2', P3'…P5', and corresponding subsites are designated s1, s2 and so on (Schechter and Berger 1967). Variability in RCL sequence largely determines target protease preference, allowing for precise regulatory control over proteolytic cascades.

Serpins can adopt multiple conformational states, including: (i) native state – the active form before protease binding; (ii) intermediate states – including the latent form, in which the RCL is inserted into β-sheet A without protease cleavage, and polymerized forms caused by abnormal intermolecular interactions; and (iii) cleaved state – after RCL cleavage, β-sheet A fully incorporates the RCL, stabilizing the serpin-protease complex for rapid clearance (Law et al. 2006; Whisstock et al. 2000). In their native state, serpins exist in a high free energy conformation in which β-sheet A is partially open, allowing for RCL mobility. Upon cleavage by a target protease, the RCL inserts into β-sheet A, and translocates the attached protease from one pole of the serpin to the other, trapping the protease in an irreversible complex that is subsequently cleared from circulation (Figure 3). However, destabilizing mutations can cause aberrant conformational changes, leading to polymerization or the formation of inactive latent states, a hallmark of serpinopathies (Law et al. 2006). There are many ways a polymer can form: the RCL of one serpin inserts into β-sheet A of another; the RCL of one serpin inserts into β-sheet C of another; or

interchain disulfide bonds between multiple serpins, all generating inactive aggregates (Zhang et al. 2008; Wilczynska et al. 2003; Lomas and Mahadeva 2002). For example, in some forms of AATD mutant *SERPINA1* polymers accumulate in hepatocytes, leading to both loss of lung protection and liver toxicity (Nunez et al. 2021).

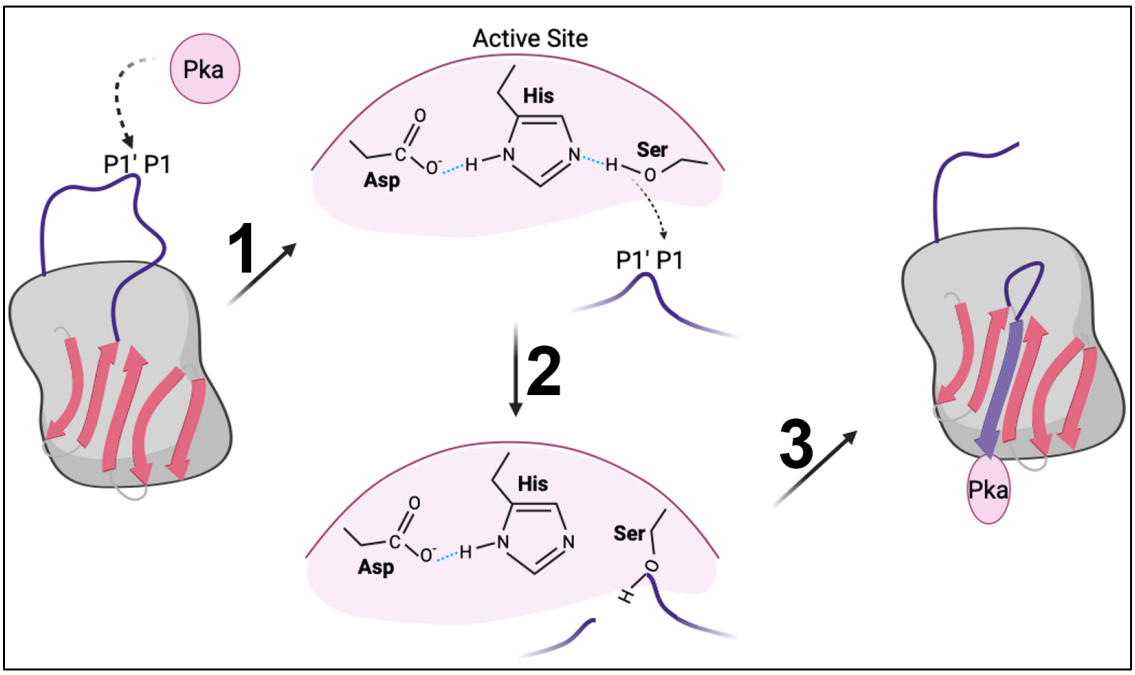

Figure 3: Serpin mechanism pathway with kallikrein. (1) Pka forms a non-covalent encounter complex with the reactive center (P1-P1') of serpin. (2) S195 of the active site of Pka performs a nucleophilic attack on the reactive center resulting in the cleavage of the reactive center and formation of an acyl-ester covalent bond between the hydroxyl of S195 and carbonyl of P1. (3) This results in a conformational change where the P1 side of reactive center loop is flipped

into β-sheet A forming as the 4th strand while distorting the oxyanion hole and plucking S195 away from the active site of Pka rendering it inactive.

The RCL is highly dynamic, and its structural fluctuations influence protease recognition and specificity (Huntington, Read, and Carrell 2000). Certain serpins, such as antithrombin, use co-factors like heparin to enhance protease recognition and maximize inhibition rates (Jin et al. 1997). Additionally, some serpins contain extra domains, such as the heavily glycosylated N-terminal domain of C1INH or the acidic N-terminal domain of heparin cofactor II (HCII) (Bos, Hack, and Abrahams 2002; Van Deerlin and Tollefsen 1991), which contribute to structural stability and function (Ghannam et al. 2016).

3.2. The Mechanism of Serpins

The inhibitory mechanism of serpins follows a highly specialized sequence of events that differentiates them from standard reversible protease inhibitors. The process begins when a target protease recognizes and binds to the serpin's RCL, forming a Michaelis, or encounter complex, where the protease's catalytic triad (Ser-His-Asp) aligns with the scissile bond at P1-P1′. This interaction is stabilized by non-covalent forces between the RCL and the protease's active site, forming a tetrahedral intermediate (Huntington, Read, and Carrell 2000). Proteolytic cleavage at P1-P1′ induces a major conformational change, releasing stored energy from the metastable native serpin state (Chang et al. 1996). This energy powers rapid insertion of the RCL into β-sheet A as the 4th strand, converting it from a 5-stranded to a 6-stranded structure, and simultaneously

dragging the covalently linked protease from one pole of the serpin to the other (Stratikos and Gettins 1998; Cabrita and Bottomley 2004). This process translocates the protease by over 70Å, effectively distorting its tertiary structure and misaligning its active site.

During this transition, the protease forms a covalent acyl-enzyme intermediate, where its catalytic serine hydroxyl group (Ser195) is esterified to the carbonyl of the serpin's P1 residue. This step is critical, as the translocation prevents proper hydrolysis, effectively trapping the protease in an inactive conformation (Ye et al. 2001; Law et al. 2006; Dementiev et al. 2003). Unlike traditional inhibitors that function by blocking substrate access, serpins physically distort and disable the protease, rendering it inactive. The resulting serpin-protease complex is highly stable, with a half-life ranging from hours to days, preventing protease reactivation (Law et al. 2006).

3.3. Serpin Clearance

Serpins play a crucial role in regulating proteolytic activity, ensuring that proteases are tightly controlled to prevent excessive or unregulated proteolysis. Once a serpin has inhibited its target protease, forming a stable serpin-protease complex, it must be rapidly removed from circulation to maintain protease homeostasis, prevent accumulation of inactive complexes. The clearance of serpin-protease complexes is mediated through cellular uptake and degradation pathways, primarily involving receptor-mediated endocytosis, non-receptor mediated endocytosis, and lysosomal degradation. The primary clearance pathway for serpin-enzyme complexes is facilitated by low-density lipoprotein

receptor-related protein (LRP1), a major scavenger receptor that recognizes and internalizes serpin-protease complexes for degradation (Strickland, Muratoglu, and Antalis 2011). However, alternative mechanisms such as mannose receptor recognition or proteasomal degradation contribute to the clearance of serpins (Lee et al. 2002; Kroeger et al. 2009). Additionally, glycosylation patterns and post-translational modifications can influence serpin clearance rates.

3.3.1. Overview of LRP1 mechanism

To prevent the accumulation of inactive serpin-protease complexes and maintain protease homeostasis, these complexes undergo rapid clearance from circulation, primarily through LRP1. LRP1 is a high-capacity scavenger receptor belonging to the LDL receptor family, widely expressed on hepatocytes, macrophages, fibroblasts, and endothelial cells (Lillis et al. 2008). It plays a crucial role in removing protease-inhibited serpins, ensuring that they do not disrupt physiological proteolytic cascades (Kounnas et al. 1996). LRP1 is a transmembrane glycoprotein that consists of two main subunits: (i) the extracellular α-chain which contains four ligand-binding clusters (I–IV), responsible for recognizing and binding serpin-protease complexes; and (ii) the membrane-anchored β-chain which contains a single transmembrane domain and a cytoplasmic tail, which regulates endocytosis and intracellular signaling via interactions with adaptor proteins (Moestrup et al. 1993; Jeon et al. 2001). Clusters contain complement-type repeats, which mediate high-affinity interactions with serpin-protease complexes, targeting them for internalization and degradation (Mikhailenko et al. 2001).

The mechanism of LRP1-mediated clearance follows a well-defined pathway. First, LRP1 recognizes specific motifs on the serpin-protease complex that are exposed when a serpin undergoes conformational changes upon protease inhibition (Herz and Strickland 2001). LRP1 primarily recognizes these complexes through electrostatic interactions between basic residues on the serpin and acidic residues on LRP1. Following receptor binding, the complex is internalized via clathrin-mediated endocytosis, forming an early endosome. The complex is subsequently trafficked to lysosomes, where both the serpin and its bound protease undergo enzymatic degradation into small peptides and amino acids (Herz and Strickland 2001). Meanwhile, LRP1 is recycled back to the plasma membrane to facilitate further clearance cycles.

LRP1-mediated clearance is highly efficient, particularly for serpins that regulate coagulation, fibrinolysis, and inflammation (He et al. 2021; Strickland and Medved 2006; Gonias and Campana 2014). Additionally, glycosylation of serpins can modulate their clearance efficiency. For example, C1INH is a heavily glycosylated serpin, and variations in its glycosylation pattern influence its binding affinity to LRP1, thereby affecting its clearance rate (Zeerleder et al. 2021). Similarly, heparin-binding serpins, such as antithrombin, interact with glycosaminoglycans, altering their circulatory half-life and clearance dynamics (Gettins 2002). Impaired LRP1 function or receptor availability can lead to serpinopathies.

3.3.2. LRP1-independent Clearance and Catabolism of Native Plasma Proteins

Although LRP1-mediated endocytosis is the primary route for clearing serpin-protease complexes, several alternative pathways contribute to the removal of serpins. These include endocytosis via other receptors, renal and hepatic clearance, proteasomal degradation of misfolded intracellular serpins, and non-receptor mediated endocytosis.

In addition to LRP1, other receptors participate in serpin clearance, particularly those that recognize glycoproteins and modified proteins. One such receptor is the asialoglycoprotein receptor (ASGPR), expressed on hepatocytes, which removes desialylated serpins from circulation (Stockert 1995). Desialylation occurs naturally as glycoproteins age, exposing galactose or N-acetylgalactosamine residues, which ASGPR recognizes and internalizes for lysosomal degradation (Ashwell and Harford 1982). Additionally, certain glycosylated serpins may be cleared by mannose receptors on macrophages and endothelial cells, though direct evidence of mannose receptor involvement in serpin clearance is limited. While the mannose receptor primarily recognizes glycoproteins with terminal mannose residues, its role in serpin turnover requires further investigation (Taylor and Drickamer 1993; Lee et al. 2002).

Smaller sized proteins may undergo renal filtration followed by urinary excretion (Turnier et al. 2019). However, most serpin clearance occurs via the liver, where glycosylation state and receptor recognition determine the rate of hepatic uptake and degradation.

While extracellular serpin-protease complexes are primarily cleared via LRP1 and lysosomal degradation, misfolded or polymerized intracellular serpins undergo clearance via the endoplasmic reticulum (ER)-associated degradation pathway. In this pathway, misfolded serpins are retrotranslocated from the ER to the cytoplasm, where they are ubiquitinated and degraded by the proteasome (Teckman and Perlmutter 2000; Kroeger et al. 2009). This process is crucial for preventing toxic intracellular serpin accumulation. Emerging evidence suggests that misfolded serpins may also be packaged into extracellular vesicles or exosomes and secreted from cells, providing an alternative clearance route (Park et al. 2022).

4. Introduction to C1-esterase Inhibitor

C1INH is a heavily glycosylated serpin that circulates in human plasma at a concentration of approximately 0.25 mg/mL (3.5 μM) (Gregorek et al. 1991). It is primarily synthesized by hepatocytes, but other cell types, including monocytes, macrophages, and fibroblasts, also contribute to its production (Prada, Zahedi, and Davis 1998). C1INH is an acute-phase protein, meaning its plasma levels increase in response to systemic inflammation, infections, or tissue injury, a characteristic that underscores its broader physiological significance beyond homeostatic regulation (Bergamaschini et al. 2001; Lathem, Bergsbaken, and Welch 2004; Huisman, van Griensven, and Kluft 1995). The glycosylation profile of C1INH plays a crucial role in its stability, plasma half-life, and interaction with various proteases, with variations in glycan composition influencing its

clearance rate and functional efficacy (Bos, Hack, and Abrahams 2002; Ghannam et al. 2016). Unlike many other serpins, which primarily act through suicide substrate inhibition, C1INH exhibits a relatively slow but efficient inhibitory mechanism, forming stable complexes with its target proteases. Given its role in regulating multiple proteolytic cascades, alterations in C1INH levels or activity are associated with a range of pathological conditions, most notably HAE (Davis 1988).

4.1. The Structure of C1INH

Comprising 500 amino acid residues, including a 22-residue signal peptide, C1INH has a molecular weight of approximately 110 kDa, with a significant portion of its mass attributed to extensive glycosylation (Zahedi, Prada, and Davis 1993). The protein is composed of two primary domains: a highly glycosylated N-terminal domain spanning 116 amino acids and a C-terminal serpin domain consisting of 362 amino acids. The N-terminal domain is dispensable for protease inhibition but contributes to structural stability and interactions with other proteins (Wagenaar-Bos and Hack 2006). Within this region, 10 N-glycosylation sites and 24 O-glycosylation sites have been identified (Stavenhagen et al. 2018). Notably, all O-linked glycans, along with most N-linked glycans, except those at N238, N253, and N352, are located within this domain, while the C-terminal serpin domain harbors the remaining glycosylation sites. N-linked glycans leads to accelerated clearance with no effect on function (Reboul, Prandini, and Colomb 1987; Zeerleder et al. 2021), whereas depletion of O-linked glycans can compromise protein stability and alter its conformational

flexibility (Stavenhagen et al. 2018). The serpin domain of C1INH is critical for its inhibitory function, housing the RCL, which serves as the primary binding site for target proteases (Bos, Lubbers, et al. 2003). The cleavage site for protease inhibition is located at Arg466-Thr467, a key determinant of its activity (Eldering et al. 1992).

One of the defining structural features that sets C1INH apart from other serpins is its reliance on two critical disulfide bonds between residues 101-406 and 108-183, which are crucial for maintaining proper folding, stability, and function (Bock et al. 1986). These disulfide linkages provide structural rigidity that is essential for its ability to act as an inhibitor across multiple proteolytic cascades. Unlike intracellular serpins, which can be expressed in bacterial systems due to their simpler folding requirements, C1INH cannot be efficiently produced in prokaryotic expression systems such as *Escherichia coli (E. coli)* due to its reliance on proper disulfide bond formation and glycosylation, unless it is grown in bacterial strains that permit the formation of disulfide bonds (Lamark et al. 2001). For example, a study by Simonovic and Patston (2000) demonstrated that reducing the disulfide bonds of C1INH induces significant conformational changes, leading to monomeric intermediates that closely resemble polymerization-prone states. These structural alterations result in the insertion of the RCL into β-sheet A, a characteristic feature of inactive serpins (Simonovic and Patston 2000). These findings underscore the indispensable role of disulfide

bonds in maintaining C1INH's metastable fold, ensuring proper positioning of the RCL and preserving its inhibitory activity.

4.2. C1INH Involvement in Multiple Pathways

C1INH serves as a broad-spectrum serpin, targeting key proteases in multiple biological pathways. Its inhibitory activity extends across the contact system, complement system, coagulation cascade, and fibrinolysis, while its non-inhibitory functions contribute to immune modulation, endothelial protection, and anti-inflammatory responses (Davis, Mejia, and Lu 2008).

The complement system is a critical component of innate immunity, responsible for pathogen clearance, immune complex elimination, and cell lysis (Dunkelberger and Song 2010). It is initiated through three distinct pathways: classical, lectin, and alternative. The classical pathway is activated when C1q binds to antigen-antibody complexes, leading to the sequential activation of C1r and C1s, which cleave C4 and C2 to generate the C3 convertase (Dunkelberger and Song 2010). The lectin pathway, triggered by pattern recognition molecules like mannose-binding lectin, follows a similar activation cascade through MASP-1 and MASP-2, which also cleave C4 and C2 (Dunkelberger and Song 2010). C1INH is the principal inhibitor of the classical and lectin pathways, preventing uncontrolled complement activation and excessive inflammation. It does so by binding to and inactivating C1r and C1s (second order rate constant (k_2) 4.4 x10^4 $M^{-1}s^{-1}$), thereby preventing C1 complex activation and the downstream complement cascade. Similarly, C1INH inhibits MASP-1 and MASP-2 (k_2 0.2 x10^4 $M^{-1}s^{-1}$), blocking lectin pathway activation before it can generate the C3

convertase (Zubareva et al. 2021; Hor et al. 2020). C1INH, via a reversible interaction with C3b that appears to interfere with the C3b-factor B interaction, also can inhibit alternative pathway activation which is not required for protease inhibition (Jiang et al. 2001). By regulating these proteases, C1INH prevents excessive complement-mediated inflammation, endothelial damage, and tissue injury.

The contact system is crucial for BK generation, which controls vascular permeability and inflammatory responses, as mentioned above. C1INH is the primary endogenous inhibitor of the contact system, preventing excessive BK production. It inhibits FXIIa (k_2 3.0 x10^4 $M^{-1}s^{-1}$) and Pka (k_2 2.6 x10^4 $M^{-1}s^{-1}$), thereby blocking both FXII autoactivation and PK activation (Maat, Prins, and Brussaard 2019). This inhibition is critical in preventing pathological vascular leakage, as seen in HAE.

The coagulation cascade consists of intrinsic and extrinsic pathways that converge to form the common pathway, ultimately leading to fibrin clot formation (Park and Park 2024). The intrinsic pathway is closely linked to the contact system, as FXIIa also activates FXI, propagating thrombin generation. The extrinsic pathway, initiated by tissue factor, activates FVII, leading to fibrin deposition (Park and Park 2024). C1INH modulates coagulation by inhibiting FXIa (k_2 0.1 x10^4 $M^{-1}s^{-1}$) (Zhao et al. 1998). Additionally, C1INH inhibits thrombin, though its efficiency in doing so is lower compared to other serpins like

antithrombin (Cugno et al. 2001). By regulating these pathways, C1INH acts as an anticoagulant, preventing excessive clot formation.

The fibrinolytic system ensures that excess fibrin clots are degraded to maintain vascular homeostasis (Chapin and Hajjar 2015). This process is driven by plasmin, which cleaves fibrin into soluble degradation products. Plasmin is generated when tissue plasminogen activator (tPA) or urokinase plasminogen activator convert plasminogen into active plasmin (Chapin and Hajjar 2015). C1INH helps regulate fibrinolysis by inhibiting plasmin (k_2 1.3 x10^4 $M^{-1}s^{-1}$) and tPA, ensuring that clot breakdown occurs in a controlled manner (de Maat, Sanrattana, et al. 2019; Huisman, van Griensven, and Kluft 1995). This inhibitory function is particularly relevant in conditions where excessive fibrinolysis can lead to bleeding disorders.

C1INH has been extensively studied for its protective effects against endotoxin shock (Liu et al. 2003). It achieves this by directly binding to bacterial endotoxins and lipopolysaccharides (LPS) on the outer membranes of gram-negative bacteria via its N-terminal residues Asn^3, Arg^{18}, Lys^{22}, Lys^{30}, and Lys^{55} (Liu et al. 2005). This binding prevents LPS from engaging to macrophages thereby reducing the subsequent release of pro-inflammatory cytokines such as tumour necrosis factor alpha (TNF-α) (Liu et al. 2003). By mitigating the LPS-induced cytokine storm, C1INH reduces systemic inflammation.

C1INH plays a crucial role in modulating leukocyte trafficking and endothelial cell function during inflammation (Cai and Davis 2003). It has been

shown that C1INH expresses the sialyl Lewis^x tetrasaccharide on the N-terminus which binds to E-selectin and P-selectin, key adhesion molecules on endothelial cells that mediate the recruitment of neutrophils and monocytes to inflamed tissues (Davis, Mejia, and Lu 2008). By interfering with selectin-mediated rolling and adhesion, C1INH reduces excessive leukocyte extravasation, thereby preventing excessive cytokine production.

4.3. C1INH Expressed Across Multiple Platforms

Recombinant C1INH (rC1INH) has been successfully expressed in functional form using various systems, including bacteria, yeast, insect, and mammalian cells (Bos, de Bruin, et al. 2003; Rossi et al. 2010; Eldering et al. 1992). However, only eukaryotic expression systems demonstrate the ability to properly fold and post-translationally modify C1INH, ensuring protease inhibition rates comparable to pdC1INH. The choice of expression system significantly impacts protein yield, stability, glycosylation patterns, and inhibitory function.

Attempts have been made to express rC1INH in *E. coli* due to its rapid growth and cost-effectiveness. However, bacterial systems lack the necessary post-translational modification machinery, which is crucial for C1INH's stability and activity, as mentioned above. Consequently, rC1INH produced in *E.coli* often results in misfolded proteins with reduced or absent functional activity (Lamark et al. 2001). However, rC1INH produced in an *E. coli* strain, such as AD494, enabling the formation of disulfide bonds, appeared to be active,

suggesting that other than disulfide bonds, no post-translational modifications are needed to express C1INH (Lamark et al. 2001).

Yeast systems, such as *Pichia pastoris (P. pastoris)*, have been explored for rC1INH production. While yeast can perform some post-translational modifications, their glycosylation patterns differ from those in humans, potentially affecting protein function (Trimble et al. 1991). For instance, yeast-expressed rC1INH has been shown to have different glycosylation profiles compared to pdC1INH, potentially affecting its activity and half-life (Bos, de Bruin, et al. 2003).

The baculovirus-insect cell system has been utilized to express rC1INH (Wolff et al. 2001; Rossi et al. 2010). Insect cells can perform post-translational modifications more like mammalian cells, including glycosylation, although differences still exist. Research has demonstrated that truncated rC1INH lacking glycosylation produced in insect cells is properly folded and biologically active, making this system a viable option for producing functional rC1INH (Rossi et al. 2010). However, the glycosylation patterns in insect cells differ from those in humans, specifically shorter N-glycans, with little sialylation are seen compared to humans, which may influence the protein's stability and immunogenicity (Wolff et al. 2001).

Mammalian cells, such as Chinese Hamster Ovary (CHO) cells or COS-1 monkey cells, produce rC1INH with native-like post-translational modifications (Eldering, Nuijens, and Hack 1988; Zubareva et al. 2021). Studies have successfully expressed functional rC1INH in CHO cells, but not achieving

glycosylation patterns comparable to those of pdC1INH although the inhibitory activity was similar (Zubareva et al. 2021). Similarly, studies have successfully expressed functional rC1INH in COS-1 cells, but not achieving the exact glycosylation patterns due to COS-1 not being able to reproduce the exact glycosylation and/or process oligosaccharide chains (Eldering, Nuijens, and Hack 1988).

5. Introduction to Alpha-1 Antitrypsin

While extending the half-life of C1INH addresses the challenge of improving its pharmacokinetics for prophylaxis, enhancing the activity and specificity of serpin inhibitors remains an important complementary goal for improving the safety and efficacy of kallikrein inhibitors. AAT presents a promising alternative scaffold for this purpose due to its well-characterized structure and its M358R mutation, which alters its natural protease specificity and makes it a candidate for RCL-based engineering. The RCL sequence plays a critical role in determining which protease the serpin will inhibit. Therefore, engineering the RCL is a promising strategy for altering serpin specificity to inhibit different target proteases.

5.1. Structural Features of AAT

AAT is a 394 residue 52 kDa glycoprotein encoded by the *SERPINA1* gene (Brantly, Nukiwa, and Crystal 1988; Carrell et al. 1982). AAT is the most abundant serpin in human plasma, circulating at a concentration of 20-53 μmol/L

(Crystal 1989). It is primarily synthesized in hepatocytes and secreted into the bloodstream, where it plays a crucial role in serine protease regulation.

The primary function of AAT is to inhibit neutrophil elastase (NE) (k_2 6.5 $x10^7$ $M^{-1}s^{-1}$), a serine protease responsible for degrading extracellular matrix components such as elastin, collagen, and fibronectin (McCarthy, Reeves, and McElvaney 2016; Janciauskiene et al. 2018; Scott et al. 1986). AAT also inhibits other proteases such has proteinase 3 (k_2 8.1 $x10^6$ $M^{-1}s^{-1}$) and cathepsin G (k_2 4.1 $x10^5$ $M^{-1}s^{-1}$) (Janciauskiene et al. 2018). NE is released by activated neutrophils during inflammation and plays a role in host defense, but excessive NE activity leads to lung tissue damage (Janciauskiene et al. 2018). AAT maintains homeostasis by neutralizing NE before it can cause proteolytic injury, particularly in the alveolar space. However, mutations in the *SERPINA1* gene can lead to AATD due to intracellular polymerization and retention within hepatocytes, which results in unregulated NE activity and contributes to chronic obstructive pulmonary disease (COPD) and emphysema (Wells et al. 2019; Abboud, Ford, and Chapman 2005).

Beyond its role in elastase inhibition, AAT exhibits broader anti-inflammatory and immunomodulatory functions, independent of its protease inhibitory activity. For example, AAT has been shown to directly interact with pro-inflammatory cytokines and their receptors, such as by binding to interleukin-8 and TNF-α receptors inhibiting their actions and leading to reduced cytokine release (Song 2018). AAT contributes to the reduction of oxidative stress by

inhibiting the activity of leukotriene B4 (LTB4), a potent chemoattractant involved in neutrophil activation (Song 2018). By binding to LTB4, AAT prevents neutrophil infiltration and the subsequent release of reactive oxygen species, thereby mitigating oxidative stress and tissue damage (O'Dwyer et al. 2015). Moreover, AAT possesses anti-apoptotic properties that are crucial in protecting tissues from injury during inflammatory responses. It can directly inhibit active caspases, such as caspase-1 and caspase-3, to prevent apoptosis (Petrache et al. 2006; Toldo et al. 2011). Studies have demonstrated that both native and oxidized forms of AAT are effective in preventing acute liver injury by inhibiting caspases, thereby reducing apoptosis in liver cells (Jedicke et al. 2014).

AAT is highly susceptible to oxidation, which can contribute to COPD and emphysema even in the absence of genetic mutations (Li et al. 2009; Taggart et al. 2000). The AAT protein contains nine methionine residues, two of which are located in the RCL, M358 (P1) and M351 (near the hinge region of the RCL) (Janciauskiene et al. 2018; Scott and Sheffield 2020). Oxidation of these residues results in their conversion to methionine sulfoxide, which significantly impairs AAT function. Specifically, oxidation at M358 disrupts the formation of the AAT-protease complex, effectively diminishing or abolishing AAT's inhibitory activity. However, this modification does not interfere with the initial interaction between AAT and the target protease (Janciauskiene et al. 2018; Rosenberg et al. 1984). Another residue of structural and functional importance is C232, the only cysteine in AAT. (Janciauskiene et al. 2018). Due to its positively charged local

environment, this cysteine is highly reactive and prone to oxidation, making it particularly susceptible to crosslinking with other cysteine residues. Such modifications can contribute to protein aggregation and altered AAT function (Scott and Sheffield 2020; Janciauskiene et al. 2018).

5.2. Mutational Studies Done on AAT M358R

Given AAT's high plasma stability and well characterized inhibitory mechanism, AAT serves as an attractive scaffold for rational engineering to enhance specificity for target proteases involved in disease pathways. Given that the RCL sequence dictates target specificity, replacing or modifying the RCL has been an effective strategy to reprogram AAT's inhibitory profile for therapeutic applications.

One well-characterized variant of AAT which features a single amino acid substitution in the RCL at M358R (AAT M358R; also known as AAT 'Pittsburgh') alters its specificity of NE (decreasing to k_2 2.2 x10^3 $M^{-1}s^{-1}$) (Lewis et al. 1978; Travis et al. 1986). This mutation enables AAT to act as a potent thrombin inhibitor, increasing from k_2 48 $M^{-1}s^{-1}$ to 3.1 x10^5 $M^{-1}s^{-1}$, and effectively regulating other coagulation cascade proteases, including FXIIa (k_2 2.4 x10^4 $M^{-1}s^{-1}$), FXIa (k_2 5.1 x10^5 $M^{-1}s^{-1}$), and Pka (k_2 8.9 x10^4 $M^{-1}s^{-1}$) (Scott et al. 1986; Travis et al. 1986).

Several research laboratories have attempted to alter the RCL residues of AAT M358R to increase activities or alter specificities (Izaguirre and Olson 2006; Scott and Sheffield 2020; Izaguirre, Rezaie, and Olson 2009; Polderdijk et al. 2017; de Maat, Sanrattana, et al. 2019). These studies have explored changes to

RCL sequences to enhance inhibition against Pka. For example, de Maat et al., aimed to engineer AAT M358R variants with enhanced specificity for contact system proteases, Pka and FXIIa, while minimizing off-target effects on thrombin and activated protein C (aPC). The authors modified RCL of AAT M358R to create SMTR/S and SLLR/S, followed by a P1' substitution (Ser to Val) to generate SMTR/V and SLLR/V. Both SMTR/V and SLLR/V are superior to C1INH in reducing BK production in plasma as they have increased specificity towards Pka by 3- and 5-fold, respectively (de Maat, Sanrattana, et al. 2019). Another example is seen in Schapira et al., where researchers engineered an AAT M358R variant by introducing a mutation at position 357, replacing the native residue with alanine to mimic C1INH P2-P1 (AR). *In vitro* assays demonstrated that AR exhibited superior inhibitory activity against Pka compared to C1INH by 21.2 fold (Schapira et al. 1987). A final example is seen by Sulikowski et al., where researchers engineered variants of AAT M358R to selectively inhibit Pka. By altering the P3-P2-P1 residues from isoleucine-proline-methionine to leucine-glycine-arginine (LGR) and proline-phenylalanine-arginine (PFR), they aimed to mimic the specificity of C1INH toward Pka. Although LGR increased selectivity towards Pka compared to C1INH by ~8-fold, it was not specific. However, PFR variant exhibited enhanced reactivity and specificity with Pka by ~4-fold compared to C1INH (Sulikowski, Bauer, and Patston 2002).

5.3. Implementing Phage Display with AAT M358R

One approach to implementing an effective strategy for achieving productive RCL mutation involves generating a large library of serpins

hypervariable at the desired RCL positions and functionally screening it to identify candidates with the desired specificity via phage display (de Souza et al. 2018). Phage display is a high-throughput screening technique in which engineered proteins are displayed on the surface of bacteriophages, allowing researchers to screen for serpin binding and inhibition against target proteases (Vodnik et al. 2011). This approach is particularly effective for serpin engineering, as it enables the selection of variants with optimized inhibitory kinetics. If fully degenerate codons are used to randomize RCL positions, probing the library at sufficient multiplicity to avoid missing promising candidates can only be done if the number of hypervariable positions is limited to at most 5 (de Souza et al. 2018). Given the RCL's integral role in serpin-protease interactions, it remains the primary target for specificity engineering through phage display-based mutagenesis.

Two commonly used bacteriophage platforms for phage display are the T7 and M13 phage systems, each with distinct advantages (Wang et al. 2023; Deng et al. 2018). M13 phage display is a filamentous bacteriophage that infects *E. coli* via the F-pilus. Its major coat protein (pVIII) and minor coat proteins (pIII, pVI, pVII, pIX) are commonly used for displaying foreign peptides and proteins (Wang et al. 2023). A major advantage of M13 is that it allows for multivalent display which is particularly useful for affinity selection due to strong protein-protein interactions (Wang et al. 2023). However, a significant limitation is that M13 is less suited for displaying large proteins like full-length serpins, as the phage's secretion-based assembly process can lead to protein misfolding (Wang et al.

2023). T7 phage display, in contrast, is a lytic phage that infects *E. coli* via direct genome injection and displays proteins on the T7 capsid protein 10B at the C-terminal end (Deng et al. 2018). This system is ideal for larger proteins like serpins, as protein folding occurs in the cytoplasm, reducing misfolding issues (Deng et al. 2018). Unlike M13, T7 phage does not require secretion, which helps preserve the functional integrity of displayed proteins. However, a drawback is that the number of fusion proteins displayed per phage particle can vary, affecting the sensitivity and consistency of biopanning assays (Ebrahimizadeh and Rajabibazl 2014).

Several studies have successfully utilized phage display for serpin engineering, demonstrating its potential to improve specificity and inhibitory activity. For example, a study by Bhakta et al., aimed to enhance the specificity of AAT M358R for inhibiting FXIa while minimizing off-target inhibition of thrombin. To achieve this, phage display technology was employed to engineer AAT variants with modified RCLs, focusing on P13-P8, P7-P3, and P2-P3′ positions to enhance inhibitory activity toward FXIa. Recombinant expression and kinetic analysis of P7-P3 (CLEVE) demonstrated a 2.1-fold decrease in FXIa inhibition compared to unmodified AAT M358R but a 48-fold reduction in thrombin inhibition, resulting in a 23-fold increase in selectivity for FXIa over thrombin. Whereas P2-P3′ (PRSTE) demonstrated a 34-fold increases in selectivity for FXIa over thrombin. This study highlights the effectiveness of phage display technology in serpin engineering (Bhakta et al. 2021). Another study is seen by

Scott et al., where researchers aimed to increase thrombin inhibition of AAT M358R via phage display. After five rounds of biopanning, DITMA and AAFVS emerged as the top-performing variants, showing a 2.1-fold increase in thrombin inhibition rates compared to the original FLEAI sequence in AAT M358R (Scott et al. 2014).

5.4. Implementing RCL Loop Exchange with AAT

Loop exchange, also known as RCL swapping, is a targeted engineering strategy in which the RCL from one serpin is transplanted into another. Because the RCL dictates a serpin's protease specificity, exchanging this region allows for precise reprogramming of inhibitory profiles. This approach leverages the stability and structural integrity of a well characterized serpin scaffold while introducing novel specificity derived from another serpin with desired protease inhibition characteristics.

For example, Hopkins et al., successfully substituted residues from the RCL of antithrombin into AAT M358R scaffold, testing these chimeras against thrombin, activated FX (FXa), and aPC (Hopkins, Pike, and Stone 2000). The study showed substantial variations in protease inhibition rates based on the loop substitutions. Specifically, for FXa and thrombin, the fastest and slowest variants exhibited significant differences in their association rates (5.5- and 88-fold, respectively; LS4-3' and LS7-2', and LS7-3/P1R and LS3-3', respectively), reflecting the profound impact of RCL sequence on specificity. Moreover, one variant (LS1) demonstrated exceptionally high specificity for aPC (12,500-fold), with a remarkable difference in the association rate compared to thrombin and

FXa (Hopkins, Pike, and Stone 2000). By leveraging the native aPC-specificity inherent to antithrombin's RCL, the engineered AAT variant retained the stability benefits of AAT while effectively redirecting its inhibitory activity toward a therapeutically relevant target (Hopkins, Pike, and Stone 2000).

Another example is seen in Filion et al., where the researchers sought to enhance the thrombin inhibitory activity of AAT by substituting it with different segments from HCII (Filion et al. 2004). The findings revealed that substituting the P16-P3' region of AAT with the corresponding HCII sequence increased its antithrombin activity to levels comparable to heparin-free HCII. Notably, replacing only the P2'-P3' dipeptide resulted in an even higher enhancement of thrombin inhibition. However, the presence of an arginine residue at the P1 position was critical for maximal inhibitory activity; variants lacking P1 Arg exhibited less than 2% of the thrombin inhibition rate observed in the AAT M358R variant (Filion et al. 2004).

A final example is seen in Chaillan-Huntington et al., where the researchers investigated the role of specific regions within the RCL of serpins in determining their inhibitory efficacy (Chaillan-Huntington et al. 1997). They focused on the P12-P2 segment of the RCL, encompassing residues P12 to P7 and P6 to P2, to assess their individual contributions to serpin functionality against trypsin and NE. The findings revealed that both the P12-P7 and P6-P2 substitutions adversely affected the inhibition kinetics, as evidenced by altered rates and stoichiometries of inhibition for both proteases. Notably, the P12-P2

variant exhibited a complete loss of inhibitory function against elastase and retained only minimal activity against trypsin, indicating that the P12-P7 and P6-P2 exhibited nonadditive/cooperativity effects (Chaillan-Huntington et al. 1997).

5.5. AAT Expressed in Multiple Systems

Like C1INH, recombinant AAT M358R has also been successfully produced using many platforms including bacteria, yeast, mammalian and insect cells.

AAT M358R can be expressed at high levels in *E. coli*, often forming inclusion bodies that require refolding (Krishnan et al. 2017). However, *E. coli* lacks the machinery for N-glycosylation, so AAT M358R is produced unglycosylated in bacteria. Native human AAT has three N-linked glycosylation sites, but the bacterially expressed protein has none, which results in a lower apparent molecular weight (~46 kDa vs ~51 kDa for plasma AAT) (Sarkar and Wintrode 2011; Krishnan et al. 2017; Bianchera et al. 2022). Despite lacking glycans, bacterially produced AAT M358R can fold into an active conformation. Absence of glycosylation does not eliminate inhibitory function *in vitro*. When properly refolded, *E. coli*-derived AAT M358R is functionally active. Studies have shown that recombinant AAT produced in bacteria can achieve high elastase-inhibitory activity; the AAT M358R variant retains its ability to form stable complexes with target proteases like thrombin (Bianchera et al. 2022; Scott et al. 2014).

In contrast, *P. pastoris*, for example, can secrete AAT into the culture medium, simplifying recovery. Yields in yeast are moderate and can surpass those in bacteria for correctly folded protein (Arjmand et al. 2011). Yeasts perform N-glycosylation, but the glycan structures differ from human ones. Recombinant AAT from *P. pastoris* is glycosylated with high-mannose type N-glycans, lacking the terminal sialic acids and galactose found in human AAT. As a result, yeast AAT runs as a broader, heavier band on sodium dodecyl sulfate polyacrylamide gel electrophoresis (Arjmand et al. 2011). The presence of N-glycans in yeast AAT does not prevent inhibitory function. In *P. pastoris*, the secreted recombinant AAT could form complexes with and inhibit NE comparably to the native protein (Arjmand et al. 2011).

Mammalian expression systems can produce AAT with high fidelity and increasingly high yields (Rocamora et al. 2024). Mammalian systems currently offer the highest yield of properly folded and glycosylated AAT, but the trade-off is longer development time. Mammalian cells provide authentic human-like post-translational modifications for AAT M358R. For example, CHO-expressed AAT is glycosylated at the same sites and with similar structures as plasma-derived AAT (pdAAT) (Arjmand et al. 2011). There is evidence that matching the native glycosylation improves AAT's overall efficacy. One study demonstrated that a glycoengineered CHO-derived AAT was biochemically and functionally equivalent to pdAAT (Rocamora et al. 2024). A study that stood out was by Gierczak et al., where researchers explored the functional implications of expressing the AAT

M358R variant as a membrane-tethered serpin in mammalian cells (Gierczak et al. 2011). They created fusion proteins by anchoring AAT M358R to the cell membrane using non-cleavable N-terminal signal sequences. Functional assays revealed that the membrane-bound AAT M358R successfully formed stable, inhibitory complexes with thrombin on the cell surface, but slightly reducing the kinetics of thrombin inhibition compared to soluble AAT M358R (Gierczak et al. 2011). The study demonstrated for the first time that serpins like AAT could retain functional activity even when immobilized on cellular membranes.

Lastly, insect cell expression can produce moderate yields of AAT; generally lower than yeast or CHO (Castilho et al. 2014). Although insect cells provide eukaryotic folding and some post-translational processing, their N-glycosylation pattern is different from mammals (hang et al. 2003). However, there is limited evidence to show that these modifications generally do not impair the *in vitro* inhibitory function of AAT.

6. Rationale, Hypothesis and Objectives

The rationale behind this research stems from the limitations of current therapeutic approaches for HAE, particularly concerning specificity and pharmacokinetic profiles of existing treatments. Although rC1INH effectively inhibits Pka, its clinical utility is restricted by a relatively short circulatory half-life. Similarly, AAT, despite its therapeutic potential due to serpin-protease inhibition, lacks sufficient specificity for Pka, limiting its direct therapeutic application for HAE. Therefore, there is an unmet need to develop modified versions of these

serpins with improved pharmacokinetics and enhanced target specificity, addressing existing therapeutic limitations and improving patient outcomes.

This research tests several hypotheses aimed at overcoming these therapeutic challenges: (i) a non-glycosylated, truncated rC1INH-albumin fusion protein will inhibit Pka as effectively as unfused rC1INH; (ii) fusing rC1INH with albumin will prolong its circulatory half-life in mice; (iii) specific AAT M358R variants for Pka can be identified within the sequence space of hypervariable positions in the RCL P7-P3'; and (iv) chimeric AAT M358R constructs incorporating C1INH RCL regions may exhibit enhanced specificity for Pka within this sequence space.

To systematically test these hypotheses, the following objectives were established: first, design and produce a non-glycosylated, truncated rC1INH-albumin fusion protein, then evaluate its inhibitory efficiency against Pka relative to unfused rC1INH. Second, investigate the pharmacokinetic properties of the rC1INH-albumin fusion in a mouse model, determining its potential to prolong circulatory half-life. Third, utilize phage display technology to identify optimized AAT M358R variants with increased selectivity for Pka from a diverse sequence space covering the hypervariable RCL region. Lastly, generate and characterize chimeric AAT M358R proteins containing strategic RCL substitutions from C1INH, assessing their specificity enhancements toward Pka. By achieving these objectives, this research aims to provide novel insights into serpin engineering, ultimately contributing to improved therapeutic strategies for treating HAE.

CHAPTER 2

Prolonging the circulatory half-life of C1 esterase inhibitor via albumin fusion

Sangavi Sivananthan[1], Varsha Bhakta[1,2], Negin Chaechi Tehrani[1], William P. Sheffield[1,2,*]

[1]Department of Pathology and Molecular Medicine, McMaster University, Hamilton, Ontario, Canada. [2]Canadian Blood Services, Innovation and Portfolio Management, Hamilton, Ontario, Canada

*Corresponding author; e-mail sheffiel@mcmaster.ca

Sivananthan, S., Bhakta, V., Chaechi Tehrani, N., & Sheffield, W. P. (2024). Prolonging the circulatory half-life of C1 esterase inhibitor via albumin fusion. PloS one, 19(10), e0305719. https://doi.org/10.1371/journal.pone.0305719

This chapter addresses the clinical limitation of short half-life in current C1INH therapies. Recombinant albumin fusion is explored as a strategy to enhance the half-life of C1INH by leveraging the FcRn-mediated recycling pathway. Chapter 2 presents the generation, purification, and inhibitory activity toward Pka alongside *in vivo* pharmacokinetics in mice. The findings provide insight into the trade-offs

between structural fusion and functional retention when extending serpin half-life through C-terminal modifications.

1. Abstract

Hereditary Angioedema (HAE) is an autosomal dominant disease characterized by episodic swelling, arising from genetic deficiency in C1-esterase inhibitor (C1INH), a regulator of several proteases including activated Plasma kallikrein (Pka). Many existing C1INH treatments exhibit short circulatory half-lives, precluding prophylactic use. Hexahistidine-tagged truncated C1INH (trC1INH lacking residues 1-97) with Mutated N-linked Glycosylation Sites N216Q/N231Q/N330Q (H_6-trC1INH(MGS)), its murine serum albumin (MSA) fusion variant (H_6-trC1INH(MGS)-MSA), and H_6-MSA were expressed in *Pichia pastoris* and purified via nickel-chelate chromatography. Following intravenous injection in mice, the mean terminal half-life of H_6-trC1INH(MGS)-MSA was significantly increased versus that of H_6-trC1INH(MGS), by 3-fold, while remaining ~35% less than that of H_6-MSA. The extended half-life was achieved with minimal, but significant, reduction in the mean second order rate constant of Pka inhibition of H_6-trC1INH(MGS)-MSA by 33% relative to that of H_6-trC1INH(MGS). Our results validate albumin fusion as a viable strategy for half-life extension of a natural inhibitor and suggest that H_6-trC1INH(MGS)-MSA is worthy of investigation in a murine model of HAE.

2. Introduction

Hereditary Angioedema (HAE) is an autosomal dominant disease characterized by an acute episodic swelling in the stomach, face, limbs, and throat; if the airways are involved HAE attacks can be life-threatening [1, 2]. There are two subtypes of HAE. Type 1 is characterized by both reduced C1 inhibitor (C1INH) antigen and activity levels, while type 2 is marked by normal antigenic but reduced activity C1INH levels. Both stem from mutations in *SERPING1* [3]. C1INH is a glycoprotein serine protease inhibitor belonging to the serpin superfamily [4, 5]. The multifaceted activities of C1INH include roles in vascular permeability, anti-inflammatory function, coagulation, and fibrinolysis [6-9]

C1INH is the largest serpin (110kDa) and is hyperglycosylated with 10 sites of N-glycosylation and 24 sites of O-glycosylation [10, 11]. Most of these sites lie in a 100 amino acid N-terminal extension not found in other members of the serpin superfamily [5], with the exception of 3 N-linked glycosylation sites, N216, N231, and N330 [11] (numbered according to mature protein sequence). Several research groups have demonstrated that recombinant C1INH retains wild-type-like inhibitory activity when its N-terminal 97 residues were deleted [12-14], but, at least in the baculovirus/insect cell expression system, combining this truncation with the triple mutation N216Q/N231Q/N330Q to eliminate glycosylation abrogated detectable expression [13].

C1INH plays a pivotal role in inhibiting various proteases, including C1s in the complement system and plasma kallikrein (Pka) [15]. Following cleavage,

Pka catalyzes the cleavage of high molecular weight kininogen, liberating bradykinin. Bradykinin controls fluid balance between the circulation and tissues via the B2 receptor, whose binding results in endothelial cell contraction, vasodilation, and nitric oxide production [16]. Bradykinin levels correlate with HAE attack severity and are higher in affected limbs than unaffected limbs in the same HAE patients during attacks [17, 18]. These observations, combined with the clinical efficacy of replacement therapy with either C1INH concentrates or drugs inhibiting Pka, support a causative role for unregulated bradykinin activity in HAE [19-22].

Over the last decade, the clinical management of HAE has expanded from treating attacks acutely to preventing attacks via prophylactic treatment [23]. Fewer drugs are approved for HAE prophylaxis than for acute treatment; for example, the only existing recombinant C1INH in clinical use, Conestat Alfa, is unsuitable for prophylactic use due to its short half-life [24]. Theoretically, prophylactic coverage for HAE patients would be easier to achieve with extended half-life (EHL) products, as has been demonstrated with protein drugs used to treat patients with hemophilia [25]. One approach to an EHL for HAE treatment would be a C1INH-albumin fusion protein. Fusing a therapeutic protein to albumin typically extends its plasma residency time, becoming more like that of albumin; plasma-derived human serum albumin (HSA) exhibits a plasma half-life of 19 days [26]. We hypothesized that albumin fusion would not impair C1INH-mediated inhibition of Pka and would extend its circulatory half-life *in vivo*. To

facilitate an EHL strategy for C1INH, we simplified C1INH by removal of its N-terminal 97 amino acids, mutation of its serpin domain N-linked glycosylation sites and addition of an N-terminal hexahistidine tag to facilitate purification. We report that the inhibitory properties of simplified, truncated, non-glycosylated C1INH were largely unaffected by genetic fusion to mouse serum albumin (MSA) and that this fusion protein acquired an extended plasma residency time in mice *in vivo* approaching that of hexahistidine-tagged recombinant MSA.

3. Methods

3.1. Expression and Purification of H_6-trC1INH(MGS), H_6-MSA, and H_6-trC1INH(MGS)-MSA Fusion Protein in P. pastoris

Clone Manager 10 (Sci Ed Software LLC) was used for design and oligonucleotides, or other synthetic DNA sequences (gBlock™) were purchased from Integrated DNA Technologies (IDT). All restriction and DNA modification enzymes were bought from Thermo Fisher Scientific (Waltham, Massachusetts, United States) (XhoI, catalogue number (cat. #) FD0694, EcoRI, cat. # FD0274, AccIII, cat. # FD0534). A hexahistidine-tagged truncated $C1INH_{98-478}$ with Mutated Glycosylation Sites (MGS; N216Q/N231Q/N330Q) (H_6-trC1INH(MGS)) was designed and the resulting 1192 base pair (bp) H_6-C1INH gBlock™ product was restricted with XhoI and EcoRI and inserted between these sites in pPICZ9ssamp [27, 28] to yield pPICZ9ssH_6-trC1INH(MGS). An MSA cDNA was modified for expression via PCR, as directed by sense oligonucleotide 5'-TCTCTCGAGA AAAGACATCA CCATCACCAT CACGAAGCAC ACAAGAGTGA

GATCGCC-3' and antisense oligonucleotide 5'-CCTAGGGAAT TCCTAGGCTA AGGCGTCTTT GCATCTAGTG AC-3' and catalyzed by heat-stable polymerase Phusion under conditions directed by its manufacturer (Thermo Fisher Scientific, cat. # F530L). The resulting amplicon was restricted with XhoI and EcoRI and inserted between these sites in pPICZ9ssamp to form pPICZ9ssH_6-MSA. Fusion construct H_6-trC1INH(MGS)-MSA, was assembled by ligating a 1206 bp H_6-trC1INH(MGS)-$(G_4S)_3$ gBlock^{TM} product restricted with XhoI and AccIII, and a 1797 bp $(G_4S)_3$-MSA gBlock^{TM} product restricted with AccIII and EcoRI. These fragments were then inserted between the Xho1 and EcoRI sites of pPICZ9ssamp vector to yield pPICZ9ssH_6-trC1INH(MGS)-MSA. All plasmid candidates were verified by Sanger dideoxy sequencing of the relevant open reading frames by the McMaster University Genomics Facility. Purified plasmid DNA was linearized with appropriate restriction enzymes and were used to transform *Pichia pastoris (P. pastoris)* strain X-33 to Zeocin resistance. The transformed cell lines were cultured, induced with methanol, and the secreted proteins H_6-trC1INH(MGS), H_6-trC1INH(MGS)-MSA, and H_6-MSA were purified from conditioned media using nickel-chelate affinity chromatography, as previously described [29].

3.2. Protease Inhibition Assays with H_6-trC1INH(MGS) and H_6-trC1INH(MGS)-MSA

Second-order rate constants (k_2) and stoichiometries of inhibition (SI) were determined using chromogenic assays as previously described [30]. Pka was purchased from Enzyme Research Laboratories (South Bend, IN, USA) (cat. # 1303) and complement component 1, s subcomponent (C1s), activated, two chain form, was bought from Sigma Aldrich (Oakville, ON, Canada) (cat. # 204879-250UG). The velocity of amidolysis of chromogenic substrate S2302 (DiaPharma, West Chester, OH, USA) (cat.# 82034039) by Pka or of chromogenic substrate Pefachrome™-C1E (CH_3CO- benzyloxycarbonyl Lys-Gly-Arg-para-nitroanilide monoacetate) (DiaPharma) (cat. # DPG08703) by C1s was assessed in 96-well flat-bottom microtiter plates (Immulon IV, Thermo Fisher Scientific) (cat. # 1424563) at 37°C in PPNE buffer (20 mM sodium phosphate pH 7.4, 0.1% (w/vol) polyethylene glycol 8000, 100 mM sodium chloride, and 0.1 mM disodium ethylenediaminetetraacetic acid). The measurements were performed at a wavelength of 405 nm using an Elx808 Absorbance Microplate Reader (Biotek, Winooski, VT, USA). For the determination of k_2, reactions included 10 nM Pka (Enzyme Research, South Bend, USA) or C1s (Millipore Sigma, Massachusetts, USA) and 200 nM pdC1INH (Athens Research and Technology, Athens, Georgia, USA) (cat. # 16-16-031509) or C1INH recombinant variants, incubated at 30-second intervals and halted with 100 μM S2302 or 400 μM Pefachrome™-C1E chromogenic substrate. To ascertain the SI, reactions

included 10 nM Pka and 10-50 nM pdC1INH/C1INH recombinant variants, incubated for 2-hours and stopped with 100 µM S2302.

3.3. Electrophoretic Analysis of H_6-trC1INH(MGS) and Pka Interaction

The electrophoretic profile of the interaction between pdC1INH/H_6-trC1INH(MGS) with Pka was visualized on 10% (w/vol) sodium dodecyl sulfate (SDS)-polyacrylamide gels (SDS-PAGE, under reducing conditions. Reactions involved a final concentration of 5 µM pdC1INH/H_6-trC1INH(MGS) and 1 µM Pka in PPNE buffer and were conducted at 37°C for 5-minutes. Reactions were then terminated by adding 1/3 the reaction volume of concentrated 4x SDS-PAGE sample buffer, and samples containing the entire reaction volume were subjected to electrophoresis. Gels were stained with Coomassie Brilliant Blue as described previously [31]. Polyacrylamide gels were imaged by scanning using a model XR GelDoc system (Bio-Rad Laboratories, Mississauga, ON, Canada) and nitrocellulose immunoblots prepared as described [30] were imaged by scanning using a model Azure 280 system (Azure Biosystems, CA, USA), generating Tagged Image File (TIF) format outputs.

3.4. Detection of C1INH Binding to Kallikrein by Modified ELISA

An enzyme-linked immunosorbent assay (ELISA) was employed to detect H_6-trC1INH(MGS)-MSA: Pka complexes, as described, with modifications [31]. In 96-well flat-bottom microtiter plates, 250 ng of Pka (in 0.1 ml of PBS) was coated

overnight. Subsequently, unbound Pka was removed, and the wells were washed with PBS-T (136 mM sodium chloride, 2.7 mM potassium chloride, 10 mM disodium phosphate, 1.8 mM monopotassium phosphate, and 0.1% Tween-20). H_6-trC1INH(MGS)-MSA (1 µg or 5 µg) or pdC1INH (500 ng or 1 µg) were diluted in 1% bovine serum albumin (BSA) in PBS-T and incubated in the Pka-coated 96-well flat bottom microtiter plates for 1-hour. Wells were subsequently washed with modified PBS-T buffers containing 1 M sodium chloride and 1% Tween-20 for the remaining washing steps. C1INH-related protein binding to immobilized Pka was detected with 100 ng per well of goat anti-human C1INH antibody conjugated to horseradish peroxidase (HRP) (Affinity Biologics, Ancaster, Canada) (cat. # GACINH-HRP); colour generation was monitored using 3,3',5,5'-Tetramethylbenzidine (TMB) substrate solution (Thermo Fisher Scientific) (cat. # 34021), 0.1 ml/well, and was stopped by adding an equal volume of 2M sulphuric acid after 5 minutes, prior to quantification using an Elx808 Absorbance Microplate Reader.

3.5. In vivo Clearance and Protein Detection in Mice

All *in vivo* experiments in this study used CD1 mice (Charles River, Wilmington, MA, USA) and were approved by the Animal Research Ethics Board of the Faculty of Health Sciences, McMaster University, via Animal Utilization Protocol 20-02-06. The ARRIVE guidelines (https://arriveguidelines.org/arrive-guidelines) were followed (specifically the ARRIVE Essential 10). Mice were

typically 1-2 months old. All mice were acclimatized to their surroundings in the Central Animal Facility of the Faculty of Health Sciences of McMaster University for at least one week after arrival. Mice were always maintained under anesthesia during the procedure, using 3% isoflurane. For clearance studies, mice were intravenously injected with either 50 µg H_6-trC1INH(MGS), 50 µg H_6-MSA, or 100 µg H_6-trC1INH(MGS)-MSA, each in 0.2 ml of saline solution. The dose was selected in order to administer equimolar doses of the three proteins to be compared, allowing for the greater molecular weight of H_6-trC1INH(MGS)-MSA than the other two proteins, to ensure that 1% of the initial dose could be detected in plasma samples using ELISA, and to not exceed ~20% of the plasma concentration of C1INH in wild-type mice, expected to be ~0.25 mg/ml [6]. Serial blood samples were collected from the tail over time, and recombinant proteins remaining in plasma derived from these samples were quantified by ELISA with minor modifications [31]. Groups of six mice comprising three male and three female mice were used in all cases, with sample size selection being based on results of previous studies [29, 32]. Three groups were initially compared, those receiving H_6-trC1INH(MGS) or H_6-trC1INH(MGS)-MSA or H_6-MSA, the latter serving as a control. Subsequently two additional groups of six mice each receiving H_6-trC1INH(MGS) or H_6-trC1INH(MGS)-MSA were compared. A total of 30 mice were used in this study, weighing 31 ± 4 g (mean ± SD). Neither randomization nor blinding were employed. All animals were included in the analysis; there were no exclusions. After the final blood sample was drawn, mice

were euthanized by cervical dislocation under anesthetic cover. To capture H_6-trC1INH(MGS) and H_6-trC1INH(MGS)-MSA, 0.1 ml of 1 µg/ml goat anti-human C1INH (Affinity Biologics, Ancaster, ON, Canada) (cat. # GACINH) was coated, per well, on a 96-well flat-bottom microtiter plate, overnight. Bound C1INH proteins were detected using 0.3 µg/ml goat anti-human C1INH HRP-conjugated antibody in 1% BSA in PBS, with colour detection as described above. Plasma-derived C1INH was used to construct a standard curve linear between 0.5 and 20 ng/ml. For detecting H_6-MSA, plasma samples diluted 1:1 with PBS were incubated with 500ng of Biotin-SP-conjugated affinity-purified Rabbit Anti-His tag antibody (Jackson ImmunoResearch Laboratories, PA, USA) (cat. # 300-065-240) for 1-hour before transfer to streptavidin-coated plates (Thermo Fisher Scientific) (cat. # 15120). Bound antibody-MSA complexes were detected with 0.25 µg/ml HRP-conjugated goat polyclonal anti-MSA antibodies (Affinity Biologicals) (cat. # AB19195) in 1% BSA in PBS, with colour generation as described above. Purified H_6-trC1INH(MGS)-MSA was used to construct a standard curve linear between 0.5 ng/ml and 20 ng/ml. Terminal half-lives were determined using a two-compartment model and curve-stripping as previously described [33]. The area under the curve was calculated via GraphPad Prism version 9.0 (Insight Partners, New York, NY, USA).

3.6. Statistical Analysis and Significance Testing

Data are presented as the mean ± the standard deviation (SD). Statistical analysis was conducted using GraphPad Prism version 9.0. A p-value of < 0.05 was indicative of statistical significance. For multiple comparisons, data were assessed using One-way ANOVA with post-tests.

4. Results

4.1. Novel Recombinant Proteins

In this study, three recombinant proteins were designed, expressed, and purified, using a *P. pastoris* expression system, as previously described. In each case, recombinant minigenes were under the control of the methanol-inducible alcohol oxidase 1 (AOX1) promoter, and recombinant proteins were secreted into the conditioned media by the *Saccharomyces cerevisiae* yeast prepro-α factor 80 amino acid cleavable prepro signal sequence, terminating in the Kex2/Ste13 protease cleavage site (SLEKR↓EA) [34]. Each protein thus shared the Glu-Ala dipeptide followed by a hexahistidine tag on its N-terminus; their predicted primary sequences are shown in S1 Appendix. Fig. 1A shows the three recombinant proteins H_6-trC1INH(MGS), H_6-trC1INH(MGS)-MSA, and H_6-MSA, with reference to full-length plasma-derived C1INH (pdC1INH).

The electrophoretic profile of the recombinant proteins is shown in Fig. 1B, following nickel chelate affinity chromatography. H_6-trC1INH(MGS) was purified to homogeneity and contained a single polypeptide of 43 kDa, matching its predicted molecular weight of 43,697 Da. Similarly, H_6-trC1INH(MGS)-MSA

exhibited a single polypeptide band of approximately 110 kDa, consistent with its predicted molecular weight of 110, 315 Da. Both C1INH variant proteins reacted with antibodies specific to human C1INH and hexahistidine; in addition, H_6-trC1INH(MGS)-MSA acquired immunoreactivity with antibodies specific for MSA. H_6-MSA preparations comprised a major polypeptide of 67 kDa consistent with the predicted molecular weight of 66,713 Da, as well as minor polypeptide comprising approximately 10% of the total protein of approximately 55 kDa. Both the major and minor species reacted not only with anti-MSA antibodies on immunoblots but also with anti-hexahistidine, indicating that the latter was intact on its N-terminus but was missing C-terminal residues.

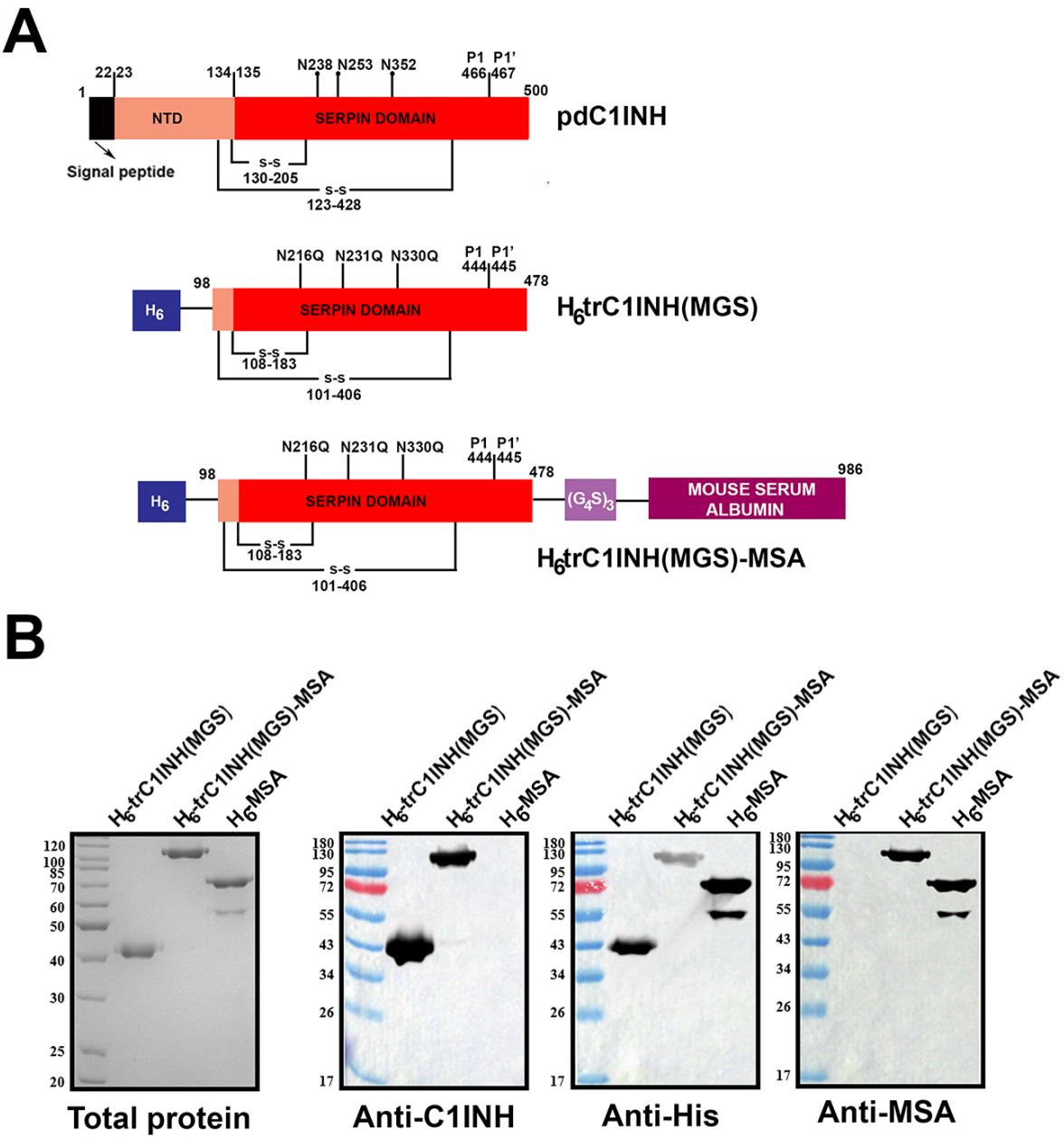

Figure 1: C1-esterase inhibitor (C1INH) recombinant proteins. A) Schematic diagram of pdC1INH and recombinant proteins. Numbers relate to C1INH mature protein except as otherwise specified. Proteins are named at right. B) Gel and immunoblot analysis of purified H_6-trC1INH(MGS), H_6-trC1INH(MGS)-MSA, and

H_6-MSA. Total protein amounts of 1 µg were electrophoresed on 10% SDS-PAGE gels that were stained with Coomassie Brilliant Blue (left) or decorated with specific antibodies identified below the panels (left centre, right centre, and right).

4.2. Characterization of Fused and Unfused Truncated, Non-glycosylated C1INH Proteins

The kinetics of protease inhibition by H_6-trC1INH(MGS) and H_6-trC1INH(MGS)-MSA were compared to that mediated by pdC1INIH, as shown in Table 1. Neither truncation, prevention of N-linked glycosylation, nor hexahistidine tagging appeared to impact inhibition of C1s, as the k_2 for C1s inhibition did not differ from pdC1INH. Adding albumin to the list of changes similarly did not impact the inhibition of C1s by H_6-trC1INH(MGS)-MSA. In contrast, small but significant reductions in mean k_2 for Pka inhibition were noted for both unfused and fused trC1INH(MGS) proteins, of 13.4% for H_6-trC1INH(MGS) and 45.2% for H_6-trC1INH(MGS)-MSA versus pdC1INH. Mean SI values were significantly increased for H_6-trC1INH(MGS) and H_6-trC1INH(MGS)-MSA compared to pdC1INH, by factors of 1.6 and 2.1, respectively, but did not differ significantly between each other. The results indicate small but significant reductions in both the rate and efficiency of inhibition for the variant recombinant C1INH proteins versus their pdC1INH counterpart.

Inhibitors of the serpin class of protease inhibitors typically form denaturation-resistant, SDS-stable complexes [35]. Inhibitory complexes between Pka and plasma-derived inhibitors were first examined by SDS-PAGE. As shown in Fig. 2A, commercial purified Pka was comprised of multiple polypeptide chains when electrophoresed under reducing conditions, including a catalytic light chain of ~37 kDa. This polypeptide chain was almost fully converted into novel, C1INH-dependent high molecular weight complexes when Pka was reacted with an excess of either pdC1INH or H_6-trC1INH(MGS), of 147 kDa or 80 kDa, respectively. In contrast, when the same reaction was carried out with Pka and excess H_6-trC1INH(MGS)-MSA (Fig. 2B), no higher molecular weight serpin-enzyme complex was formed, although the Pka catalytic light chain appeared to be consumed to a similar extent as in the reaction with H_6-trC1INH(MGS). Two new polypeptide chains were generated from H_6-trC1INH(MGS)-MSA on exposure to Pka, of ~70 kDa and ~40 kDa.

To reconcile the apparent discrepancy of a substantial k_2 for Pka inhibition with the inability to detect SDS-stable complexes between H_6-trC1INH(MGS)-MSA and Pka by SDS-PAGE, we sought independent verification of complex formation. Active Pka was immobilized on microtiter plate wells, incubated with pdC1INH or H_6-trC1INH(MGS)-MSA, washed under stringent high-salt, high detergent conditions, and captured C1INH antigenic material was detected with C1INH-specific antibodies. As shown in Fig. 2C, bound C1INH was detected when either pdC1INH or H_6-trC1INH(MGS)-MSA was reacted with immobilized

Pka, in a dose-dependent manner, although the signal was higher with pdC1INH than with H_6-trC1INH(MGS)-MSA. These results, like the k_2 findings, are suggestive of tightly bound inhibitory complex formation between Pka and H_6-trC1INH(MGS)-MSA even if the complexes are not SDS-stable.

Table 1: Pharmacokinetic characterization of activity of C1INH recombinant proteins.

Protein name	k_2 versus Pka ($X\ 10^4\ M^{-1}s^{-1}$)	k_2 versus C1s ($X\ 10^4\ M^{-1}s^{-1}$)	SI versus Pka
pdC1INH	2.3 ± 0.2***	5.7 ± 0.5	3.3 ± 0.06***^^^
H_6-trC1INH(MGS)	2.01 ± 0.07***	5 ± 0.5	5.3 ± 0.3
H_6-trC1INH(MGS)-MSA	1.3 ± 0.08	5.1 ± 0.4	6.9 ± 0.1

Results are the mean of 5 determinations (SI or k_2 for kallikrein), ± SD, or 3 determinations (k_2 for C1s). ***, $p < 0.001$ versus H_6-trC1INH(MGS)-MSA. ^^^, $p < 0.001$ versus H_6-trC1INH(MGS).

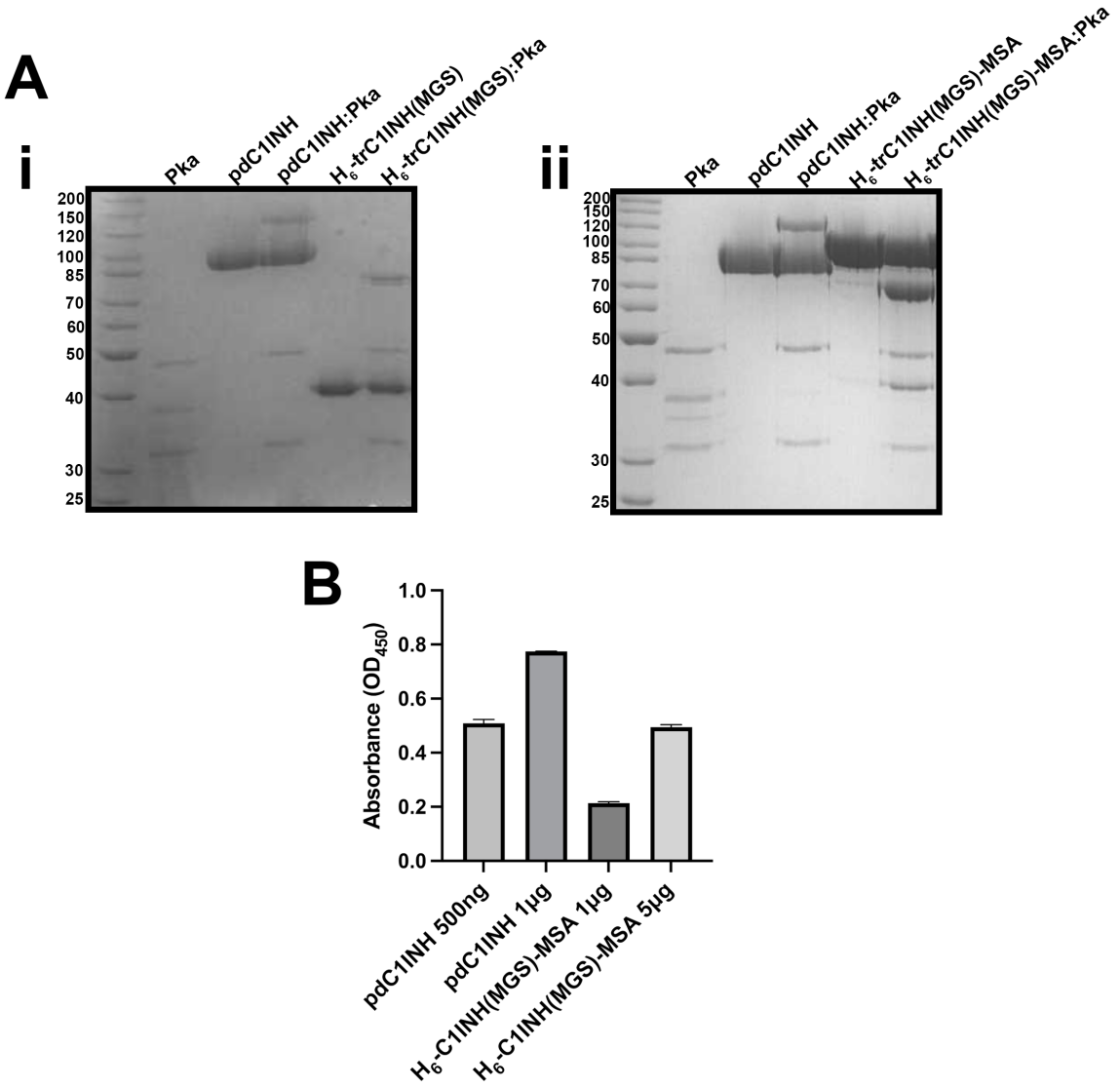

Figure 2: Complex characterization of C1INH recombinant proteins. A) i. Gel-based assays of complex formation. 10% SDS-PAGE gels are shown electrophoresed under reducing conditions and stained with Coomassie Brilliant Blue. Serpins (pdC1INH, H_6-trC1INH(MGS), or H_6-trC1INH(MGS)-MSA) were reacted with Pka at a 5:1 molar ratio for 5-minutes at 37°C. B) Graph of binding assay between pdC1INH:Pka and H_6-trC1INH(MGS)-MSA:Pka at varying ratios

(500 ng-1 µg) with PBS-T washing condition of 1M NaCl and 1% Tween-20. The mean and SD of 3 determinations is shown.

4.3. In vivo Clearance of Recombinant Proteins

H_6-trC1INH(MGS), H_6-trC1INH(MGS)-MSA, and H_6-MSA proteins were separately injected into groups of mice. The average relative recovery in serial plasma samples is shown in Fig. 3A (log-linear plot) and Fig. 3B (linear-linear plot), where the profile of H_6-trC1INH(MGS) in mice exhibited a distinct and more rapidly cleared trajectory from that of H_6-trC1INH(MGS)-MSA or H_6-MSA, within minutes of injection. After 1 hour, only 27 ± 10% of the initial dose of H_6-trC1INH(MGS) remained in the circulation, which was significantly lower than the residual levels of H_6-trC1INH(MGS)-MSA or H_6-MSA (90 ± 4% and 95 ± 3%, respectively) (Fig 3C). By 4 hours post-injection, only 2.2 ± 0.5% of the initial dose of H_6-trC1INH(MGS) remained in the circulation, significantly less than H_6-trC1INH(MGS)-MSA or H_6-MSA (48 ± 10% and 60 ± 8%, respectively) (Fig 3D). While residual levels of H_6-trC1INH(MGS)-MSA and H_6-MSA did not exhibit a significant difference at 1 hour, the difference became significant by 4 hours post-injection.

Our initial design of the *in vivo* clearance experiment was limited by local animal research ethics requirements which restricted the number of blood samples that could be taken in a 24-hour period. For H_6-trC1INH(MGS) that design covered >95% of the total clearance curve, but <50% of that of the less

rapidly cleared MSA-containing proteins (see Fig. 3A – 3D). More extrapolation was therefore required to estimate the half-life of those proteins than for H_6-trC1INH(MGS). Accordingly, an additional experiment was performed in which identical doses of H_6-trC1INH(MGS)-MSA and H_6- MSA as previously employed were administered to additional groups of 6 mice each, and blood samples were obtained 16 – 28 hours after injection. As shown in Fig. 3E, these results supported the initial, shorter experiment, and showed that substantial quantities of H_6-trC1INH(MGS)-MSA (19 ± 1%) and H_6- MSA (22 ± 1%) 18 and 28 hours after injection, respectively.

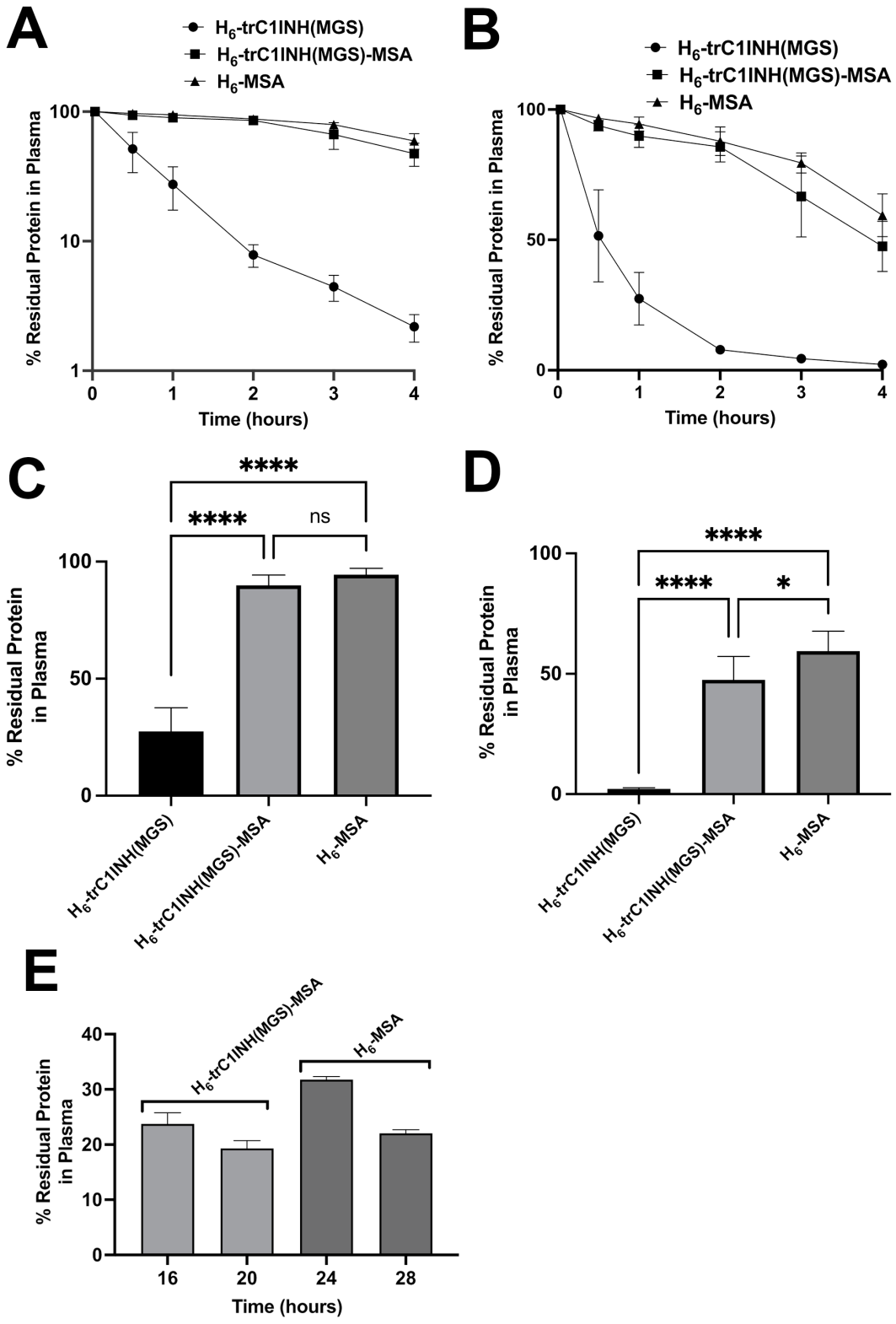
A
H6-trC1INH(MGS)
H6-trC1INH(MGS)-MSA
H6-MSA
% Residual Protein in Plasma
100
10
1
0
1
2
3
4
Time (hours)
B
H6-trC1INH(MGS)
H6-trC1INH(MGS)-MSA
H6-MSA
% Residual Protein in Plasma
100
50
0
0
1
2
3
4
Time (hours)
C
****
****
ns
% Residual Protein in Plasma
100
50
0
H6-trC1INH(MGS)
H6-trC1INH(MGS)-MSA
H6-MSA
D
****
****
*
% Residual Protein in Plasma
100
50
0
H6-trC1INH(MGS)
H6-trC1INH(MGS)-MSA
H6-MSA
E
H6-trC1INH(MGS)-MSA
H6-MSA
% Residual Protein in Plasma
40
30
20
10
0
16
20
24
28
Time (hours)

Figure 3: Protein clearance of H_6-trC1INH(MGS), H_6-trC1INH(MGS)-MSA, and H_6-MSA. A) Logarithmic-linear plot of H_6-trC1INH(MGS), H_6-trC1INH(MGS)-MSA, and H_6-MSA percentage residual protein in plasma versus time in hours post-injection. B) Linear plot of H_6-trC1INH(MGS), H_6-trC1INH(MGS)-MSA, and H_6-MSA percentage residual protein in plasma versus time in hours post-injection. C) Percentage residual protein in plasma at 1-hour post-injection. D) Percentage residual protein in plasma at 4-hours post-injection. E) Percentage residual protein in plasma at the times, in hours, specified on the x axis, following injection of H_6-trC1INH(MGS)-MSA (light grey bars) or H_6-MSA (dark grey bars). The mean of 6 determinations ± SD is shown in all cases. *, $p < 0.05$, ****, $p<0.0001$ for statistical comparisons indicated by horizontal bars (ns denotes non-significant).

4.4. Pharmacokinetic Analysis

The use of a two-compartment model to resolve clearance curves allowed the calculation of terminal half-lives, alongside the area under the curve (AUC) for the three proteins, are presented in Table 2. Fusion to albumin significantly extended the mean terminal half-life of C1INH by 3.0-fold. However, H_6-trC1INH(MGS)-MSA still exhibited a 1.5-fold more rapid clearance compared to H_6-MSA. Furthermore, there was a significant 3.8-fold increase in the observed AUC for H_6-trC1INH(MGS)-MSA versus H_6-trC1INH(MGS), while remaining 1.1-fold less than the AUC of H_6-MSA. The results suggest that albumin fusion

significantly extended the plasma residency time of H_6-trC1INH(MGS)-MSA compared to H_6-trC1INH(MGS), as well as the terminal half-life, supporting our hypothesis, although the extension fell short of achieving the longer values observed for H_6-MSA. No effect of sex on terminal half-life was noted for any of the three proteins; when half-life values were grouped by sex for each protein, no significant differences were noted (as indicated by p values of 0.1 to 0.7 by Mann-Whitney non-parametric test). Similarly, no effect of body weight was noted for any of the three proteins; when half-life values were divided into heavier half versus lighter half per protein per group, no significant differences were noted (as indicated by p values of 0.4 to 0.99 by Mann-Whitney non-parametric test).

Table 2: H_6-trC1INH(MGS), H_6-trC1INH(MGS)-MSA, H_6-MSA pharmacokinetic analysis of clearance.

Protein name	Terminal half-life (hours)	Area Under the observed Curve (AUC; %-hours)
H_6-trC1INH(MGS)	5 ± 2	80 ± 20
H_6-trC1INH(MGS)-MSA	14 ± 3*	310 ± 20***
H_6-MSA	21 ± 8***	340 ± 8***
Results are the mean of 6 determinations, ± SD. *, $p < 0.05$; ***, $p < 0.001$ versus H_6-trC1INH(MGS).		

5. Discussion

The chief findings of this study were that the inhibitory properties of C1INH were maintained in a truncated, non-glycosylated variant, that these properties were largely maintained when this variant was fused to serum albumin, and that the fusion protein remained in the circulation of mice after intravenous injection for considerably longer than its unfused equivalent. Although the results supported our initial hypothesis, the extension in plasma residency fell short of that exhibited by recombinant albumin alone.

Unfused H_6-trC1INH(MGS) left the circulation rapidly after injection, as expected for a protein of 43 kDa, below the glomerular filtration limit. Such proteins are expected to be filtered in the glomerular structures of the kidneys, and not re-adsorbed in the renal tubules [36]. Consistent with this expectation, the clearance curve for H_6-trC1INH(MGS) diverged from those of H_6-trC1INH(MGS)-MSA or H_6-MSA at the earliest sampled time point. Both plasma residency time, as quantified by the observed AUC, and terminal catabolism, as quantified by the terminal half-life, increased 3- to 4-fold when MSA was fused to H_6-trC1INH(MGS). H_6-trC1INH(MGS)-MSA approached, but did not reach, the long plasma residency and slow rate of terminal clearance of H_6-MSA, achieving mean levels of 92% of the AUC and 66% of the terminal half-life of that hexahistidine-tagged albumin. The mean terminal half-life of H_6-MSA, 21.4 hours, was less than that reported for plasma-derived MSA in previous studies (27.7 hours [37] – 35 hours [38]), a difference potentially arising either from hexahistidine tagging, recombinant production, or methodological differences

such as protein radioiodination in previous studies. In this work we elected to follow the fusion proteins without modification via ELISA of plasma samples, in part due to initial observations that pdC1NH lost the ability to form SDS-stable complexes with Pka after iodination. Our results were nonetheless internally consistent and showed a significant extension of half-life and reduction in clearance rate for H_6-trC1INH(MGS)-MSA versus H_6-trC1INH(MGS). The improved pharmacokinetic profile was likely obtained by the combined mechanisms of avoidance of renal filtration and the conferring of recycling via murine FcRn [39].

Fusion to albumin generally increases the plasma half-life of fused proteins, but it can interfere with the biological function of the attached protein, to varying extents. Miyakawa et al. reported that fusion of interferon γ to MSA increased the observed clearance AUC of the fusion protein 10-fold versus unfused interferon γ, but at the cost of the loss of ~99% of its biological activity [40]. Less dramatic losses in activity were reported by our laboratory in fusing the Kunitz Protease Inhibitor (KPI) domain of Protease Nexin 2 to HSA, where the affinity of KPI for its target protease FXIa significantly declined 2.1-fold with fusion [41]. Similarly, fusing FIX to HSA resulted in substantial losses in specific activity compared to unfused recombinant FIX of up to 100-fold, unless a cleavable spacer was used that could liberate FIX from HSA [42]. In this study the rate of C1s inhibition by H_6-trC1INH(MGS) was unaffected by MSA fusion and the rate of Pka inhibition was reduced 1.8-fold. These outcomes likely arose from favourable

interactions between the H_6-trC1INH(MGS) moiety of the fusion protein and the target proteases, unimpeded by MSA, which was designed to be distanced from that moiety by a substantive triplicated Gly_4Ser spacer.

Previous investigators have established that truncated, glycosylated recombinant C1 inhibitor retained the inhibitory capacity of full-length C1INH against several protease targets. Coutinho et al. deleted the N-terminal 97 residues of C1INH and showed, qualitatively, similar inhibitory activity of the deletion mutant as wild-type C1INH produced in cultured COS-1 cells [12]. Bos et al. expressed the same truncation mutant (Δ97) in *P. pastoris* and reported comparable association rate constants differing by less than two-fold for wild-type and truncated C1INH for C1s, Pka, and FXIIa [14]. Rossi et al. made the Δ97 truncation using baculovirus expression vectors expressed in cultured Sf21 insect cells, finding equivalent complex formation with C1s on gel analysis both for truncated and hexahistidine-tagged C1inhΔ97-ht and for untagged C1inhΔ97, and for truncated variants with mutated N216 and/or N231 sites; truncated variants with mutated N216, N231, and N330 sites failed to be expressed [13]. Our results contrasted with those of Rossi et al. in that we were able to obtain enough hexahistidine-tagged, truncated, non-glycosylated H_6-trC1INH(MGS) to determine quantitatively its identical kinetics of C1s inhibition and its similar (85%) kinetics of Pka inhibition to its plasma-derived counterpart. The discordance suggests that glycosylation on N330 is obligatory only for expression in Sf21 insect cells [13] and not for eukaryotic cells in general.

While many studies of albumin fusion proteins employ HSA as a fusion partner rather than a species-matched albumin, it is known that the serum half-life of HSA fusion proteins can be underestimated in mice. This underestimation arises because the binding affinity of HSA to murine FcRn is about 10-fold weaker than its binding to human FcRn [43]. Moreover, HSA-conjugated drugs persist longer in the circulation of transgenic mice expressing human FcRn than in wild-type mice [44]. Site-specific conjugation of superfolder green fluorescent protein (sfGFP) to MSA or HSA resulted in a significantly longer mean half-life for the sfGFP-MSA conjugate (27.7 hours) than for sfGFP-HSA (16.3 hours) [45]. In addition, use of MSA as the fusion partner could make it easier to determine proof-of-concept for the utility of H_6-trC1INH(MGS)-MSA in knockout mice genetically deficient in C1INH [6].

Purified plasma-derived C1INH concentrates have been reported to have mean half-lives in HAE patients ranging from 32.7 [46] to 74.1 hours [47]. These values might seem longer than those reported in this study for both H_6-trC1INH(MGS) and H_6-trC1INH(MGS)-MSA were it not for the principle of allometric scaling, which holds that drug or protein clearance is proportional to the body weight of an animal or human [48]. The mean terminal catabolic half-life of HSA in humans is 19 days [26]. Extrapolating from our results in mice, we speculate that the half-life of a H_6-trC1INH(MGS)-HSA fusion protein would be significantly longer than that of plasma-derived C1INH concentrates, although it is unlikely that the full extension of half-life to 19 days would be achieved.

Although H_6-trC1INH(MGS)-MSA inhibited Pka with similar kinetics to either unfused H_6-trC1INH(MGS) or pdC1INH, in contrast to those proteins, the fusion protein did not form detectable SDS-stable complexes with Pka. Our failure to detect covalent serpin-protease complexes with this combination of serpin and protease may have arisen for several reasons. Firstly, our choice of reaction conditions could have been responsible; greater excesses of H_6-trC1INH(MGS)-MSA over Pka might have been required because of its mean SI of 6.8, versus 5.3 for H_6-trC1INH(MGS) (although these values did not differ statistically) and 3.2 for pdC1INH; others have estimated the latter value, for pdC1INH, at approximately 2 [14]. Secondly, it is possible that the fusion protein formed a strongly stabilized non-covalent inhibitory complex. There are precedents for such unusual variant serpins. Ciaccia et al. did not detect a covalent complex between the L444R variant of heparin cofactor II and α-thrombin in the presence of heparin, despite strong inhibition of activity [49]. Similarly, Rossi et al. described the lack of covalent complex formation between Complement Component 1, r subcomponent-like protein (*C1rLP*) and C1inhΔ97, despite strong inhibition of C1rLP activity [13]. Finally, relatively few fusion proteins involving serpins have been described in the literature. Alpha-1 antitrypsin (AAT), the most abundant serpin in human plasma, loses the ability to inhibit its natural target, neutrophil elastase, when fused to the N-terminus of IgG1 Fc [50]. In contrast, AAT M358R variant retains function when fused, via its N-terminus, to the C-terminus of bacteriophage T7 coat protein 10, as evidenced

by its formation of SDS-stable complexes with thrombin [51]. Thus, H_6-trC1INH(MGS) retains potent anti-Pka activity but may inhibit its target via an atypical mechanism.

The rate of inhibition of Pka by C1INH is surprisingly low compared to those achieved by other serpins in regulating other proteases [35]. Nevertheless, the susceptibility of C1INH-deficient individuals to HAE and their successful treatment with pdC1INH concentrates show that it is high enough to maintain control of bradykinin generation. In this study we showed that fusion protein H_6-trC1INH(MGS)-MSA gains extended half-life and maintains most of rate of Pka inhibition exhibited by pdC1INH. Future studies in C1INH knockout mice will be required to determine if this profile is sufficiently favourable to warrant continued development via substitution of the MSA moiety by HSA and investigation in mice with human FcRn, or if protein engineering to re-direct a different serpin towards Pka inhibition at higher rates, like the approach taken by de Maat et al. [52] would be a superior strategy.

6. References

1. N.S. Landerman, M.E. Webster, E.L. Becker and H.E. Ratcliffe, "Hereditary angioneurotic edema. II. Deficiency of inhibitor for serum globulin permeability factor and/or plasma kallikrein," *J Allergy*, 1962. 33: p. 330-41.
2. V.H. Donaldson and R.R. Evans, "A Biochemical Abnormality in Herediatry Angioneurotic Edema: Absence of Serum Inhibitor of C' 1-Esterase," *Am J Med*, 1963. 35: p. 37-44.
3. A.E. Davis, 3rd, "C1 inhibitor and hereditary angioneurotic edema," *Annu Rev Immunol*, 1988. 6: p. 595-628.
4. H. Gregorek, M. Kokai, T. Hidvegi, G. Fust, K. Sabbouh and K. Madalinski, "Concentration of C1 inhibitor in sera of healthy blood donors as studied

by immunoenzymatic assay," *Complement Inflamm*, 1991. 8(5-6): p. 310-2.
5. R. Huber and R.W. Carrell, "Implications of the three-dimensional structure of alpha 1-antitrypsin for structure and function of serpins," *Biochemistry*, 1989. 28(23): p. 8951-66.
6. E.D. Han, R.C. MacFarlane, A.N. Mulligan, J. Scafidi and A.E. Davis, 3rd, "Increased vascular permeability in C1 inhibitor-deficient mice mediated by the bradykinin type 2 receptor," *J Clin Invest*, 2002. 109(8): p. 1057-63.
7. C. Caliezi, W.A. Wuillemin, S. Zeerleder, M. Redondo, B. Eisele and C.E. Hack, "C1-Esterase inhibitor: an anti-inflammatory agent and its potential use in the treatment of diseases other than hereditary angioedema," *Pharmacol Rev*, 2000. 52(1): p. 91-112.
8. A. Relan, K. Bakhtiari, E.S. van Amersfoort, J.C. Meijers and C.E. Hack, "Recombinant C1-inhibitor: effects on coagulation and fibrinolysis in patients with hereditary angioedema," *BioDrugs*, 2012. 26(1): p. 43-52.
9. M. Cugno, I. Bos, Y. Lubbers, C.E. Hack and A. Agostoni, "In vitro interaction of C1-inhibitor with thrombin," *Blood Coagul Fibrinolysis*, 2001. 12(4): p. 253-60.
10. K. Zahedi, A.E. Prada and A.E. Davis, 3rd, "Structure and regulation of the C1 inhibitor gene," *Behring Inst Mitt*, 1993(93): p. 115-9.
11. K. Stavenhagen, H.M. Kayili, S. Holst, C.A.M. Koeleman, R. Engel, D. Wouters, S. Zeerleder, B. Salih and M. Wuhrer, "N- and O-glycosylation Analysis of Human C1-inhibitor Reveals Extensive Mucin-type O-Glycosylation," *Mol Cell Proteomics*, 2018. 17(6): p. 1225-1238.
12. M. Coutinho, K.S. Aulak and A.E. Davis, 3rd, "Functional analysis of the serpin domain of C1 inhibitor," *J Immunol*, 1994. 153(8): p. 3648-54.
13. V. Rossi, I. Bally, S. Ancelet, Y. Xu, V. Fremeaux-Bacchi, R.R. Vives, R. Sadir, N. Thielens and G.J. Arlaud, "Functional characterization of the recombinant human C1 inhibitor serpin domain: insights into heparin binding," *J Immunol*, 2010. 184(9): p. 4982-9.
14. I.G. Bos, Y.T. Lubbers, D. Roem, J.P. Abrahams, C.E. Hack and E. Eldering, "The functional integrity of the serpin domain of C1-inhibitor depends on the unique N-terminal domain, as revealed by a pathological mutant," *J Biol Chem*, 2003. 278(32): p. 29463-70.
15. I. Gigli, J.W. Mason, R.W. Colman and K.F. Austen, "Interaction of plasma kallikrein with the C1 inhibitor," *J Immunol*, 1970. 104(3): p. 574-81.
16. J.B. Su, "Kinins and cardiovascular diseases," *Curr Pharm Des*, 2006. 12(26): p. 3423-35.
17. J. Nussberger, M. Cugno, M. Cicardi and A. Agostoni, "Local bradykinin generation in hereditary angioedema," *J Allergy Clin Immunol*, 1999. 104(6): p. 1321-2.
18. J. Nussberger, M. Cugno, C. Amstutz, M. Cicardi, A. Pellacani and A. Agostoni, "Plasma bradykinin in angio-oedema," *Lancet*, 1998. 351(9117): p. 1693-7.

19. H. Duffey and R. Firszt, "Management of acute attacks of hereditary angioedema: role of ecallantide," *J Blood Med*, 2015. 6: p. 115-23.
20. H. Farkas and L. Varga, "Ecallantide is a novel treatment for attacks of hereditary angioedema due to C1 inhibitor deficiency," *Clin Cosmet Investig Dermatol*, 2011. 4: p. 61-8.
21. N.M. Johnson and M.A. Phillips, "New Treatments for Hereditary Angioedema," *Skin Therapy Lett*, 2018. 23(1): p. 6-8.
22. H. Longhurst, "Optimum Use of Acute Treatments for Hereditary Angioedema: Evidence-Based Expert Consensus," *Front Med (Lausanne)*, 2017. 4: p. 245.
23. H.H. Li, "Hereditary angioedema: Long-term prophylactic treatment," *Allergy Asthma Proc*, 2020. 41(Suppl 1): p. S35-S37.
24. B. Davis and J.A. Bernstein, "Conestat alfa for the treatment of angioedema attacks," *Ther Clin Risk Manag*, 2011. 7: p. 265-73.
25. L.M. Malec, D. Cheng, C.M. Witmer, J. Jaffray, P.A. Kouides, K.M. Haley, R.F. Sidonio, Jr., K. Johnson, M. Recht, G. White, S.E. Croteau and M.V. Ragni, "The impact of extended half-life factor concentrates on prophylaxis for severe hemophilia in the United States," *Am J Hematol*, 2020. 95(8): p. 960-965.
26. T. Peters, Jr., "Serum albumin," *Adv Protein Chem*, 1985. 37: p. 161-245.
27. W.P. Sheffield, I.J. Smith, S. Syed and V. Bhakta, "Prolonged in vivo anticoagulant activity of a hirudin-albumin fusion protein secreted from Pichia pastoris," *Blood Coagul Fibrinolysis*, 2001. 12(6): p. 433-43.
28. W.P. Sheffield, B. Wilson, L.J. Eltringham-Smith, S. Gataiance and V. Bhakta, "Recombinant albumins containing additional peptide sequences smaller than barbourin retain the ability of barbourin-albumin to inhibit platelet aggregation," *Thromb Haemost*, 2005. 93(5): p. 914-21.
29. W.P. Sheffield, L.J. Eltringham-Smith, S. Gataiance and V. Bhakta, "A long-lasting, plasmin-activatable thrombin inhibitor aids clot lysis in vitro and does not promote bleeding in vivo," *Thromb Haemost*, 2009. 101(5): p. 867-77.
30. V. Bhakta, M. Hamada, A. Nouanesengsy, J. Lapierre, D.L. Perruzza and W.P. Sheffield, "Identification of an alpha-1 antitrypsin variant with enhanced specificity for factor XIa by phage display, bacterial expression, and combinatorial mutagenesis," *Sci Rep*, 2021. 11(1): p. 5565.
31. B.V. Hamada M, Andres SN, Sheffield WP, "Stepwise reversion of multiply mutated recombinant antitrypsin reveals a selective inhibitor of coagulation factor XIa as active as the M358R variant," *Frontiers in Cardiovascular Medicine*, 2021. 8.
32. W.P. Sheffield, L.J. Eltringham-Smith, S. Gataiance and V. Bhakta, "A plasmin-activatable thrombin inhibitor reduces experimental thrombosis and assists experimental thrombolysis in murine models," *J Thromb Thrombolysis*, 2015. 39(4): p. 443-51.

33. W.P. Sheffield, A. Mamdani, G. Hortelano, S. Gataiance, L. Eltringham-Smith, M.E. Begbie, R.A. Leyva, P.S. Liaw and F.A. Ofosu, "Effects of genetic fusion of factor IX to albumin on in vivo clearance in mice and rabbits," *Br J Haematol*, 2004. 126(4): p. 565-73.
34. W.P. Sheffield, T.R. McCurdy and V. Bhakta, "Fusion to albumin as a means to slow the clearance of small therapeutic proteins using the Pichia pastoris expression system: a case study," *Methods Mol Biol*, 2005. 308: p. 145-54.
35. P.G. Gettins, "Serpin structure, mechanism, and function," *ChemRev*, 2002. 102(12): p. 4751-4804.
36. B.J. Ballermann, J. Nystrom and B. Haraldsson, "The Glomerular Endothelium Restricts Albumin Filtration," *Front Med (Lausanne)*, 2021. 8: p. 766689.
37. F.J. Dixon, P.H. Maurer and M.P. Deichmiller, "Half-lives of homologous serum albumins in several species," *Proc Soc Exp Biol Med*, 1953. 83(2): p. 287-8.
38. C. Chaudhury, S. Mehnaz, J.M. Robinson, W.L. Hayton, D.K. Pearl, D.C. Roopenian and C.L. Anderson, "The major histocompatibility complex-related Fc receptor for IgG (FcRn) binds albumin and prolongs its lifespan," *J Exp Med*, 2003. 197(3): p. 315-22.
39. H.Y. Tao, R.Q. Wang, W.J. Sheng and Y.S. Zhen, "The development of human serum albumin-based drugs and relevant fusion proteins for cancer therapy," *Int J Biol Macromol*, 2021. 187: p. 24-34.
40. N. Miyakawa, M. Nishikawa, Y. Takahashi, M. Ando, M. Misaka, Y. Watanabe and Y. Takakura, "Prolonged circulation half-life of interferon gamma activity by gene delivery of interferon gamma-serum albumin fusion protein in mice," *J Pharm Sci*, 2011. 100(6): p. 2350-7.
41. W.P. Sheffield, L.J. Eltringham-Smith and V. Bhakta, "Fusion to Human Serum Albumin Extends the Circulatory Half-Life and Duration of Antithrombotic Action of the Kunitz Protease Inhibitor Domain of Protease Nexin 2," *Cell Physiol Biochem*, 2018. 45(2): p. 772-782.
42. S. Schulte, "Half-life extension through albumin fusion technologies," *Thromb Res*, 2009. 124 Suppl 2: p. S6-8.
43. J. Nilsen, M. Bern, K.M.K. Sand, A. Grevys, B. Dalhus, I. Sandlie and J.T. Andersen, "Human and mouse albumin bind their respective neonatal Fc receptors differently," *Sci Rep*, 2018. 8(1): p. 14648.
44. D. Viuff, F. Antunes, L. Evans, J. Cameron, H. Dyrnesli, B. Thue Ravn, M. Stougaard, K. Thiam, B. Andersen, S. Kjaerulff and K.A. Howard, "Generation of a double transgenic humanized neonatal Fc receptor (FcRn)/albumin mouse to study the pharmacokinetics of albumin-linked drugs," *J Control Release*, 2016. 223: p. 22-30.
45. B. Yang, J.C. Kim, J. Seong, G. Tae and I. Kwon, "Comparative studies of the serum half-life extension of a protein via site-specific conjugation to a

species-matched or -mismatched albumin," *Biomater Sci*, 2018. 6(8): p. 2092-2100.
46. J.A. Bernstein, B. Ritchie, R.J. Levy, R.L. Wasserman, A.K. Bewtra, D.S. Hurewitz, K. Obtulowicz, A. Reshef, D. Moldovan, T. Shirov, V. Grivcheva-Panovska, P.C. Kiessling, F. Schindel and T.J. Craig, "Population pharmacokinetics of plasma-derived C1 esterase inhibitor concentrate used to treat acute hereditary angioedema attacks," *Ann Allergy Asthma Immunol*, 2010. 105(2): p. 149-54.
47. I. Martinez-Saguer, K. Bork, T. Latysheva, L. Zabrodska, V. Chopyak, N. Nenasheva, A. Totolyan and V. Krivenchuk, "Plasma-derived C1 esterase inhibitor pharmacokinetics and safety in patients with hereditary angioedema," *J Allergy Clin Immunol Glob*, 2024. 3(1): p. 100178.
48. A.B. Nair and S. Jacob, "A simple practice guide for dose conversion between animals and human," *J Basic Clin Pharm*, 2016. 7(2): p. 27-31.
49. A.V. Ciaccia, A.J. Willemze and F.C. Church, "Heparin promotes proteolytic inactivation by thrombin of a reactive site mutant (L444R) of recombinant heparin cofactor II," *J Biol Chem*, 1997. 272(2): p. 888-93.
50. D. Jonigk, M. Al-Omari, L. Maegel, M. Muller, N. Izykowski, J. Hong, K. Hong, S.H. Kim, M. Dorsch, R. Mahadeva, F. Laenger, H. Kreipe, A. Braun, G. Shahaf, E.C. Lewis, T. Welte, C.A. Dinarello and S. Janciauskiene, "Anti-inflammatory and immunomodulatory properties of alpha1-antitrypsin without inhibition of elastase," *Proc Natl Acad Sci U S A*, 2013. 110(37): p. 15007-12.
51. B.M. Scott, W.L. Matochko, R.F. Gierczak, V. Bhakta, R. Derda and W.P. Sheffield, "Phage display of the serpin alpha-1 proteinase inhibitor randomized at consecutive residues in the reactive centre loop and biopanned with or without thrombin," *PLoS One*, 2014. 9(1): p. e84491.
52. S. de Maat, W. Sanrattana, R.K. Mailer, N.M.J. Parr, M. Hessing, R.M. Koetsier, J.C.M. Meijers, G. Pasterkamp, T. Renne and C. Maas, "Design and characterization of alpha1-antitrypsin variants for treatment of contact system-driven thromboinflammation," *Blood*, 2019.

7. Supporting Information

(1) Protein sequences and lengths

Below can be found the primary amino acid sequence of each recombinant C1INH- or MSA-related recombinant protein used in this study, in each case with length in amino acids, predicted molecular weight, and calculated isoelectric point (pI).

H_6-trC1INH(MGS)

EAHHHHHHGSFCPGPVTLCSDLESHSTEAVLGDALVDFSLKLYHAFSAMKK
VETNMAFSPFSIASLLTQVLLGAGENTKTNLESILSYPKDFTCVHQALKGFTT
KGVTSVSQIFHSPDLAIRDTFVQASRTLYSSSPRVLSQNSDANLELINTWVAK
NTNNKISRLLDSLPSDTRLVLLNAIYLSAKWKTTFDPKKTRMEPFHFKNSVIK
VPMMNSKKYPVAHFIDQTLKAKVGQLQLSHQLSLVILVPQNLKHRLEDMEQ
ALSPSVFKAIMEKLEMSKFQPTLLTLPRIKVTTSQDMLSIMEKLEFFDFSYDL
NLCGLTEDPDLQVSAMQHQTVLELTETGVEAAAASAISVARTLLVFEVQQPF
LFVLWDQQHKFPVFMGRVYDPRA

389 amino acids

43,697 Da

pI 7.09

H_6-trC1INH(MGS)-MSA

EAHHHHHHGSFCPGPVTLCSDLESHSTEAVLGDALVDFSLKLYHAFSAMKK
VETNMAFSPFSIASLLTQVLLGAGENTKTNLESILSYPKDFTCVHQALKGFTT
KGVTSVSQIFHSPDLAIRDTFVQASRTLYSSSPRVLSQNSDANLELINTWVAK
NTNNKISRLLDSLPSDTRLVLLNAIYLSAKWKTTFDPKKTRMEPFHFKNSVIK
VPMMNSKKYPVAHFIDQTLKAKVGQLQLSHQLSLVILVPQNLKHRLEDMEQ
ALSPSVFKAIMEKLEMSKFQPTLLTLPRIKVTTSQDMLSIMEKLEFFDFSYDL
NLCGLTEDPDLQVSAMQHQTVLELTETGVEAAAASAISVARTLLVFEVQQPF
LFVLWDQQHKFPVFMGRVYDPRAGGGGSGGGGSGGGGSHKSEIAHRYND

LGEQHFKGLVLIAFSQYLQKCSYDEHAKLVQEVTDFAKTCVADESAANCDK
SLHTLFGDKLCAIPNLRENYGELADCCTKQEPERNECFLQHKDDNPSLPPFE
RPEAEAMCTSFKENPTTFMGHYLHEVARRHPYFYAPELLYYAEQYNEILTQ
CCAEADKESCLTPKLDGVKEKALVSSVRQRMKCSSMQKFGERAFKAWAVA
RLSQTFPNADFAEITKLATDLTKVNKECCHGDLLECADDRAELAKYMCENQ
ATISSKLQTCCDKPLLKKAHCLSEVEHDTMPADLPAIAADFVEDQEVCKNYA
EAKDVFLGTFLYEYSRRHPDYSVSLLLRLAKKYEATLEKCCAEANPPACYGT
VLAEFQPLVEEPKNLVKTNCDLYEKLGEYGFQNAILVRYTQKAPQVSTPTLV
EAARNLGRVGTKCCTLPEDQRLPCVEDYLSAILNRVCLLHEKTPVSEHVTKC
CSGSLVERRPCFSALTVDETYVPKEFKAETFTFHSDICTLPEKEKQIKKQTAL
AELVKHKPKATAEQLKTVMDDFAQFLDTCCKAADKDTCFSTEGPNLVTRCK
DALA

986 amino acids

110,315 Da

pI 6.00

H_6-MSA

EAHHHHHHHKSEIAHRYNDLGEQHFKGLVLIAFSQYLQKCSYDEHAKLVQE
VTDFAKTCVADESAANCDKSLHTLFGDKLCAIPNLRENYGELADCCTKQEPE
RNECFLQHKDDNPSLPPFERPEAEAMCTSFKENPTTFMGHYLHEVARRHP
YFYAPELLYYAEQYNEILTQCCAEADKESCLTPKLDGVKEKALVSSVRQRMK
CSSMQKFGERAFKAWAVARLSQTFPNADFAEITKLATDLTKVNKECCHGDL

LECADDRAELAKYMCENQATISSKLQTCCDKPLLKKAHCLSEVEHDTMPAD

LPAIAADFVEDQEVCKNYAEAKDVFLGTFLYEYSRRHPDYSVSLLLRLAKKY

EATLEKCCAEANPPACYGTVLAEFQPLVEEPKNLVKTNCDLYEKLGEYGFQ

NAILVRYTQKAPQVSTPTLVEAARNLGRVGTKCCTLPEDQRLPCVEDYLSAI

LNRVCLLHEKTPVSEHVTKCCSGSLVERRPCFSALTVDETYVPKEFKAETFT

FHSDICTLPEKEKQIKKQTALAELVKHKPKATAEQLKTVMDDFAQFLDTCCK

AADKDTCFSTEGPNLVTRCKDALA

590 amino acids

66,713 Da

pI 5.68

(2) All data from Table 1

Protein name	k_2 versus Pka ($X 10^4 M^{-1}s^{-1}$)	k_2 versus C1s ($X 10^4 M^{-1}s^{-1}$)	SI versus Pka
Trial 1	2.35	5.3	3.3
Trial 2	2.25	5.6	3.3
Trial 3	2.00	6.3	3.2
Trial 4	2.45	-	3.3
Trial 5	2.55	-	3.2
pdC1INH average	2.3 ± 0.2***	5.7 ± 0.5	3.3 ± 0.06***^^^
Trial 1	2.00	4.3	5.3
Trial 2	2.10	4.7	5.8
Trial 3	1.95	5.7	5.2
Trial 4	1.95	-	5.1
Trial 5	2.05	-	5.5
H_6-trC1INH(MGS) average	2.01 ± 0.07***	5.0 ± 0.5	5.3 ± 0.3
Trial 1	1.2	4.68	7.0
Trial 2	1.25	5.42	6.9
Trial 3	1.35	5.22	6.7
Trial 4	1.2	-	6.8
Trial 5	1.35	-	7.1
H_6-trC1INH(MGS)-MSA average	1.3 ± 0.08	5.1 ± 0.4	6.9 ± 0.1

Results are the mean of 5 determinations (SI or k_2 for kallikrein), ± SD, or 3 determinations (k_2 for C1s). ***, $p < 0.001$ versus H_6-trC1INH(MGS)-MSA. ^^^, $p < 0.001$ versus H_6-trC1INH(MGS). Each trial is shown.

(3) All data from Figure 2B

	pdC1INH 500ng	pdC1INH 1000ng	H6-trC1INH(MGS)-MSA 1000ng	H6-trC1INH(MGS)-MSA 5000ng
OD450-1	0.524	0.776	0.218	0.485
OD450-2	0.481	0.775	0.204	0.512
OD450-3	0.521	0.773	0.22	0.488
Mean	0.509	0.775	0.214	0.495
SD	0.024	0.002	0.009	0.015

(4) All data from Figure 3A, 3B, 3C, and 3D

Time after injection (hours)	H_6-trC1INH(MGS) Relative residual amount in plasma (%)					
	Mouse 1	Mouse 2	Mouse 3	Mouse 4	Mouse 5	Mouse 6
0.0333	100	100	100	100	100	100
0.5	42.8	40.7	74.1	27.4	67.1	57.2
1	30.4	19.5	24.8	16.9	45.3	27.9
2	8.3	5.1	8.8	9.6	7.4	7.9
3	4.2	3.7	5.3	4.5	5.9	3.2
4	3.0	2.4	1.7	1.8	2.5	1.7
Time after injection (hours)	H_6-trC1INH(MGS)-MSA Relative residual amount in plasma (%)					
	Mouse 1	Mouse 2	Mouse 3	Mouse 4	Mouse 5	Mouse 6
0.0333	100.0	100.0	100.0	100.0	100.0	100.0
0.5	93.6	92.4	91.7	93.3	97.5	94.3
1	92.0	83.7	90.7	85.5	95.3	91.8
2	91.9	82.1	78.1	84.6	93.1	84.1
3	50.8	80.1	69.1	47.9	87.1	64.9
4	46.4	59.5	30.7	45.1	51.8	51.6
Time after injection (hours)	H_6-MSA Relative residual amount in plasma (%)					
	Mouse 1	Mouse 2	Mouse 3	Mouse 4	Mouse 5	Mouse 6
0.0333	100.0	100.0	100.0	100.0	100.0	100.0
0.5	96.1	93.9	96.9	96.4	97.3	99.4
1	93.4	91.1	96.0	92.4	95.3	98.6
2	87.7	81.6	94.2	85.2	83.7	94.9
3	80.1	73.8	84.7	76.4	81.0	81.0
4	64.6	69.3	45.7	59.0	62.6	55.7

(5) All data from Figure 3E

	H_6-trC1INH(MGS)-MSA		**H_6-MSA**	
Time (hours after injection)	**16**	**18**	**24**	**28**
Mouse 1	20.5	17.1	32.5	22.6
Mouse 2	25.6	21.0	32.2	21.0
Mouse 3	22.6	18.9	31.1	22.0
Mouse 4	25.7	20.6	31.8	22.0
Mouse 5	23.2	18.7	31.5	22.8
Mouse 6	24.8	19.4	31.4	21.8

(6) All data from Table 2

Protein name	**Terminal half-life (hours)**	**Area Under the observed Curve (AUC; %-hours)**
Trial 1	5.3	81
Trial 2	8.1	68
Trial 3	3.1	93
Trial 4	3.1	64
Trial 5	5.1	104
Trial 6	3.3	84
H_6-trC1INH(MGS) average	5 ± 2	80 ± 20
Trial 1	12.9	303

Trial 2	20.2	323
Trial 3	10.8	298
Trial 4	11.7	288
Trial 5	14.5	348
Trial 6	14.4	313
H_6-trC1INH(MGS)-MSA average	14 ± 3*	310 ± 20***
Trial 1	21.6	340
Trial 2	35.9	327
Trial 3	13.3	344
Trial 4	18.3	330
Trial 5	24.2	338
Trial 6	15.1	349
H_6-MSA average	21 ± 8***	340 ± 8***
Results are the mean of 6 determinations, ± SD. *, $p < 0.05$; ***, $p < 0.001$ versus H_6-trC1INH(MGS).		

(7) All data relating to effect of sex or weight on terminal half-life, by protein

Half-life values by injected protein and sex

H_6-trC1INH(MGS)		**H_6-trC1INH(MGS)-MSA**		**H_6-MSA**	
Male	Female	Male	Female	Male	Female
0.338693	0.219536	1.907285	1.531063	4.014926	2.587195
0.129881	0.127471	1.497898	1.997685	2.70063	2.602597

	0.210745	0.138842	1.754144	1.759024	3.106161	2.600269
Average	0.22644	0.16195	1.7197757	1.76259067	3.273906	2.596687
SD	0.105287	0.050194	0.2068461	0.23333145	0.673014	0.008302

Half-life values by injected protein and weight (stratified, 2 groups)

	H_6-trC1INH(MGS)		**H_6-trC1INH(MGS)-MSA**		**H_6-MSA**	
	Heavier	Lighter	Heavier	Lighter	Heavier	Lighter
	0.338693	0.219536	1.531063	1.907285	4.014926	2.587195
	0.129881	0.210745	1.997685	1.497898	2.70063	3.106161
	0.127471	0.138842	1.754144	1.759024	2.602597	2.600269
Average	0.198682	0.189708	1.760964	1.72140233	3.106051	2.764542
SD	0.121259	0.04427	0.2333857	0.20727029	0.788634	0.295923

(8) All data relating to mouse weight

Weight of mice whose data is shown in Fig 3A-D

H_6-trC1INH(MGS)	H_6-trC1INH(MGS)-MSA	H_6-MSA
26.6	28	24.4
33.8	29	41.6
28.4	31	34.8

	29.2	32	31
	28	40.6	25.8
	27.8	25	26.6
Average	28.96666667	30.93333333	30.7
SD	2.515286597	5.331666406	6.576017

Weight of mice whose data is shown in Fig 3E

	H_6-trC1INH(MGS)-MSA	H_6-MSA
	34	30
	31.4	33
	35.6	27.8
	29	30
	29.5	34.8
	27.8	31.4
Average	31.21666667	31.16667
SD	3.050519082	2.476826

Weight of all mice (n=30)
26.6
33.8
28.4

29.2
28
27.8
28
29
31
32
40.6
25
24.4
41.6
34.8
31
25.8
26.6
34
31.4
35.6
29
29.5
27.8
30

	33
	27.8
	30
	34.8
	31.4
Average	30.73448276
SD	4.102689054

S1 Appendix. (1) Protein sequences and lengths. The primary sequence of all recombinant proteins employed in this study are shown, along with the length in amino acids, the molecular weight in Daltons, and the calculated isoelectric point. (2) Raw data shown in Table 1. (3) Raw data shown in Figure 2B. (4) Raw data shown in Figure 3A, 3B, 3C, and 3D. (5) Raw data shown in Figure 3E. (6) Raw data shown in Table 2. (7) All data relating to effect of sex or weight on terminal half-life, by protein. (8) All data relating to mouse weight.

CHAPTER 3

N-terminal fusion of albumin enhances the plasma residency time of C1-esterase inhibitor

Sangavi Sivananthan[1], Varsha Bhakta[1,2], Negin Chaechi Tehrani[1], William P. Sheffield[1,2,*]

[1]Department of Pathology and Molecular Medicine, McMaster University, Hamilton, Ontario, Canada. [2]Canadian Blood Services, Innovation and Portfolio Management, Hamilton, Ontario, Canada

[*]Corresponding author

E-mail sheffiel@mcmaster.ca

Building on the concept of albumin fusion seen in Chapter 2, bridging Chapter 3 investigates whether N-terminal fusion to MSA preserves or enhances the inhibitory function of C1INH while still extending plasma residency. Comparative analyses of N- versus C-terminal fusions are performed to evaluate differences in activity, SDS stability, and *in vivo* behavior. These experiments inform optimal fusion orientation by balancing pharmacokinetics with protease inhibitory capacity, with broader implications for designing long-acting serpin therapeutics.

1. Abstract

Hereditary Angioedema (HAE) is a genetic disorder inherited in an autosomal dominant manner, characterized by unpredictable episodes of swelling due to insufficient levels or function of C1-esterase inhibitor (C1INH). C1INH plays a critical role in regulating several proteases, including plasma kallikrein (Pka). Despite its therapeutic use, most available C1INH treatments are limited by rapid clearance from circulation, reducing their effectiveness for long-term preventive therapy. Hexahistidine-tagged truncated C1INH (trC1INH lacking residues 1-97) with Mutated N-linked Glycosylation Sites N216Q/N231Q/N330Q fused to murine serum albumin (MSA) at the N-terminal (H_6-MSA-trC1INH(MGS)) was expressed in *Pichia pastoris* and purified via nickel-chelate chromatography. Twenty hours after intravenous injection in mice, the percentage dose of protein remaining in the circulation was 1.8-fold greater for H_6-MSA-trC1INH(MGS) faster than the previous fusion construct, H_6-trC1INH(MGS)-MSA, seen in Chapter 2. H_6-MSA-trC1INH(MGS) and H_6-trC1INH(MGS)-MSA did not differ significantly in second order rate constants for inhibition of Pka or C1s or in reaction stoichiometry with Pka. Our results highlight the impact of fusion orientation in modulating the pharmacokinetics of C1INH and demonstrate that N-terminal fusion with albumin enhances circulatory half-life more effectively than C-terminal fusion. These findings support further evaluation of H_6-MSA-trC1INH(MGS) in murine models of HAE.

2. Introduction

Hereditary Angioedema (HAE) is a rare autosomal dominant disorder characterized by sudden, recurrent episodes of swelling affecting the skin, gastrointestinal tract, and upper airways. Laryngeal edema, in particular, can obstruct the airway and pose a serious risk of asphyxiation [1, 2]. The condition arises from mutations in the *SERPING1* gene, which impair the production or function of C1-esterase inhibitor (C1INH), a critical serine protease inhibitor (serpin) of the contact, complement, and fibrinolytic cascades [3-9]. In type 1 HAE, both the antigenic and functional levels of C1INH are reduced, whereas in type 2 HAE, C1INH is present at normal levels but is functionally inactive.

C1INH is the largest serpin (110kDa) and its structure includes an unusual 100-residue N-terminal extension, not found in most other serpins, which houses the majority of its 10 N-linked and 24 O-linked glycosylation sites, with the exception of 3 N-linked glycosylation sites, N216, N231, and N330 (numbered according to mature protein sequence) on the serpin domain [4, 10, 11]. While studies have shown that the removal of the N-terminal extension of 97 amino acids does not significantly impair its inhibitory function, expression of a triple deglycosylation at serpin domain, truncated variant in insect cells proved challenging, pointing to a minimal requirement for glycosylation for proper folding and stability [12-14].

Among the proteases regulated by C1INH is plasma kallikrein (Pka), a key enzyme in the contact pathway [15]. Once activated, Pka cleaves high molecular weight kininogen to release bradykinin (BK), a peptide mediator that increases

vascular permeability by activating the B2 receptor on endothelial cells [16]. BK is directly implicated in the pathophysiology of HAE, with elevated levels correlating with both the severity and localization of angioedema during attacks [17, 18]. Therapeutics that replace functional C1INH or inhibit Pka have been effective in controlling disease symptoms, further supporting the central role of BK in HAE [19-22].

As clinical focus has shifted toward long-term prevention of attacks, the demand for prophylactic treatments with sustained activity has increased [23]. Unfortunately, currently approved recombinant C1INH therapies, such as Conestat Alfa, have limited circulatory half-lives and require frequent dosing, making them less suitable for prophylaxis [24]. Efforts to improve drug persistence in circulation have drawn inspiration from other protein replacement therapies where fusion to long-lived carriers like albumin has successfully extended half-life without compromising bioactivity [25-28]. Fusion of therapeutic proteins to serum albumin enhances their half-life by taking advantage of albumin's inherent longevity in circulation. This effect is largely attributed to albumin's size, stability, and ability to engage the neonatal Fc receptor (FcRn), which protects it from lysosomal degradation [29, 30]. Human serum albumin (HSA) exhibits a plasma half-life of approximately 19 days [31].

Chapter 2 demonstrated that fusion of mouse serum albumin (MSA) to the C-terminus of a simplified, truncated, and non-glycosylated form of C1INH significantly extended its half-life by 3-fold *in vivo* while preserving protease

inhibitory function. However, fusion orientation, the placement of albumin on either the N-terminus or C-terminus of the target protein, can profoundly influence the half-life of the resulting fusion construct [32, 33]. Several studies have shown that N-terminal and C-terminal fusions can differ in terms of protein stability, expression yield, steric accessibility of functional domains, and interaction with cellular receptors such as FcRn. For instance, in albumin fusion constructs involving human lactoferrin, N-terminal fusion exhibited superior pharmacokinetic profiles and biological activity compared to their C-terminal counterpart [32].

We hypothesized that the orientation of albumin fusion could also influence the pharmacokinetic properties of C1INH by further extension of plasma residence time *in vivo*, and this orientation would also not impair C1INH-mediated inhibition of Pka. Hexahistidine-tagged truncated C1INH (trC1INH lacking residues 1-97) with Mutated N-linked Glycosylation Sites N216Q/N231Q/N330Q fused to MSA at the N-terminal (H_6-MSA-trC1INH(MGS)) was compared to C-terminal fusion (H_6-trC1INH(MGS)-MSA) described in Chapter 2. We report that while both constructs retained comparable inhibitory activity toward Pka, H_6-MSA-trC1INH(MGS) exhibited further increase in circulatory half-life in mice.

3. Methods

3.1. Expression and Purification of H_6-MSA-trC1INH(MGS) in Pichia pastoris

Clone Manager 10 (Sci Ed Software LLC) was used to design oligonucleotides and synthetic DNA sequences (gBlock™) were purchased from Integrated DNA Technologies (IDT). All restriction and DNA modification

enzymes were bought from Thermo FisherScientific (Waltham, Massachusetts, United States) (XhoI, catalogue number (cat. #) FD0694, EcoRI, cat. # FD0274, AccIII, cat. # FD0534). A hexahistidine-tagged truncated C1INH98-478 with Mutated Glycosylation Sites (MGS; N216Q/N231Q/N330Q) fused to MSA in between hexahistidine-tag and $(G_4S)_3$ linker, H_6-MSA-trC1INH(MGS), was assembled by ligating a 1797 bp H_6-MSA-$(G_4S)_3$ gBlock™ product restricted with XhoI and AccIII, and a 1206 bp $(G_4S)_3$-trC1INH(MGS) gBlock™ product restricted with AccIII and EcoRI [34, 35]. These fragments were then inserted between the XhoI and EcoRI sites of pPICZ9ssamp vector to yield pPICZ9ssH_6-MSA-trC1INH(MGS). All plasmid candidates were verified by Sanger dideoxy sequencing of the relevant open reading frames by the McMaster University Genomics Facility. Purified plasmid DNA was linearized with appropriate restriction enzymes and were used to transform *Pichia pastoris (P. pastoris)* strain X-33 to Zeocin resistance. The transformed cell lines were cultured, induced with methanol, and secreted H_6-MSA-trC1INH(MGS) was purified from conditioned media using nickel-chelate affinity chromatography, as previously described [36].

3.2. Protease Inhibition Assays with H_6-MSA-trC1INH(MGS)

Second-order rate constants (k_2) and stoichiometries of inhibition (SI) were determined using chromogenic assays as described in Chapter 2. In this Chapter, the inhibitory activity of H_6-MSA-trC1INH(MGS) was evaluated against Pka and

C1s. All reagents and substrates were sourced identically as in Chapter 2, with Pka purchased from Enzyme Research Laboratories (South Bend, IN, USA; cat. # 1303), C1s from Sigma Aldrich (Oakville, ON, Canada; cat. # 204879-250UG), S2302 chromogenic substrate from DiaPharma (West Chester, OH, USA; cat.# 82034039), and Pefachrome™-C1E from DiaPharma (cat. # DPG08703). Absorbance readings were recorded at 405 nm using an Elx808 Microplate Reader (Biotek, Winooski, VT, USA). All assay conditions and data acquisition parameters were consistent with those described in Chapter 2.

3.3. Electrophoretic Analysis of H_6-MSA-trC1INH(MGS) and Pka Interaction

The formation of sodium dodecyl sulfate (SDS)-stable complexes between Pka and H_6- trC1INH(MGS)/ H_6-MSA-trC1INH(MGS) was assessed by SDS-polyacrylamide gels (SDS-PAGE), following the same procedure described in Chapter 2. Briefly, reactions containing 5 µM H_6-MSA-trC1INH(MGS) and 1 µM Pka were incubated at 37°C for 5 minutes in PPNE buffer. Reactions were terminated with 4x SDS-PAGE sample buffer, and the full reaction volumes were loaded onto 10% SDS-PAGE gels under reducing conditions. Protein bands were visualized with Coomassie Brilliant Blue staining, and gels were imaged using a Bio-Rad XR GelDoc system (Bio-Rad Laboratories, Mississauga, ON, Canada) [37].

3.4. In vivo Clearance and Protein Detection in Mice

All animal procedures were conducted using CD1 mice (Charles River, Wilmington, MA, USA) in accordance with McMaster University's Animal Research Ethics Board under Animal Utilization Protocol 20-02-06. The ARRIVE Essential 10 guidelines were followed throughout the study. Mice aged 1–2 months were housed in the Central Animal Facility and acclimatized for at least one week prior to experimentation. Anesthesia was maintained using 3% isoflurane for all procedures. The pharmacokinetic protocol followed was as described in Chapter 2, with the following modifications. In this study, only H_6-MSA-trC1INH(MGS) and control H_6-MSA were evaluated. Mice received intravenous injections of 100 µg H_6-MSA-trC1INH(MGS) or 50 µg H_6-MSA in 0.2 ml saline to ensure equimolar dosing. Blood samples were collected at 16-20 hour time points for H_6-MSA-trC1INH(MGS) and at 24-28 hour time points for H_6-MSA, based on clearance data observed in Chapter 2 and practical logistics of available space and time in the McMaster Faculty of Health Sciences Central Animal Facility. A total of 6 mice were used in this study, weighing 31 ± 4 g (mean ± standard deviation (SD)). Protein concentrations in plasma were quantified by Enzyme-Linked Immunosorbent Assay (ELISA), as previously described, using anti-human C1INH (Affinity Biologics, Ancaster, ON, Canada; cat. # GACINH) for H_6-MSA-trC1INH(MGS) detection or anti-His tag/anti-MSA (Jackson ImmunoResearch Laboratories, PA, USA; cat. # 300-065-240) for H_6-MSA detection. Standard curves ranged from 0.5 to 20 ng/ml for all constructs.

Pharmacokinetic parameters, including terminal half-life, were calculated using a two-compartment model with curve-stripping as described previously [38].

3.5. Statistical Analysis and Significance Testing

Statistical analyses were identical to those described in Chapter 2. To compare between two data sets, t-tests with Welch's corrections were conducted. Data are presented as the mean ± SD. A p-value of < 0.05 was indicative of statistical significance.

4. Results

4.1. Expression and Purification of H_6-MSA-trC1INH(MGS)

To assess the impact of albumin fusion orientation on C1INH properties, a fourth recombinant protein, H_6-MSA-trC1INH(MGS), was generated using the same *P. pastoris* expression system described in Chapter 2. Like the previously characterized constructs, H_6-trC1INH(MGS), H_6-trC1INH(MGS)-MSA, and H_6-MSA, this variant was also expressed under control of the AOX1 promoter and secreted via the *Saccharomyces cerevisiae* prepro-α factor signal sequence. Figure 1A presents a schematic overview of the recombinant constructs evaluated in this and the preceding Chapter. It consists of the first three constructs in Chapter 2, pdC1INH, H_6-trC1INH(MGS), and H_6-trC1INH(MGS)-MSA; and the new construct in this Chapter, H_6-MSA-trC1INH(MGS), in which mouse serum albumin was fused to the N-terminus of truncated, non-

glycosylated C1INH. The schematic highlights the relative positioning of the hexahistidine tag, MSA, and the trC1INH(MGS) domains across all constructs.

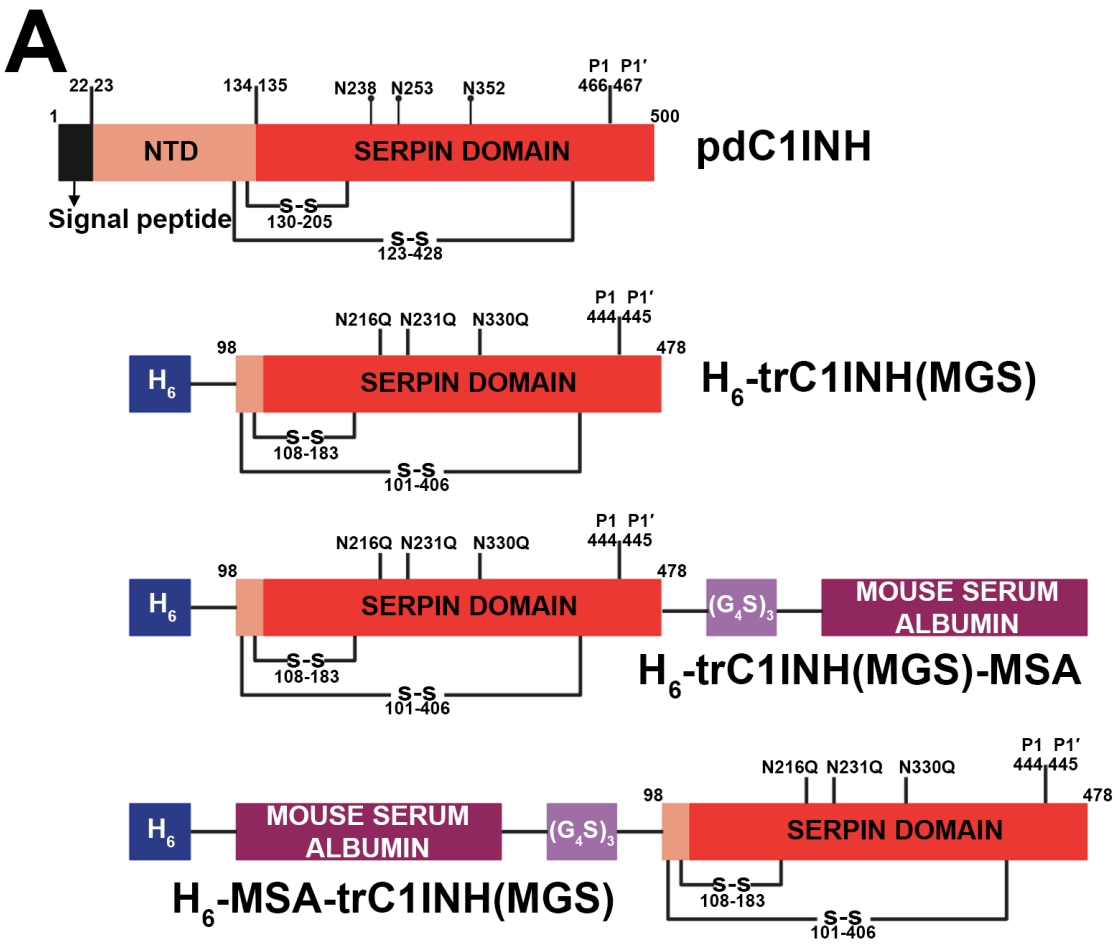

Figure 1: Schematic diagram of C1INH recombinant proteins. A) Domain organization of pdC1INH and three recombinant proteins: H_6-trC1INH(MGS) and H_6-trC1INH(MGS)-MSA as previously described in Chapter 2, and the newly generated H_6-MSA-trC1INH(MGS).

4.2. Characterization of H_6-MSA-trC1INH(MGS) compared to Chapter 2

The kinetics of protease inhibition by H_6-MSA-trC1INH(MGS) were compared to those seen in Chapter 2 for H_6-trC1INH(MGS), H_6-trC1INH(MGS)-MSA, and pdC1INH (Table 1). The inhibitory effects of H_6-MSA-trC1INH(MGS) on C1s were comparable to those observed for H_6-trC1INH(MGS), H_6-trC1INH(MGS)-MSA, and pdC1INH. Additionally, H_6-MSA-trC1INH(MGS) and H_6-trC1INH(MGS)-MSA similarly inhibited Pka by a 1.5-fold reduction, relative to pdC1INH. Similarly, the mean SI values showed a significant 2-fold increase regardless of position of the MSA fusion, relative to pdC1INH. These results indicate modest but significant reductions in both the rate and efficiency of inhibition for the rC1INH variants compared to their pdC1INH counterpart.

Table 1: Pharmacokinetic characterization of activity of C1INH proteins.

Protein name	k_2 vs Pka (x $10^4 M^{-1}s^{-1}$)	k_2 vs C1s (x $10^4 M^{-1}s^{-1}$)	SI with Pka
pdC1INH	2.3 ± 0.2^^****°°°°	5.7 ± 0.5	3.3 ± 0.06^^^****°°°°
H_6-trC1INH(MGS)	2.01 ± 0.07****°°°	5 ± 0.5	5.3 ± 0.3**°°°
H_6-trC1INH(MGS)-MSA	1.3 ± 0.08	5.1 ± 0.4	6.9 ± 0.1
H_6-MSA-trC1INH(MGS)	1.5 ± 0.2	5.1 ± 0.2	7.4 ± 1.0
Results are the mean of 3-5 determinations, ± SD; ^^, p<0.01 versus H_6-trC1INH(MGS); ^^^, p<0.001 versus H_6-trC1INH(MGS); **, p<0.01 versus H_6-trC1INH(MGS)-MSA; ****,			

p<0.0001 versus H_6-trC1INH(MGS)-MSA; ˚˚˚, p<0.001 versus H_6-MSA-trC1INH(MGS); ˚˚˚˚, p<0.0001 versus H_6-MSA-trC1INH(MGS)

In Chapter 2, it was noted that C1INH-dependent high molecular weight complexes formed when Pka was reacted with an excess of either pdC1INH or H_6-trC1INH(MGS), with complex sizes of approximately 142 kDa and 80 kDa, respectively. However, no high molecular weight serpin-enzyme complex was observed with H_6-trC1INH(MGS)-MSA. Instead, when Pka was incubated with excess H_6-trC1INH(MGS)-MSA, the Pka catalytic light chain was consumed to a similar extent as in the reaction with H_6-trC1INH(MGS), but two new polypeptide chains of approximately 70 kDa and 40 kDa were generated from H_6-trC1INH(MGS)-MSA. It was unclear if a H_6-trC1INH(MGS)-Pka covalent complex (80 kDa) also formed and comigrated with the broad unreacted H_6-trC1INH(MGS)-MSA band. In this study, we demonstrated that changing the MSA fusion from the C-terminus to the N-terminus allowed the detection of C1INH-dependent high molecular weight complexes (Figure 2A). Under identical conditions, reactions with Pka and excess H_6-MSA-trC1INH(MGS) resulted in the formation of high molecular weight complexes of approximately 147 kDa. This was compared to H_6-trC1INH(MGS) which mediated the formation of high molecular weight complexes of approximately 80 kDa.

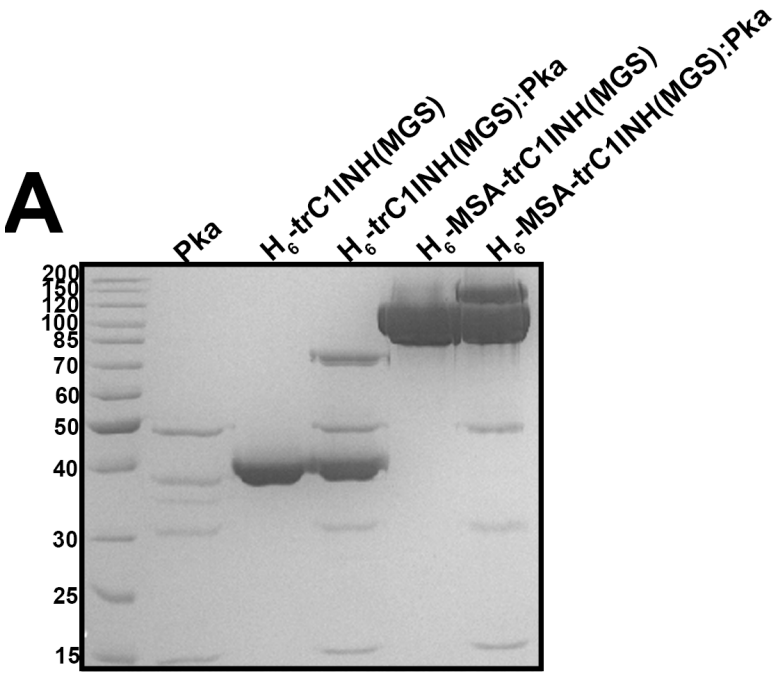

Figure 2: Complex characterization of C1INH proteins. Gel-based assays of complex formation. 10% SDS-PAGE gels are shown electrophoresed under reducing conditions and stained with Coomassie Brilliant Blue. A) Serpins (H_6-trC1INH(MGS), H_6-MSA-trC1INH(MGS)) were reacted with Pka at a 5:1 molar ratio for 5 minutes at 37°C.

4.3. Further Extension of Plasma Half-life with H_6-MSA-trC1INH(MGS)

In Chapter 2, we established that fusion of MSA to the C-terminus of trC1INH(MGS) significantly enhanced its circulatory half-life in mice compared to the unfused variant. However, clearance profiles for MSA containing constructs, H_6-trC1INH(MGS)-MSA and H_6-MSA, remained incompletely resolved beyond the 4-hour time point due to animal sampling restrictions, prompting a follow-up experiment with additional sampling at 16-28 hours post-injection. Those results

showed that H_6-trC1INH(MGS)-MSA and H_6-MSA persisted in the plasma at levels of 19 ± 1% and 22 ± 1%, respectively, at 16–28 hours. Building on these findings, we next sought to determine whether N-terminal fusion of albumin, H_6-MSA-trC1INH(MGS), could further enhance circulatory half-life. Mice were injected with either H_6-MSA-trC1INH(MGS) or H_6-MSA at equimolar doses, and plasma samples were collected between 16-28 hours post-injection. As shown in Figure 3A, H_6-trC1INH(MGS)-MSA were compared to H_6-MSA-trC1INH(MGS) and H_6-MSA. H_6-MSA-trC1INH(MGS) exhibited significantly improved plasma residency compared to the previously tested C-terminal fusion. After 20 hours, 35 ± 2% of H_6-MSA-trC1INH(MGS) remained in circulation, representing a 1.8-fold increase over the 19 ± 1% observed for H_6-trC1INH(MGS)-MSA.

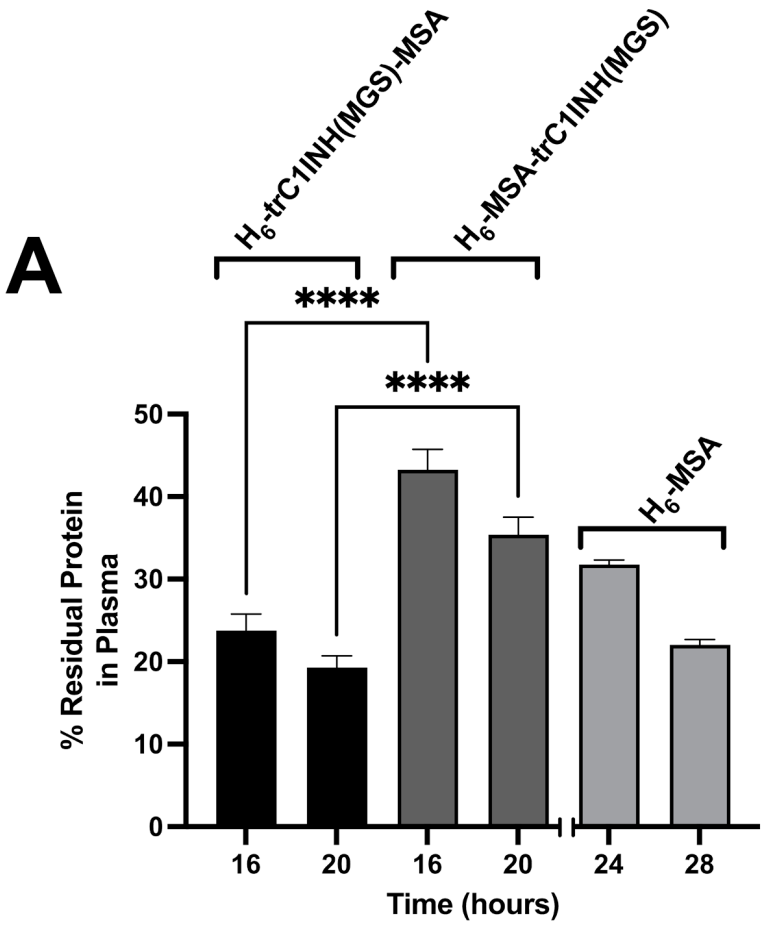

Figure 3: Protein clearance of H_6-trC1INH(MGS)-MSA, H_6-MSA-trC1INH(MGS), and H_6-MSA. Percentage residual protein in plasma at the times, in hours, specified on the x axis, following injection of H_6-trC1INH(MGS)-MSA (black bars), H_6-MSA-trC1INH(MGS) (dark grey bars) or H_6-MSA (light grey bars).

5. Discussion

The overarching objective of this research was to enhance the pharmacokinetic properties of C1INH through a different orientation of fusion with MSA based on results observed in Chapter 2, thereby addressing the limitations

associated with approved on-demand available treatments' rapid clearance from circulation [19, 39]. Building upon the findings from Chapter 2, where the C-terminal fusion construct H_6-trC1INH(MGS)-MSA demonstrated prolonged plasma half-life compared to the unfused variant, this Chapter explored the effects of N-terminal fusion, resulting in the novel construct H_6-MSA-trC1INH(MGS).

The inhibitory efficacy of C1INH against its target proteases, particularly Pka and, less importantly, C1s, is pivotal for its therapeutic potential in conditions like HAE [40]. In Chapter 2, H_6-trC1INH(MGS)-MSA retained substantial inhibitory activity against C1s, comparable to pdC1INH. However, a notable reduction in Pka inhibition was observed, with a 45.2% decrease in k_2 compared to pdC1INH. This Chapter introduced H_6-MSA-trC1INH(MGS), with the hypothesis that repositioning MSA might alleviate the reduction of Pka inhibition observed with the C-terminal fusion. However, H_6-MSA-trC1INH(MGS) inhibited Pka similarly to H_6-trC1INH(MGS)-MSA, therefore it was still below the level of activity demonstrated by pdC1INH. Moreover, the SI remained elevated for both fusion constructs relative to pdC1INH, suggesting that while fusion orientation influenced activity, complete restoration to pdC1INH levels may require additional modifications. The observed decrease in Pka inhibition could be attributed to specific steric or conformational hindrance, as C1s inhibition remained unaffected. Previous studies indicate that C1INH possesses multiple secondary sites for C1s interaction [41, 42], but such sites do not exist for Pka. Since Pka

inhibition primarily relies on active site interactions, the MSA fusion may cause C1INH to adopt a different conformation or introduce steric hindrance, limiting its efficacy against Pka. While the $(G_4S)_3$ linker is widely used to provide flexibility between protein domains in fusion constructs, its effectiveness can vary depending on the specific proteins involved. In some cases, the $(G_4S)_3$ linker may not provide sufficient separation between domains, potentially leading to steric hindrance or conformational constraints that affect the functionality of the fusion protein. For instance, studies have shown that flexible $(G_4S)_3$ linkers did not increase the hydrodynamic radius of fused IgG molecule, suggesting this linker does not provide increased separation between domains in certain contexts [43]. Xylose containing glycans have recently been observed at Ser residues in $(G_4S)_3$ linkers as “GSG” is a motif for O-xylosation [44, 45]. This can result in undesirable heterogeneity that may affect protein quality, a potential reason why the fused constructs lost equivalent function. While the $(G_4S)_3$ linker is a common choice for providing flexibility in fusion proteins, its suitability should be evaluated in the context of the specific proteins being fused. Alternative linkers, such as longer flexible linkers or rigid linkers, may be more appropriate in cases where greater separation between domains is necessary to maintain functionality [46].

An intriguing observation from Chapter 2 was the apparent inability of H_6-trC1INH(MGS)-MSA to form detectable SDS-stable complexes with Pka, despite evidence of inhibitory activity. This phenomenon raised questions about the nature of the interaction between the fusion protein and Pka. In contrast, H_6-

MSA-trC1INH(MGS) demonstrated the formation of such complexes, akin to pdC1INH and the unfused truncated variant. The formation of SDS-stable complexes is indicative of a covalent interaction between the serpin and its target protease, a hallmark of effective inhibition. The lack of such complexes in the C-terminal fusion suggests either difficulties in visualizing the covalent complex band on SDS-PAGE gels, a possible shift towards a non-covalent inhibitory mechanism, or an altered conformational state that precluded stable complex formation. While there are limited studies on serpin-albumin fusion proteins, such effects have been observed in non-serpin fusion proteins. For example, thioredoxin-1 (Trx), a redox-active protein involved in maintaining homeostasis, retains only 60% of its activity when fused to HSA at the C-terminus [47]. Further studies indicated that potential protein-protein interactions between Trx and HSA contributed to this reduction in activity. Extrapolating from this example, future studies could investigate potential interactions between C1INH and MSA to determine their impact on Pka interactions. This discrepancy emphasizes the influence of fusion orientation on the mechanistic aspects of protease inhibition and warrants further structural investigations to elucidate the underlying causes.

A central aim of this research was to extend the circulatory half-life of C1INH, thereby enhancing its therapeutic utility. Chapter 2 demonstrated that H_6-trC1INH(MGS)-MSA significantly prolonged plasma residency compared to the unfused variant, attributed to the increased molecular weight and potential engagement with FcRn recycling pathway [48]. Building upon this, this Chapter

assessed the pharmacokinetics of H_6-MSA-trC1INH(MGS). The findings revealed a further enhancement in plasma residence time, with the N-terminal fusion exhibiting a 1.8-fold increase in residual levels at 20 hours post-injection compared to the C-terminal fusion. This trend aligns with findings from studies comparing N-terminal and C-terminal HSA fusions. For instance, Ueda et al., evaluated the clearance of human lactoferrin (hLF) fused to HSA at either terminus and found that while both configurations extended the half-life, hLF-HSA and HSA-hLF exhibited approximately 3.3- and 20.7-fold increases in circulation time, respectively [32]. These data suggest that the positioning of albumin in the fusion construct plays a critical role in influencing circulatory half-life, emphasizing the need for strategic placement in the design of fusion proteins to optimize pharmacokinetics.

The prolonged pharmacokinetics and functional stability observed with N-terminal albumin fusion compared to C-terminal fusion constructs may be attributed to structural preservation and optimal receptor engagement. Albumin interacts with FcRn primarily through its domain III, located near the C-terminal region [49]. Fusion at the albumin C-terminus places C1INH at a position that is less disruptive to albumin's critical internal FcRn-binding domains, thereby preserving its interaction with FcRn, promoting efficient receptor mediated recycling, and prolonging the circulating half-life of the fusion construct. Although the C-terminal domain III of albumin contains the principal binding site, the N-terminal domain I is important for optimal FcRn binding [49]. This suggests that

perhaps N-terminal end of albumin needs to be free for optimal binding otherwise it can indirectly perturb the albumin structure and hinder FcRn binding sites.

The insights gained from this research have significant implications for the development of long-acting C1INH therapeutics. The enhanced plasma half-life observed with the N-terminal fusion suggests a promising avenue for therapeutic optimization. However, the residual reduction in activity compared to pdC1INH indicates that further refinements are necessary. Future strategies may involve the incorporation of cleavable linkers to release active C1INH post-circulation, thereby mitigating steric hindrance. Additionally, exploring alternative fusion partners or engineering mutations to enhance protease specificity and binding affinity could further improve therapeutic efficacy. The use of HSA in place of MSA is obligatory for clinical translation, considering immunoreactivity and species-specific interactions with FcRn. Moreover, evaluating the performance of these constructs in humanized mouse models expressing human FcRn would provide more accurate assessments of their pharmacokinetic and pharmacodynamic profiles, facilitating the progression towards clinical application [50, 51].

This study underscores the critical role of fusion orientation in modulating the functional and pharmacokinetic properties of C1INH fusion proteins. The N-terminal fusion construct, H_6-MSA-trC1INH(MGS), demonstrated superior pharmacokinetic attributes compared to its C-terminal counterpart. These findings contribute valuable knowledge to the field of therapeutic protein engineering and

lay the groundwork for the potential development of optimized long-acting C1INH therapies for conditions such as HAE.

6. References

1. Donaldson, V.H. and R.R. Evans, *A Biochemical Abnormality in Herediatry Angioneurotic Edema: Absence of Serum Inhibitor of C' 1-Esterase.* Am J Med, 1963. **35**: p. 37-44.
2. Landerman, N.S., et al., *Hereditary angioneurotic edema. II. Deficiency of inhibitor for serum globulin permeability factor and/or plasma kallikrein.* J Allergy, 1962. **33**: p. 330-41.
3. Davis, A.E., 3rd, *C1 inhibitor and hereditary angioneurotic edema.* Annu Rev Immunol, 1988. **6**: p. 595-628.
4. Huber, R. and R.W. Carrell, *Implications of the three-dimensional structure of alpha 1-antitrypsin for structure and function of serpins.* Biochemistry, 1989. **28**(23): p. 8951-66.
5. Gregorek, H., et al., *Concentration of C1 inhibitor in sera of healthy blood donors as studied by immunoenzymatic assay.* Complement Inflamm, 1991. **8**(5-6): p. 310-2.
6. Caliezi, C., et al., *C1-Esterase inhibitor: an anti-inflammatory agent and its potential use in the treatment of diseases other than hereditary angioedema.* Pharmacol Rev, 2000. **52**(1): p. 91-112.
7. Cugno, M., et al., *In vitro interaction of C1-inhibitor with thrombin.* Blood Coagul Fibrinolysis, 2001. **12**(4): p. 253-60.
8. Han, E.D., et al., *Increased vascular permeability in C1 inhibitor-deficient mice mediated by the bradykinin type 2 receptor.* J Clin Invest, 2002. **109**(8): p. 1057-63.
9. Relan, A., et al., *Recombinant C1-inhibitor: effects on coagulation and fibrinolysis in patients with hereditary angioedema.* BioDrugs, 2012. **26**(1): p. 43-52.
10. Zahedi, K., A.E. Prada, and A.E. Davis, 3rd, *Structure and regulation of the C1 inhibitor gene.* Behring Inst Mitt, 1993(93): p. 115-9.
11. Stavenhagen, K., et al., *N- and O-glycosylation Analysis of Human C1-inhibitor Reveals Extensive Mucin-type O-Glycosylation.* Mol Cell Proteomics, 2018. **17**(6): p. 1225-1238.
12. Coutinho, M., K.S. Aulak, and A.E. Davis, 3rd, *Functional analysis of the serpin domain of C1 inhibitor.* J Immunol, 1994. **153**(8): p. 3648-54.
13. Bos, I.G., et al., *The functional integrity of the serpin domain of C1-inhibitor depends on the unique N-terminal domain, as revealed by a pathological mutant.* J Biol Chem, 2003. **278**(32): p. 29463-70.

14. Rossi, V., et al., *Functional characterization of the recombinant human C1 inhibitor serpin domain: insights into heparin binding.* J Immunol, 2010. **184**(9): p. 4982-9.
15. Gigli, I., et al., *Interaction of plasma kallikrein with the C1 inhibitor.* J Immunol, 1970. **104**(3): p. 574-81.
16. Su, J.B., *Kinins and cardiovascular diseases.* Curr Pharm Des, 2006. **12**(26): p. 3423-35.
17. Nussberger, J., et al., *Plasma bradykinin in angio-oedema.* Lancet, 1998. **351**(9117): p. 1693-7.
18. Nussberger, J., et al., *Local bradykinin generation in hereditary angioedema.* J Allergy Clin Immunol, 1999. **104**(6): p. 1321-2.
19. Farkas, H. and L. Varga, *Ecallantide is a novel treatment for attacks of hereditary angioedema due to C1 inhibitor deficiency.* Clin Cosmet Investig Dermatol, 2011. **4**: p. 61-8.
20. Duffey, H. and R. Firszt, *Management of acute attacks of hereditary angioedema: role of ecallantide.* J Blood Med, 2015. **6**: p. 115-23.
21. Johnson, N.M. and M.A. Phillips, *New Treatments for Hereditary Angioedema.* Skin Therapy Lett, 2018. **23**(1): p. 6-8.
22. Longhurst, H., *Optimum Use of Acute Treatments for Hereditary Angioedema: Evidence-Based Expert Consensus.* Front Med (Lausanne), 2017. **4**: p. 245.
23. Li, H.H., *Hereditary angioedema: Long-term prophylactic treatment.* Allergy Asthma Proc, 2020. **41**(Suppl 1): p. S35-S37.
24. Davis, B. and J.A. Bernstein, *Conestat alfa for the treatment of angioedema attacks.* Ther Clin Risk Manag, 2011. **7**: p. 265-73.
25. Malec, L.M., et al., *The impact of extended half-life factor concentrates on prophylaxis for severe hemophilia in the United States.* Am J Hematol, 2020. **95**(8): p. 960-965.
26. Pestel, S., et al., *FVIII half-life extension by coadministration of a D'D3 albumin fusion protein in mice, rabbits, rats, and monkeys.* Blood Adv, 2020. **4**(9): p. 1870-1880.
27. Chia, J., et al., *Increased potency of recombinant VWF D'D3 albumin fusion proteins engineered for enhanced affinity for coagulation factor VIII.* J Thromb Haemost, 2021. **19**(11): p. 2710-2725.
28. Pasca, S. and E. Zanon, *Albumin-Fusion Recombinant FIX in the Management of People with Hemophilia B: An Evidence-Based Review.* Drug Des Devel Ther, 2022. **16**: p. 3109-3116.
29. Sleep, D., J. Cameron, and L.R. Evans, *Albumin as a versatile platform for drug half-life extension.* Biochim Biophys Acta, 2013. **1830**(12): p. 5526-34.
30. Andersen, J.T., et al., *Extending serum half-life of albumin by engineering neonatal Fc receptor (FcRn) binding.* J Biol Chem, 2014. **289**(19): p. 13492-502.
31. Peters, T., Jr., *Serum albumin.* Adv Protein Chem, 1985. **37**: p. 161-245.

32. Ueda, K., et al., *Albumin fusion at the N-terminus or C-terminus of human lactoferrin leads to improved pharmacokinetics and anti-proliferative effects on cancer cell lines.* Eur J Pharm Sci, 2020. **155**: p. 105551.
33. Li, T., et al., *Albumin Fusion at the N-Terminus or C-Terminus of HM-3 Leads to Improved Pharmacokinetics and Bioactivities.* Biomedicines, 2021. **9**(9).
34. Sheffield, W.P., et al., *Prolonged in vivo anticoagulant activity of a hirudin-albumin fusion protein secreted from Pichia pastoris.* Blood Coagul Fibrinolysis, 2001. **12**(6): p. 433-43.
35. Sheffield, W.P., et al., *Recombinant albumins containing additional peptide sequences smaller than barbourin retain the ability of barbourin-albumin to inhibit platelet aggregation.* Thromb Haemost, 2005. **93**(5): p. 914-21.
36. Sheffield, W.P., et al., *A long-lasting, plasmin-activatable thrombin inhibitor aids clot lysis in vitro and does not promote bleeding in vivo.* Thromb Haemost, 2009. **101**(5): p. 867-77.
37. Hamada, M., et al., *Stepwise Reversion of Multiply Mutated Recombinant Antitrypsin Reveals a Selective Inhibitor of Coagulation Factor XIa as Active as the M358R Variant.* Front Cardiovasc Med, 2021. **8**: p. 647405.
38. Sheffield, W.P., et al., *Effects of genetic fusion of factor IX to albumin on in vivo clearance in mice and rabbits.* Br J Haematol, 2004. **126**(4): p. 565-73.
39. Riedl, M., *Recombinant human C1 esterase inhibitor in the management of hereditary angioedema.* Clin Drug Investig, 2015. **35**(7): p. 407-17.
40. Levi, M., D.M. Cohn, and S. Zeerleder, *Hereditary angioedema: Linking complement regulation to the coagulation system.* Res Pract Thromb Haemost, 2019. **3**(1): p. 38-43.
41. He, S., R.B. Sim, and K. Whaley, *A secondary C1s interaction site on C1-inhibitor is essential for formation of a stable enzyme-inhibitor complex.* FEBS Lett, 1997. **405**(1): p. 42-6.
42. He, S., et al., *Role of the distal hinge region of C1-inhibitor in the regulation of C1s activity.* FEBS Lett, 1997. **412**(3): p. 506-10.
43. Klein, J.S., et al., *Design and characterization of structured protein linkers with differing flexibilities.* Protein Eng Des Sel, 2014. **27**(10): p. 325-30.
44. Wen, D., et al., *Discovery and investigation of O-xylosylation in engineered proteins containing a (GGGGS)n linker.* Anal Chem, 2013. **85**(9): p. 4805-12.
45. Spahr, C., et al., *High-resolution mass spectrometry confirms the presence of a hydroxyproline (Hyp) post-translational modification in the GGGGP linker of an Fc-fusion protein.* MAbs, 2017. **9**(5): p. 812-819.
46. Chen, X., J.L. Zaro, and W.C. Shen, *Fusion protein linkers: property, design and functionality.* Adv Drug Deliv Rev, 2013. **65**(10): p. 1357-69.
47. Ikuta, S., et al., *Albumin fusion of thioredoxin--the production and evaluation of its biological activity for potential therapeutic applications.* J Control Release, 2010. **147**(1): p. 17-23.

48. Tao, H.Y., et al., *The development of human serum albumin-based drugs and relevant fusion proteins for cancer therapy.* Int J Biol Macromol, 2021. **187**: p. 24-34.
49. Sand, K.M., et al., *Interaction with both domain I and III of albumin is required for optimal pH-dependent binding to the neonatal Fc receptor (FcRn).* J Biol Chem, 2014. **289**(50): p. 34583-94.
50. Conner, C.M., et al., *A precisely humanized FCRN transgenic mouse for preclinical pharmacokinetics studies.* Biochem Pharmacol, 2023. **210**: p. 115470.
51. Proetzel, G. and D.C. Roopenian, *Humanized FcRn mouse models for evaluating pharmacokinetics of human IgG antibodies.* Methods, 2014. **65**(1): p. 148-53.

CHAPTER 4

Enhancement of plasma kallikrein specificity of antitrypsin variants identified by phage display and partial reversion

Sangavi Sivananthan[1], Tyler Seto[1], Negin C. Tehrani[1], Varsha Bhakta[1,2], and William P. Sheffield[1,2,3]

[1]Department of Pathology and Molecular Medicine, McMaster University, Hamilton, Ontario, Canada. [2]Canadian Blood Services, Innovation and Portfolio Management, Medical Affairs and Innovation, Hamilton, Ontario, Canada

[3]To whom correspondence should be addressed:

Dr. William P. Sheffield, Professor, Department of Pathology and Molecular Medicine HSC 4H19, McMaster University, 1280 Main Street West, Hamilton, ON L8S 4K1 Canada; E-mail: sheffiel@mcmaster.ca

Sivananthan, S., Seto, T., Tehrani, N. C., Bhakta, V., & Sheffield, W. P. (2025). Enhancement of plasma kallikrein specificity of antitrypsin variants identified by phage display and partial reversion. *BMC Biotechnology*, *25*(1), 22. https://doi.org/10.1186/s12896-025-00956-8

Chapter 4 employs T7 phage display to screen the hypervariable regions of the AAT M358R RCL. Separate libraries spanning the P7-P3 and P2-P3′ regions are

constructed and screened against Pka. Enrichment analysis via deep sequencing identifies consensus motifs, which are then validated using biochemical assays. This high-throughput approach uncovers selective motifs for Pka inhibition and characterizes the contribution of specific residues to target specificity.

1. Abstract

Background: The naturally occurring variant Alpha-1 Antitrypsin M358R (AAT M358R), modified at the P1 position of the reactive center loop (RCL), shifts its inhibitory protease target from neutrophil elastase to multiple coagulation and contact proteases, including activated plasma kallikrein (Pka; KLKB1). Our aim was to increase the specificity of AAT M358R for Pka as a potential novel therapeutic agent to treat pathological swelling arising from elevated Pka levels in patients with Hereditary Angioedema (HAE).

Results: Two AAT M358R T7Select phage display libraries randomized at RCL positions P7-P3 and P2-P3' were iteratively probed with Pka. The most abundant Pka-inhibitory motifs from phage display were P7-P3, **Q**L**IPS**; and P2-P3', **V**R**RAY** (mutated residues in bold). AAT variants expressing these motifs, alone or in combination, as well as six less-mutated P7-P3' revertant proteins were expressed, purified, and characterized kinetically. Variants AAT M358R (QLIPS) (designated 7-QLIPS-3) and 7-FLEPS-3 exhibited significantly enhanced selectivity for Pka (over factor XIa) by factors of 6.9 and 9.2, respectively, without

increasing the stoichiometry of inhibition (SI) or decreasing the inhibition rate relative to AAT M358R. No other variants matched this profile.

Conclusions: Pro substitution at P4 was found to be important for enhanced inhibition of Pka by AAT M358R. Two novel variants with this substitution are more rapid and selective inhibitors of Pka than AAT M358R and may provide better control of Pka *in vivo* than existing HAE therapeutics.

Word count: 229

Keywords

Phage display, alpha-1 antitrypsin, plasma kallikrein, mutagenesis, reactive centre loop, hereditary angioedema

2. Introduction

Hereditary Angioedema (HAE) is an autosomal dominant disease marked by recurrent episodes of acute swelling affecting different body regions (Donaldson and Evans 1963; Landerman, et al. 1962; Wedner 2020). HAE is classified into three types: Type 1, arising from quantitative genetic deficiency of C1-esterase inhibitor (C1INH); Type 2, arising from quantitative genetic deficiency of functional C1INH; and the more rare Type 3, arising from genetic lesions in genes other than that encoding C1INH (C1INH) (Davis 1988; Sinnathamby, et al. 2023; Zahedi, et al. 1993). C1INH, a serpin that regulates biological processes, plays a pivotal role in inhibiting various proteases, including activated plasma kallikrein (Pka) (Gigli, et al. 1970; Grover, et al. 2023;

Karnaukhova 2022). Pka catalyzes the cleavage of high molecular weight kininogen, liberating bradykinin, a key mediator of vasodilation and increased permeability during inflammation (Lin, et al. 2017; Motta, et al. 2023; Schmaier 2016; Wu 2015). Despite C1INH being recognized as the primary inhibitor of Pka, and replacement therapy with C1INH concentrates being the first specific therapy to show efficacy in ameliorating HAE, C1INH has limitations due to its broad-spectrum inhibition of various proteases and its relatively slow speed of inhibition of Pka illustrated by a mean second order rate constant (k_2) of ~2.55 x 10^4 $M^{-1}s^{-1}$ (Kajdacsi, et al. 2020; Wuillemin, et al. 1996). While many pharmacological agents have been licensed for Pka control, some suffer from short half-lives (Markland, et al. 1996; Martello, et al. 2012; Stolz and Horn 2010) rendering them unsuitable for prophylactic administration, while other newer agents appropriate for prophylaxis are associated with high costs (Banerji, et al. 2022; Syed 2019; Wedi 2019). Opportunities remain, therefore, to develop new molecules for the optimal control of Pka in HAE, including engineered versions of other serpins.

The most abundant serpin in plasma, Alpha-1 Antitrypsin (AAT), exerts minimal influence on the contact system and primarily targets neutrophil elastase. However, a point mutation changing M358 to R358 (M358R), in the reactive center of AAT changes its specificity from inhibiting neutrophil elastase to inhibiting multiple coagulation/contact system proteases (Heeb, et al. 1990; Owen, et al. 1983; Schapira, et al. 1986; Scott, et al. 1986; Travis, et al. 1986). Inspired by this “experiment of nature”, researchers have made additional

modifications within the reactive center loop (RCL) of AAT M358R to enhance specificity toward coagulation and contact proteases (Bhakta, et al. 2021; de Maat, et al. 2019; Hamada, et al. 2021; Patston, et al. 1990; Scott, et al. 2014). One strategy for introducing and assessing RCL mutations involves creating serpin libraries with hypervariable RCL positions. Such a library can be functionally screened through phage display and biopanning, a method utilizing bait proteases in solution to probe variant proteins expressed on the T7 phage surface (de Souza, et al. 2018; Deng, et al. 2018).

Herein, two AAT M358R phage display libraries hypervariable between P7-P3' were screened with Pka. Novel AAT M358R variants were expressed corresponding to the most abundant motifs, their combination, and their reversion towards AAT M358R. Our findings indicated that two novel mutated proteins demonstrated enhanced selectivity for Pka over activated factor XI (FXIa) without altering the rate of PKa inhibition or increasing the stoichiometry of inhibition (SI) relative to AAT M358R.

3. Methods

3.1. Materials

Purified human proteases Pka and FXIa were purchased from Enzyme Research Labs (South Bend, IN, USA). Chromogenic substrates (S-2302 for Pka and S-2366 for FXIa) were purchased from Diapharma (West Chester, OH, USA). Oligonucleotides were obtained from Integrated DNA Technologies (Coralville, IO, USA). Restriction endonucleases, thermostable DNA polymerase

and buffers for PCR, gel extraction/purification kits, and glutathione agarose were obtained from ThermoFisher Scientific (Waltham, MA, USA). Nickel-nitrilotriacetic acid (Ni-NTA) agarose resin for nickel chelate affinity chromatography was obtained from Qiagen (Mississauga, Canada). PreScission protease, a fusion protein of glutathione sulfotransferase (GST)-human rhinovirus (HRV) 3C protease, was acquired from ThermoFisher Scientific. Phage display libraries and plasmids pBAD-$H_6\alpha_1$PI M358R and pGEX-AAT M358R were generated previously by the Sheffield Laboratory (Bhakta, et al. 2021).

3.2. DNA Manipulation

Standard DNA manipulation techniques, including restriction digestion, electrophoresis, gel purification, ligation, and transformation of *E. coli*, were employed as previously described (Bhakta, et al. 2021). Cloning steps involved the use of *E. coli* DH5α, while *E. coli* BL21 was utilized for protein expression. All AAT M358R variant plasmids were verified by DNA sequencing at the Mobix Lab central facility, located in the Faculty of Health Sciences at McMaster University.

3.3. Biopanning of Phage Display Libraries

T7Select10-3b API M358R(P7-P3ran) and T7Select10-3b API M358R(P2-P3' ran) bacteriophage libraries were biopanned as previously described, with minor modifications (Scott, et al. 2014). Briefly, five rounds of biopanning with or without Pka were performed with each library, starting with 10^9 pfu/ml

bacteriophage in liquid lysates. Phage populations reacting with Pka were captured using a biotinylated affinity-purified rabbit anti-human kallikrein IgG polyclonal antibody (Cusabio Technology, Houston, USA) and streptavidin-coated magnetic beads (Dynabeads, Invitrogen). The phage-antibody-bead assembly was used to infect *E. coli* BLT5403 cells to start subsequent rounds of biopanning.

To determine the phage titer in the lysate, a plaque assay was performed. *E. coli* BLT5403 was inoculated in Luria Broth (LB) with M9 salts (M9LB) and incubated at 37°C until the OD_{600} reached 1.0. Phage lysate dilutions (in LB) were separately plated on LB with ampicillin (LB-Amp) agar plates with *E. coli* BLT5403 M9LB growth culture (250µl), a dilution of phage lysate (100µl), and top agarose (4ml). The plates were inverted, covered, and incubated overnight at room temperature for plaque counting.

3.4. Deep Sequencing

Variant RCL sequences selected by AAT M358R phage display were determined using deep sequencing of polymerase chain reaction (PCR) products, as previously described (Scott, et al. 2014). Amplification of candidates was performed using phage lysates from: the starting library, the round 2 library selected with or without Pka, and the round 5 library selected with or without Pka. Sense oligonucleotides P504 and P505 were used, paired with antisense oligonucleotides P710, P711, and P712. The amplified products were analyzed

on a 1.2% agarose gel, purified using a gel extraction kit (GeneJet Gel Extraction kit, ThermoFisher), and subjected to direct deep sequencing at McMaster University's Farncombe Metagenomics Facility, using an Illumina Nextra XT library kit. For sequence analysis, Linux operating software was used to convert FASTQ raw data files into FASTA format. The most abundant DNA and translated protein sequences in the phage lysate were identified using Clone Manager 7.11 software (Sci Ed Software, Westminster, Colorado, USA).

3.5. GST Expression and Purification

Expression vector pGEX-AAT M358R was created previously as described (Bhakta, et al. 2021). Each novel variant in this study was mobilized as a 1221 bp SalI-NcoI-ended minor fragment and ligated to the 4960 bp major fragment of pGEX-AAT M358R to create pGEX-AAT M358R(X) (where X is the motif of interest). *E. coli* BL21 transformed with pGEX-AAT M358R(X) variants were induced using 0.1mM isopropyl β-D-1-thiogalactopyranoside (IPTG), and purified using GST and nickel chelate (Ni-NTA) affinity chromatography purification methods, as previously described (Bhakta, et al. 2021).

3.6. Protease Inhibition Assays with AAT M358R Variants

k_2 and SI values were determined for all AAT M358R variants by a discontinuous method, under pseudo-first order conditions, using chromogenic assays. The velocity of amidolysis of chromogenic substrates S-2302 and S-2366

was evaluated at 37°C in PPNE buffer (20mM sodium phosphate (pH 7.4), 0.1% (w/v) polyethylene glycol 8000, 100mM sodium chloride, and 0.1mM disodium ethylenediaminetetraacetic acid) using an Elx808 Absorbance Microplate Reader (Biotek, Winooski, VT, USA) at 405nm. For k_2 determination, reactions included 10nM Pka/FXIa and 200nM AAT M358R variants, incubated for 8-30s intervals and stopped with 100μM S-2302/S-2366 chromogenic substrate, respectively. For SI determination, reactions included 10nM Pka/FXIa and 10-1000nM AAT M358R variants, incubated for 2h and stopped with 100μM S-2302/S-2366 chromogenic substrate. k_2 and SI were calculated as described previously (Bhakta, et al. 2021).

3.7. Plasma Clotting Tests

The effects of AAT M358R or AAT M358R(X) proteins on *in vitro* clotting were assessed by measuring the diluted Activated Partial Thromboplastin Time, as previously described (Bhakta, et al. 2021; de Maat, et al. 2019). Briefly, STA PTTA reagent (Diagnostica Stago, Asnières, France) was diluted 1:15 with Owren-Koller buffer (Diagnostica Stago). Normal human pooled plasma was supplemented with AAT M358R or variant protein to 3 μM final concentration, combined with diluted PTTA reagent, and pre-heated to 37ºC. Citrate anticoagulation was overcome by the addition of 50 μL of 25 mM $CaCl_2$, and clotting time was determined using a STA-IV clotting analyzer (Diagnostica Stago).

3.8. Electrophoretic Analysis of AAT M358R Variants with Pka/FXIa Interactions

The electrophoretic profiles of the interaction between AAT M358R or AAT M358R(X) variants with Pka/FXIa were visualized on 10% (w/vol) sodium dodecyl sulfate (SDS)-polyacrylamide (SDS-PAGE) gels under reducing conditions. Reactions involved a final concentration of 2μM AAT M358R or AAT M358R(X) and 1μM Pka/0.2μM FXIa in PPNE buffer and were incubated at 37°C for 1-5-minutes. Reactions were then terminated by adding 1/3 the reaction volume of concentrated 4x SDS-PAGE sample buffer and samples containing the entire reaction volume were subjected to electrophoresis. The gels were stained with Coomassie Brilliant Blue and destained as described previously (Hamada, et al. 2021). Gels were imaged by using a model XR GelDoc system (Bio-Rad Laboratories, Mississauga, ON, Canada), and immunoblots were imaged by using a model Azure 280 system (Azure Biosystems, CA, USA).

3.9. Protein Modeling

The Michaelis complexes between AAT M358R or AAT M358R(X) with Pka/FXIa were modeled separately using PyMOL Molecular Graphics System 2.5 (https://pymol.org/2/) and ClusPro 2.0 (https://cluspro.bu.edu/login.php), as previously described (Hamada, et al. 2021; Kozakov, et al. 2017). Protein Data Base (PDB) files 1OPH, 2ANY, and 1ZJD were used, for AAT M358R, the Pka catalytic domain, and the FXIa catalytic domain, respectively. The distance

between the alpha carbon of M358R in AAT M358R or AAT M358R variants and the hydroxyl side group of S195 in Pka/FXIa was determined in each case (Dementiev, et al. 2003; Navaneetham, et al. 2005; Tang, et al. 2005). Rendered figures were also made using PyMOL.

3.10. Statistical Analysis and Significance Testing

Data are presented as the mean ± the standard deviation (SD). Statistical analysis was conducted using GraphPad Prism version 10 (GraphPad Software, Boston, MA, USA). A p-value of <0.05 was taken to be indicative of statistical significance, with AAT M358R serving as the comparator. For multiple comparisons, data were assessed using Brown and Forsythe and Welch one-way ANOVA with Dunnett's T3 post-tests, which is a parametric approach assuming Gaussian distribution of data but not equivalence of standard deviations.

4. Results

4.1. Phage Display of AAT M358R P7-P3' and Characterization of 7-QLIPS-3 and 2-VRRAY-3'

We conducted two phage display screens to identify AAT M358R RCL sequences that were the most enriched by biopanning with Pka. To generate libraries amenable to productive phage display probing, no more than five RCL codons were randomized at a time (Bhakta, et al. 2013; Scott, et al. 2014). Two phage display experiments were carried out, spanning from P7-P3 (wild-type AAT sequence FLEAI) and P2-P3' (AAT M358R sequence PRSIP). After five rounds

of biopanning with Pka, the most abundant P7-P3 motif was identified as QLIPS, while the most abundant P2-P3' motif was identified as VRRAY. The corresponding soluble purified recombinant proteins were named for the motif being probed, with P-numbering identified, as 7-QLIPS-3 and 2-VRRAY-3' (Figure 1).

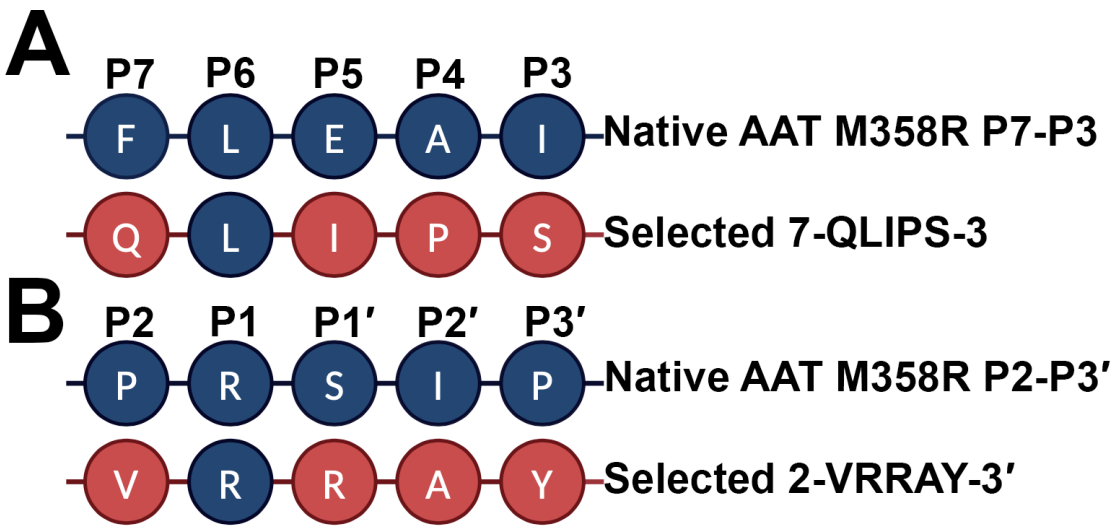

Figure 1: Schematic representation of the native AAT M358R and selected AAT M358R variants at positions P7-P3'. Native AAT M358R P7-P3' compared to (A) selected AAT M358R P7-P3 and (B) selected AAT M358R P2-P3' obtained through phage display.

These proteins were characterized by measuring k_2 and SI. Table 1 presents a summary of the kinetic parameters of AAT M358R, 7-QLIPS-3, and 2-VRRAY-3' with Pka and FXIa. The recombinant protein bearing the motif from P7-P3 phage display, 7-QLIPS-3, inhibited Pka faster than AAT M358R, by 2.2-fold ($p < 0.0001$) without significant change to the SI. In contrast to the results

with Pka, the protease used for positive selection, 7-QLIPS-3 was significantly slower in inhibiting FXIa, as evidenced by a 3.1-fold reduction in k_2, and was also a less efficient inhibitor, as indicated by its greatly elevated SI, 32.8-fold higher than that of AAT M358R for FXIa. Selectivity for Pka over FXIa was increased 9.2-fold for 7-QLIPS-3 over AAT M358R.

In contrast, the recombinant protein bearing the motif from P2-P3' phage display, 2-VRRAY-3', was a significantly less rapid inhibitor of Pka than AAT M358R, on average by 2.1-fold (Table 1). Nevertheless, its selectivity was increased 10.6-fold, on average, due to its greater loss of anti-FXIa activity (23.2-fold) than anti-Pka activity. The efficiency of Pka inhibition by 2-VRRAY-3' was diminished with respect to AAT M358R, as evidenced by its 2.2-fold increase in SI.

Table 1: Kinetic characterization of protease inhibition by AAT M358R, 7-QLIPS-3, and 2-VRRAY-3'.

Name	Second order rate constant (k_2) versus Pka ($x10^5\ M^{-1}s^{-1}$)	Second order rate constant (k_2) versus FXIa ($x10^5\ M^{-1}s^{-1}$)	Selectivity (Pka k_2: FXIa k_2)	Stoichiometry of Inhibition (SI) for Pka	Stoichiometry of Inhibition (SI) for FXIa
AAT M358R	0.394 ± 0.019	2.18 ± 0.084	0.181	3.21 ± 0.10	3.47 ± 0.36
7-QLIPS-3	0.870 ± 0.077 ****	0.696 ± 0.049 ****	1.25	2.92 ± 0.42	113 ± 2.7 ****
2-VRRAY-3'	0.180 ± 0.012 ****	0.0940 ± 0.0055 ****	1.91	7.14 ± 0.42 ***	10.4 ± 1.1 ****

Results are the mean of 5 determinations, ± SD. ***, p<0.001****, p <0.0001 versus AAT M358R.

The reactions of AAT M358R, 7-QLIPS-3, and 2-VRRAY-3' with Pka and FXIa were next examined separately using electrophoresis (Figure 2). Purified AAT M358R and purified 7-QLIPS-3 migrated as single polypeptide bands of ~45 kDa. When reacted in molar excess with either Pka or FXIa, a portion of these recombinant AAT proteins was converted into covalent AAT-protease complexes of 75 – 80 kDa, with concomitant disappearance of the catalytic light chains of the proteases from the gel profile. No differences were noted in reaction profiles of AAT M358R or 7-QLIPS-3 with Pka, while with FXIa, 7-QLIPS-3 exhibited a more rapidly migrating polypeptide band of ~41 kDa likely representing 7-QLIPS-3 cleaved at R358-S359, consistent with the elevated SI of 7-QLIPS-3 for FXIa

inhibition (Table 1). In contrast, 2-VRRAY-3' was heterogeneous, comprising a major full-length ~45 kDa polypeptide and a minor small polypeptide of ~41 kDa. While it formed similar high molecular weight complexes with Pka and FXIa, these were also more heterogeneous than AAT M358R-protease complexes.

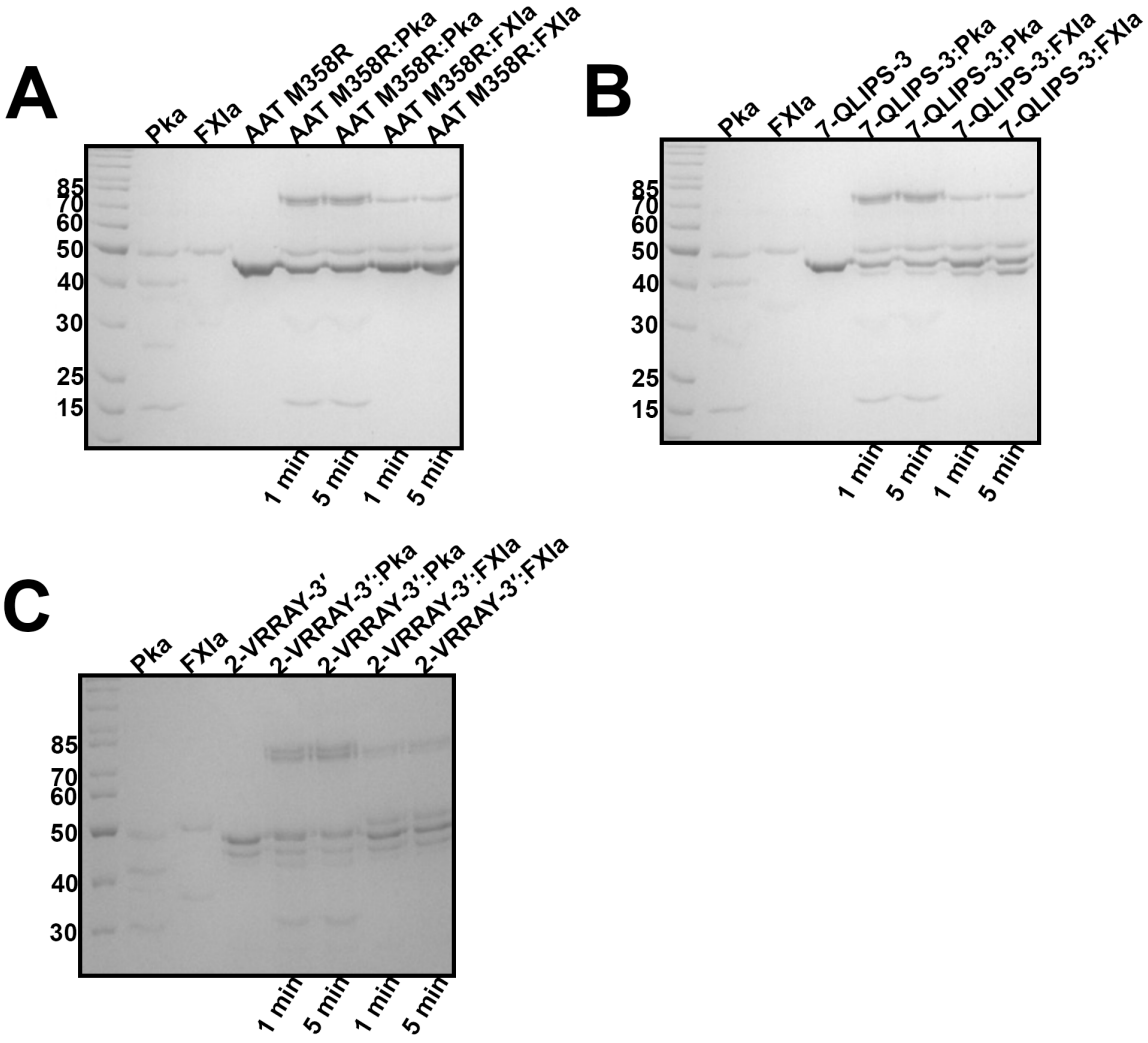

Figure 2: Electrophoretic profile of reactions of AAT M358R, 7-QLIPS-3, and 2-VRRAY-3' with Pka or FXIa. Reactions of 2μM (A) AAT M358R, (B) 7-QLIPS-3, or (C), 2-VRRAY-3' with Pka (1μM) or FXIa (0.2μM), for 1-5min.

4.2. *Characterization of Revertants and Combinatorial Mutagenesis of Selected Variants*

The mutational strategy involved starting with 7-QLIPS-3 and 2-VRRAY-3', each containing four unique amino acid substitutions between P7-P3', compared to AAT M358R, and systematically reversing the mutations, one at a time, back toward the AAT M358R sequence. This generated a total of 6 revertant variants from 7-QLIPS-3 and 2-VRRAY-3': 7-FLIPS-3, 7-FLEPS-3, 7-FLEAS-3, 2-PRRAY-3', 2-PRSAY-3', and 2-PRSIY-3' (Figure 3A and 3B). In addition, the combined variant 7-QLIPSVRRAY-3' was also expressed (Figure 3C).

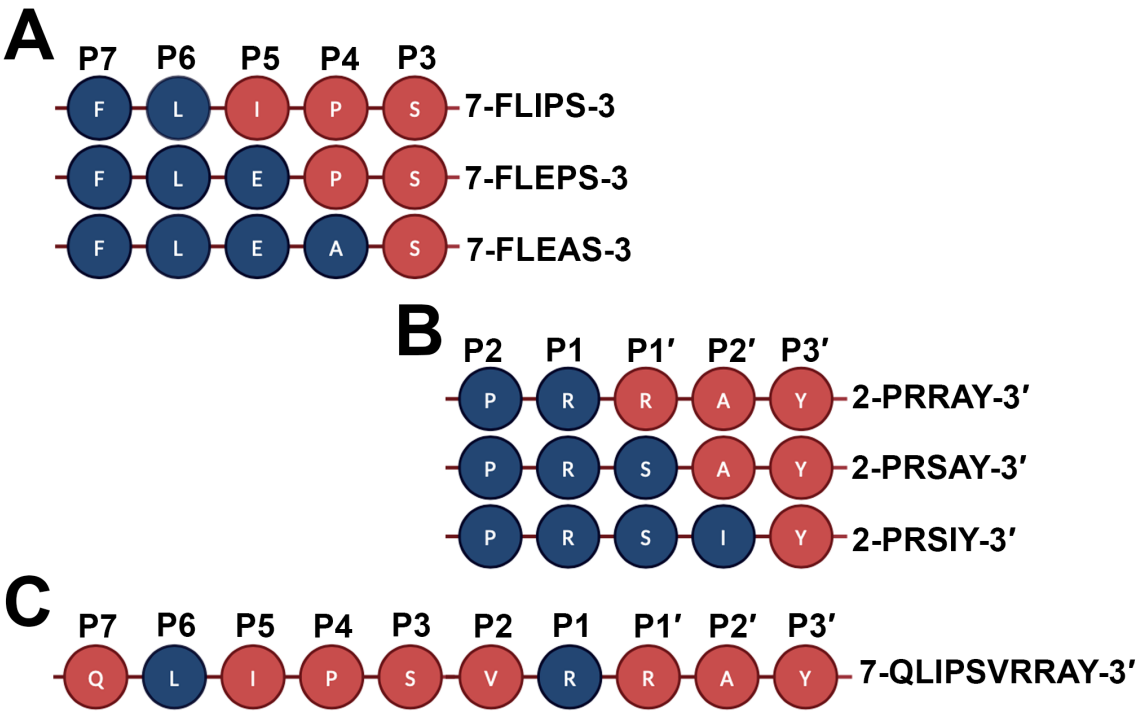

Figure 3: Schematic diagrams of reversion mutations and combination of selective AAT M358R mutants. Reversion of (A) phage-selected 7-QLIPS-3 to

original AAT M358R, (B) phage-selected 2-VRRAY-3' to original AAT M358R, and (C) the combination of 7-QLIPS-3 and 2-VRRAY-3' (7-QLIPSVRRAY-3').

Table 2 summarizes the kinetic activity of AAT M358R, 7-FLIPS-3, 7-FLEPS-3, 7-FLEAS-3, 2-PRRAY-3', 2-PRSAY-3', 2-PRSIY-3', and 7-QLIPSVRRAY-3' with Pka and FXIa for both k_2 and SI. Revertants of 7-QLIPS-3 were without exception found to be more rapid inhibitors of Pka and FXIa than revertants of 2-VRRAY-3'. Their average k_2 values for Pka inhibition were between 1.6-fold and 4.5-fold greater than that of AAT M358R. In contrast revertants of 2-VRRAY-3' on average only exhibited 9.6% to 18.3% of the k_2 value of AAT M358R for Pka inhibition. Selectivity for Pka was somewhat more favourable due to even greater losses in anti-FXIa activity, with all revertants found to have enhanced selectivity for Pka over FXIa, ranging from 0.66 to 2.00 compared to 0.18 for AAT M358R. This increase in selectivity was offset not only by the decreased rate of inhibition but also by decreased efficiency, as indicated by increased mean SI values ranging from 5.7 to 19.9 (versus 3.18 for AAT M358R).

All three 7-QLIPS-3 revertants exhibited increased rates of Pka inhibition, coupled in two cases (7-FLIPS-3 and 7-FLEPS-3) with decreases in the rate of FXIa inhibition (of 8.9- and 2.1-fold, respectively). 7-FLEAS-3 was the only revertant in which the rate of FXIa inhibition was increased relative to AT M358R, by ~1.5-fold. While the SI for Pka inhibition increased 3.8-fold for 7-FLIPS-3, 7-

FLEPS-3 showed no change in SI. Both 7-FLIPS-3 and 7-FLEPS-3 were inefficient inhibitors of FXIa, as judged by substantial increases in SI for FXIa inhibition of 53.2- and 25.2-fold, respectively.

Combining the two motifs in 7-QLIPSVRRAY-3' resulted in a 2.4-fold decrease in Pka inhibition and abolished detectable k_2 determination of anti-FXIa activity. Furthermore, the SI of 7-QLIPSVRRAY-3' for Pka and FXIa inhibition increased by 3.36- and 894-fold, respectively. For these reasons the combined variant was not further modified or investigated.

Table 2: Kinetic characterization of back mutants and combinatorial mutagenesis.

Name	Second order rate constant (k_2) versus Pka ($x10^5\ M^{-1}s^{-1}$)	Second order rate constant (k_2) versus FXIa ($x10^5\ M^{-1}s^{-1}$)	Selectivity (Pka k_2: FXIa k_2)	Stoichiometry of Inhibition (SI) for Pka	Stoichiometry of Inhibition (SI) for FXIa
AAT M358R	0.394 ± 0.019	2.18 ± 0.084	0.181	3.18 ± 0.10	3.48 ± 0.36
7-FLIPS-3	0.620 ± 0.035 ***	0.244 ± 0.011 ****	2.54	5.78 ± 0.31****	185 ± 9.2****
7-FLEPS-3	1.76 ± 0.13 ***	1.06 ± 0.14 ****	1.66	3.18 ± 0.085	87.7 ± 1.0****
7-FLEAS-3	1.33 ± 0.081 ****	3.24 ± 0.18 ***	0.410	1.79 ± 0.035****	1.49 ± 0.028**
2-PRRAY-3'	0.0400 ± 0.0071 ****	0.020 ± 0.01 ****	2.00	19.9 ± 2.4***	28.8 ± 8.2**
2-PRSAY-3'	0.0380 ± 0.0045 ****	0.060 ± 0.01 ****	0.633	16.9 ± 1.9***	14.2 ± 0.84****
2-PRSIY-3'	0.0720 ± 0.0045 ****	0.096 ± 0.006 ****	0.750	11.2 ± 0.54****	9.44 ± 0.24****
7-QLIPSVRRAY-3'	0.164 ± 0.0055 ****	ND	ND	10.7 ± 0.14****	3110 ± 290****

Results are the mean of 5 determinations, ± SD. **, p<0.01, ***, p<0.001, ****, p <0.0001 versus AAT M358R.

The reactions of all revertant proteins and the double motif combination variant were next examined separately using electrophoresis (Figure 4). In general, the electrophoretic profiles were consistent with the kinetic analysis. All

six revertants formed SDS-stable complexes with both Pka and FXIa, as observed with AAT M358R, 7-QLIPS-3, and 2-VRRAY-3', with or without the appearance of the ~41 kDa cleaved AAT polypeptide, depending on the conditions selected for the 1- or 5-minute reactions (Figure 4A-4F). In contrast, 7-QLIPSVRRAY-3' showed little or no complex formation with FXIa, and greater cleaved AAT with either Pka or FXIa than any of the revertant proteins, consistent with the remarkably elevated SI values measured for this double motif combination (Figure 4G).

Additional insights into 7-QLIPS-3 and 7-FLIPS-3 were sought using 7-FLIAI-3 (Additional Files 1 and 2) but it was found to be heterogenous after purification. The variant formed covalent complexes with Pka and FXIa (Additional File 2). Estimates of its kinetic parameters were obtained (Supplemental Table 1, Additional File 1) but they must be treated with caution given the heterogeneity and the unknown consequences of the contaminating proteins. At face value, a significant but minor contribution of the E362I mutation in 7-QLIPS-3 and 7-FLIPS-3 to enhanced selectivity for Pka (2.6-fold, on average) at the cost of a similar decrease in the rate of Pka inhibition was observed.

AAT M358R, 7-QLIPS-3, 7-FLEPS-3, and 7-QLIPSVRRAY-3' all exhibited anticoagulant activity in plasma, as indicated by all variants mediating a significant prolongation of the diluted APTT. AAT M358R prolonged clotting the

most, followed by 7-QLIPS-3 and 7-FLEPS-3, which had equivalent activity, followed by 7-QLIPSVRRAY-3' (Supplemental Figure 2, Additional File 3).

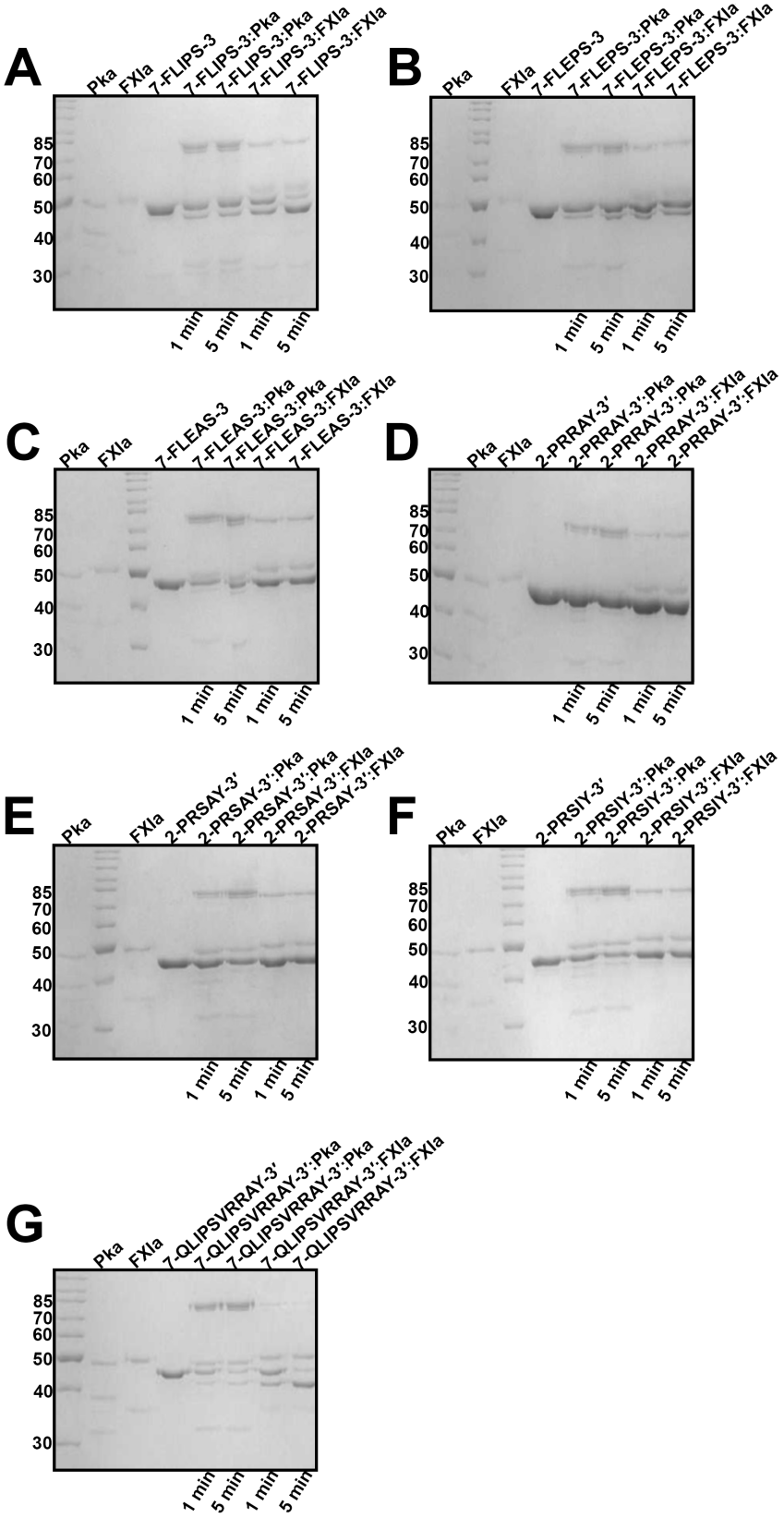
A
Pka
FXIa
7-FLIPS-3
7-FLIPS-3:Pka
7-FLIPS-3:Pka
7-FLIPS-3:FXIa
7-FLIPS-3:FXIa
B
Pka
FXIa
7-FLEPS-3
7-FLEPS-3:Pka
7-FLEPS-3:Pka
7-FLEPS-3:FXIa
7-FLEPS-3:FXIa
C
Pka
FXIa
7-FLEAS-3
7-FLEAS-3:Pka
7-FLEAS-3:Pka
7-FLEAS-3:FXIa
7-FLEAS-3:FXIa
D
Pka
FXIa
2-PRRAY-3'
2-PRRAY-3':Pka
2-PRRAY-3':Pka
2-PRRAY-3':FXIa
2-PRRAY-3':FXIa
E
Pka
FXIa
2-PRSAY-3'
2-PRSAY-3':Pka
2-PRSAY-3':Pka
2-PRSAY-3':FXIa
2-PRSAY-3':FXIa
F
Pka
FXIa
2-PRSIY-3'
2-PRSIY-3':Pka
2-PRSIY-3':Pka
2-PRSIY-3':FXIa
2-PRSIY-3':FXIa
G
Pka
FXIa
7-QLIPSVRRAY-3'
7-QLIPSVRRAY-3':Pka
7-QLIPSVRRAY-3':Pka
7-QLIPSVRRAY-3':FXIa
7-QLIPSVRRAY-3':FXIa
85
70
60
50
40
30
1 min
5 min
1 min
5 min

Figure 4: Electrophoretic profile of reactions of revertants and combination variant with Pka and FXIa. Reaction of (2μM) AAT variants (identified above the stained gel images) with Pka (1μM) or FXIa (0.2μM) for times specified below each panel.

4.3. Molecular Modeling suggests Correlation between the Distance and Activity

We sought molecular explanations for the selectivity of AAT M358R variants for Pka/FXIa. Utilizing the ClusPro 2.0 web server, we docked modeled AAT M358R variants to modeled protease catalytic domains and selected the lowest free energy version of ten modeled encounter complexes to gain insights into potential molecular explanations. Table 3 delineates the distances (in angstroms, Å) between the alpha carbon of M358R in AAT M358R variants and the hydroxyl side chain of S195 in Pka/FXIa, as one potential measure of the ease or difficulty of proceeding along the reaction pathway following formation of an initial complex between these protein reactants.

Table 3: Modeled distances between alpha carbon of R358 and S195 hydroxyl side chain in AAT M358R and variant encounter complexes

Name of inhibitor protein	Pka distance (Å)	FXIa distance (Å)
AAT M358R	11.5	3.3
7-QLIPS-3	4.4	4.9
7-FLIPS-3	6.3	8.7
7-FLEPS-3	3.3	3.6
7-FLEAS-3	3.4	3.1
2-VRRAY-3'	12.8	18.2
2-PRRAY-3'	27.1	43.9
2-PRSAY-3'	27.0	23.9
2-PRSIY-3'	23.4	15.0
7-QLIPSVRRAY-3'	15.6	54.9

The modeled distance between the catalytic domain of Pka and S195, and the reactive bond of R358 in AAT M358R, was 11.5Å. Conversely, the modeled distance between the catalytic domain of FXIa and S195, and the reactive bond of R358 in AAT M358R, was 3.3Å. For 7-QLIPS-3 and the revertants representing faster reactions for Pka and slower reactions for FXIa, shorter distances between RCL and Pka, and longer distances between RCL and FXIa, were observed. For instance, there was a reduction of 71.3% in this distance between 7-FLEPS-3 and Pka, while an increase of 8.3% was noted between 7-

FLEPS-3 and FXIa. Conversely, for 2-VRRAY-3' and the revertants representing slower reactions for both Pka and FXIa, longer distances between RCL and Pka/FXIa were modeled; between 2-PRRAY-3' and Pka, this distance increased by 135.6%, and by 1230% between 2-PRRAY-3' and FXIa.

Figure 5 represents a close-up model of the initial, non-covalent encounter complex of the light chain catalytic domain of Pka/FXIa (cyan/purple) docked to AAT M358R or 7-FLEPS-3 or 2-PRRAY-3' RCL (green, orange for changed residues). This figure provides visual insight into the differences among the initial, optimal, and least favorable interactions for the three selected mutants.

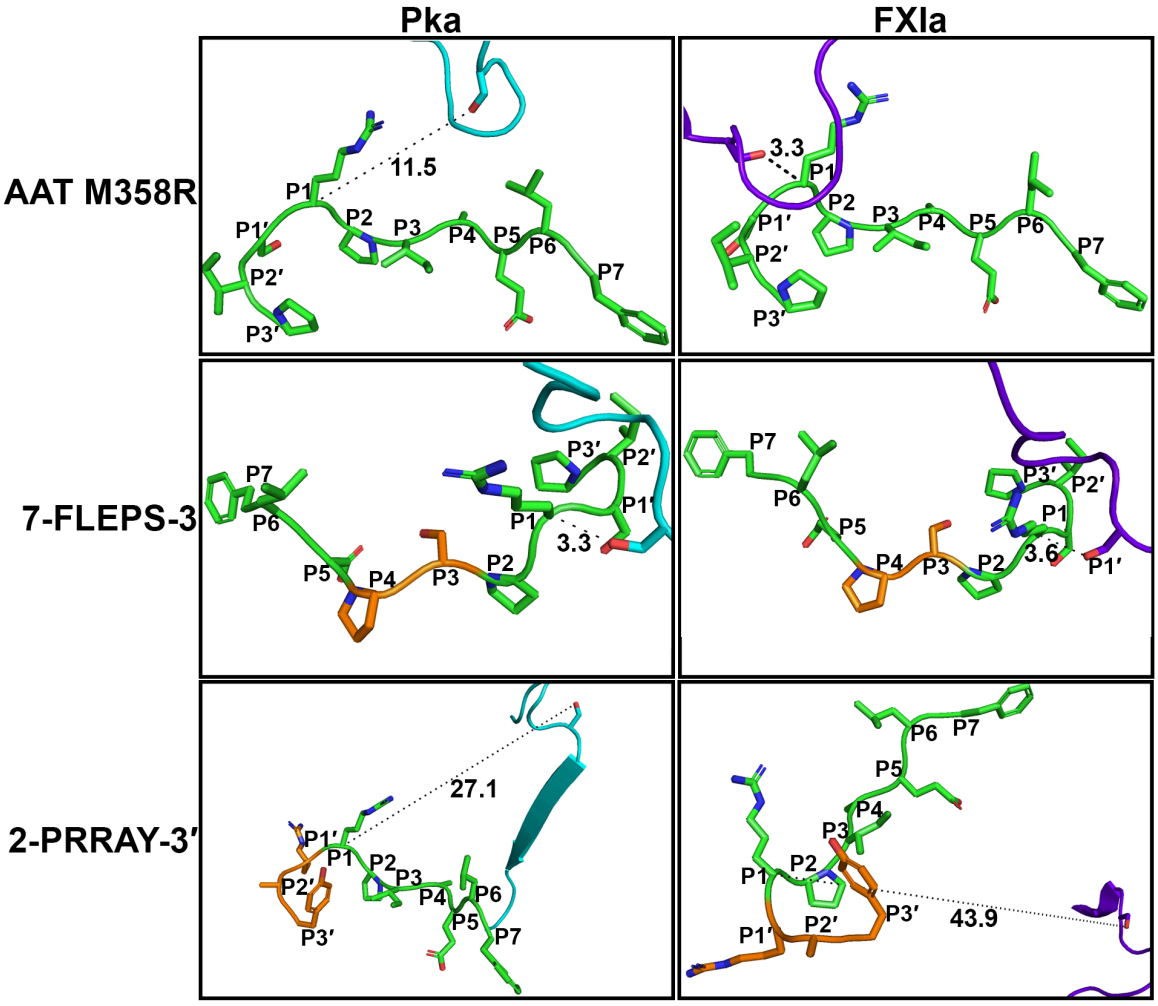

Figure 5: Molecular models of Pka and FXIa encounter complex to AAT M358R variants. Crystal structures of the catalytic domain of Pka (cyan, PDB 2ANY) or catalytic domain of FXIa (purple, PDB 1ZJD), and AAT M358R (original sequence in green; variants in orange, PDB 1OPH) were docked using ClusPro 2.0 as described in Methods. Black dashed lines indicate distance (Å) predicted between the alpha carbon of R358 in AAT M358R variants and the hydroxyl side chain of S195 in Pka/FXIa.

5. Discussion

The current study sought to replicate the success of a previous strategy of biopanning phage-displayed hypervariable AAT libraries with a bait protease, combinatorial mutagenesis, and partial reversion of mutant sequences toward the wild-type, substituting Pka for FXIa (Bhakta, et al. 2021). Our previous work using FXIa identified AAT-RC-2, a form of AAT M358R with three additional mutations (P7-P3' FLEA**E**P**R**S**TE**, substitutions bolded) as being 25-fold more selective for FXIa over Pka than AAT M358R, and 470-fold more selective for FXIa over thrombin than AAT M358R (Hamada, et al. 2021). AAT RC-2 was the most FXIa-specific inhibitor of a set of four candidate proteins comprising two motifs selected by phage or bacterial display (AAT-RC) and stepwise revertants (AAT RC-1, 2, and -3) that changed the AAT RC RCL sequence back towards AAT M358R one residue at a time. AAT-RC-2's increased selectivity towards FXIa was achieved with a 31% increase in its rate of FXIa inhibition and no increase in SI for FXIa compared to those kinetic parameters of AAT M358R (Hamada, et al. 2021). In the current study, the analogous optimal variant was 7-FLEPS-3, a revertant of the phage display-selected motif 7-QLIPS-3. 7-FLEPS-3 was 9.2-fold more selective for Pka over FXIa than AAT M358R, a gain in selectivity achieved with a concomitant 4.5-fold increase in the rate of Pka inhibition and no significant increase in SI. In contrast to our previous studies, no gain in selectivity was achieved by combining the RCL motifs identified by separate biopanning campaigns in 7-QLIPSVRRAY-3', although the possibility that stepwise reversion

of the combined motif towards the AAT M358R might have yielded gains in selectivity cannot be excluded.

RCL motifs identified using T7 phage display of AAT are subject to several uncertainties. They may behave differently with respect to their interaction with proteases when expressed in the molecular context of a stand-alone soluble protein than when expressed as a coat protein-serpin fusion protein on the bacteriophage surface (Danner and Belasco 2001). Although we formally demonstrated that AAT M358R fused to T7 bacteriophage coat protein 10 formed a covalent complex with thrombin (Scott, et al. 2014) this may not be the case with other bait proteases, for which a high affinity non-covalent encounter complex may be sufficient for selection. Moreover, because the screened library is hypervariable, not all mutations in the selected motif may contribute to enhanced interactions with the bait protease, and stepwise reversion may reveal variants with superior properties than the full selected motif.

The QLIPS motif yielded a more active Pka inhibitor than the VRRAY motif when expressed as soluble AAT M358R proteins 7-QLIPS-3 and 2-VRRAY-3'. Reverting 7-QLIPS-3 to 7-FLIPS-3 yielded higher selectivity for Pka at the cost of increased SI. Reverting 7-FLIPS-3 to 7-FLEPS-3 produced the most selective Pka inhibitor of the P7-P3' mutants, without increasing SI. Finally, reverting 7-FLEPS-3 to 7-FLEAS-3 enhanced FXIa inhibition more than Pka inhibition, eliminating most of the gains in selectivity achieved with 7-FLEPS-3. This comparison identifies the P4 mutation A355P as being the most important

contributor to the increased Pka selectivity of 7-QLIPS-3, 7-FLIPS-3, and 7-FLEPS-3. This mutation has not previously been described in the literature, either in mutagenesis studies (Scott and Sheffield 2020) or in patients with AAT deficiency (Strnad, et al. 2020). Pigment epithelium-derived factor (PEDF) is the only serpin known to contain a proline at P4, and it is non-inhibitory (Sanrattana, et al. 2019). Proline residues are helix-breaking, and the increased peptide rigidity they elicit could lock the 7-FLEPS-3 RCL into a favourable conformation for interacting with Pka, especially in combination with Pro357 at P2. 7-FLEPS-3 was the most selective variant tested whose selectivity was not gained at the cost of increased SI. Increased SI is undesirable given that it indicates not only reduced efficiency as an inhibitor, due to cleavage rather than complexation, but also the possibility of promoting inflammation, given that cleaved AAT has been shown to be pro-inflammatory in cell culture (Moraga, et al. 2001).

Our results overlap with some previous studies of wild-type AAT. Previously Phe352 was mutated to Glu in the wild-type AAT background without decreasing its rate of elastase inhibition, consistent with our finding that F352Q in the 7-QLIPS-3 (AAT M358R) context was functional. Mutations to the P5 Glu residue in wild-type AAT were also previously shown to increase the SI by ~4-fold (Chaillan-Huntington and Patston 1998), consistent with our findings that restoration of P5 Glu in 7-FLEPS-3 reduced the SI relative to 7-FLIPS-3, although the similar SI of 7-QLIPS-3 argues for cooperativity between residues in that

context. RCL cooperativity has been noted in previous mutagenic studies of AAT (Hopkins, et al. 2000).

The VRRAY motif selected via biopanning of the second phage display library was not as effective as the QLIPS motif when recreated in soluble recombinant 2-VRRAY-3'. While this variant formed covalent complexes with Pka and FXIa and inhibited the proteases at measurable rates, its rate of inhibition of Pka was 2.5-fold lower than AAT M358R and its increased selectivity was achieved at the cost of an elevated SI. There are no natural serpins with a natural Arg-Arg reactive centre. AAT variants with P2-P1' sequences of RRS, PRR, and RRC were found to be more efficient inhibitors of Activated Protein C than a KRK variant (Sanrattana, et al. 2021) . Reversion of 2-VRRAY-3' to 2-PRRAY-3' further reduced the rate of inhibition of Pka, and SI values were elevated for all VRRAY-related variants, including 2-PRSIY-3', which is a single residue mutant (P361Y). Given the preference of Pka for cleaving substrates C-terminal to Arg residues (Capraro, et al. 2015; Duckert, et al. 2004; Xie, et al. 2020), it is possible that the observed SI elevation could have arisen from Pka cleavage at either P1-P1' or P1'-P2', with the latter leading to substrate rather than inhibitor behaviour of 2-VRRAY-3'. This feature may have led to enhanced recognition in biopanning of phage exhibiting this motif that was not reproduced when transferred to soluble serpin form. Alternatively, the VRRAY-bearing phage may have harboured an unforeseen growth advantage that along with their reactivity with Pka promoted their abundance in the Pka-selected pool.

Our approach was to alter AAT to make it a specific inhibitor of Pka, like other therapeutic agents used to treat or control HAE or envisioned for such use. Others have sought to make AAT simultaneously able to inhibit Pka, FXIIa, and FXIa, and no other proteases, reasoning that such an engineered protein could have multiple clinical uses in disorders related to thromboinflammation (de Maat, et al. 2019). The AAT variant with the most potent inhibition of the three target proteases, SLLR/V (P4-P1'), perhaps unsurprisingly, has no overlap to the QLIPS or VRRAY series of variants described in this study. The 7-FLEAS-3 variant, intriguingly, inhibited both Pka and FXIa with rate constants higher than AAT M358R, in both cases, and could be considered as a candidate for control of thromboinflammation. A consideration for all mutagenesis studies is that the more modifications are introduced into a human protein, the greater the likelihood of eliciting an immune response in patients; 7-FLEAS-3 has only two variant residues compared to five in SLLR/V.

We found that the overall fitness of our variant AAT molecules as Pka inhibitors correlated reasonably well with the ClusPro 2.0-modeled distance to the active site S195 of Pka, suggesting that we had selected for effective encounter complex formation. In the serpin mechanism, nucleophilic attack by the active site serine of the protease on the carbonyl carbon of the serpin P1 residue in the P1-P1' peptide bond is an essential step in the progression from encounter complex to tetrahedral intermediate to acyl intermediate to stable serpin-enzyme complex (Huntington 2011). We assumed that a modeled complex in which the protease

hydroxyl group of the protease serine residue was closer to its reactive centre target in an AAT variant would predict faster inhibition rates than for a variant in which this distance was greater. Our assumption was supported by the measured distances, because variants with shorter distances than in AAT M358R between the key reactive groups were faster inhibitors of the modeled protease than AAT M358R and those with longer distances inhibited the modeled protease less rapidly. However, the modeled distance between the groups in AAT M358R, for Pka, was a substantial 11.5 Å, which indicates that energy-minimized ClusPro 2.0 modeling provides only an early model of a reversible encounter complex, one which must evolve to bring the reactant groups into closer proximity. While compatibility between RCL residues and protease active sites would seem a more critical parameter in assessing encounter complex fitness than the distance on which we focused, our modeling did not identify electrostatic or hydrophobic interactions between these residues that were strengthened by acceleratory variants, unlike in our previous use of ClusPro 2.0 to rationalize AAT M35R variant interactions with FXIa. The latter approach identified the facilitation of hydrogen bonds to K192 in FXIa as correlating with enhanced rates of FXI inhibition (Hamada, et al. 2021). Thus, the modeled distances serve only as a rough guide to variant fitness as an inhibitor, especially for distances of 20 Å or more.

Altering serpin specificity via protein engineering is a task with multiple molecular hurdles. The engineered serpin must form an encounter complex with

the target protease efficiently, ideally by engaging the active site without clashes, and its reactive centre must be efficiently cleaved. The engineered RCL must then integrate into the underlying β sheet of the serpin rapidly; failure to do so will allow escape of the trapped protease. Incompatibilities in the last step can underlie SI elevation (Hamada, et al. 2021). Modelling the fitness of the variant inhibitor for SI elevation would require advanced molecular dynamics modelling beyond the scope of this study and the capabilities of our laboratory.

Others have used structural modeling *a priori* to design AAT mutagenesis (Polderdijk, et al. 2017), or a combination of cleavage preference information and functional testing of a protein library to change AAT specificity (de Maat, et al. 2019; Sanrattana, et al. 2021). All strategies have yielded novel variants with desired or more optimal properties for the biotechnological problem at hand; it is therefore not possible to endorse one method over another as being more efficient or successful.

6. Conclusion

Purified C1INH products are currently used to prevent or treat HAE, despite C1INH's relatively slow rate of Pka inhibition of ~2.6 x 10^4 $M^{-1}s^{-1}$ (Kajdacsi, et al. 2020; Wuillemin, et al. 1996). Our results in this study suggest that 7-FLEPS-3, an AAT M358R variant with two additional substitutions, is a candidate for further testing in animal models of HAE, given its 7-fold faster rate of Pka inhibition. Further, while we found that phage display and subsequent

refinement of variant sequences by reversion mutagenesis were successful in identifying this promising variant, combining different RCL motifs identified in separate parts of the RCL was more effective when FXIa was the target than when Pka was employed (Hamada, et al. 2021).

7. List of Abbreviations

AAT	Alpha-1 Antitrypsin
AAT M358R	Alpha-1 Antitrypsin M358R
APC	Activated protein C
7-FLEAS-3	Alpha-1 Antitrypsin I356S, M358R
7-FLEPS-3	Alpha-1 Antitrypsin A355P, I356S, M358R
7-FLIAI-3	Alpha-1 Antitrypsin E354I, M358R
7-FLIPS-3	Alpha-1 Antitrypsin E354I, A355P, I356S, M358R
2-PRRAY-3'	Alpha-1 Antitrypsin M358R, S359R, I360A, P361Y
2-PRSAY-3'	Alpha-1 Antitrypsin M358R, I360A, P361Y
2-PRSIY-3'	Alpha-1 Antitrypsin M358R, P361Y
7-QLIPS-3	Alpha-1 Antitrypsin F352Q, E354I, A355P, I356S, M358R
7-QLIPSVRRAY-3'	Alpha-1 Antitrypsin F352Q, E354I, A355P, I356S, P357V, M358R, S359R, I360A, P361Y
2-VRRAY-3'	Alpha-1 Antitrypsin P357V, M358R, S359R, I360A, P361Y
C1INH	C1-inhibitor

Coomassie Brilliant Blue	0.1% Coomassie R-250 in 40% ethanol and 10% acetic acid
Destain	10% acetic acid and 50% methanol
E. coli	*Escherichia coli*
FXIa	Activated Factor XI
FXIIa	Activated Factor XII
h	Hour
HAE	Hereditary Angioedema
IPTG	Isopropyl β-D-1-thiogalactopyranoside
k_2	Second-order rate constant
kDa	Kilodalton
LB	Luria broth
LB-amp	Luria broth with ampicillin
M9LB	M9 salts in Luria broth
M	Molar
$M^{-1}s^{-1}$	Moles per liter per second
mM	Millimolar
min	Minute
mg	Milligram
µg	Microgram
µl	Microliter
µM	Micromolar

ml	Milliliter
nM	Nanomolar
PBS	Phosphate buffered saline
PEDF	Pigment epithelium-derived factor
pfu	Plaque forming units
PPNE Buffer	20mM sodium phosphate (pH 7.4), 0.1% (w/v) polyethylene glycol 8000, 100mM sodium chloride, and 0.1mM disodium ethylenediaminetetraacetic acid
Pka	Plasma kallikrein (KLKB1)
RCL	Reactive center loop
rpm	Revolutions per minute
RR	Arginine-Arginine
s	Second
S-2302	Chromogenic substrate for activated plasma kallikrein
S-2366	Chromogenic substrate for activated Factor XI
SD	Standard deviation
SDS	Sodium dodecyl sulphate
SDS Buffer	0.2M Tris-HCl (pH 6.8), 0.4M DTT, 277mM SDS, 6mM bromophenol blue, and 4.3M glycerol
SI	Stoichiometry of inhibition
v/v	Volume/volume
w/v	Weight/volume

Å	Angstrom
°C	Degree in Celsius
%	Percentage
±	Plus or minus

8. Declarations

Ethics approval and consent to participate: Not applicable.

Consent for publication: Not applicable.

Availability of data and materials: All data generated or analyzed during this study are included in this published article and its supplementary information (additional) files.

Competing interests: The authors declare that they have no competing interests.

Funding: Canadian Blood Services Discovery Research Grant DRG-WS2023 award to William P. Sheffield, and Canadian Blood Services Graduate Fellowship Program award to Sangavi Sivananthan.

Authors' contributions: SS conducted phage display of AAT M358R P2-P3', analyzed the pharmacokinetics of all the variants, and was a major contributor in writing and revising the manuscript. TS conducted phage display of AAT M358R P7-P3. NCT expressed revertants and combined forms of the AAT M358R variants. VB helped SS, TS, and NCT with their contributions. WPS supervised the experiments and was a major contributor in writing and revising the manuscript. All authors read and approved the final manuscript.

Acknowledgements: Not applicable.

9. References

Banerji, A., et al.
2022 Long-term prevention of hereditary angioedema attacks with lanadelumab: The HELP OLE Study. Allergy 77(3):979-990.
Bhakta, V., R. F. Gierczak, and W. P. Sheffield
2013 Expression screening of bacterial libraries of recombinant alpha-1 proteinase inhibitor variants for candidates with thrombin inhibitory capacity. J Biotechnol 168(4):373-81.
Bhakta, V., et al.
2021 Identification of an alpha-1 antitrypsin variant with enhanced specificity for factor XIa by phage display, bacterial expression, and combinatorial mutagenesis. Sci Rep 11(1):5565.
Capraro, J., et al.
2015 Proteolytic cleavage at twin arginine residues affects structural and functional transitions of lupin seed 11S storage globulin. PLoS One 10(2):e0117406.
Chaillan-Huntington, C. E., and P. A. Patston
1998 Influence of the P5 residue on alpha1-proteinase inhibitor mechanism. J Biol Chem 273(8):4569-73.
Danner, S., and J. G. Belasco
2001 T7 phage display: a novel genetic selection system for cloning RNA-binding proteins from cDNA libraries. Proc Natl Acad Sci U S A 98(23):12954-9.
Davis, A. E., 3rd
1988 C1 inhibitor and hereditary angioneurotic edema. Annu Rev Immunol 6:595-628.
de Maat, S., et al.
2019 Design and characterization of alpha1-antitrypsin variants for treatment of contact system-driven thromboinflammation. Blood 134(19):1658-1669.
de Souza, L. R., et al.
2018 Serpin Phage Display: The Use of a T7 System to Probe Reactive Center Loop Libraries with Different Serine Proteinases. Methods Mol Biol 1826:41-64.
Dementiev, A., et al.
2003 Canonical inhibitor-like interactions explain reactivity of alpha1-proteinase inhibitor Pittsburgh and antithrombin with proteinases. J Biol Chem 278(39):37881-7.
Deng, X., et al.

2018 Advances in the T7 phage display system (Review). Mol Med Rep 17(1):714-720.

Donaldson, V. H., and R. R. Evans
1963 A Biochemical Abnormality in Herediatry Angioneurotic Edema: Absence of Serum Inhibitor of C' 1-Esterase. Am J Med 35:37-44.

Duckert, P., S. Brunak, and N. Blom
2004 Prediction of proprotein convertase cleavage sites. Protein Eng Des Sel 17(1):107-12.

Gigli, I., et al.
1970 Interaction of plasma kallikrein with the C1 inhibitor. J Immunol 104(3):574-81.

Grover, S. P., et al.
2023 C1 inhibitor deficiency enhances contact pathway-mediated activation of coagulation and venous thrombosis. Blood 141(19):2390-2401.

Hamada, M., et al.
2021 Stepwise Reversion of Multiply Mutated Recombinant Antitrypsin Reveals a Selective Inhibitor of Coagulation Factor XIa as Active as the M358R Variant. Front Cardiovasc Med 8:647405.

Heeb, M. J., et al.
1990 Inhibition of activated protein C by recombinant alpha 1-antitrypsin variants with substitution of arginine or leucine for methionine358. J Biol Chem 265(4):2365-9.

Hopkins, P. C., R. N. Pike, and S. R. Stone
2000 Evolution of serpin specificity: cooperative interactions in the reactive-site loop sequence of antithrombin specifically restrict the inhibition of activated protein C. J Mol Evol 51(5):507-15.

Huntington, J. A.
2011 Serpin structure, function and dysfunction. J Thromb Haemost 9 Suppl 1:26-34.

Kajdacsi, E., et al.
2020 Patterns of C1-Inhibitor/Plasma Serine Protease Complexes in Healthy Humans and in Hereditary Angioedema Patients. Front Immunol 11:794.

Karnaukhova, E.
2022 C1-Inhibitor: Structure, Functional Diversity and Therapeutic Development. Curr Med Chem 29(3):467-488.

Kozakov, D., et al.
2017 The ClusPro web server for protein-protein docking. Nat Protoc 12(2):255-278.

Landerman, N. S., et al.
1962 Hereditary angioneurotic edema. II. Deficiency of inhibitor for serum globulin permeability factor and/or plasma kallikrein. J Allergy 33:330-41.

Lin, L., M. Wu, and J. Zhao

2017 The initiation and effects of plasma contact activation: an overview. Int J Hematol 105(3):235-243.

Markland, W., A. C. Ley, and R. C. Ladner
1996 Iterative optimization of high-affinity protease inhibitors using phage display. 2. Plasma kallikrein and thrombin. Biochemistry 35(24):8058-67.

Martello, J. L., M. R. Woytowish, and H. Chambers
2012 Ecallantide for treatment of acute attacks of hereditary angioedema. Am J Health Syst Pharm 69(8):651-7.

Moraga, F., S. Lindgren, and S. Janciaskiene
2001 Effects of noninhibitory alpha-1-antitrypsin on primary human monocyte activation in vitro. Arch Biochem Biophys 386(2):221-6.

Motta, G., L. Juliano, and J. R. Chagas
2023 Human plasma kallikrein: roles in coagulation, fibrinolysis, inflammation pathways, and beyond. Front Physiol 14:1188816.

Navaneetham, D., et al.
2005 Structural and mutational analyses of the molecular interactions between the catalytic domain of factor XIa and the Kunitz protease inhibitor domain of protease nexin 2. J Biol Chem 280(43):36165-75.

Owen, M. C., et al.
1983 Mutation of antitrypsin to antithrombin. alpha 1-antitrypsin Pittsburgh (358 Met leads to Arg), a fatal bleeding disorder. N Engl J Med 309(12):694-8.

Patston, P. A., et al.
1990 Reactivity of alpha 1-antitrypsin mutants against proteolytic enzymes of the kallikrein-kinin, complement, and fibrinolytic systems. J Biol Chem 265(18):10786-91.

Polderdijk, S. G., et al.
2017 Design and characterization of an APC-specific serpin for the treatment of hemophilia. Blood 129(1):105-113.

Sanrattana, W., C. Maas, and S. de Maat
2019 SERPINs-From Trap to Treatment. Front Med (Lausanne) 6:25.

Sanrattana, W., et al.
2021 A reactive center loop-based prediction platform to enhance the design of therapeutic SERPINs. Proc Natl Acad Sci U S A 118(45).

Schapira, M., et al.
1986 Recombinant alpha 1-antitrypsin Pittsburgh (Met 358----Arg) is a potent inhibitor of plasma kallikrein and activated factor XII fragment. J Clin Invest 77(2):635-7.

Schmaier, A. H.
2016 The contact activation and kallikrein/kinin systems: pathophysiologic and physiologic activities. J Thromb Haemost 14(1):28-39.

Scott, B. M., et al.

2014 Phage display of the serpin alpha-1 proteinase inhibitor randomized at consecutive residues in the reactive centre loop and biopanned with or without thrombin. PLoS One 9(1):e84491.

Scott, B. M., and W. P. Sheffield
2020 Engineering the serpin alpha(1) -antitrypsin: A diversity of goals and techniques. Protein Sci 29(4):856-871.

Scott, C. F., et al.
1986 Alpha-1-antitrypsin-Pittsburgh. A potent inhibitor of human plasma factor XIa, kallikrein, and factor XIIf. J Clin Invest 77(2):631-4.

Sinnathamby, E. S., et al.
2023 Hereditary Angioedema: Diagnosis, Clinical Implications, and Pathophysiology. Adv Ther 40(3):814-827.

Stolz, L. E., and P. T. Horn
2010 Ecallantide: a plasma kallikrein inhibitor for the treatment of acute attacks of hereditary angioedema. Drugs Today (Barc) 46(8):547-55.

Strnad, P., N. G. McElvaney, and D. A. Lomas
2020 Alpha(1)-Antitrypsin Deficiency. N Engl J Med 382(15):1443-1455.

Syed, Y. Y.
2019 Lanadelumab: A Review in Hereditary Angioedema. Drugs 79(16):1777-1784.

Tang, J., et al.
2005 Expression, crystallization, and three-dimensional structure of the catalytic domain of human plasma kallikrein. J Biol Chem 280(49):41077-89.

Travis, J., et al.
1986 Kinetic studies on the interaction of alpha 1-proteinase inhibitor (Pittsburgh) with trypsin-like serine proteinases. Biol Chem Hoppe Seyler 367(9):853-9.

Wedi, B.
2019 Lanadelumab to treat hereditary angioedema. Drugs Today (Barc) 55(7):439-448.

Wedner, H. J.
2020 Hereditary angioedema: Pathophysiology (HAE type I, HAE type II, and HAE nC1-INH). Allergy Asthma Proc 41(Suppl 1):S14-S17.

Wu, Y.
2015 Contact pathway of coagulation and inflammation. Thromb J 13:17.

Wuillemin, W. A., et al.
1996 Modulation of contact system proteases by glycosaminoglycans. Selective enhancement of the inhibition of factor XIa. J Biol Chem 271(22):12913-8.

Xie, Z., et al.
2020 Discovery and development of plasma kallikrein inhibitors for multiple diseases. Eur J Med Chem 190:112137.

Zahedi, K., A. E. Prada, and A. E. Davis, 3rd

1993 Structure and regulation of the C1 inhibitor gene. Behring Inst Mitt (93):115-9.

10. List of Additional Files

Supplemental Table 1. *Kinetic characterization of 7-FLIAI-3.* A table showing second order rate constant of inhibition values (n=5) for AAT M358R and AAT variant 7-FLIAI-3 for Pka and FXIa

Name	**k_2 versus Pka (x 10^5 $M^{-1}s^{-1}$)**	**k_2 versus FXIa (x 10^5 $M^{-1}s^{-1}$)**	**Selectivity (Pka k_2: FXIa k_2)**
AAT M358R	0.394 ± 0.019	2.18 ± 0.084	0.181
7-FLIAI-3	0.162 ± 0.013 ****	0.344 ± 0.017 ****	0.471

Supplementary Table 1. Results are the mean of 5 determinations, ± SD. ****, p <0.001 versus AAT M358R.

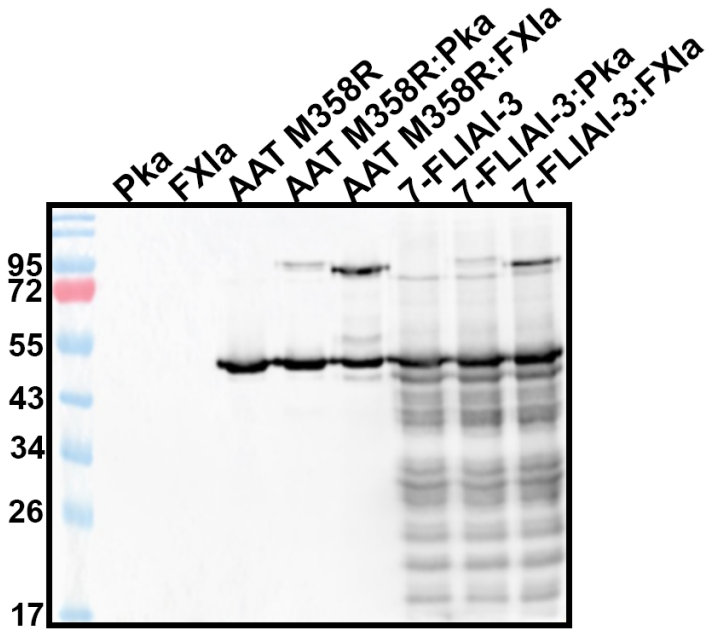

Supplementary Figure 1. *Immunoblot of 7-FLIAI-3 with or without protease reaction.* Immunoblot decorated by anti-human AAT IgG, showing reactions between AAT M358R or 7-FLIAI-3 with Pka, FXIa, or neither. Serpin: protease reactions were at a 5:1 molar ratio for 5min at 37°C. AAT M358R or 7-FLIAI-3 (45 kDa) reacts with the light chain of Pka (45 kDa) or the light chain of FXIa (30 kDa) to form stable covalent SDS complexes of 90 kDa or 75 kDa, respectively.

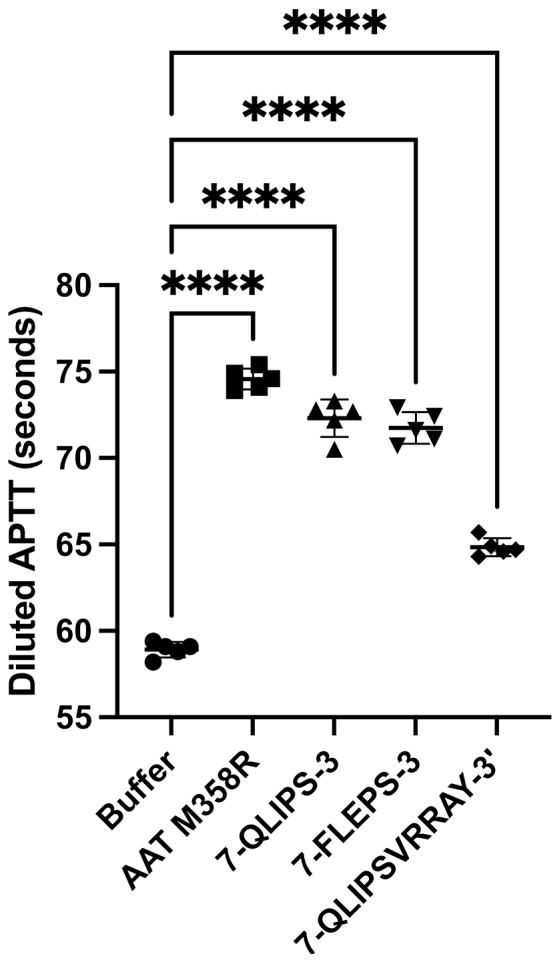

Supplemental Figure 2. *Diluted APTT Assay.* Clotting times are shown for diluted APTT reactions supplemented with 3 μM AAT M358R or variants identified on the x axis. Each data point is a separate technical replicate. Horizontal lines show the mean and error bars represent the SD. ****, $p < 0.0001$ versus Buffer.

Supplemental Table 2. *Raw data for all quantitative results of the study.*

(1) The table below shows individual data points for k_2 versus Pka (x 10^5 $M^{-1}s^{-1}$) used to calculate mean and SD values in Tables 1 and 2.

	Group A	Group B	Group C	Group D	Group E	Group F	Group G	Group H	Group I	Group J
	AATR + Pka	QLIPS + Pka	FLIPS + Pka	FELPS + Pka	FLEAS + Pka	VRRAY + Pka	PRRAY + Pka	PRSAY + Pka	PRSIY + Pka	QLIPSVRRAY + Pka
1	0.40	0.82	0.62	1.80	1.38	0.18	0.03	0.04	0.07	0.16
2	0.41	0.89	0.64	1.81	1.27	0.17	0.04	0.04	0.07	0.17
3	0.36	0.97	0.65	1.84	1.24	0.18	0.04	0.03	0.08	0.16
4	0.40	0.90	0.63	1.81	1.44	0.17	0.04	0.04	0.07	0.16
5	0.40	0.77	0.56	1.53	1.33	0.20	0.05	0.04	0.07	0.17

(2) The table below shows individual data points for k_2 versus FXIa (x 10^5 $M^{-1}s^{-1}$) used to calculate mean and SD values in Tables 1 and 2.

	Group A	Group B	Group C	Group D	Group E	Group F	Group G	Group H	Group I
	AATR + FXIa	QLIPS + FXIa	FLIPS + FXIa	FLEPS + FXIa	FLEAS + FXIa	VRRAY + FXIa	PRRAY + FXIa	PRSAY + FXIa	PRSIY + FXIa
1	2.10	0.75	0.26	1.00	3.24	0.09	0.01800	0.060	0.09
2	2.30	0.66	0.24	0.95	3.50	0.09	0.01800	0.060	0.09
3	2.20	0.75	0.24	1.10	3.25	0.10	0.01800	0.060	0.10
4	2.10	0.66	0.23	0.97	2.99	0.09	0.01800	0.060	0.10
5	2.20	0.66	0.25	1.30	3.24	0.10	0.01600	0.062	0.10

(3) The table below shows individual data points for SI for Pka used to calculate mean and SD values in Tables 1 and 2.

	Group A	Group B	Group C	Group D	Group E	Group F	Group G	Group H
	AAT-R	FLIPS	FLEPS	FLEAS	PRRAY	PRSAY	PRSIY	QV
1	3.295	5.667	3.294	1.823	16.450	17.740	11.140	10.86
2	3.185	6.293	3.056	1.768	22.220	18.300	10.640	10.56
3	3.052	5.913	3.200	1.805	21.070	16.420	10.950	10.70
4	3.311	5.483	3.194	1.803	21.700	14.090	12.080	10.49
5	3.196	5.705	3.168	1.736	19.220	18.890	11.310	10.65

(4) The table below shows individual data points for SI for FXIa used to calculate mean and SD values in Tables 1 and 2.

	Group A	Group B	Group C	Group D	Group E	Group F	Group G	Group H
	AATR + FXIa	FLIPS + FXIa	FLEPS + FXIa	FLEAS+ FXIa	PRRAY+ FXIa	PRSAY+ FXIa	PRSIY+ FXIa	QV+ FXIa
1	3.216	202.000	89.090	1.459	37.430	14.620	9.479	3472.00
2	3.728	180.900	87.260	1.466	26.670	13.170	9.043	3279.00
3	3.157	181.800	86.380	1.530	31.710	14.360	9.631	2750.00
4	3.279	180.300	87.850	1.481	39.340	13.820	9.483	3230.00
5	3.962	183.100	88.040	1.498	19.290	15.390	9.625	2933.00

Note that in Items 1-4 above short forms are used for AAT variant proteins. Short forms are identified below.

Short form	**Long form**
AATR	AAT M358R
FLIPS	7-FLIPS-3
FLEPS	7-FLEPS-3
FLEAS	7-FLEAS-3
PRRAY	2-PRRAY-3'
PRSAY	2-PRSAY-3'
QLIPSVRRAY	7-QLIPSVRRAY-3'
QV	7-QLIPSVRRAY-3'

(5) The table below shows individual data points for k_2 versus Pka and versus FXIa (x 10^5 $M^{-1}s^{-1}$) for AAT M358R and variant protein 7-FLIAI-3 from the supplementary table in Additional File 1.

AAT M358R		**7-FLIAI-3**	
k_2 vs. Pka	k_2 vs. FXIa	k_2 vs. Pka	k_2 vs. FXIa
0.400	2.10	0.365	0.875
0.410	2.30	0.368	0.796
0.360	2.20	0.317	0.789
0.400	2.10	0.301	0.601
0.400	2.20	0.333	0.570

(6) The table below shows individual data points for diluted APTT clotting times for the AAT proteins identified at the top of each column. The results are also shown graphically in Supplementary Figure 2.

Buffer	**AAT M358R**	**7-QLIPS-3**	**7-FLEPS-3**	**7-QLIPSVRRAY-3'**
58.2	74.1	72.7	71.1	64.9
59.1	74.9	72.2	72.9	64.3
58.8	75.4	73.3	72.4	64.7
59.1	74.6	72.8	71.6	64.6
59.4	73.9	70.5	70.7	65.7

CHAPTER 5

Substitution of reactive centre loop residues from C1 Esterase inhibitor increases the inhibitory specificity of Alpha-1 Antitrypsin for plasma kallikrein[#]

Sangavi Sivananthan[*], S. Ameer Ahmed[*], Ammaar M. Baig[*], Varsha Bhakta[†], and William P. Sheffield[*†1]

[*]Department of Pathology and Molecular Medicine, McMaster University, Hamilton, Ontario, Canada, and [†]Canadian Blood Services, Innovation and Portfolio Management, Medical Affairs and Innovation, Hamilton, Ontario, Canada

[1]Address correspondence to: Dr. William P. Sheffield, Ph.D. McMaster University, Department of Pathology and Molecular Medicine, HSC 4H19 1280 Main Street West, Hamilton, ON, Canada, L8S 4K1. Tel: (905) 525-9140 x22701 E-mail: sheffiel@mcmaster.ca

[#]Financial support: Canadian Blood Services Discovery Research Grant DRG-WS2023 award to William P. Sheffield, and Canadian Blood Services Graduate Fellowship Program award to Sangavi Sivananthan. The sponsor had no role in the design or execution of the study.

Conflict of interest: The authors declare that they have no conflicts of interest, financial or otherwise, in this work.

Sivananthan, S., Ahmed, S. A., Baig, A. M., Bhakta, V., & Sheffield, W. P. (2025). Substitution of reactive centre loop residues from C1 esterase inhibitor increases

the inhibitory specificity of alpha-1 antitrypsin for plasma kallikrein. *Journal of biotechnology*, *405*, 205–214. https://doi.org/10.1016/j.jbiotec.2025.05.013

Chapter 5 explores loop exchange between C1INH and AAT. Chimeric variants incorporating C1INH-derived segments into the AAT M358R backbone are generated, with a focus on the P10–P3′ region. Functional assays assess inhibitory efficiency and selectivity for Pka and FXIa. The results demonstrate how broader structural remodeling of the RCL can drive enhanced selectivity, expanding the toolkit for rational serpin design.

1. Abstract

C1 esterase inhibitor (C1INH) is a member of the serpin superfamily of proteins and controls plasma kallikrein (Pka). Purified C1INH concentrates are effective in controlling C1INH deficiency (Hereditary Angioedema, HAE). Because C1INH is a relatively slow inhibitor of Pka, we sought to develop a more effective inhibitor by exchanging reactive centre loop (RCL) residues in another serpin, alpha-1 antitrypsin (AAT) variant M358R, with the corresponding residues of C1INH. Novel, soluble, N-terminally hexahistidine-tagged variants were expressed in *E. coli*, purified by nickel chelate chromatography, and

characterized kinetically. **A**AT/**C**1INH loop exchange mutants were designated by the RCL residues exchanged using the reactive centre P1-P1' convention. Maximal exchange mutant AC (10-4') inhibited Pka 78-fold and activated Factor XI (FXIa) 350-fold less rapidly than AAT M358R. Eleven additional variants were expressed, restoring AAT residues stepwise. The most selective variant was AC (10-3/4'), which restored AAT residues from P2-P3' compared to AC (10-4'), and inhibited Pka 1.9-fold more rapidly, and FXIa 1.6-fold less rapidly, for a gain in selectivity of 2.8-fold ($p<0.0001$), without increasing the stoichiometry of inhibition (SI). The most active variant was AC (10-3), in which both the rate of Pka and FXIa inhibition were elevated relative to AAT M358R values, without SI elevation. Other variants exhibited slower reaction rates and/or elevated SI values. These results indicate that RCL exchanges can be productively employed to change serpin specificity and selectivity, but that the most effective exchanges may not be contiguous due to cooperativity between RCL residues.

Keywords

Alpha-1 antitrypsin, C1 esterase inhibitor, plasma kallikrein, reactive centre loop, Hereditary Angioedema

2. Introduction

Hereditary Angioedema (HAE) is a rare autosomal dominant disorder caused by dysregulation of the contact pathway, resulting in excessive activation of bradykinin, a potent vasodilator (Longhurst and Cicardi 2012, Wettschureck,

Strilic et al. 2019, Wilkerson and Moellman 2022). This overactivity results in increased vascular permeability and recurrent episodes of acute swelling in various body regions, with the most severe risk being life-threatening airway obstruction (Landerman, Webster et al. 1962, Donaldson and Evans 1963, Wedner 2020). Many HAE cases are linked to heterozygous mutations in the *SERPING1* gene, which encodes C1 esterase inhibitor (C1INH). These mutations either reduce C1INH antigen levels or impair its functional capacity (Davis 1988, Zahedi, Prada et al. 1993, Wilkerson and Moellman 2022, Sinnathamby, Issa et al. 2023). C1INH is a serine protease inhibitor (SERPIN) capable of inhibiting key biological proteases involved in the complement, coagulation, fibrinolytic, and contact systems (Levi, Cohn et al. 2019, Long, Fujioka et al. 2024). It plays a pivotal role in controlling the contact system by acting as the primary inhibitor of plasma kallikrein (Pka) and activated Factor XII (FXIIa) (Gigli, Mason et al. 1970, Karnaukhova 2022, Grover, Kawano et al. 2023). Through these interactions, C1INH effectively limits the generation of bradykinin, since Pka catalyzes the cleavage of high molecular weight kininogen to release bradykinin (Wu 2015, Schmaier 2016, Lin, Wu et al. 2017, Motta, Juliano et al. 2023).

Replacement therapy with purified plasma-derived C1INH concentrates is effective in controlling and preventing HAE episodes (Karnaukhova 2022). Plasma-derived C1INH concentrates suffer from the limitation that C1INH is a complex glycoprotein present at relatively low levels in plasma, complicating fractionation and purification. In addition, C1INH-mediated inhibition of Pka is

relatively slow, as demonstrated by a mean second-order rate constant (k_2) of ~2.55 x 10^4 $M^{-1}s^{-1}$ (Wuillemin, Eldering et al. 1996, Kajdacsi, Jandrasics et al. 2020), likely necessitating larger doses than would be needed with a more rapid inhibitor.

Another circulating member of the serpin superfamily of protease inhibitors, alpha-1 antitrypsin (AAT, product of the *SERPINA1* gene), primarily regulates neutrophil elastase (Strnad, McElvaney et al. 2020), and shows only marginal reactivity with other proteases. A point mutation in codon 358 of AAT, altering methionine to arginine (M358R), was found to shift its inhibitory profile to target multiple proteases (Owen, Brennan et al. 1983, Schapira, Ramus et al. 1986, Scott, Carrell et al. 1986, Travis, Matheson et al. 1986, Heeb, Bischoff et al. 1990). Researchers extended this seminal observation and introduced additional mutations in the reactive centre loop (RCL) of AAT M358R to hone its specificity for specific coagulation and contact pathway proteases (Patston, Roodi et al. 1990, Scott, Matochko et al. 2014, Polderdijk, Adams et al. 2017, de Maat, Sanrattana et al. 2019, Bhakta, Hamada et al. 2021, Hamada, Bhakta et al. 2021). Serpins interact with their cognate proteases principally via their reactive centre loops (Huntington 2011), which are protruding surface structures, whose residues are numbered by convention N-terminal or C-terminal to the scissile reactive centre bond P1-P1' (Schechter and Berger 1967). Substituting all or part of a serpin RCL for that of another serpin can change inhibitory specificity, as has

been previously noted for other serpin pairs (Chaillan-Huntington, Gettins et al. 1997, Filion, Bhakta et al. 2004).

Recombinant AAT M358R could hold advantages over plasma-derived or recombinant C1INH as a protein therapeutic in HAE. Firstly, both serpins share Arg at P1 (Huber and Carrell 1989). Secondly, AAT M358R is known to inhibit Pka at a faster rate than C1INH (Scott, Carrell et al. 1986). Thirdly, AAT has a longer circulatory half-life than C1INH after intravenous injection (Strnad, McElvaney et al. 2020, Karnaukhova 2022). Recently, this laboratory reported that novel variants of AAT M358R selected by probing hypervariable AAT phage display libraries with Pka were more rapid and more selective Pka inhibitors than AAT M358R (Sivananthan, Seto et al. 2025).

In this study, portions of the C1INH RCL were swapped for the corresponding residues of AAT M358R, between P10-P4' positions, inclusive. Our hypothesis was that AAT M358R variants specific for Pka inhibition exist within the sequence space defined by full or partial substitution of P10-P4' AAT residues with those of C1INH. We report that swapping 7 of the maximum 12 mismatched or non-aligned residues increased the selectivity of RCL-exchanged AAT M358R for Pka, increasing the rate of inhibition without increasing the stoichiometry of inhibition (SI) relative to AAT M358R. Other swaps provided structure/function insights.

3. Materials and Methods

3.1. Reagents and Materials

Purified human proteases, Pka, coagulation factor XIa (FXIa), thrombin, factor Xa (FXa), and factor XIIa (FXIIa) were purchased from Enzyme Research Labs (South Bend, IN, USA). Chromogenic substrates specific to Pka and FXIIa (S-2302), FXIa (S-2366), thrombin (S-2238), and FXa (S-2222) were purchased from Diapharma (West Chester, OH, USA). Synthetic DNA sequences (gBlock^{TM}) were obtained from Integrated DNA Technologies (Coralville, IO, USA). Restriction endonucleases, gel extraction/purification kits, glutathione agarose, and PreScission protease (a fusion protein of glutathione sulfotransferase (GST)-human rhinovirus (HRV) 3C protease) were obtained from ThermoFisher Scientific (Waltham, MA, USA). Nickel-nitrilotriacetic acid (Ni-NTA) agarose resin was obtained from Qiagen (Mississauga, Canada).

3.2. DNA Manipulations

Standard DNA manipulation techniques, including restriction digestion, electrophoresis, gel purification, ligation, and *E. coli* transformation, were used as previously described (Bhakta, Hamada et al. 2021). The design of AAT M358R variants was facilitated using Clone Manager 10 (Sci Ed Software LLC). Figure 1 illustrates the structural representation of AAT M358R and C1INH, highlighting the relevant RCL positions from P17 to P5' for AAT M358R and P17 to P4' for C1INH.

RCL segments P10-P4'/d2 (indicating the peptide spanning P10 to P4', with a deletion at P2) (AC (P10-P4'/d2), P10-P4' (AC (P10-P4')) and P10-P3 (AC (10-3)) in AAT M358R were swapped with the corresponding segments from C1INH (see Table 1 for aligned sequences).

Table 1: Aligned reactive centre loop sequences of C1INH, AAT M358R, and initial constructs

Protein	P17	P16	P15	P14	P13	P12	P11	P10	P9	P8	P7	P6	P5	P4	P3	P2	P1	P1'	P2'	P3'	P4'	P5'
C1INH	E	T	G	V	E	A	A	A	A	S	A	I	S	V	A		R	T	L	L	V	
AAT M358R	E	K	G	T	E	A	A	G	A	M	F	L	E	A	I	P	R	S	I	P	P	E
AC (10-4'/d2)	E	K	G	T	E	A	A	**A**	A	**S**	**A**	**I**	**S**	**V**	**A**		R	**T**	**L**	**L**	**V**	E
AC (10-4')	E	K	G	T	E	A	A	**A**	A	**S**	**A**	**I**	**S**	**V**	**A**	**P**	R	**T**	**L**	**L**	**V**	E
AC (10-3)	E	K	G	T	E	A	A	**A**	A	**S**	**A**	**I**	**S**	**V**	**A**	P	R	S	I	P	P	E

Using AC (10-4') as a backbone, the substituted RCL sequences from C1INH were then sequentially reversed toward the original AAT M358R sequence. We created three C-terminal variants: P2'-P4' (AC (10-3/2'-4')), P3'-P4' (AC (10-3/3'-4')), and P4' (AC (10-3/4')). Additionally, five N-terminal loop exchange variants were expressed: P10-P4 (AC (10-4)), P10-P5 (AC (10-5)), P10-P6 (AC (10-6)), P10-P7 (AC (10-7)), and P10-P8 (AC (10-8)) (see Table 2 for additional aligned sequences).

Table 2: Amino acid configuration of AAT M358R constructs showing stepwise reversion from AC (10-4') to AC (10-8).

Protein	P17	P16	P15	P14	P13	P12	P11	P10	P9	P8	P7	P6	P5	P4	P3	P2	P1	P1'	P2'	P3'	P4'	P5'
AC (10-3/2'-4')	E	K	G	T	E	A	A	**A**	A	**S**	**A**	**I**	**S**	**V**	**A**	P	R	S	**L**	**L**	**V**	E
AC (10-3/3'-4')	E	K	G	T	E	A	A	**A**	A	**S**	**A**	**I**	**S**	**V**	**A**	P	R	S	I	**L**	**V**	E
AC (10-3/4')	E	K	G	T	E	A	A	**A**	A	**S**	**A**	**I**	**S**	**V**	**A**	P	R	S	I	P	**V**	E
AC (10-4)	E	K	G	T	E	A	A	**A**	A	**S**	**A**	**I**	**S**	**V**	I	P	R	S	I	P	P	E
AC (10-5)	E	K	G	T	E	A	A	**A**	A	**S**	**A**	**I**	**S**	A	I	P	R	S	I	P	P	E
AC (10-6)	E	K	G	T	E	A	A	**A**	A	**S**	**A**	**I**	E	A	I	P	R	S	I	P	P	E
AC (10-7)	E	K	G	T	E	A	A	**A**	A	**S**	**A**	L	E	A	I	P	R	S	I	P	P	E
AC (10-8)	E	K	G	T	E	A	A	**A**	A	**S**	F	L	E	A	I	P	R	S	I	P	P	E

E. coli strain DH5α was employed for DNA manipulations, while *E. coli* strain BL21 was employed for protein expression. All AAT M358R variant plasmids were confirmed by DNA sequencing at the Mobix Lab central facility, located within the Faculty of Health Sciences at McMaster University.

3.3. Expression and Purification of GST-fusion Constructs

The expression vector pGEX-AAT M358R was previously created as described (Bhakta, Hamada et al. 2021). For each variant in this study, a 942 or 945 bp DNA fragment containing the desired mutation, flanked by Kpn2I and EcoRI restriction sites, was cloned into a pGEX-AAT M358R vector backbone, resulting in the variant construct pGEX-AC (X), where X is the exchanged loop of interest, as described above (see Suppl. Fig. S1). The resulting plasmids were transformed into *E. coli* BL21 cells, and expression was induced with 0.1 mM isopropyl β-D-1-thiogalactopyranoside. After induction, cells were harvested and lysed, and the fusion proteins were isolated through GST affinity chromatography and specific proteolytic elution, followed by purification using Ni-NTA affinity

chromatography to ensure high purity following previously established protocols (Bhakta, Hamada et al. 2021). Full details of DNA sequences and primary sequences of all expressed proteins are provided in Suppl. Fig. S1.

3.4. Protease Inhibition Assays for AAT M358R Variants

The rate and efficiency of protease inhibition, represented by k_2 constants and SI values, respectively, was evaluated for each AAT M358R variant using chromogenic assays. Rate determinations were carried out under pseudo-first-order conditions. Reactions were conducted at 37°C in PPNE buffer (20 mM sodium phosphate, pH 7.4; 0.1% (w/v) polyethylene glycol 8000; 100 mM sodium chloride; 0.1 mM disodium EDTA), with amidolysis rates measured at 405 nm on a Synergy H1 Microplate Reader (Biotek, Winooski, VT, USA). For k_2 determination, 10 nM Pka or FXIa was incubated with 200 nM of each AAT M358R variant. Reactions proceeded for intervals between 8 or 30 seconds, after which they were terminated by the addition of 100 μM of the respective chromogenic substrate (S-2302 for Pka or S-2366 for FXIa). To determine SI values, each reaction contained 10 nM Pka or FXIa and varying concentrations (10-500 nM) of AAT M358R variants, incubated for 2 hours before termination with 100 μM chromogenic substrate. All inhibition constants were calculated based on methods outlined previously (Bhakta, Hamada et al. 2021). The k_2 values for inhibition of selected AAT M358R variants and AAT M358R were

determined in an analogous manner to that described above for thrombin, FXa, and FXIIa, using substrates S-2238, S-2222, and S-2302, respectively.

3.5. Electrophoretic Analysis of AAT M358R Variants and Protease Complex Formation

To assess complex formation between AAT M358R or AAT M358R(X) and the proteases Pka or FXIa, reaction mixtures were prepared and analyzed via 10% (w/v) sodium dodecyl sulfate-polyacrylamide gel electrophoresis (SDS-PAGE) under reducing conditions. Each reaction included 2 μM of AAT M358R or variant AC (X) and either 1 μM Pka or 0.2 μM FXIa in PPNE buffer. Reactions were incubated at 37°C for 1 or 5 minutes then terminated by adding 4x SDS-PAGE sample buffer in a 1:3 ratio relative to the reaction volume. The entire reaction volume was then loaded onto SDS-PAGE gels. Following electrophoresis, gels were stained with Coomassie Brilliant Blue to visualize protein bands, then destained as described previously (Hamada, Bhakta et al. 2021). Gels were imaged by using a model XR GelDoc system (Bio-Rad Laboratories, Mississauga, ON, Canada).

3.6. Intrinsic Fluorescence of AAT M358R and AC (10-3/4')

The intrinsic fluorescence profiles of purified AAT M358R and AC (10-3/4') were determined in a Synergy H1 Microplate Reader. Samples of the two proteins in phosphate-buffered saline (PBS) at 4.0 μM concentrations, with or

without heating to 95ºC for ten minutes, were separately introduced into the wells of a 384 well black microtiter plate and subjected to excitation at 280 nm. Emission from wavelengths ranging from 310 nm to 450 nm was measured at 10 nm increments.

3.7. Protein Modeling of AAT M358R Variants and Protease Complexes

To model the Michaelis complexes between AAT M358R or AC (X) and proteases Pka or FXIa, PyMOL Molecular Graphics System 2.5 (https://pymol.org/2/) and AlphaFold 3 (https://alphafoldserver.com) were used following established protocols (Hamada, Bhakta et al. 2021, Abramson, Adler et al. 2024). In each model, the distance between the alpha carbon of the M358R residue in AAT M358R (PDB file 1OPH) or AC (X) and the hydroxyl side chain of S195 in Pka (PDB file 2ANY) or FXIa (PDB file 1ZJD) was measured (Dementiev, Simonovic et al. 2003, Navaneetham, Jin et al. 2005, Tang, Yu et al. 2005). Key intermolecular hydrogen bonds between AAT M358R or AC (X) and Pka or FXIa, as well as intramolecular interactions within AAT M358R or AC (X), were identified and analyzed (Hamada, Bhakta et al. 2021). Rendered figures were also made using PyMOL.

3.8. Statistical Analysis and Evaluation of Testing

Data are presented as the mean ± the standard deviation (SD). Statistical analysis was conducted using GraphPad Prism version 10 (GraphPad Software,

Boston, MA, USA). A p-value of <0.05 was considered indicative of statistical significance, with AAT M358R serving as the control group. For multiple comparisons, the data were analyzed using the Brown-Forsythe and Welch one-way ANOVA, complemented by Dunnett's T3 post hoc test. This parametric approach assumes a Gaussian distribution of the data while allowing for the possibility of unequal variances among groups.

4. Results

4.1. Characterization of Maximal AAT M358R-C1INH Loop Exchanged Variants

Inspection of the aligned RCL sequences of C1INH and AAT M358R in Table 1 showed the portion of both loops most clearly separated from the serpin body in crystal structures lies between P13 and P5' (see Fig. 1), and that the two sequences differed at 14 of 18 positions, including two gaps introduced to account for the shorter RCL of C1INH compared to AAT (see Table 1). Accordingly, residues P10-P4' were exchanged to create AC (10-4'/d2), in which peptide GAMFLEAIPRSIPP of AAT M358R was substituted by peptide AASAISVA-RTLLV (with a gap at P2).

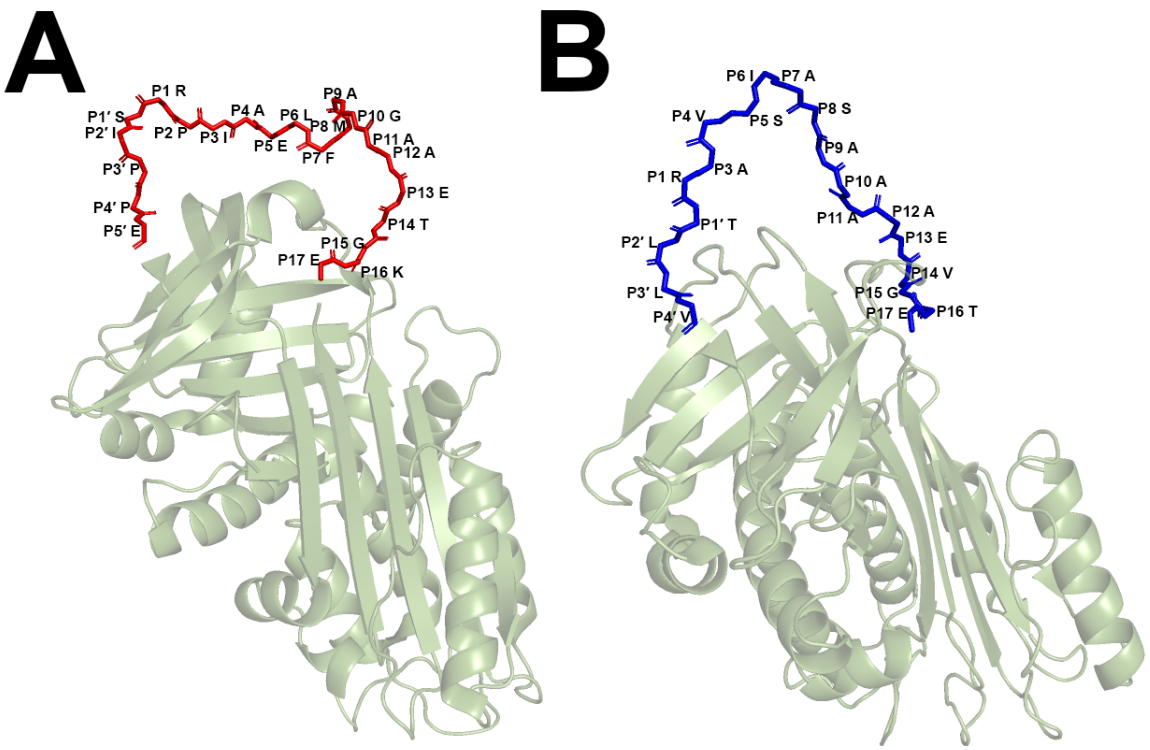

Figure 1: Structural Representation of AAT M358R and C1INH RCL Positions. (A) AAT M358R highlighting RCL (red) from P17-P5' compared to (B) C1INH highlighting RCL (blue) from P17-P4'. Serpin bodies are depicted in light green. Figures were created from Protein Data Base (PDB) files 1OPH (A) and 7AKV (B).

As shown in Table 3, this substantial substitution reduced both the average rate of Pka inhibition, by 74-fold, and that of FXIa inhibition, by 350-fold, essentially converting AC (10-4'/d2) into primarily a substrate of both proteases, as evidenced by average SI values found to exceed 300 in both cases. Electrophoretic analysis of AC (10-4'/d2) (see Suppl. Fig. S2A and S2B) showed that it was largely converted into a more rapidly migrating polypeptide by both

proteases, consistent with substrate behavior and cleavage within the RCL, without detectable formation of a covalent AAT-protease complex.

Table 3: Kinetic parameters of inhibition of Pka or FXIa by AAT M358R and initial constructs.

Protein	k_2 vs Pka ($x10^5$ $M^{-1}s^{-1}$)	k_2 vs FXIa ($x10^5$ $M^{-1}s^{-1}$)	Selectivity Pka:FXIa	SI vs Pka	SI vs FXIa
C1INH	0.23 ± 0.03[a]	ND	ND	3.3 ± 0.06[a]	ND
AAT M358R	0.37 ± 0.03	1.4 ± 0.1	0.27	2.5 ± 0.2	2.36 ± 0.06
AC (10-4'/d2)	0.005 ± 0.002 ****	0.004 ± 0.002 ****	1.3	300 ± 200 *	400 ± 200 *
AC (10-4')	0.016 ± 0.002 ****	0.012 ± 0.002 ****	1.4	58 ± 2****	ND
AC (10-3)	1.4 ± 0.2 ****	2.6 ± 0.2 ****	0.53	1.22 ± 0.05 ****	1.74 ± 0.07 ****

Results are the mean of 5 determinations, ± SD. *, p<0.05; ****, p <0.0001 versus AAT M358R. ND signifies Not Determined. Selectivity = k_2 vs Pka/ k_2 vs FXIa. [a] From (Sivananthan, Bhakta et al. 2024).

Eliminating the gap arising from the difference in length of the RCL in AAT and C1INH by incorporating the Pro residue at P2 in AC (10-4') restored some measure of inhibitory function and increased the rate of Pka and FXIa inhibition by ~3-fold compared to AC (10-4'/d2), but the reactions remained 23-fold and 120-fold slower than those of AAT M358R (Table 3). In contrast to AC (10-4'/d2), AC (10-4') formed denaturation-resistant high molecular weight inhibitory complexes with both Pka and FXIa. As shown in Suppl. Fig. 2A, incubation of either AAT M358R or AC (10-4') converted these 45 kDa polypeptides into 79 kDa or 77 kDa AAT-protease complexes, consistent with reaction with the 38 kDa

catalytic chain of Pka or the 36 kDa catalytic chain of FXIa, and loss of the 4 kDa S359-K394 under reducing conditions following reactive centre cleavage.

Further reducing the extent of RCL residue swapping in AC (10-3) resulted in increased rates of inhibition of both Pka and FXIa, by 3.8-fold and 1.9-fold, respectively, leading to a 2-fold increase in selectivity for Pka over FXIa versus AAT M358R. The selectivity index is the ratio of the k_2 rate constants of inhibition for Pka: FXIa, as previously defined (Hopkins, Crowther et al. 1995, Hopkins, Pike et al. 2000). Interestingly, this enhanced selectivity was achieved with a significant reduction in reaction stoichiometry, as evidenced by reductions of SI values for both proteases, and covalent complex formation was evident on electrophoretic examination (see Fig. 2).

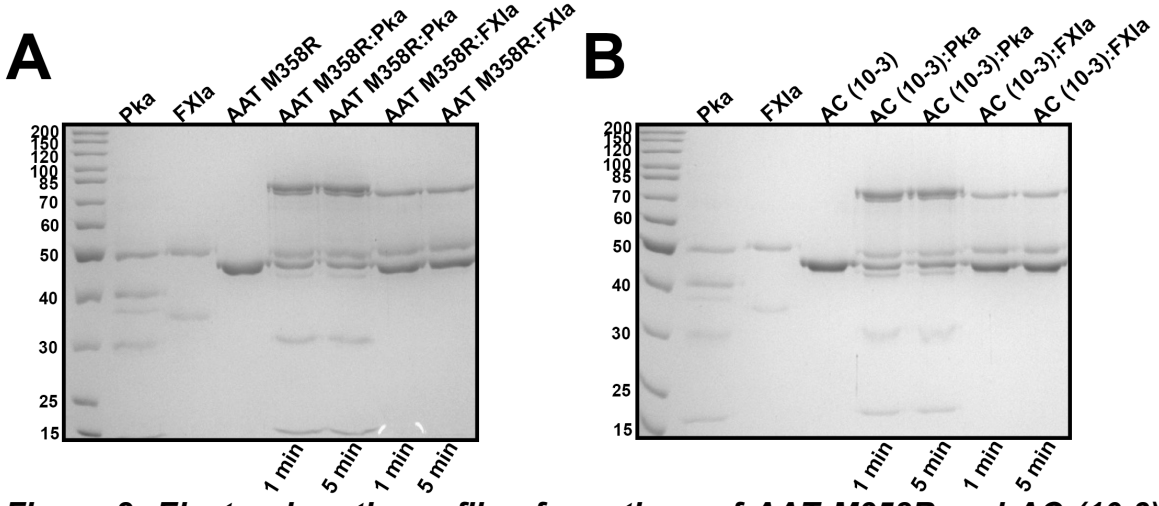

Figure 2: Electrophoretic profile of reactions of AAT M358R and AC (10-3) with Pka or FXIa. Reactions of 2 μM (A) AAT M358R, (B) AC (10-3) with Pka (1 μM) or FXIa (0.2 μM), for 1-5 minutes.

4.2. Characterization of additional AAT M358R-C1INH Loop Exchanged Variants

Because of the likelihood of cooperativity between different parts of the RCL in engineered serpins (Hopkins, Pike et al. 2000), we next determined if reducing substitutions C-terminal to the reactive centre, while maintaining N-terminal substitutions, would improve reactivity and selectivity for Pka. As shown in Table 4, restoring AAT M358R Ser or Ser-Ile residues at P1' or P1' and P2' did little to change the inhibitory profiles of AC (10-3/2'-4') or AC (10-3/3'-4'), which remained less active inhibitors of Pka than AAT M358R, as evidenced by their low rates of inhibition, and less efficient inhibitors of Pka than AAT M358R, as evidenced by their elevated SI values. Restoring the Pro residue from AAT at P3' while maintaining the Val residue from C1INH at P4' yielded AC (10-3/4'), which demonstrated a 1.7-fold increased rate of Pka inhibition, a 1.6-fold decreased rate of FXIa inhibition, and decreases in SI for both proteases, all of which were statistically significant. Taken together, these changes in the reaction profile combined for a 2.8-fold increase in selectivity for Pka, showing the greatest change in selectivity among variants with an increased rate of Pka inhibition of those listed in Tables 3 or 4.

Table 4: Kinetic parameters of inhibition of Pka or FXIa by AAT M358R and constructs produced to study stepwise reversion from AC (10-3/2'-4') to AC (10-8).

Protein	k_2 vs Pka ($x10^5$ $M^{-1}s^{-1}$)	k_2 vs FXIa ($x10^5$ $M^{-1}s^{-1}$)	Selectivity Pka:FXIa	SI vs Pka	SI vs FXIa
AAT M358R	0.37 ± 0.03	1.4 ± 0.1	0.27	2.5 ± 0.2	2.36 ± 0.06
AC (10-3/2'-4')	0.070 ± 0.004 ****	0.041 ± 0.002 ****	1.7	7.0 ± 0.3 ****	10.0 ± 0.4 ****
AC (10-3/3'-4')	0.077 ± 0.003 ****	0.059 ± 0.004 ****	1.3	7.0 ± 0.2 ****	8.2 ± 0.3 ****
AC (10-3/4')	0.64 ± 0.01 ****	0.87 ± 0.04 ****	0.75	1.86 ± 0.09 **	2.1 ± 0.1 *
AC (10-4)	0.61 ± 0.05 ****	1.4 ± 0.1	0.45	1.87 ± 0.08 **	4.8 ± 0.3 ***
AC (10-5)	0.73 ± 0.03 ****	1.5 ± 0.2	0.50	4 ± 2	4.1 ± 0.1 ****
AC (10-6)	0.30 ± 0.02	1.79 ± 0.04 ***	0.17	1.6 ± 0.1 ***	4.6 ± 0.1 ****
AC (10-7)	0.29 ± 0.08	1.3 ± 0.2	0.22	1.60 ± 0.06 ***	3.50 ± 0.02 ****
AC (10-8)[a]	0.088 ± 0.002 ****	2.2 ± 0.4 ****	0.07	2.1 ± 0.2	4.55 ± 0.08 ****

Results are the mean of 5 or 4[a] determinations, ± SD. *, p<0.05; **, p<0.01; ***, p<0.001; ****, p <0.0001 versus AAT M358R. Selectivity = k_2 vs Pka/ k_2 vs FXIa.

As shown in Fig. 3A, the electrophoretic profile of this variant was unchanged compared to AAT M358R and denaturation-resistant higher molecular weight complexes were readily observed following reactions with both proteases.

Further reductions in the number of C1INH residues substituted into the AAT M358R RCL restored or improved the rate of FXIa inhibition and elevated FXIa reaction stoichiometry without enhancing Pka selectivity (Table 4), although all remaining variants (AC (10-4), AC (10-5), AC (10-6), AC (10-7) and AC (10-8)) demonstrated similar electrophoretic reaction profiles (Fig. 3B and Suppl. Fig. S3).

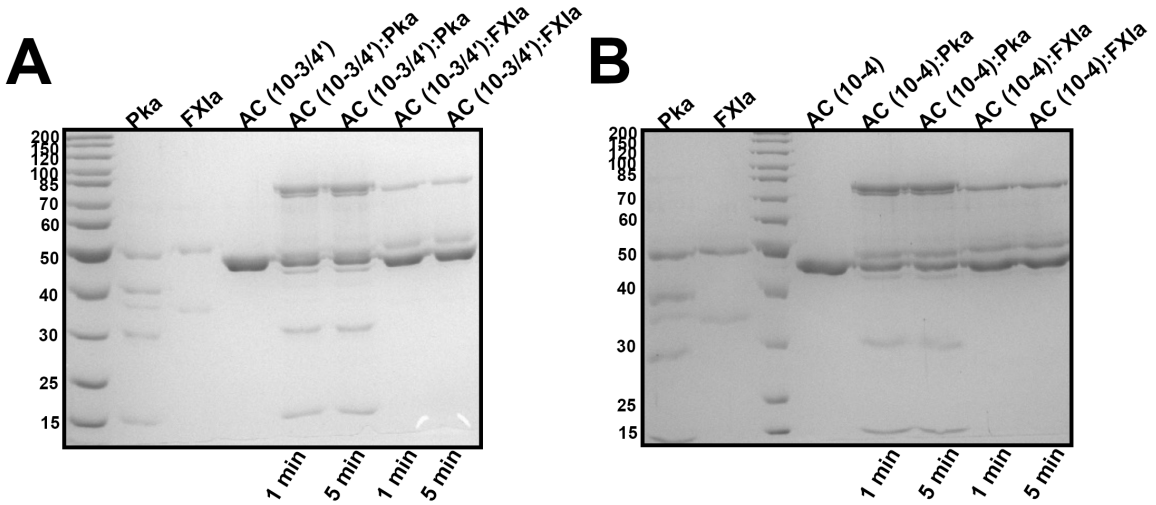

Figure 3: Electrophoretic profile of reactions of AC (10-3/4') and AC (10-4) with Pka or FXIa. Reactions of 2 μM (A) AC (10-3/4'), (B) AC (10-4) with Pka (1 μM) or FXIa (0.2 μM), for 1-5 minutes, are shown.

4.3. Inhibition of Thrombin, Factor Xa, and Factor XIIa by Selected Variants

While most of this study focused on AAT M358R variant inhibition of Pka versus FXIa, the rate of inhibition of thrombin, FXa, and FXIIa was tested for AAT M358R and two variants. As shown in Table 5, both AC (10-3/3'-4') and AC (10-3/4') were slower inhibitors of thrombin (by 6.4- and 8.6-fold, respectively) and FXIIa (by factors of 25- and 16.2-fold, respectively) than AAT M358R. In contrast, FXa inhibition diverged for AC (10-3/3'-4') and AC (10-3/4'), with the former exhibiting a mean k_2 value 73-fold less than that of AAT M358R, and the latter exhibiting a mean k_2 value 1.3-fold higher than AAT M358R. Covalent inhibitory complex formation was consistent with the kinetic values (see Suppl. Fig. S4).

These reductions in k_2 values were mirrored in increased selectivity for Pka over thrombin and FXIIa than had been observed for FXIa for AC (10-3/4') (Table 5).

Table 5: Kinetic parameters of inhibition of thrombin, FXa, or FXIIa by AAT M358R, AC (10-3/3'-4'), and AC (10-3/4').

Protein	k_2 vs thrombin ($x10^5$ $M^{-1}s^{-1}$)	k_2 vs FXa ($x10^5$ $M^{-1}s^{-1}$)	k_2 vs FXIIa ($x10^5$ $M^{-1}s^{-1}$)	Selectivity Pka:thrombin	Selectivity PKa:FXa	Selectivity Pka:FXIIa
AAT M358R	1.8 ± 0.03	0.29 ± 0.1	0.21 ± 0.02	0.21	1.3	1.76
AC (10-3/3'-4')	0.28 ± 0.03****	0.004 ± 0.001****	0.0084 ± 0.0001[a] ****	0.28	19.3	9.17
AC (10-3/4')	0.21 ± 0.03****	0.38 ± 0.01****	0.013 ± 0.003****	3.10	1.7	50.00

Results are the mean of 5 or 3[a] determinations, ± SD. ****, p <0.0001 versus AAT M358R. Selectivity = k_2 vs Pka/ k_2 vs thrombin, FXa, or FXIIa, respectively.

4.4. Intrinsic Fluorescence of AAT M358R and AC (10-3/4')

To gain insight into the folding and conformation of AC (10-3/4'), the most selective variant without an elevated SI in this study, its intrinsic fluorescence profile was compared to that of AAT M358R. As shown in Suppl. Fig. S5A, following excitation at 280 nm, the profile of emitted fluorescence from 310 nm to 450 nm was largely superimposable for both proteins. Heating the proteins caused substantial divergence of the profiles, reinforcing the folding dependence of the spectra (see Suppl. Fig. S5B).

4.5. Molecular Modeling of AAT M358R and Variant Encounter Complexes with Pka and FXIa

The structure of the RCL in the AAT variants when docked to either Pka or FXIa was modeled using the Alphafold 3 deep-learning framework. Fig. 4 shows a rendering of the RCL only, from models of all AAT variants docked to Pka, grouped from maximal to minimal loop exchanges. Initially these structural models were used to visualize and align the RCL segments of all AAT M358R variants, as shown in Fig. 4. As expected, the RCL that aligned least closely with that of AAT M358R was AC (10-4'/d2), which exhibited both a flatter, less protruding loop than AAT M358R, but also considerable distortion of the N-terminal hinge region; extension of the loop via re-introduction of the Pro at P2 improved the alignment of the RCL of AC (10-4') to AAT M358R in the hinge region and also elevated the reactive centre above the serpin body (see Fig. 4A). As the degree of RCL substitution diminished, progressing through the variant sequences presented in Fig. 4B, 4C, and 4D, the alignments improved on the C-terminal portions of the RCL of the variants, with predicted structural differences remaining more pronounced on the N-terminal hinge region.

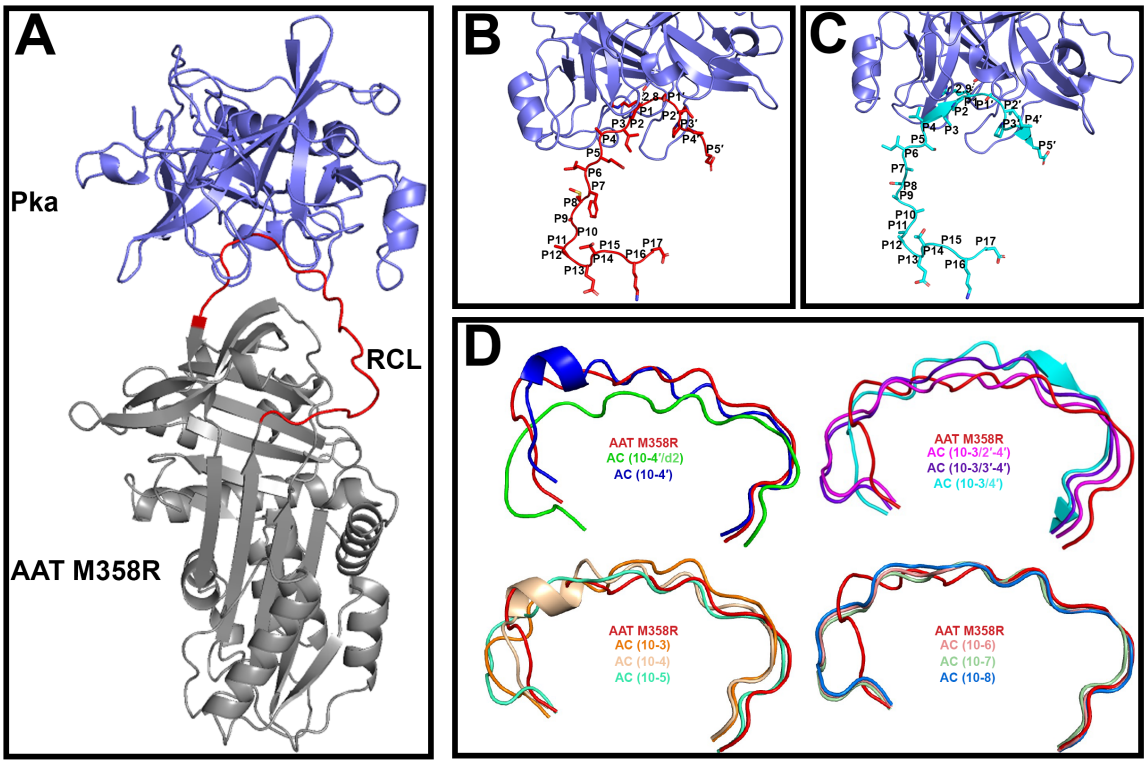

Figure 4: Modeling of Pka and AAT M358R and AC variant encounter complexes. (A) Encounter complex of Pka (violet) and AAT M358R (body of serpin, grey; RCL, red). (B) Close-up of Pka and AAT M358R encounter complex, showing only the RCL and the Pka interface. Dotted line shows distance between Pka S195 hydroxyl and P1 carbon, in Angstroms, bolded. (C) as in B but for AC (10-3/4'), dotted line as in B. (D) RCL alignments from modeled Pka-AAT encounter complexes of (upper left) AAT M358R (red), AC (10-4'/d2) (neon green), AC (10-4') (dark blue), (upper right) AC (10-3/2'-4') (pink), AC (10-3/3'-4') (purple), AC (10-3/4') (cyan), (lower left) AC (10-3) (orange), AC (10-4) (tan), AC (10-5) (turquoise), and (lower right) AC (10-6) (light pink), AC (10-7) (light green), and AC (10-8) (light blue).

Given that a reaction is more likely to take place when reactive groups are situated closely in space, the distance (in angstroms, Å) between the alpha carbon of M358R in AAT variants and the hydroxyl side chain of the active site serine S195 in Pka and FXIa was measured in each modeled encounter complex to ascertain any patterns. As shown in Table 5, these distances did not vary more than 10 – 15% across variants differing in their rates of reaction by up to 150-fold, suggesting that other considerations were more important in driving specificity and selectivity of these reactions. The models were also interrogated to count the number of intramolecular and intermolecular hydrogen bonds between serpin and protease in the modeled complexes. Neither intramolecular nor intermolecular hydrogen bonding correlated well with the rate of inhibition, except that AAT M358R variants with more predicted intermolecular hydrogen bonds than AAT M358R were more likely to react more rapidly with Pka than those with fewer intermolecular hydrogen bonds. This imperfect correlation suggests that some intermolecular hydrogen bonds were more important than others in driving the reaction, or that other more critical determinants were in play.

Table 6: Modeled distances (Å) between alpha carbon of R358 in AAT M358R and S195 hydroxyl side chain of protease in AAT M358R: protease encounter complexes in AAT M358R and variant encounter complexes, and number of intramolecular modeled hydrogen bonds in the AAT M358R or variant RCL residues or intermolecular modeled hydrogen bonds between the AAT M358R or variant RCL and Pka or FXIa.

Protein	Distance with Pka (Å)	Distance with FXIa (Å)	# Intramolecular interactions	# Intermolecular interactions with Pka	# Intermolecular interactions with FXIa
AAT M358R	2.8	3.0	15	9	7
AC (10-4'/d2)	2.9	2.8	12	5	8
AC (10-4')	2.6	2.8	18	7	9
AC (10-3/2'-4')	2.8	2.9	12	7	7
AC (10-3/3'-4')	2.8	3.0	16	14	7
AC (10-3/4')	2.9	3.0	15	11	8
AC (10-3)	2.9	3.0	11	14	7
AC (10-4)	2.8	2.4	15	11	7
AC (10-5)	2.9	3.0	11	12	7
AC (10-6)	2.9	3.0	17	13	7
AC (10-7)	2.9	3.0	23	10	7
AC (10-8)	2.9	3.0	17	11	7

5. Discussion

The results of this study supported our hypothesis that AAT M358R variants with increased specificity for Pka inhibition over AAT M358R existed within the sequence space defined by full or partial substitution of P10-P4' AAT residues with those of C1INH. Among the 11 AAT M358R variants expressed and tested herein, four exhibited a significantly increased rate of Pka inhibition compared to AAT M358R, by up to 4-fold. In terms of enhanced specificity, however, only one variant (AC (10-3/4') exhibited both an increased rate of Pka inhibition and a decreased rate of inhibition of FXIa. FXIa was chosen as a comparator because, unlike Pka or FXIIa, it is not directly involved in bradykinin

generation and because FXI deficiency, unlike deficiency in Pka or FXII, is associated with a small bleeding risk (Ali and Becker 2024). Additionally, for two of the four variants with increased initial rates of Pka inhibition (AC (10-4) and AC (10-5)), the gain in specificity came at the cost of increased SI values for either Pka or FXIa or both, signifying decreased efficiency and the probable generation of cleaved serpin reaction products. Reduced efficiency of inhibition is undesirable in a Pka inhibitor, as would be the inactivation of another protease, FXIa, as a “side-effect”.

Design choices in this loop-exchange study had to reflect the shorter RCL of C1INH. The RCL in C1INH is two residues shorter than in AAT, one residue shorter N-terminal to the R444-T445 reactive centre scissile bond, and one residue shorter C-terminal to it (Bock, Skriver et al. 1986, Bos, Lubbers et al. 2004). Most alignments have positioned the former gap at P2, consistent with the conservation of P12 Ala throughout the serpin superfamily and the identity of P1 in C1INH as R444 (Huber and Carrell 1989, Bos, Hack et al. 2002). Accordingly, the maximal loop exchange was made, spanning the P10 to P4' residues of the two serpins, comprising either 11 (AC (10-4'/d2)) or 12 (AC (10-4')) substitutions, depending on whether Pro at P2 was restored. The maximal exchange severely impacted AC (10-4'/d2) function as both an inhibitor of Pka and FXIa. This outcome could have arisen due to the shorter length of the transplanted RCL or due to the changes in individual residues. Adding back a residue in (AC (10-4')) only improved the rate of inhibition of Pka or FXIa by 3-fold, and the efficiency of

Pka inhibition by 5-fold, versus AC (10-4'/d2), suggesting that residue identity was a greater contributor to this poor inhibitory profile than RCL length. Zhou et al. found that shortening the AAT M358R RCL by deletion of A355 at P4 only reduced the rate constant for FXa inhibition by ~3-fold, without SI alteration, whereas Bos et al. found a 1.5-fold increase in rate constant for Pka inhibition for recombinant C1INH with an Ala insertion at P2, supporting a modest contribution of RCL length variation by a single residue. Limiting the loop exchange to 7 residues N-terminal to P3 in AC (10-3) increased the rate of inhibition of both Pka and FXIa, without SI elevation, but did not advance the goal of increasing AAT M358R selectivity for Pka.

To explore the possibility that negative cooperativity between different parts of the RCL in AC (10-4') was impairing reactivity with Pka, exchanged residues C-terminal to the reactive centre were reverted stepwise towards the AAT M358R sequence. These changes enhanced the rate constant for Pka inhibition in AC (10-3/2'-4') and AC (10-3/3'-4'), albeit with elevated reaction stoichiometries. Restoring Pro at P3' instead of the transferred Leu residue, in AC (10-3/4') increased the rate of Pka inhibition above that of AAT M358R while maintaining the rate of FXIa inhibition below that of AAT M358R, with optimal SI values. Therefore, it is likely that the Leu-Leu dipeptide cooperated negatively with the rest of the exchanged RCL and the Val residue at P4' either was less negatively cooperative or more positively cooperative than these other residues. Enhanced specificity for Pka was lost when the loop-exchanged sequence was

reduced to AC (10-4), further highlighting the effect of either the P4' Val substitution or the removal of the P3' Leu substitution.

Cooperativity between RCL residues in serpins was first noted by Hopkins et al., who reported large and small cooperative effects in a comprehensive study substituting residues from antithrombin into the RCL of AAT M358R (Hopkins, Pike et al. 2000). Of note was the finding that the P361N substitution at P3' had a 196-fold greater effect on the rate of activated protein C (aPC) inhibition in AAT M358R than in the loop-exchanged variant LS7–3', which contained RCL sequences from antithrombin substituted for those of AAT between P7 and P2, as well as the antithrombin-specific P361N substitution at P3'. This finding mirrors our observation of the effects of the P3' Leu residue (P362L) whose effects were removed in comparing AC (10-3/3'-4') to AC (10-3/4'). Cooperativity was also noted when this laboratory combined variant RCL motifs identified in screening different libraries of phage-displayed AAT M358R and compared their effects in isolation (Bhakta, Hamada et al. 2021).

The context-dependent effects noted above explain some of the variation in outcomes in other RCL exchange studies in the literature. Substitution of the P16-P3' RCL of heparin cofactor II, a thrombin-specific serpin, for the corresponding residues of AAT, increased the slow rate of thrombin inhibition by AAT by 5-fold, but did not approach the rate of thrombin inhibition unless Arg was introduced at P1; the resulting AAT (P16-P3' /M358R) variant was reduced 3-fold in its rate of thrombin inhibition versus AAT M358R but 70-fold in its rate of aPC

inhibition, for a >20-fold increase in selectivity for thrombin over aPC (Filion, Bhakta et al. 2004). Gains in selectivity for thrombin over aPC were even greater when eight non-consecutive residues of antithrombin were substituted for those at AAT M358R, as noted above (Hopkins, Crowther et al. 1995, Hopkins, Pike et al. 2000). Replacing the P6-P1 RCL residues of AAT with those of the natural furin inhibitor Serpin B8 increased the inhibition of furin 10-fold over Serpin B8 (Izaguirre, Qi et al. 2013). Substitution of the P12-P2 residues of ovalbumin into AAT impaired antitrypsin activity to a greater extent than separate substitution of P12-P7 and P6-P2 (Chaillan-Huntington, Gettins et al. 1997).

The ability of AAT M358R to inhibit thrombin and other coagulation proteases rapidly was thought to have led to the bleeding diathesis from which the index case succumbed (Owen, Brennan et al. 1983, Scott, Carrell et al. 1986). At least with respect to AC (10-3/4'), rates of inhibition of thrombin and FXIIa were each reduced, by 8.6- and 16.2-fold, which could cumulatively reduce the bleeding risk considerably. This possibility will need to be tested, initially in a C1INH-knockout mouse (Han, MacFarlane et al. 2002), as part of future preclinical testing of AC (10-3/4') or any other AAT M358R-based variant of potential utility in HAE (Sivananthan, Seto et al. 2025).

Empirical mutagenesis efforts such as this study would be unnecessary if *in silico* protein modelling could be exploited to predict the optimal structure of a serpin inhibitor of a given protease. The complexity of the serpin mechanism greatly complicates this task. The serpin RCL must not only present an optimal

structure for protease recognition and formation of an initial encounter complex, but it must also contain optimal residues for bond cleavage and for rapid insertion of the cleaved RCL into the serpin body, as a novel β-strand of an underlying β-sheet (Huntington 2011). Previously our laboratory was able to rationalize the enhanced specificity of AAT M358R variants for FXIa inhibition based on the ability to form hydrogen bonds with Lys192 of FXIa in modelled encounter complexes (Hamada, Bhakta et al. 2021). In contrast, *in silico* modeling did not identify a unique interaction correlated with enhanced specificity in this study. This outcome may have arisen due to the lesser magnitude of the specificity enhancement, to the distribution of the effect over multiple hydrogen bonds, or to the introduced changes having more impact on steps in the serpin mechanism distinct from the initial encounter complex. It is nevertheless intriguing that *in silico* modeling predicted an extremely pronounced turn at P17-P14 in minimally active AC (10-4'/d2), one not seen in AC (10-4') or any other variant with P2 Pro restored. AC (10-4') also exhibited a modeled four-residue α-helix from P12-P9 which was absent in RCLs from other variant except for a similarly positioned but longer helix in the more active AC (10-4) variant, highlighting the complexity of the structural environment. Despite the accuracy of the artificial intelligence-driven software used for the structural predictions (Abramson, Adler et al. 2024), it must be remembered that they constitute a static prediction and cannot take protein dynamics, especially that of the flexible RCL, into account.

Rather than seeking specificity, de Maat et al. sought to engineer AAT to inhibit three contact factor pathway enzymes simultaneously: Pka, FXIIa, and FXIa (de Maat, Sanrattana et al. 2019). This goal was achieved in AAT M358R variant SLLR/V, named for its P4-P1' sequence. AAT SLLR/V inhibited both ferric chloride-induced thrombosis and acute carrageenan-induced tissue edema in mice; promotion of *in vivo* bleeding was not assessed. It is not yet clear if inhibition of all three contact pathway factors is safe for further development. If it becomes clear that it is, then it is noteworthy that AC (10-3) is more active than AAT M358R both in inhibiting Pka and FXIa, and that its SI values for both proteases indicate better efficiency of inhibition than AAT M358R, as well.

Any mutagenesis study comes with the possibility that the introduced changes will affect protein folding. At least with AC (10-3/4'), we addressed this possibility by probing the protein's intrinsic fluorescence spectral profile (Royer 2006). It was found to be virtually indistinguishable from that of AAT M358R, suggesting that both proteins were similarly folded. For other variant proteins reported in this study, we cannot eliminate the possibility of misfolding but consider it unlikely because all variant proteins all had measurable activity as inhibitors, versus at least two proteases, and all proteins were expressed as soluble proteins in *E. coli* without interdiction by bacterial chaperone systems and/or aggregation.

There were other limitations to our study. Our recombinant proteins were expressed as non-glycosylated hexahistidine-tagged proteins in *E. coli*, and their

properties could differ in other expression systems or in the absence of the affinity tag. The AAT variants would likely require expression in a system capable of N-linked glycosylation or albumin fusion or chemical modification with polyethylene glycol to achieve a reasonable circulatory half-life *in vivo*, although we have previously tested bacterially expressed AAT M358R in murine models of thrombosis (Sheffield, Eltringham-Smith et al. 2012). Our concept that variant AAT M358R proteins could replace C1INH assumes that non-inhibitor functions of C1INH, especially those dependent on its unique N-terminal domain, are not relevant to its efficacy in replacement therapy. While this has not been firmly established, for instance using truncated recombinant C1INH *in vivo*, it seems likely due to the clinical efficacy of non-C1INH drugs such as engineered monoclonal antibody anti-Pka and anti-FXIIa agents (Reshef, Hsu et al. 2025). Finally, the stepwise reversion approach that was taken left other variants uninvestigated, such as those that would have arisen from gapped reversion or reversion in the opposite direction (N-terminal to C-terminal).

In conclusion, our findings suggest that RCL exchange between C1INH and AAT was a useful strategy to increase the selectivity of AAT M358R as an inhibitor of Pka. Consistent with exchange studies of other serpins, too large a substitution greatly impaired inhibitory function, and needed to be optimized by stepwise reversion to the AAT M358R sequence. The optimal sequence, in AC (10-3/4'), involved non-contiguous mutated residues. It was 2.8-fold more selective for Pka than FXIa, inhibited Pka 3 times more rapidly than AAT M358R,

and exhibited a favourable reaction stoichiometry less than AAT M358R for both proteases. Although this strategy led to a successful outcome, *in vivo* experimentation will be required to determine if different AAT M358R variants, discovered using an alternative strategy, involving phage display of AAT hypervariable libraries spanning RCL residues P7-P3', constitute superior agents compared to AC (10-3/4'). Of note, variant 7-FLEPS-3, with only two additional mutations in addition to M358R, conferred 9.2-fold greater selectivity for Pka over FXIa than AAT M358R (Sivananthan, Seto et al. 2025).

6. References

Abramson, J., J. Adler, J. Dunger, R. Evans, T. Green, A. Pritzel, O. Ronneberger, L. Willmore, A. J. Ballard, J. Bambrick, S. W. Bodenstein, D. A. Evans, C. C. Hung, M. O'Neill, D. Reiman, K. Tunyasuvunakool, Z. Wu, A. Zemgulyte, E. Arvaniti, C. Beattie, O. Bertolli, A. Bridgland, A. Cherepanov, M. Congreve, A. I. Cowen-Rivers, A. Cowie, M. Figurnov, F. B. Fuchs, H. Gladman, R. Jain, Y. A. Khan, C. M. R. Low, K. Perlin, A. Potapenko, P. Savy, S. Singh, A. Stecula, A. Thillaisundaram, C. Tong, S. Yakneen, E. D. Zhong, M. Zielinski, A. Zidek, V. Bapst, P. Kohli, M. Jaderberg, D. Hassabis and J. M. Jumper (2024). "Accurate structure prediction of biomolecular interactions with AlphaFold 3." Nature **630**(8016): 493-500.

Ali, A. E. and R. C. Becker (2024). "Factor XI: structure, function and therapeutic inhibition." J Thromb Thrombolysis **57**(8): 1315-1328.

Bhakta, V., M. Hamada, A. Nouanesengsy, J. Lapierre, D. L. Perruzza and W. P. Sheffield (2021). "Identification of an alpha-1 antitrypsin variant with enhanced specificity for factor XIa by phage display, bacterial expression, and combinatorial mutagenesis." Sci Rep **11**(1): 5565.

Bock, S. C., K. Skriver, E. Nielsen, H. C. Thogersen, B. Wiman, V. H. Donaldson, R. L. Eddy, J. Marrinan, E. Radziejewska, R. Huber and et al. (1986). "Human C1 inhibitor: primary structure, cDNA cloning, and chromosomal localization." Biochemistry **25**(15): 4292-4301.

Bos, I. G., C. E. Hack and J. P. Abrahams (2002). "Structural and functional aspects of C1-inhibitor." Immunobiology **205**(4-5): 518-533.

Bos, I. G., Y. T. Lubbers, E. Eldering, J. P. Abrahams and C. E. Hack (2004). "Effect of reactive site loop elongation on the inhibitory activity of C1-inhibitor." Biochim Biophys Acta **1699**(1-2): 139-144.
Chaillan-Huntington, C. E., P. G. Gettins, J. A. Huntington and P. A. Patston (1997). "The P6-P2 region of serpins is critical for proteinase inhibition and complex stability." Biochemistry **36**(31): 9562-9570.
Davis, A. E., 3rd (1988). "C1 inhibitor and hereditary angioneurotic edema." Annu Rev Immunol **6**: 595-628.
de Maat, S., W. Sanrattana, R. K. Mailer, N. M. J. Parr, M. Hessing, R. M. Koetsier, J. C. M. Meijers, G. Pasterkamp, T. Renne and C. Maas (2019). "Design and characterization of alpha1-antitrypsin variants for treatment of contact system-driven thromboinflammation." Blood **134**(19): 1658-1669.
Dementiev, A., M. Simonovic, K. Volz and P. G. Gettins (2003). "Canonical inhibitor-like interactions explain reactivity of alpha1-proteinase inhibitor Pittsburgh and antithrombin with proteinases." J Biol Chem **278**(39): 37881-37887.
Donaldson, V. H. and R. R. Evans (1963). "A Biochemical Abnormality in Herediatry Angioneurotic Edema: Absence of Serum Inhibitor of C' 1-Esterase." Am J Med **35**: 37-44.
Filion, M. L., V. Bhakta, L. H. Nguyen, P. S. Liaw and W. P. Sheffield (2004). "Full or partial substitution of the reactive center loop of alpha-1-proteinase inhibitor by that of heparin cofactor II: P1 Arg is required for maximal thrombin inhibition." Biochemistry **43**(46): 14864-14872.
Gigli, I., J. W. Mason, R. W. Colman and K. F. Austen (1970). "Interaction of plasma kallikrein with the C1 inhibitor." J Immunol **104**(3): 574-581.
Grover, S. P., T. Kawano, J. Wan, P. Tanratana, Z. Polai, Y. J. Shim, O. Snir, S. Braekkan, S. Dhrolia, R. R. Kasthuri, P. K. Bendapudi, K. R. McCrae, A. S. Wolberg, J. B. Hansen, H. Farkas and N. Mackman (2023). "C1 inhibitor deficiency enhances contact pathway-mediated activation of coagulation and venous thrombosis." Blood **141**(19): 2390-2401.
Hamada, M., V. Bhakta, S. N. Andres and W. P. Sheffield (2021). "Stepwise Reversion of Multiply Mutated Recombinant Antitrypsin Reveals a Selective Inhibitor of Coagulation Factor XIa as Active as the M358R Variant." Front Cardiovasc Med **8**: 647405.
Han, E. D., R. C. MacFarlane, A. N. Mulligan, J. Scafidi and A. E. Davis, 3rd (2002). "Increased vascular permeability in C1 inhibitor-deficient mice mediated by the bradykinin type 2 receptor." J Clin Invest **109**(8): 1057-1063.
Heeb, M. J., R. Bischoff, M. Courtney and J. H. Griffin (1990). "Inhibition of activated protein C by recombinant alpha 1-antitrypsin variants with substitution of arginine or leucine for methionine358." J Biol Chem **265**(4): 2365-2369.
Hopkins, P. C., D. C. Crowther, R. W. Carrell and S. R. Stone (1995). "Development of a novel recombinant serpin with potential antithrombotic properties." J Biol Chem **270**(20): 11866-11871.

Hopkins, P. C., R. N. Pike and S. R. Stone (2000). "Evolution of serpin specificity: cooperative interactions in the reactive-site loop sequence of antithrombin specifically restrict the inhibition of activated protein C." J Mol Evol **51**(5): 507-515.
Huber, R. and R. W. Carrell (1989). "Implications of the three-dimensional structure of alpha 1-antitrypsin for structure and function of serpins." Biochemistry **28**(23): 8951-8966.
Huntington, J. A. (2011). "Serpin structure, function and dysfunction." J Thromb Haemost **9 Suppl 1**: 26-34.
Izaguirre, G., L. Qi, M. Lima and S. T. Olson (2013). "Identification of serpin determinants of specificity and selectivity for furin inhibition through studies of alpha1PDX (alpha1-protease inhibitor Portland)-serpin B8 and furin active-site loop chimeras." J Biol Chem **288**(30): 21802-21814.
Kajdacsi, E., Z. Jandrasics, N. Veszeli, V. Mako, A. Koncz, D. Gulyas, K. V. Kohalmi, G. Temesszentandrasi, L. Cervenak, P. Gal, J. Dobo, S. de Maat, C. Maas, H. Farkas and L. Varga (2020). "Patterns of C1-Inhibitor/Plasma Serine Protease Complexes in Healthy Humans and in Hereditary Angioedema Patients." Front Immunol **11**: 794.
Karnaukhova, E. (2022). "C1-Inhibitor: Structure, Functional Diversity and Therapeutic Development." Curr Med Chem **29**(3): 467-488.
Landerman, N. S., M. E. Webster, E. L. Becker and H. E. Ratcliffe (1962). "Hereditary angioneurotic edema. II. Deficiency of inhibitor for serum globulin permeability factor and/or plasma kallikrein." J Allergy **33**: 330-341.
Levi, M., D. M. Cohn and S. Zeerleder (2019). "Hereditary angioedema: Linking complement regulation to the coagulation system." Res Pract Thromb Haemost **3**(1): 38-43.
Lin, L., M. Wu and J. Zhao (2017). "The initiation and effects of plasma contact activation: an overview." Int J Hematol **105**(3): 235-243.
Long, L. H., T. Fujioka, T. J. Craig and H. Hitomi (2024). "Long term outcome of C1-esterase inhibitor deficiency." Asian Pac J Allergy Immunol **42**(3): 222-232.
Longhurst, H. and M. Cicardi (2012). "Hereditary angio-oedema." Lancet **379**(9814): 474-481.
Motta, G., L. Juliano and J. R. Chagas (2023). "Human plasma kallikrein: roles in coagulation, fibrinolysis, inflammation pathways, and beyond." Front Physiol **14**: 1188816.
Navaneetham, D., L. Jin, P. Pandey, J. E. Strickler, R. E. Babine, S. S. Abdel-Meguid and P. N. Walsh (2005). "Structural and mutational analyses of the molecular interactions between the catalytic domain of factor XIa and the Kunitz protease inhibitor domain of protease nexin 2." J Biol Chem **280**(43): 36165-36175.
Owen, M. C., S. O. Brennan, J. H. Lewis and R. W. Carrell (1983). "Mutation of antitrypsin to antithrombin. alpha 1-antitrypsin Pittsburgh (358 Met leads to Arg), a fatal bleeding disorder." N Engl J Med **309**(12): 694-698.

Patston, P. A., N. Roodi, J. A. Schifferli, R. Bischoff, M. Courtney and M. Schapira (1990). "Reactivity of alpha 1-antitrypsin mutants against proteolytic enzymes of the kallikrein-kinin, complement, and fibrinolytic systems." J Biol Chem **265**(18): 10786-10791.
Polderdijk, S. G., T. E. Adams, L. Ivanciu, R. M. Camire, T. P. Baglin and J. A. Huntington (2017). "Design and characterization of an APC-specific serpin for the treatment of hemophilia." Blood **129**(1): 105-113.
Reshef, A., C. Hsu, C. H. Katelaris, P. H. Li, M. Magerl, K. Yamagami, M. Guilarte, P. K. Keith, J. A. Bernstein, J. P. Lawo, H. Shetty, M. Pollen, L. Wieman, T. J. Craig and V. S. Group (2025). "Long-term safety and efficacy of garadacimab for preventing hereditary angioedema attacks: Phase 3 open-label extension study." Allergy **80**(2): 545-556.
Royer, C. A. (2006). "Probing protein folding and conformational transitions with fluorescence." Chem Rev **106**(5): 1769-1784.
Schapira, M., M. A. Ramus, S. Jallat, D. Carvallo and M. Courtney (1986). "Recombinant alpha 1-antitrypsin Pittsburgh (Met 358----Arg) is a potent inhibitor of plasma kallikrein and activated factor XII fragment." J Clin Invest **77**(2): 635-637.
Schechter, I. and A. Berger (1967). "On the size of the active site in proteases. I. Papain." Biochem.Biophys.Res.Commun. **27**(2): 157-162.
Schmaier, A. H. (2016). "The contact activation and kallikrein/kinin systems: pathophysiologic and physiologic activities." J Thromb Haemost **14**(1): 28-39.
Scott, B. M., W. L. Matochko, R. F. Gierczak, V. Bhakta, R. Derda and W. P. Sheffield (2014). "Phage display of the serpin alpha-1 proteinase inhibitor randomized at consecutive residues in the reactive centre loop and biopanned with or without thrombin." PLoS One **9**(1): e84491.
Scott, C. F., R. W. Carrell, C. B. Glaser, F. Kueppers, J. H. Lewis and R. W. Colman (1986). "Alpha-1-antitrypsin-Pittsburgh. A potent inhibitor of human plasma factor XIa, kallikrein, and factor XIIf." J Clin Invest **77**(2): 631-634.
Sheffield, W. P., L. J. Eltringham-Smith, V. Bhakta and S. Gataiance (2012). "Reduction of thrombus size in murine models of thrombosis following administration of recombinant alpha1-proteinase inhibitor mutant proteins." Thromb Haemost **107**(5): 972-984.
Sinnathamby, E. S., P. P. Issa, L. Roberts, H. Norwood, K. Malone, H. Vemulapalli, S. Ahmadzadeh, E. M. Cornett, S. Shekoohi and A. D. Kaye (2023). "Hereditary Angioedema: Diagnosis, Clinical Implications, and Pathophysiology." Adv Ther **40**(3): 814-827.
Sivananthan, S., V. Bhakta, N. Chaechi Tehrani and W. P. Sheffield (2024). "Prolonging the circulatory half-life of C1 esterase inhibitor via albumin fusion." PLoS One **19**(10): e0305719.
Sivananthan, S., T. Seto, N. C. Tehrani, V. Bhakta and W. P. Sheffield (2025). "Enhancement of plasma kallikrein specificity of antitrypsin variants identified by phage display and partial reversion." BMC Biotechnol **25**(1): 22.

Strnad, P., N. G. McElvaney and D. A. Lomas (2020). "Alpha(1)-Antitrypsin Deficiency." N Engl J Med **382**(15): 1443-1455.
Tang, J., C. L. Yu, S. R. Williams, E. Springman, D. Jeffery, P. A. Sprengeler, A. Estevez, J. Sampang, W. Shrader, J. Spencer, W. Young, M. McGrath and B. A. Katz (2005). "Expression, crystallization, and three-dimensional structure of the catalytic domain of human plasma kallikrein." J Biol Chem **280**(49): 41077-41089.
Travis, J., N. R. Matheson, P. M. George and R. W. Carrell (1986). "Kinetic studies on the interaction of alpha 1-proteinase inhibitor (Pittsburgh) with trypsin-like serine proteinases." Biol Chem Hoppe Seyler **367**(9): 853-859.
Wedner, H. J. (2020). "Hereditary angioedema: Pathophysiology (HAE type I, HAE type II, and HAE nC1-INH)." Allergy Asthma Proc **41**(Suppl 1): S14-S17.
Wettschureck, N., B. Strilic and S. Offermanns (2019). "Passing the Vascular Barrier: Endothelial Signaling Processes Controlling Extravasation." Physiol Rev **99**(3): 1467-1525.
Wilkerson, R. G. and J. J. Moellman (2022). "Hereditary Angioedema." Emerg Med Clin North Am **40**(1): 99-118.
Wu, Y. (2015). "Contact pathway of coagulation and inflammation." Thromb J **13**: 17.
Wuillemin, W. A., E. Eldering, F. Citarella, C. P. de Ruig, H. ten Cate and C. E. Hack (1996). "Modulation of contact system proteases by glycosaminoglycans. Selective enhancement of the inhibition of factor XIa." J Biol Chem **271**(22): 12913-12918.
Zahedi, K., A. E. Prada and A. E. Davis, 3rd (1993). "Structure and regulation of the C1 inhibitor gene." Behring Inst Mitt(93): 115-119.

7. Supplementary Information

5’ACGGAGATTCCGGAGGCTCAGATCCATGAAGGCTTCCAGGAGCTCCTCC

GTACCCTCAACCAGCCAGACAGCCAGCTCCAGCTGACCACCGGCAATGGC

CTGTTCCTCAGCGAGGGCCTGAAGCTAGTGGATAAGTTTTTGGAGGATGTTA

AAAAGTTGTACCACTCAGAAGCCTTCACTGTCAACTTCGGGGACACCGAAG

AGGCCAAGAAACAGATCAACGATTACGTGGAGAAGGGTACTCAAGGGAAAA

TTGTGGATTTGGTCAAGGAGCTTGACAGAGACACAGTTTTTGCTCTGGTGAA

TTACATCTTCTTTAAAGGCAAATGGGAGAGACCCTTTGAAGTCAAGGACACC

GAGGAAGAGGACTTCCACGTGGACCAGGTGACCACCGTGAAGGTGCCTAT

GATGAAGCGTTTAGGCATGTTTAACATCCAGCACTGTAAGAAGCTGTCCAGC
TGGGTGCTGCTGATGAAATACCTGGGCAATGCCACCGCCATCTTCTTCCTG
CCTGATGAGGGGAAACTACAGCACCTGGAAAATGAACTCACCCACGATATC
ATCACCAAGTTCCTGGAAAATGAAGACAGAAGGTCTGCCAGCTTACATTTAC
CCAAACTGTCCATTACTGGAACCTATGATCTGAAGAGCGTCCTGGGTCAACT
GGGCATCACTAAGGTCTTCAGCAATGGGGCTGACCTCTCCGGGGTCACAGA
GGAGGCACCCCTGAAGCTCTCCAAGGCCGTGCATAAGGCTGTGCTGACCAT
CGATGAGAAAGGGACTGAAGCTGCTGCTGCTAGTGCCATTTCAGTTGCTCG
TACTCTACTTGTAGAGGTCAAGTTCAACAAACCCTTTGTCTTCTTAATGATTG
AACAAAATACCAAGTCTCCCCTCTTCATGGGAAAAGTGGTGAATCCCACCCA
AAAATAAGAATTCGTACTG3’

Supplemental Figure S1A. *DNA sequence of synthetic DNA fragment (gene block) encoding 3’ sector of open reading frame (ORF) encoding AC (10-4′/d2).* Only the coding strand of the 942 bp double-stranded fragment is shown.

MSPILGYWKIKGLVQPTRLLLEYLEEKYEEHLYERDEGDKWRNKKFELGLEFPN
LPYYIDGDVKLTQSMAIIRYIADKHNMLGGCPKERAEISMLEGAVLDIRYGVSRIA
YSKDFETLKVDFLSKLPEMLKMFEDRLCHKTYLNGDHVTHPDFMLYDALDVVLY
MDPMCLDAFPKLVCFKKRIEAIPQIDKYLKSSKYIAWPLQGWQATFGGGDHPPK
SDLEVLFQGPMG*HHHHHH***E**DPQGDAAQKTDTSHHDQDHPTFNKITPNLAEFAF
SLYRQLAHQSNSTNIFFSPVSIATAFAMLSLGTKADTHDEILEGLNFNLTEIPEAQI
HEGFQELLRTLNQPDSQLQLTTGNGLFLSEGLKLVDKFLEDVKKLYHSEAFTVN

FGDTEEAKKQINDYVEKGTQGKIVDLVKELDRDTVFALVNYIFFKGKWERPFEV
KDTEEEDFHVDQVTTVKVPMMKRLGMFNIQHCKKLSSWVLLMKYLGNATAIFFL
PDEGKLQHLENELTHDIITKFLENEDRRSASLHLPKLSITGTYDLKSVLGQLGITK
VFSNGADLSGVTEEAPLKLSKAVHKAVLTIDEKGTEAAAASAISVA_RTLLVEVKF
NKPFVFLMIEQNTKSPLFMGKVVNPTQ**K**

Supplemental Figure S1B. *Amino acid sequence of full GST-AC (10-4'/d2) fusion protein ORF designed for expression using plasmid pGEX-AC AC (10-4'/d2).* GST residues and LEVLFQ↓ PreScission protease cleavage sites are not highlighted, while hexahistidine-tagged (italics) AC (10-4'/d2) protein liberated by cleavage and purified by nickel chelate chromatography is highlighted in yellow. P10-P4' residues are underlined, with a gap introduced at P2 (d2). Glu1 (**E**) and Lys394 (**K**) of AAT are bolded.

AAT Variant Name	**DNA sequence**
AC (10-4')	GCTGCTAGTGCCATTTCAGTTGCTCCGCGTACTCTACTTGTA
AC (10-3/2'-4')	GCTGCTAGTGCCATTTCAGTTGCTCCGCGTTCTCTACTTGTA
AC (10-3/3'-4')	GCTGCTAGTGCCATTTCAGTTGCTCCGCGTTCTATCCTTGTA
AC (10-3/4')	GCTGCTAGTGCCATTTCAGTTGCTCCGCGTTCTATCCCCGTA
AC (10-3)	GCTGCTAGTGCCATTTCAGTTGCTCCCAGGTCTATCCCCCCT
AC (10-4)	GCTGCTAGTGCCATTTCAGTTATACCGCGTTCTATCCCCCCT
AC (10-5)	GCTGCTAGTGCCATTTCAGCCATACCGCGTTCTATCCCCCCT

AC (10-6)	GCTGCTAGTGCCATTGAGGCCATACCGCGTTCTATCCCCCCT
AC (10-7)	GCTGCTAGTGCCTTAGAGGCCATACCGCGTTCTATCCCCCCT
AC (10-8)	GCTGCTAGTTTTTTAGAGGCCATACCGCGTTCTATCCCCCCT
AAT M358R	**GGGGCCATGTTTTTAGAGGCCATACCCAGGTCTATCCCCCCT**

Supplemental Figure S1C*. Synthetic DNA sequences (gene blocks) identical to those shown in Supplemental Figure 1A except for codons shown above, between P10 and P4', were employed to make 10 additional pGEX-AC (X) constructs.* AAT M358R sequence (last row, bolded) is shown for comparison.

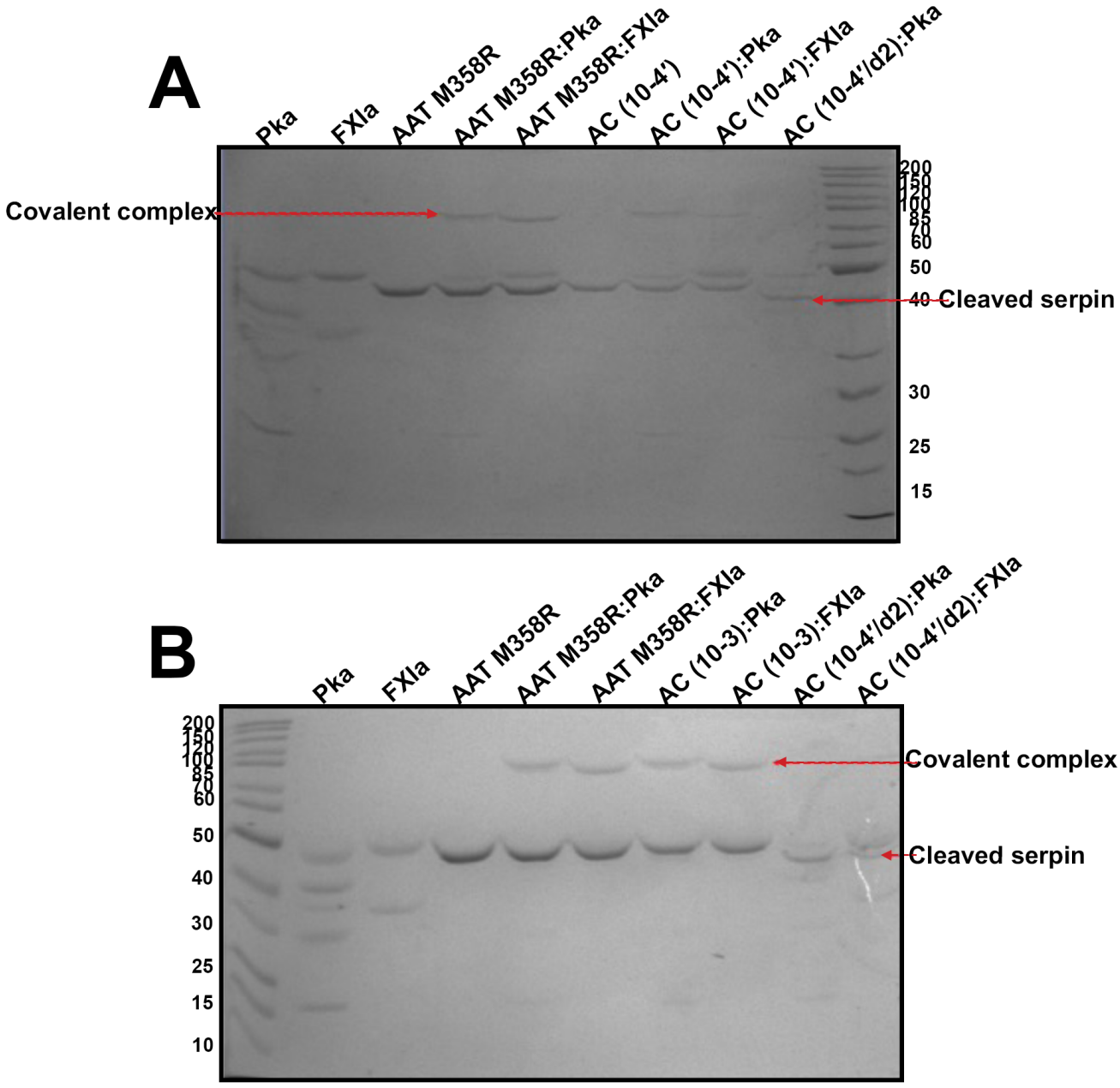

Supplemental Figure S2*. Electrophoretic profile of reactions of AAT M358R, AC (10-3), AC (10-4'), and AC (10-4'/d2), with Pka or FXIa.* (A) Reactions of 2 μM AAT M358R and AC (10-4') with and without 1 μM Pka or 0.2 μM FXIa, and 2 μM AC (10-4') with 1 μM Pka, are shown. (B) Reactions of 2 μM AAT M358R, AC (10-3), and AC (10-4') with 1 μM Pka or 0.2 μM FXIa, are shown.

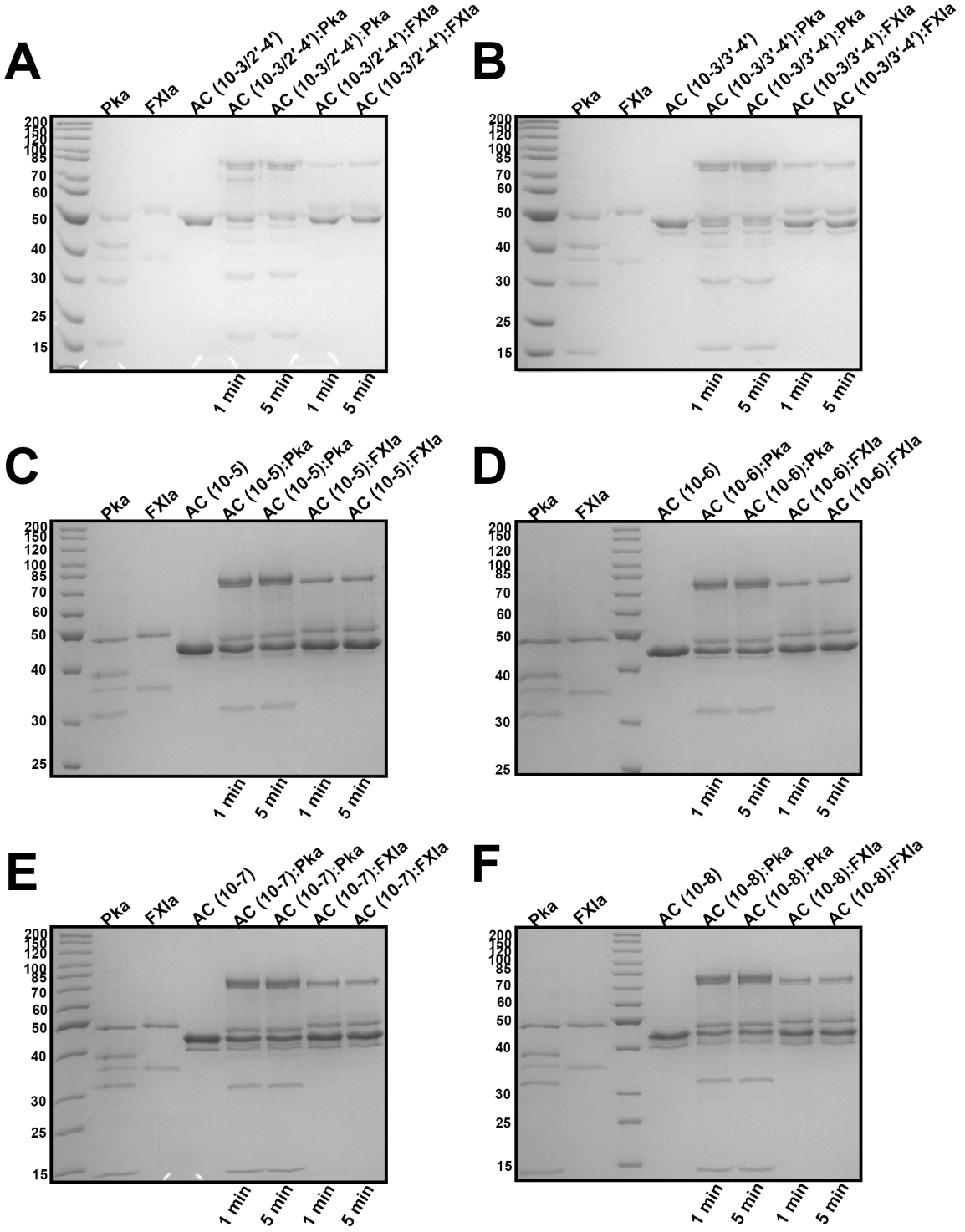

Supplemental Figure S3*. Electrophoretic profile of reactions of additional revertant variants with Pka or FXIa.* Reactions of 2 μM (A) AC (10-3/2'-4'), (B) AC

(10-3/3'-4'), (C) AC (10-5), (D) AC (10-6), (E) AC (10-7), or (F) AC (10-8) with Pka (1 μM) or FXIa (0.2 μM), for 1-5 minutes, are shown.

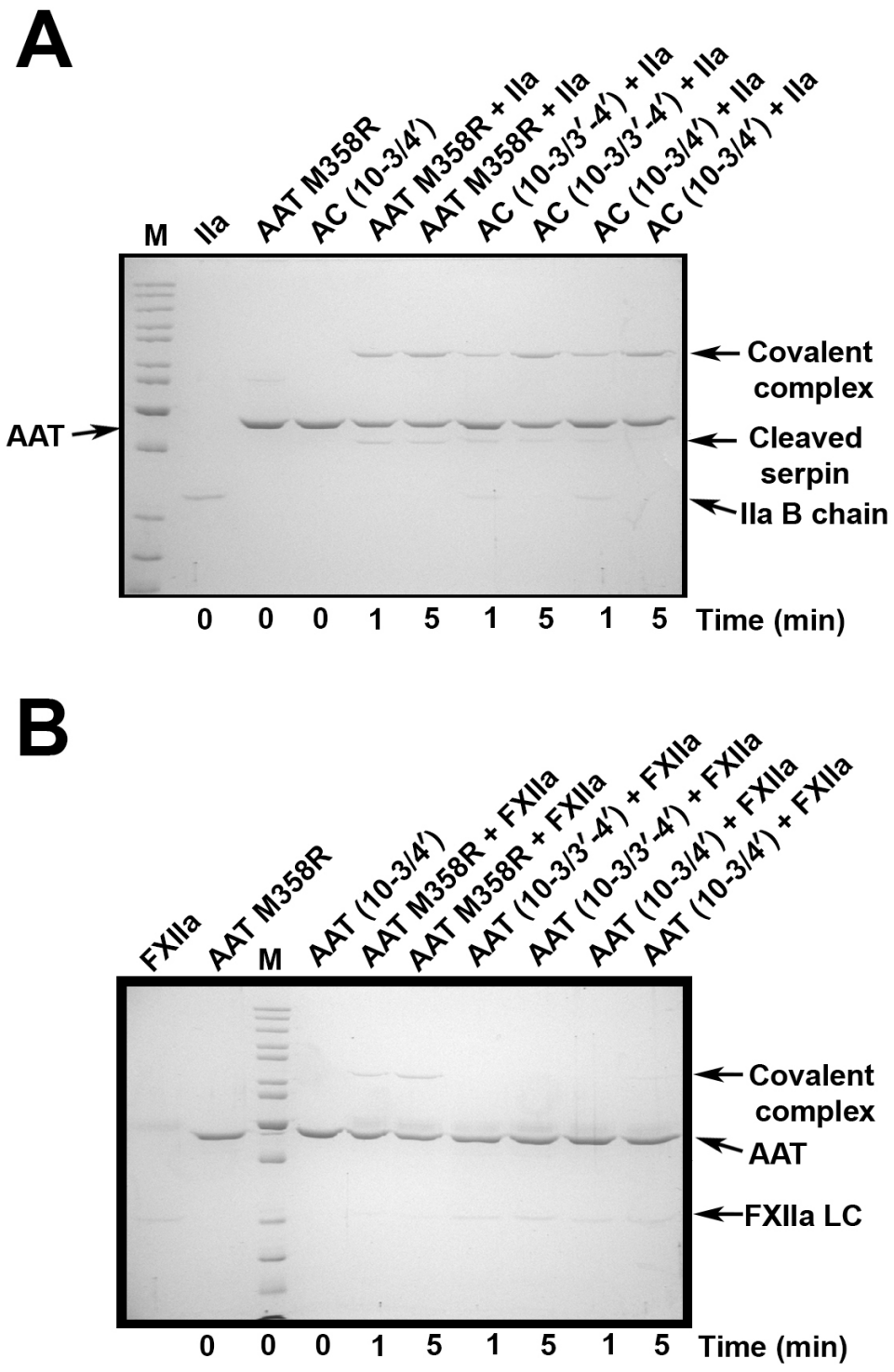

Supplemental Figure S4. *Electrophoretic profiles of reactions of selected variants with thrombin or FXIIa.* Reactions of 2 μM AAT M358R or AC (10-3/3'-4') or AC (10-3/4') with 0.4 μM thrombin (IIa) (A) or 0.4 μM FXIIa, for 0 (no protease), 1, or 5 minutes, are shown. The positions of AAT-IIa or AAT-FXIIa covalent complexes, cleaved AAT (serpin) and the catalytic chain of IIa (IIa B chain) or FXIIa (FXIIa light chain, LC) are shown beside the panels.

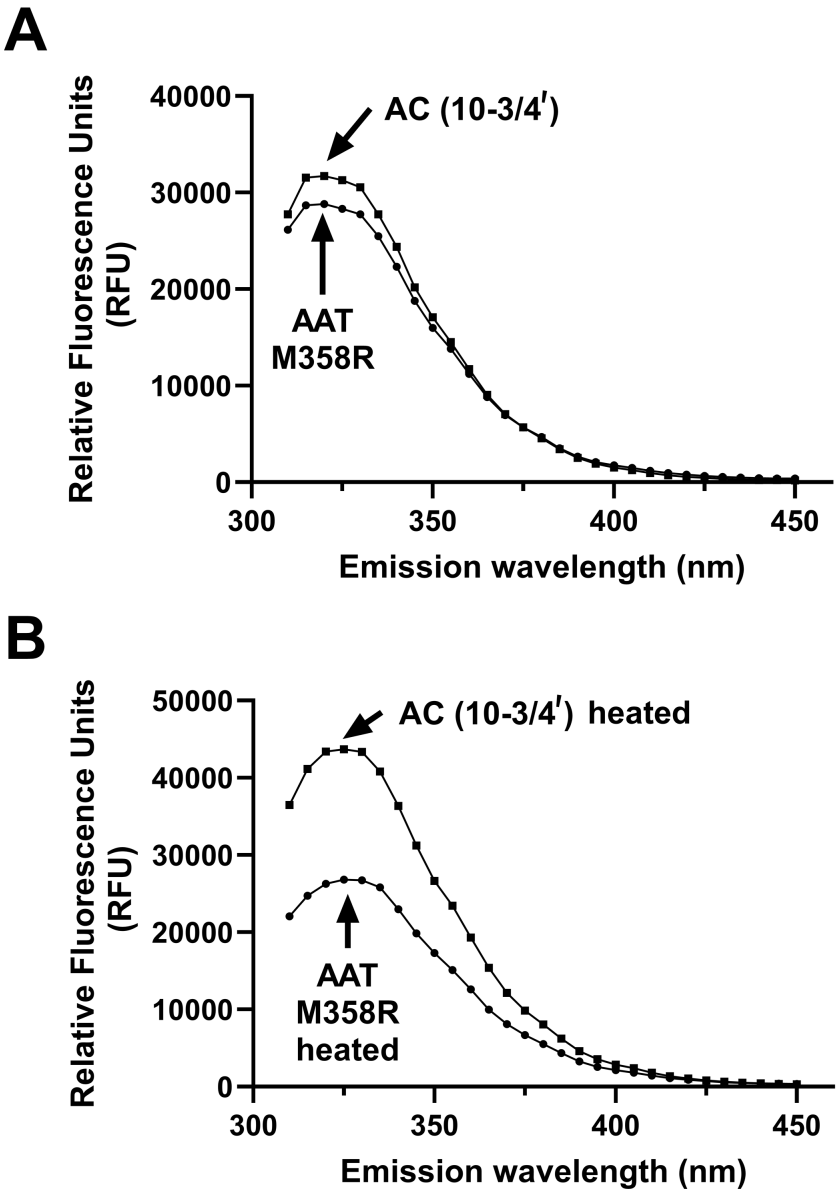

Supplemental Figure S5*. Intrinsic fluorescence profiles of AAT M358R and AC (10-3/4').* Emission spectra of 4.0 μM solutions of AAT M358R (circles) or AC (10-3/4') (squares) in PBS were determined using excitation at 280 nm and emission from 310 to 450 nm. Results are shown with PBS background subtracted, either without (A) or with (B) heating at 95ºC for 10 minutes.

8. Highlights

- C1 esterase inhibitor (C1INH) deficiency causes Hereditary Angioedema (HAE)
- HAE arises due to overactive plasma kallikrein (Pka) activity
- Alpha-1 antitrypsin variants containing full or partial substitutions of their reactive centre loops with the corresponding residues of C1INH were produced
- One of 11 variants tested, AC (10-3/4'), was 2.8-fold more selective for Pka than another protease, activated coagulation factor XI, without increasing reaction stoichiometry
- The novel inhibitor could be a first step towards improved recombinant protein treatments for HAE.

CHAPTER 6 - DISCUSSION

1. Overall Context and Contributions to Knowledge

This thesis explored strategic protein engineering approaches aimed at enhancing serpin therapeutics for targeted protease inhibition and prolonged pharmacokinetics. Chapter 2 highlighted the fusion of MSA to the C-terminus of H_6-trC1INH(MGS) resulting in a 3-fold increase in half-life compared to unfused C1INH, retaining approximately 67% of the half-life observed for unfused H_6-MSA control. Recognizing the potential importance of fusion orientation, Chapter 3 explored the repositioning of MSA to the N-terminus of H_6-trC1INH(MGS), further increasing plasma residency by an additional 1.8-fold relative to the C-terminal fusion, showing the significant impact of fusion topology on pharmacokinetics. Building on the therapeutic goal of specificity and potency, subsequent projects shifted focus toward enhancing the anti-Pka activity of AAT M358R. Chapter 4 exploited the use of phage display. The variant 7-FLEPS-3 emerged as a potent candidate, exhibiting a 4.5-fold increase in inhibitory activity against Pka with a notable selectivity of 1.66. Molecular modeling suggested that this improved inhibition might result from a substantially reduced distance, by 85%, between the serpin's P1 carbonyl group and the catalytic serine hydroxyl of Pka, facilitating a more efficient encounter complex formation. In Chapter 5, a different mutagenic paradigm was employed, loop exchange between AAT and C1INH. This Chapter identified the variant AC (10-3/4') as having enhanced specificity, achieving a 2.8-fold improvement in selective inhibition of Pka versus AAT M358R. Interestingly, a critical insight was obtained through AC (10-4'/d2), where reducing the reactive

center loop length by a single residue converted the serpin into a substrate, underscoring loop length as a crucial factor in maintaining inhibitory function. Collectively, these interconnected studies showcase and demonstrate the worth of two strategies for generating improved Pka inhibitors: C1INH simplification and optimal albumin fusion of the simplified serpin; and manipulation of AAT M358R RCL composition and length using either motifs uncovered by phage display or substitution of parts of the C1INH RCL.

2. Potential Therapeutic Implications

The findings presented in this thesis have implications for the therapeutic landscape for HAE, pending further development and possible translation. Currently available prophylactic treatments for HAE are limited in number and often impose substantial financial burdens, exemplified by therapies like Lanadelumab (Zuraw 2019). This work directly addresses these limitations by exploring cost effective and scalable serpin production in yeast (*P. pastoris*) and bacterial expression systems, possibly positioning these engineered serpins as advantageous alternatives. By extending the half-life of H_6-trC1INH(MGS) via fusion with MSA, particularly in the optimized N-terminal orientation, this research directly addresses the clinical limitation of frequent dosing associated with current HAE treatments, providing that the relevant properties of the MSA fusion are maintained when it is humanized by substitution of HSA for MSA. A prolonged circulating half-life can potentially translate into improved patient compliance, reduced treatment burden, and enhanced quality of life. Concurrently, the

discovery and characterization of the highly specific AAT-derived variants, notably 7-FLEPS-3 and AC (10-3/4'), establish promising new candidates for targeted anti-Pka therapeutics, demonstrating increased inhibitory potency and selectivity compared to AAT M358R. These engineered serpins, optimized through meticulous analysis of RCL composition and length, provide increased Pka activity while minimizing potential off-target effects, thus potentially enhancing safety profiles if their *in vitro* promise translates into improved control of vascular permeability in mice. Moreover, the use of microbial expression systems not only facilitates rapid production timelines but also significantly reduces manufacturing costs, providing a competitive advantage over existing prophylactic biologics (Karbalaei, Rezaee, and Farsiani 2020; Zerbs, Giuliani, and Collart 2014).

The research outlined in this thesis possesses substantial translational potential, bridging protein engineering with clinical applications for patients with HAE. The development of serpins with enhanced half-life, as demonstrated through the optimized H_6-MSA-trC1INH(MGS) fusions, could offer a pathway toward clinical translation by addressing key barriers such as dosing frequency and patient adherence (Cruz 2015; Sinnathamby et al. 2023; Eidelman 2010; Leach et al. 2015). By utilizing cost effective and scalable microbial expression systems like *P. pastoris* and bacterial hosts, these serpins become accessible alternatives to high-cost biologics currently dominating the prophylactic treatment landscape (Wang et al. 2020; Busse and Kaplan 2022). The identification of

potent and selective anti-Pka variants, such as 7-FLEPS-3 and AC (10-3/4'), provides a promising basis for the clinical development of targeted therapeutics compared to conventional therapies. Additionally, the insights derived from detailed structural analyses inform rational design strategies that can be extended beyond HAE, facilitating broader applications in diseases involving dysregulated protease activity.

This thesis introduces significant methodological advancements in the engineering and optimization of therapeutic serpins. By leveraging fusion protein strategies, this work demonstrates for the first time the critical importance of orientation when fusing MSA to H_6-trC1INH(MGS), showing that N-terminal fusion significantly outperforms traditional C-terminal approaches, and an albumin fusion can work on a serpin as well. Additionally, the application of phage display technology represents a substantial methodological advancement in serpin specificity engineering. Traditionally limited to antibodies or smaller peptide scaffolds, the adaptation of phage display to screen combinatorial libraries of serpin reactive center loops represents a substantial methodological innovation, enabling the discovery of highly effective variants such as 7-QLIPS-3 and 2-VRRAY-3' motifs. This approach significantly expands the possibilities for serpin inhibitor design beyond conventional rational methods and the use of T7 bacteriophage instead of M13 phage. Furthermore, the comprehensive loop exchange strategy between AAT and C1INH employed in this thesis advances

the methodology of serpin engineering by demonstrating successful exchange of large, specificity determining loops across different serpins.

3. Albumin Fusion

The genetic fusion of C1INH to albumin represents a novel strategy to extend the half-life of C1INH by leveraging albumin's long circulatory residence (19 days) and its recycling via FcRn pathway (Andersen et al. 2014). FcRn is crucial protein that regulates the homeostasis of plasma proteins such as IgG and albumin (Kim et al. 1999; Sand, Bern, Nilsen, Dalhus, et al. 2014). FcRn is predominantly localized within acidified endosomal compartments. First, IgG and albumin are internalized into cells via fluid-phase pinocytosis. Within the acidic environment of the endosome, FcRn selectively binds to these ligands in a strictly pH dependent manner where the interactions occur efficiently at low pH but are negligible at physiological pH (Sand, Bern, Nilsen, Noordzij, et al. 2014; Pyzik et al. 2015; Grevys et al. 2018). FcRn recognizes the CH2–CH3 interdomain region of IgG, whereas binding to albumin requires structural input from both domain I and domain III (Kim et al. 1999; Sand, Bern, Nilsen, Dalhus, et al. 2014). Once bound, the FcRn–protein complexes are sorted away from lysosomes, thereby preventing degradation. The complexes are then transported back to the cell surface. Upon reaching the neutral pH of the extracellular environment, FcRn releases IgG and albumin back into the circulation (Sand, Bern, Nilsen, Noordzij, et al. 2014; Pyzik et al. 2015; Grevys et al. 2018). While albumin fusion is a well-established approach for prolonging the pharmacokinetics of biologics, it had not

previously been applied to C1INH. Existing C1INH therapies, whether plasma derived (half-life 36-48 hours) or recombinant (half-life 3 hours), require frequent dosing, limiting patient convenience and increasing treatment burden (Bernstein et al. 2010; Hayes et al. 2021; Prematta, Prematta, and Craig 2008). Similar concepts have been used with other proteins, such as coagulation factors, which have been fused to the IgG Fc domain to protect them from clearance (Powell et al. 2012; Shapiro et al. 2012). Fusing C1INH directly to albumin provided similar benefits, conferring FcRn recycling, increasing molecular size and resisting renal clearance, offering an alternative to antibody-based half-life extension strategies. Unlike IgG or Fc, albumin is not glycosylated, allowing for recombinant production of C1INH fusion proteins in economical and scalable systems such as *P. pastoris* rather than mammalian cell culture hosts such as CHO or HEK 293 cells. The albumin-fused C1INH construct achieved a prolonged half-life approaching that of albumin itself while largely retaining C1INH's inhibitory activity. This innovation, creating a recombinant C1INH with extended circulatory residency without compromising function, resembled the sustained Pka inhibition seen with long acting monoclonal antibodies like Lanadelumab. As such, this strategy introduces a promising and previously unexplored modality for C1INH based HAE prophylaxis, excluding patents for C1INH half-life extensions mentioned below.

4. Mutagenic Strategies

The systematic selection and refinement leading to the variant 7-FLEPS-3 represents a departure from prior rational design approaches, which typically

involved only one or two amino acid substitutions, in that five residues were simultaneously randomized (Polderdijk et al. 2017; Schapira et al. 1987). In contrast, phage display enabled simultaneous discovery of multiple substitutions, uncovering sequence motifs not readily predictable by rational design. For example, Sulikowski et al., (2002) engineered an AAT mutant by substituting the P3–P1 residues (IPM to PFR) to target Pka (Sulikowski, Bauer, and Patston 2002). The optimal anti-Pka variant in Chapter 4, 7-FLEPS-3, differs notably, introducing proline at P4 and serine at P3, combinations previously unreported. De Maat et al., (2019) created AAT variants such as SMTR and SLLR (P4–P1) for contact system inhibition, aiming to eliminate off-target protease inhibition (de Maat, Sanrattana, et al. 2019). Their lead variant, α_1AT-SLLR/V, achieved specificity without extensive modifications beyond the cleavage site. By contrast, the variant 7-QLIPS-3 achieved enhanced specificity and maintained SI despite multiple amino acid substitutions upstream and downstream of P1, including the unconventional selection of arginine at P1' in 2-VRRAY-3', an atypical feature in serpins, which usually feature serine at this position (Sanrattana, Maas, and de Maat 2019). The inclusion of arginine at P1' could potentially strengthen enzyme serpin interactions but risked creating a cleavable substrate. Importantly, attempts to combine multiple beneficial motifs (e.g., merging 7-QLIPS-3 and 2-VRRAY-3' motifs) did not yield additive improvements, reinforcing the concept that optimized inhibition often requires a carefully balanced mutation set rather than extensive modification. This observation aligns with previous findings. For

example, Sulikowski et al., reported that adding extra residues (P4' Glu in the LGR variant) reduced performance, highlighting the risk of over engineering (Sulikowski, Bauer, and Patston 2002). Overall, the phage display strategy demonstrated superior capability to explore serpin sequence plasticity compared to rational approaches, leading to optimized variants such as 7-FLEPS-3 with enhanced specificity and maintained inhibitory function.

Replacing AAT's RCL with that of C1INH aimed to transfer C1INH's promiscuous specificity for Pka, FXIIa, and C1s onto AAT's stable backbone, and then hone in on Pka specificity via back-mutation towards AAT M358R. Unlike point mutations, this loop exchange approach is a comprehensive substitution that can substantially alter serpin specificity and inhibitory profiles. Previous studies have demonstrated the feasibility of loop exchanges. For example, Chaillan-Huntington et al., (1997) showed that swapping the P12-P2 segment of AAT with ovalbumin's sequence drastically reduced inhibition, highlighting the critical role of specific RCL residues (Chaillan-Huntington et al. 1997). Filion et al., (2004) further demonstrated that extensive loop substitutions (P16-P3') from HCII into AAT effectively conferred thrombin inhibition (Filion et al. 2004). This suggests that larger exchanges are tolerable and can confer new specificity, provided key residues (such as P1) align appropriately with the target protease. This current strategy uniquely incorporates residues from both sides of the cleavage site (P4-P4'), extending beyond previous studies that primarily focused on substitutions upstream of the reactive centre (P-side). Unlike prior minimal

substitutions, such as Sulikowski et al., limited P3-P1 modifications, the present design comprehensively imported the C1INH RCL sequence into AAT, and explored whether specificity was driven predominantly by loop residues rather than other structural features of C1INH (Sulikowski, Bauer, and Patston 2002). Notably, this design retains C1INH's unusual residue choices, such as Thr at P1', typically uncommon among serpins (usually Ser), potentially enhancing protease recognition or stability of the serpin-protease complex (Sanrattana, Maas, and de Maat 2019). Additionally, this approach systematically examined how RCL length affects inhibition. Prior literature indicates that optimizing loop length can enhance serpin activity, suggesting C1INH's natural RCL length may be suboptimal (Bos et al. 2004; Zhou, Carrell, and Huntington 2001). Incorporating C1INH's loop into AAT thus not only tested the direct role of sequence composition but also addressed whether extending loop length improved inhibitory efficiency. Furthermore, this targeted loop exchange isolated the inhibitory mechanism from C1INH's unique structural complexities, including its extensive glycosylation and N-terminal domain, factors that are not present in AAT (Stavenhagen et al. 2018). The successful retention of inhibitory activity after the loop swap confirmed the loop sequence itself is the primary determinant of protease specificity, complementing findings from earlier Chapters. Finally, using C1INH's loop inherently avoided undesirable off-target inhibition (e.g., thrombin), since C1INH naturally exhibits minimal thrombin inhibition, providing another layer of specificity to the engineered variant (Cugno et al. 2001).

5. Comparisons to Ecallantide and Lanadelumab

To place the engineered inhibitors in clinical context, comparisons with two approved Pka inhibitors (Ecallantide (Kalbitor®) and Lanadelumab (Takhzyro®)) are instructive. The serpin variants (7-FLEPS-3 and AC (10-3/4')) function as irreversible, suicide inhibitors, forming covalent complexes upon binding. In contrast, Ecallantide is a reversible competitive inhibitor derived from a Kunitz domain that transiently occupies Pka's active site, allowing dissociation and repeated binding of Pka molecules during its short plasma residence (Lunn and Banta 2011). Lanadelumab, a monoclonal antibody, employs a distinct mechanism by binding non-covalently and sterically blocking Pka's active site region without being consumed; its inhibition is continuous and sustained through extended plasma half-life (Kenniston et al. 2014). Specificity also differentiates these inhibitors. Lanadelumab exhibits the highest selectivity, exclusively neutralizing Pka and sparing prekallikrein and other precursors and proteases (Wang et al. 2020). Ecallantide similarly maintains specificity primarily toward Pka with minimal off-target inhibition, though minor FXIa and plasmin inhibition were reported (Al-Adimi et al. 2024). Likewise, engineered serpin variants 7-FLEPS-3 and AC (10-3/4') were designed for enhanced selectivity, achieving approximately 9-fold and 3-fold greater specificity for Pka over FXIa, respectively, thereby minimizing off-target risks compared to natural serpins or less specific engineered variants. Importantly, none of these inhibitors target the BK receptor itself, preserving specificity and targeting upstream protease control. Ecallantide, despite clinical efficacy, carries immunogenicity risks due to its non-human origin

(Lunn and Banta 2011), whereas engineered serpins that have human scaffolds are likely to exhibit lower immunogenic potential. The irreversible nature of serpin inhibition offers rapid and stable neutralization similarly to Lanadelumab. Thus, prolonged half-life strategies, as explored in albumin-fused serpins, may enhance feasibility for prophylactic use. Finally, the methodological approaches used for Chapter 4 involving phage display-driven optimization of the RCL represents overlap with the strategies used to develop Ecallantide and Landelumab. Both Ecallantide and Lanadelumab were discovered via phage display, just like 7-QLIPS-3 and 2-VRRAY-3' (Busse et al. 2019; Nixon, Sexton, and Ladner 2014). Each investigational team applied this powerful technology to distinct scaffolds, highlighting its versatility and underscoring the novelty of using serpin frameworks as to generate new candidate treatment proteins for HAE.

6. Challenges and Limitations

Although the research presented provides significant advancements in serpin engineering, several challenges and limitations were encountered that deserve consideration. Firstly, in Chapter 2, while significant half-life extension was achieved, the resultant fusion proteins still displayed only ~67% of the half-life observed for MSA alone, indicating incomplete exploitation of albumin's pharmacokinetic potential. This limitation might be attributed to steric hindrance or conformational instability caused by fusing large proteins, potentially affecting interactions with FcRn. Future studies could explore alternative linker designs, optimize fusion orientations further, or investigate other fusion partners to fully

leverage pharmacokinetic benefits. In Chapter 4, despite successfully identifying potent motifs like 7-FLEPS-3, combining the optimal sequences (7-QLIPS-3 and 2-VRRAY-3') into a single variant unexpectedly did not yield further improvements. This unexpected finding highlights a key challenge such as potential conformational or energetic incompatibilities introduced by cumulative mutations, possibly affecting reactive loop dynamics or protease serpin encounter efficiency. To better understand this phenomenon, future research could employ high-resolution structural techniques such as X-ray crystallography to elucidate precise molecular interactions and loop conformations that determine serpin activity. Finally, Chapter 5 demonstrated the importance of RCL length, as shortening by even a single amino acid unexpectedly converted the engineered serpin into a substrate, rather than an inhibitor. This finding underscores the precise and delicate structural constraints that define serpin function. Future studies should rigorously test intermediate loop lengths, systematically varying amino acid identities and hinge flexibility to identify optimal balance points. Additionally, further exploration using biophysical methods would clarify how subtle loop variations impact serpin folding pathways and inhibition mechanisms.

P. pastoris is a widely utilized expression host for recombinant protein production, particularly advantageous for secreted proteins due to several beneficial properties. Its popularity stems from its ability to achieve high level protein secretion, straightforward scalability, cost effectiveness, rapid growth, and suitability for large scale industrial production compared to mammalian cell lines

(Karbalaei, Rezaee, and Farsiani 2020). Proteins secreted by *P. pastoris* are typically easier to purify, as the yeast secretes relatively fewer endogenous proteins compared to other expression systems like *E.coli*, significantly simplifying downstream processing (Karbalaei, Rezaee, and Farsiani 2020). However, a common concern with yeast expression is its distinct glycosylation pattern, characterized by high mannose type N-glycosylation, which differs significantly from mammalian glycosylation (Karbalaei, Rezaee, and Farsiani 2020). Such differences can influence protein pharmacokinetics, stability, immunogenicity, and biological activity *in vivo* (Karbalaei, Rezaee, and Farsiani 2020; Liu et al. 2018). To mitigate potential glycosylation induced variability, many studies remove glycosylation sites through site directed mutagenesis, ensuring that the produced proteins are uniform and glycan free (Idrovo-Hidalgo et al. 2024; Jia et al. 2016). Deglycosylation or site directed mutagenesis of glycosylation sites reduces the risk of immunogenicity and variability, making results more reproducible (Idrovo-Hidalgo et al. 2024; Karbalaei, Rezaee, and Farsiani 2020; Jia et al. 2016). While some researchers might argue that expression systems such as mammalian cells could yield different outcomes due to their native glycosylation machinery, the intentional removal of glycosylation sites ensures that the glycosylation pattern does not influence the protein's half-life or activity significantly, as seen in Chapter 2 and 3 comparing second order rate constants with pdC1INH.

CD-1 mice are an outbred mouse strain commonly selected for pharmacokinetic and biodistribution studies due to their robust health, genetic diversity, consistent breeding performance, and suitability for general toxicological assessments (Jung et al. 2023). The genetic diversity within CD-1 mice better represents human genetic variability compared to inbred strains, offering broader relevance in predicting drug metabolism and pharmacokinetics (Aldinger et al. 2009). Choosing CD-1 mice for pharmacokinetic studies ensures reliable, generalizable, and robust pharmacokinetic data. While the specific strain used could potentially impact pharmacokinetic outcomes, especially when interacting with endogenous receptors like FcRn, the fundamental pharmacokinetic principles generally remain consistent across strains. Nevertheless, specific strain differences in receptor expression or affinity could be evaluated further to confirm findings broadly.

A patent application by Shire published in 2016 (now Takeda; WO2016/070156, CA2964132A1, withdrawn in both Canada, the USA, and Japan)) covers genetic fusions of C1INH to HSA to extend plasma half-life for therapeutic use (https://patents.google.com/patent/CA2964132A1/fi%20US4325121.pdf). The patent claims both N-terminal and C-terminal albumin fusions, including albumin fragments (such as HSA domain III), but provides no comparative data on orientation effectiveness, implicitly assuming equal efficacy. It emphasizes the advantage of monomeric albumin fusion constructs over dimeric IgG Fc-fusions,

citing improved stability and pharmacokinetic profiles. The same patent also covers Fc-fusion proteins of C1INH designed for extended half-life via FcRn recycling, with potential monovalent or bivalent configurations. Both albumin and Fc based fusions reportedly achieve multiple day half-lives, significantly exceeding native C1INH (2–3 days for pdC1INH). Beyond genetic fusions, several patents have taken a chemical conjugation approach to extend C1INH's half-life. The core idea is to attach an inert polymer, such as polyethylene glycol (PEG) to C1INH, increasing its hydrodynamic size and plasma persistence. Takeda pursued a refined PEGylation strategy focusing on site specific conjugation. A patent application published in 2017 (WO2017/176798, CA3019942A1, now withdrawn in both the USA, Japan, Europe, and the United Kingdom) illustrates the invention of attaching PEG or a polysialic acid (PSA) polymer to defined glycan sites on C1INH, preserving specific activity and achieving prolonged circulation. (https://patents.google.com/patent/CA3019942A1/en). The research described in Chapters 2 and 3 diverges from these patents by using MSA, which shares only 72% identity with HSA (Sheng et al. 2016). Employing MSA was strategic for preclinical murine studies, as mouse FcRn optimally recycles mouse albumin, enhancing half-life (Nilsen et al. 2018). Notably, these experiments explicitly compared N-terminal and C-terminal fusion orientations, unaddressed in existing patents, and identified a clear advantage of the N-terminal (H_6-MSA-trC1INH(MGS)) fusion for extending half-life. This orientation dependent nuance

represents a unique scientific finding absent from patent literature. It is likely that the same phenomenon will be observed when HSA is substituted for MSA in future experiments, as an MSA fusion protein is not useful for clinical development.

SerpinPC is a human AAT derived engineered serpin with a mutated RCL (KRK; P2-P1') for high specificity towards aPC (Huntington et al. 2025). Unlike endogenous protein C inhibitors, which have low potency and broad specificity, SerpinPC exhibits exceptional selectivity, with over 8,000-fold preference for aPC over thrombin, and little interaction with FXa and FXIa (Polderdijk et al. 2017). Designed as a therapeutic for hemophilia A and B, SerpinPC rebalances hemostasis by selectively inhibiting aPC, a natural anticoagulant that inactivates factor Va and VIIIa. Preclinical studies demonstrated robust efficacy due to SerpinPC reducing bleeding in hemophilia mouse models in a dose and time dependent manner (Huntington et al. 2025). Clinical development advanced through Phase 1/2a and Phase 2 trials, establishing subcutaneous dosing and demonstrating safety and dose dependent efficacy, marking it as a highly promising hemophilia therapy (Mancuso, Croteau, and Klamroth 2024; Aymonnier et al. 2021). Despite these clinical successes, SerpinPC's development was halted by Centessa Pharmaceuticals in November 2024 due to strategic and competitive market considerations, following Pfizer's approval of Marstacimab, an antibody targeting tissue factor pathway inhibitor (TFPI) (Lamb 2025). SerpinPC's journey underscores key translational and commercial

challenges relevant to engineered serpins, such as those discussed in Chapters 2–5. Bringing recombinant serpins to market involves navigating complex biologics manufacturing, ensuring proper protein folding, and managing potential polymerization risks during production. Immunogenicity remains a concern, as even minor loop mutations can trigger anti-drug antibodies (ADA), as observed in a subset of SerpinPC treated patients (Gualtierotti et al. 2022). Similar challenges could emerge for engineered serpins targeting Pka in HAE. This underscores the necessity for strategic planning and clear differentiation to support successful clinical translation and commercialization.

Lanadelumab is a human monoclonal antibody that specifically binds and inhibits Pka, as mentioned above. Clinical studies demonstrate Lanadelumab significantly reduces attack frequency, with a prolonged half-life (2 weeks), allowing convenient dosing intervals (biweekly or monthly). Importantly, Lanadelumab exhibits a low incidence of ADAs, 11.9% of treated patients (Banerji et al. 2018). Garadacimab is a human IgG4 monoclonal antibody targeting FXIIa, another critical component in the contact pathway, upstream of Pka (Craig et al. 2023). By inhibiting FXIIa, Garadacimab effectively prevents the cascade activation responsible for BK production, providing strong prophylactic efficacy in clinical studies. Remarkably, clinical trials of Garadacimab report one ADA in a patient, indicating exceptional immunological tolerance (Craig et al. 2023). Pharmacokinetic studies show Garadacimab has a prolonged half-life (18 days), supporting convenient monthly dosing, with clinical trials showing

sustained efficacy and safety profiles (Glassman et al. 2025; Craig et al. 2023). From a therapeutic standpoint, Lanadelumab currently represents the gold standard for prophylaxis due to its potent, durable, and bivalent binding and low immunogenic profile (Riedl et al. 2020). The variants that were discussed in this thesis present unique therapeutic attributes that differentiate them from monoclonal antibodies like Lanadelumab and Garadacimab, and offer potential economic advantages over these agents. Monoclonal antibodies offer strong specificity, proven safety, and low ADA-related concerns, but they also come with critical economic limitations which these engineered serpins may specifically address such as providing a unique platform allowing precise tuning of specificity and activity, reduction in production expenses when using *P. pastoris* or bacterial systems, inherently pose lower theoretical risks of immunogenicity when carefully designed, and more robust and permanent inhibition (Shah et al. 2023; Harris and Cohen 2024).

De Maat et al., (2019) has significantly advanced the field of engineered serpins by developing AAT mutants, particularly the α_1AT-SMTR/S and α_1AT-SLLR/S variants, designed explicitly to inhibit multiple proteases simultaneously (de Maat, Sanrattana, et al. 2019). These engineered serpins target critical proteases involved in the contact pathway responsible for HAE, including Pka and FXIIa. This multi-specific inhibition has been proposed as a potential solution to overcome limitations associated with the natural C1INH, which, although a key regulator of these proteases, exhibits moderate affinity and efficiency, limiting its

therapeutic efficacy at conventional dosages (Bos, Lubbers, et al. 2003). However, despite the clear therapeutic promise of these broadly inhibitory serpin variants, the experimental design in this thesis did not pursue De Maat group's strategy, instead prioritizing narrower specificity and a more precise engineering approach. First, specificity and associated safety concerns played a significant role in the decision. While broad spectrum inhibitors like α_1AT-SMTR/S and α_1AT-SLLR/S offer powerful and comprehensive therapeutic coverage, they also inherently raise concerns about off-target protease inhibition (de Maat, Sanrattana, et al. 2019). Broadly acting inhibitors carry a risk of unintentionally perturbing proteases that are essential for maintaining physiological homeostasis, possibly leading to adverse effects, especially with chronic administration. The experimental design in this thesis emphasizes high specificity by engineering serpins to target a single protease, enhancing the safety profile of engineered serpins. Secondly, the issue of therapeutic precision and personalization guided the research direction. HAE is clinically heterogeneous, with patients exhibiting variations in severity, frequency, and underlying biochemical pathways driving their symptoms (Bygum et al. 2017). By precisely engineering serpins to target individual proteases implicated in specific patient subsets, such as Pka-centric or FXIIa-driven HAE phenotypes, researchers can develop more personalized therapeutic strategies. Unlike broad spectrum inhibitors, the variants discussed in this thesis, which focus on specific molecular target, potentially allow clinicians to

tailor treatments more effectively to individual patient needs, leading to optimized therapeutic outcomes and fewer side effects.

Immunogenicity, the potential of therapeutic proteins to elicit an immune response, is a critical concern during the development of biologic therapies, influencing both clinical efficacy and safety (Carter and Quarmby 2024). Various factors, such as protein sequence, glycosylation patterns, formulation stability, and aggregation propensity, significantly impact the immunological profile of therapeutic proteins (Kuriakose, Chirmule, and Nair 2016). Even minor changes, such as a single amino acid substitution, can create or expose immunogenic epitopes capable of eliciting immune responses. Therefore, meticulous consideration of immunogenic risks is crucial in designing new protein-based therapeutics. A common strategy to mitigate immunogenicity involves modifying or removing glycosylation sites (Wolf et al. 2022). Glycans attached to therapeutic proteins profoundly influence their pharmacokinetics, stability, and immune recognition. Properly glycosylated proteins typically exhibit enhanced stability, reduced aggregation, and decreased immune recognition (Zhou and Qiu 2019). Conversely, aberrant or non-human glycosylation, as often seen in recombinant proteins produced by yeast or bacterial expression systems, can trigger significant immune responses (Cruz 2015; Boune et al. 2020; Wolf et al. 2022). For instance, pdC1INH currently used clinically for HAE, is naturally glycosylated and generally exhibits low immunogenicity due to its human origin and native glycosylation profile. However, even plasma-derived preparations can

provoke occasional allergic reactions or ADAs, although these responses are rare and typically mild, likely due to minor structural or glycosylation variants arising during production (Farkas et al. 2016). Conversely, Ecallantide, a small recombinant peptide based inhibitor of Pka used to treat acute HAE attacks, illustrates significant immunogenicity concerns (Stolz and Horn 2010). The immunogenicity observed with Ecallantide arises predominantly from its recombinant nature and peptide sequence differences from human proteins. Surprisingly, Ruconest™, a recombinant C1INH produced from the milk of transgenic rabbits, demonstrates an overall favorable immunogenicity profile in clinical use (Riedl 2015; Cruz 2015). Although ADAs against Ruconest™ have been observed, these antibodies generally occur at low frequencies and are predominantly non-neutralizing. Clinical studies indicate that about 0.5-2.2% of patients develop anti-C1INH antibodies after repeated exposure, none of which were neutralizing. However, antibodies targeting host-related impurities (HRIs) from the rabbit-derived production system have been detected more frequently (up to 17% after repeated doses) (Cruz 2015). Importantly, these anti-HRI antibodies were not associated with clinical adverse events or diminished therapeutic effectiveness. In contrast, monoclonal antibodies, like Lanadelumab or Garadacimab, exhibit very low immunogenicity due to their human sequence and human-like glycosylation profiles (Bova et al. 2019; Reshef et al. 2025). Lanadelumab, targeting Pka, and Garadacimab, targeting FXIIa, both demonstrate minimal ADA formation, with few instances of neutralizing

antibodies, indicating their sustained efficacy in chronic use, as illustrated above. In this thesis, the engineered serpin variants were designed using recombinant human AAT or C1INH scaffolds, specifically altering the RCL or fusing serum albumin to improve specificity or half-life, respectively. Importantly, Chapter 2 involves truncating the N-terminal domain of C1INH, which harbors all 24 O-linked glycans and most N-linked glycans, combined with targeted removal of the remaining three N-linked glycans within the serpin domain through site directed mutagenesis (N216Q, N231Q, N330Q). This targeted glycan removal substantially decreases the presence of non-human glycosylation patterns, particularly high-mannose structures typical of yeast expression systems in *P. pastoris*, thus potentially reducing epitopes recognized as foreign by the immune system. However, despite this careful approach, potential immunogenic implications remain. Truncation and selective deglycosylation might inadvertently expose previously masked epitopes or alter the local conformational stability of the protein, potentially increasing the risk of protein aggregation (Wang et al. 2013; Qi and Anand-Apte 2022; Duran-Romana et al. 2024). Aggregation is a known factor contributing to increased immunogenicity and ADA formation, even when the glycosylation associated epitopes themselves are minimized or removed. Ongoing assessments, such as structural studies, aggregation monitoring, and immunogenic profiling, will be essential to ensure these engineered serpins achieve optimal therapeutic profiles with minimal immune responses.

7. Future Experiments

While this thesis has advanced the understanding of engineered serpins, several key unanswered questions remain that provide important directions for future research. The most important question for future research is to determine if and how H_6-trC1INH(MGS), H_6-MSA-trC1INH(MGS), 7-FLEPS-3, and AC (10-3/4') function *in vivo*, compared to plasma-derived C1INH for the first two proteins and AAT M358R for the latter two. This question would best be answered in the C1INH knockout mouse model (Han et al. 2002), in which both hemizygous and homozygous gene deletion of C1INH causes increased vascular permeability, as measured by Evans Blue dye extravasation. Dose and time responses should be followed to allow fair quantitative comparisons among the proteins. The proteins should also be assessed in bleeding models to gauge possible off-target effects mediated by the inhibition of proteases other than Pka. In other experiments In Chapters 2 and 3, it remains unclear precisely how fusion orientation influences interactions with the FcRn recycling receptor at a structural or molecular level, and biophysical and biochemical studies of interactions of these proteins with soluble Fc would illuminate this issue. Additionally, questions surrounding immunogenicity and long-term tolerability of these fusion proteins in clinical contexts are yet unanswered, necessitating further investigation in more comprehensive animal studies, ideally in several species.

In the AAT phage display study, the unexpected lack of synergy between individually potent motifs (7-QLIPS-3 and 2-VRRAY-3') when combined into a single variant raises important questions about potential conformational conflicts

or structural incompatibilities within the reactive loop. It remains uncertain precisely why certain amino acid combinations are advantageous individually but detrimental in combination, warranting further structural and computational studies. Moreover, it remains to be seen whether the selectivity and potency observed *in vitro* with 7-FLEPS-3 variant will translate effectively *in vivo*, particularly regarding pharmacokinetics and bioavailability within animal models. For the loop exchange study, a significant unanswered question is why subtle changes in loop length so profoundly impact the balance between inhibitor and substrate behavior. Understanding the detailed molecular mechanisms governing this switch could significantly refine future serpin designs. Additionally, it is not yet fully understood how these engineered serpins interact with the broader protease network in physiological settings, and whether off-target or compensatory effects might arise. Addressing these unresolved questions through targeted structural, biophysical, computational, and *in vivo* experiments will be essential to fully realize the therapeutic potential of these innovative serpin variants.

8. Genetic therapies for HAE

Research presented in this thesis sought to improve replacement therapy in HAE. Genetic therapies to replace or repair a dysfunctional *SERPING1* gene constitute an alternative approach. Modern gene editing technologies, particularly clustered regularly interspaced short palindromic repeats (CRISPR)–CRISPR-associated protein 9 (Cas9), are being explored as curative strategies for HAE (Cohn et al. 2025; Longhurst et al. 2024). While directly repairing *SERPING1*

mutations via CRISPR is conceptually feasible, the approach is complicated by the diversity of mutations (Gosswein et al. 2008). Instead, a more promising strategy involves targeting *KLKB1*, the gene encoding Pka, to reduce BK production regardless of the underlying *SERPING1* mutation. One leading example is Intellia Therapeutics' NTLA-2002, an *in vivo* CRISPR/Cas9 therapy delivered via lipid nanoparticles (LNPs) to hepatocytes (Longhurst et al. 2024). By knocking out *KLKB1* in liver cells, NTLA-2002 achieves durable suppression of Pka. In a Phase 1/2 clinical trial, a single dose of NTLA-2002 led to a 95% mean reduction in monthly HAE attack rates with no serious adverse events, showcasing gene editing's potential for long-term relief (Longhurst et al. 2024). In parallel, gene therapy approaches are also being pursued. BioMarin's BMN 331 used an adeno-associated virus (AAV5) vector to deliver a healthy *SERPING1* gene to liver cells for sustained C1INH production (Riedl et al. 2024). Although early-phase trials demonstrated safety, the program was discontinued for strategic business reasons but will continue with the patients that they already have. Another effort, OTL-105, developed by Orchard Therapeutics and Pharming Group, uses *ex vivo* gene therapy which entails hematopoietic stem cells being harvested, transduced with a lentiviral vector carrying *SERPING1*, and reintroduced after conditioning chemotherapy (Smith and Riedl 2024). This approach, still in preclinical development, no results are published yet. While these gene based approaches offer the promise of a one-time cure, they face significant hurdles, such as off-target genome editing, insertional mutagenesis,

immune responses to vectors or transgene products, delivery efficiency, tissue targeting, ethical issues, and lack of reversibility (Zheng et al. 2023; Uddin, Rudin, and Sen 2020; Liu et al. 2021). In contrast, current HAE management relies on prophylactic therapies, which, although requiring repeat administration, offer controllability, reversibility, titratability, and characterized safety profiles (Gower et al. 2011). Advances in these treatments have made them increasingly convenient, with long-acting options like Lanadelumab allowing patients to lead nearly normal lives. For many, the idea of accepting irreversible risks from gene editing may not be justified, particularly when existing therapies are effective and manageable. In this context, prophylactic approaches offer a desirable balance. In conclusion, while curative gene therapies for HAE are advancing rapidly and may one day offer permanent relief, they currently face technical, clinical, and strategic barriers that limit widespread adoption. Until such therapies can demonstrate consistent, superior safety and efficacy, optimizing preventative biologics remains the most pragmatic and patient-preferred strategy. The work described in this thesis contributes to that goal by developing potent, specific, and potentially long-acting inhibitors that could offer effective prophylaxis with greater safety, lower cost, and fewer barriers to use than gene-based interventions.

In summary, this thesis presents a multifaceted approach to improving the prophylactic treatment landscape for HAE through the rational design and engineering of serpin inhibitors (Figure 1). Each project, whether extending the

half-life of C1INH via albumin fusion, refining specificity and speed of AAT variants through phage display, or harnessing loop exchange to enhance Pka targeting, contributed toward the broader goal of developing cost effective, scalable, and highly tailored biologics that overcome the limitations of current therapies. While curative strategies such as gene therapy and gene editing hold transformative potential, they are accompanied by irreversible risks, long-term uncertainty, and substantial technical and ethical challenges. In contrast, the protein-based therapeutics developed here offer a safer, more controllable, and reversible alternative that can be dynamically adapted to patient needs and evolving clinical insights. Altogether, the work presented in this thesis not only advances the understanding of serpin engineering in the context of HAE but also provides a foundation for potential future translational applications that prioritize precision, safety, and accessibility.

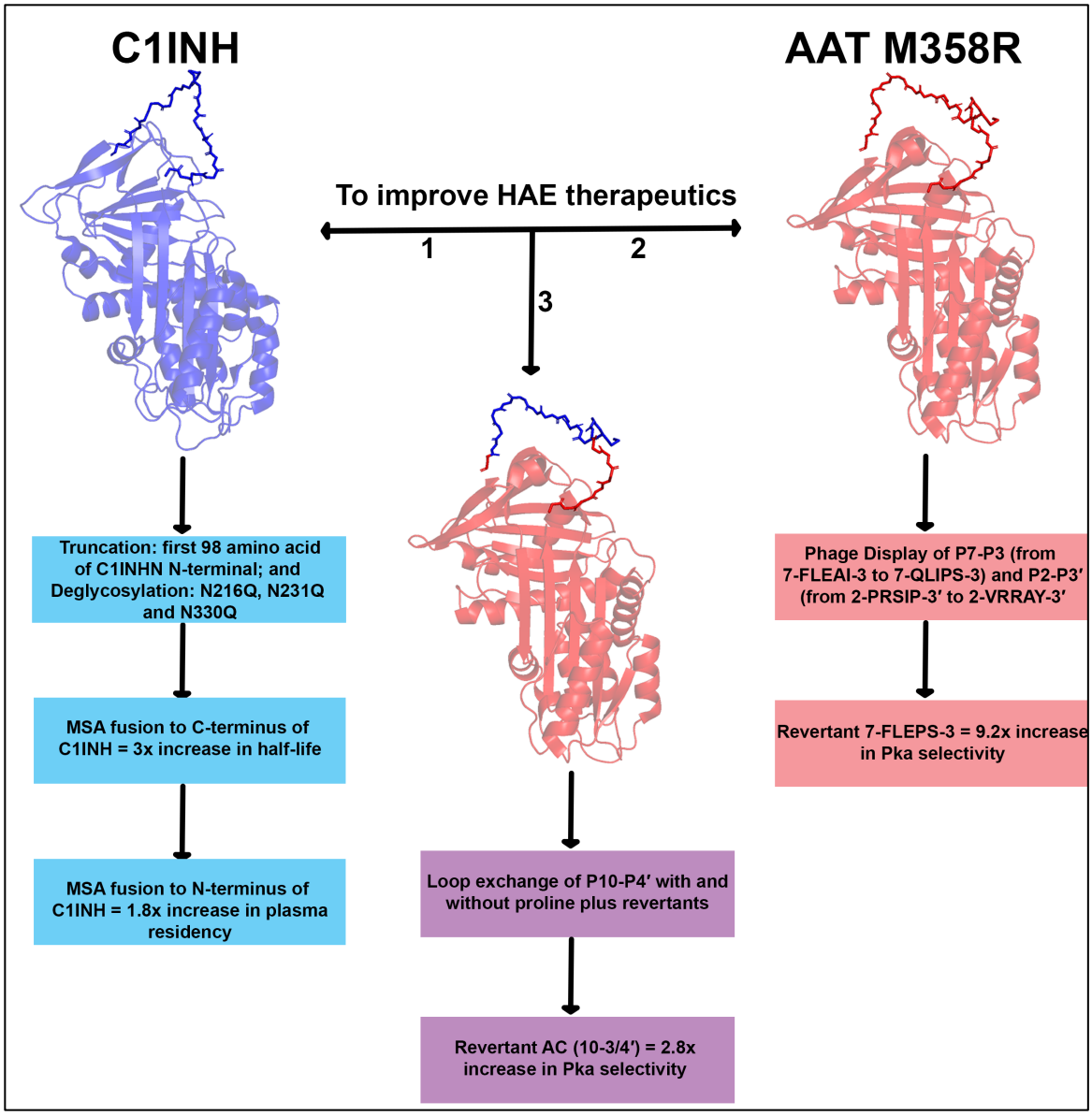

Figure 1: Summary of ways to improve HAE therapeutics. (1) Chapter 2 and 3 highlighted the importance of albumin fusion to extend half-life. Truncated deglycosylated C1INH with C-terminal fusion of MSA, seen in Chapter 2, illustrated a 3-fold increase in half-life *in vivo*. N-terminal fusion of MSA, reported in Chapter 3, showed a further 1.8-fold increase in plasma residency *in vivo*. (2) Chapter 4 highlighted the importance of phage display with AAT M358R.

Revertant 7-FLEPS-3 from the variant discovered from phage display, 7-QLIPS-3, resulted in 9.2-fold increase in Pka selectivity. (3) Chapter 5 highlighted the importance of loop exchange of AAT M358R with that of C1INH. The revertant of the loop exchange, AC (10-3/4'), resulted in 2.8-fold increase in Pka selectivity.

CHAPTER 7 - REFERENCES

Abbas, M. N., A. Chlastakova, M. A. Jmel, E. Iliaki-Giannakoudaki, J. Chmelar, and M. Kotsyfakis. 2022. 'Serpins in Tick Physiology and Tick-Host Interaction', *Front Cell Infect Microbiol*, 12: 892770.

Abboud, R. T., G. T. Ford, and K. R. Chapman. 2005. 'Emphysema in alpha1-antitrypsin deficiency: does replacement therapy affect outcome?', *Treat Respir Med*, 4: 1-8.

Agboola, F., S. Lubinga, J. Carlson, G. A. Lin, W. B. Dreitlein, and S. D. Pearson. 2019. 'The Effectiveness and Value of Lanadelumab and C1 Esterase Inhibitors for Prophylaxis of Hereditary Angioedema Attacks', *J Manag Care Spec Pharm*, 25: 143-48.

Al-Adimi, G., V. Bhakta, L. J. Eltringham-Smith, V. Shirobokov, and W. P. Sheffield. 2024. 'Extension of the circulatory half-life of recombinant ecallantide via albumin fusion without loss of anti-kallikrein activity', *J Biotechnol*, 391: 11-19.

Aldinger, K. A., G. Sokoloff, D. M. Rosenberg, A. A. Palmer, and K. J. Millen. 2009. 'Genetic variation and population substructure in outbred CD-1 mice: implications for genome-wide association studies', *PLoS One*, 4: e4729.

Andersen, J. T., B. Dalhus, D. Viuff, B. T. Ravn, K. S. Gunnarsen, A. Plumridge, K. Bunting, F. Antunes, R. Williamson, S. Athwal, E. Allan, L. Evans, M. Bjoras, S. Kjaerulff, D. Sleep, I. Sandlie, and J. Cameron. 2014. 'Extending serum half-life of albumin by engineering neonatal Fc receptor (FcRn) binding', *J Biol Chem*, 289: 13492-502.

Ar, M. C., C. Balkan, and K. Kavakli. 2019. 'Extended Half-Life Coagulation Factors: A New Era in the Management of Hemophilia Patients', *Turk J Haematol*, 36: 141-54.

Arjmand, S., E. Bidram, A. S. Lotfi, M. Shamsara, and S. J. Mowla. 2011. 'Expression and Purification of Functionally Active Recombinant Human Alpha 1-Antitrypsin in Methylotrophic Yeast Pichia pastoris', *Avicenna J Med Biotechnol*, 3: 127-34.

Ashwell, G., and J. Harford. 1982. 'Carbohydrate-specific receptors of the liver', *Annu Rev Biochem*, 51: 531-54.

Aymonnier, K., C. Kawecki, V. Arocas, Y. Boulaftali, and M. C. Bouton. 2021. 'Serpins, New Therapeutic Targets for Hemophilia', *Thromb Haemost*, 121: 261-69.

Azmy, V., J. P. Brooks, and F. I. Hsu. 2020. 'Clinical presentation of hereditary angioedema', *Allergy Asthma Proc*, 41: S18-S21.

Baglia, F. A., K. O. Badellino, C. Q. Li, J. A. Lopez, and P. N. Walsh. 2002. 'RETRACTED: Factor XI binding to the platelet glycoprotein Ib-IX-V complex promotes factor XI activation by thrombin', *J Biol Chem*, 277: 1662-8.

Banerji, A., M. A. Riedl, J. A. Bernstein, M. Cicardi, H. J. Longhurst, B. L. Zuraw, P. J. Busse, J. Anderson, M. Magerl, I. Martinez-Saguer, M. Davis-Lorton,

A. Zanichelli, H. H. Li, T. Craig, J. Jacobs, D. T. Johnston, R. Shapiro, W. H. Yang, W. R. Lumry, M. E. Manning, L. B. Schwartz, M. Shennak, D. Soteres, R. H. Zaragoza-Urdaz, S. Gierer, A. M. Smith, R. Tachdjian, H. J. Wedner, J. Hebert, S. M. Rehman, P. Staubach, J. Schranz, J. Baptista, W. Nothaft, M. Maurer, and Help Investigators. 2018. 'Effect of Lanadelumab Compared With Placebo on Prevention of Hereditary Angioedema Attacks: A Randomized Clinical Trial', *JAMA*, 320: 2108-21.

Bekassy, Z., I. Lopatko Fagerstrom, M. Bader, and D. Karpman. 2022. 'Crosstalk between the renin-angiotensin, complement and kallikrein-kinin systems in inflammation', *Nat Rev Immunol*, 22: 411-28.

Bergamaschini, L., G. Gobbo, S. Gatti, L. Caccamo, P. Prato, M. Maggioni, P. Braidotti, R. Di Stefano, and L. R. Fassati. 2001. 'Endothelial targeting with C1-inhibitor reduces complement activation in vitro and during ex vivo reperfusion of pig liver', *Clin Exp Immunol*, 126: 412-20.

Bernstein, J. A., B. Ritchie, R. J. Levy, R. L. Wasserman, A. K. Bewtra, D. S. Hurewitz, K. Obtulowicz, A. Reshef, D. Moldovan, T. Shirov, V. Grivcheva-Panovska, P. C. Kiessling, F. Schindel, and T. J. Craig. 2010. 'Population pharmacokinetics of plasma-derived C1 esterase inhibitor concentrate used to treat acute hereditary angioedema attacks', *Ann Allergy Asthma Immunol*, 105: 149-54.

Bhakta, V., M. Hamada, A. Nouanesengsy, J. Lapierre, D. L. Perruzza, and W. P. Sheffield. 2021. 'Identification of an alpha-1 antitrypsin variant with enhanced specificity for factor XIa by phage display, bacterial expression, and combinatorial mutagenesis', *Sci Rep*, 11: 5565.

Bianchera, A., E. Alomari, A. Michielon, G. Bazzoli, N. Ronda, G. Pighini, I. Zanotti, C. Giorgio, A. Mozzarelli, R. Bettini, and S. Bruno. 2022. 'Recombinant Alpha-1 Antitrypsin as Dry Powder for Pulmonary Administration: A Formulative Proof of Concept', *Pharmaceutics*, 14.

Binkley, K. E., and A. Davis, 3rd. 2000. 'Clinical, biochemical, and genetic characterization of a novel estrogen-dependent inherited form of angioedema', *J Allergy Clin Immunol*, 106: 546-50.

Boccon-Gibod, I., and L. Bouillet. 2012. 'Safety and efficacy of icatibant self-administration for acute hereditary angioedema', *Clin Exp Immunol*, 168: 303-7.

Bock, S. C., K. Skriver, E. Nielsen, H. C. Thogersen, B. Wiman, V. H. Donaldson, R. L. Eddy, J. Marrinan, E. Radziejewska, R. Huber, and et al. 1986. 'Human C1 inhibitor: primary structure, cDNA cloning, and chromosomal localization', *Biochemistry*, 25: 4292-301.

Bork, K., S. E. Barnstedt, P. Koch, and H. Traupe. 2000. 'Hereditary angioedema with normal C1-inhibitor activity in women', *Lancet*, 356: 213-7.

Bos, I. G., E. C. de Bruin, Y. A. Karuntu, P. W. Modderman, E. Eldering, and C. E. Hack. 2003. 'Recombinant human C1-inhibitor produced in Pichia pastoris has the same inhibitory capacity as plasma C1-inhibitor', *Biochim Biophys Acta*, 1648: 75-83.

Bos, I. G., C. E. Hack, and J. P. Abrahams. 2002. 'Structural and functional aspects of C1-inhibitor', *Immunobiology*, 205: 518-33.

Bos, I. G., Y. T. Lubbers, E. Eldering, J. P. Abrahams, and C. E. Hack. 2004. 'Effect of reactive site loop elongation on the inhibitory activity of C1-inhibitor', *Biochim Biophys Acta*, 1699: 139-44.

Bos, I. G., Y. T. Lubbers, D. Roem, J. P. Abrahams, C. E. Hack, and E. Eldering. 2003. 'The functional integrity of the serpin domain of C1-inhibitor depends on the unique N-terminal domain, as revealed by a pathological mutant', *J Biol Chem*, 278: 29463-70.

Boune, S., P. Hu, A. L. Epstein, and L. A. Khawli. 2020. 'Principles of N-Linked Glycosylation Variations of IgG-Based Therapeutics: Pharmacokinetic and Functional Considerations', *Antibodies (Basel)*, 9.

Bova, M., A. Valerieva, M. A. Wu, R. Senter, and F. Perego. 2019. 'Lanadelumab Injection Treatment For The Prevention Of Hereditary Angioedema (HAE): Design, Development And Place In Therapy', *Drug Des Devel Ther*, 13: 3635-46.

Brantly, M., M. Campos, A. M. Davis, J. D'Armiento, K. Goodman, K. Hanna, M. O'Day, J. Queenan, R. Sandhaus, J. Stoller, C. Strange, J. Teckman, and A. Wanner. 2020. 'Detection of alpha-1 antitrypsin deficiency: the past, present and future', *Orphanet J Rare Dis*, 15: 96.

Brantly, M., T. Nukiwa, and R. G. Crystal. 1988. 'Molecular basis of alpha-1-antitrypsin deficiency', *Am J Med*, 84: 13-31.

Busse, P. J., S. C. Christiansen, M. A. Riedl, A. Banerji, J. A. Bernstein, A. J. Castaldo, T. Craig, M. Davis-Lorton, M. M. Frank, H. H. Li, W. R. Lumry, and B. L. Zuraw. 2021. 'US HAEA Medical Advisory Board 2020 Guidelines for the Management of Hereditary Angioedema', *J Allergy Clin Immunol Pract*, 9: 132-50 e3.

Busse, P. J., H. Farkas, A. Banerji, W. R. Lumry, H. J. Longhurst, D. J. Sexton, and M. A. Riedl. 2019. 'Lanadelumab for the Prophylactic Treatment of Hereditary Angioedema with C1 Inhibitor Deficiency: A Review of Preclinical and Phase I Studies', *BioDrugs*, 33: 33-43.

Busse, P., and A. Kaplan. 2022. 'Specific Targeting of Plasma Kallikrein for Treatment of Hereditary Angioedema: A Revolutionary Decade', *J Allergy Clin Immunol Pract*, 10: 716-22.

Bygum, A., P. Busse, T. Caballero, and M. Maurer. 2017. 'Disease Severity, Activity, Impact, and Control and How to Assess Them in Patients with Hereditary Angioedema', *Front Med (Lausanne)*, 4: 212.

Cabrita, L. D., and S. P. Bottomley. 2004. 'How do proteins avoid becoming too stable? Biophysical studies into metastable proteins', *Eur Biophys J*, 33: 83-8.

Cai, S., and A. E. Davis, 3rd. 2003. 'Complement regulatory protein C1 inhibitor binds to selectins and interferes with endothelial-leukocyte adhesion', *J Immunol*, 171: 4786-91.

Carrell, R. W., J. O. Jeppsson, C. B. Laurell, S. O. Brennan, M. C. Owen, L. Vaughan, and D. R. Boswell. 1982. 'Structure and variation of human alpha 1-antitrypsin', *Nature*, 298: 329-34.

Carrell, R. W., and D. A. Lomas. 1997. 'Conformational disease', *Lancet*, 350: 134-8.

Carter, P. J., and V. Quarmby. 2024. 'Immunogenicity risk assessment and mitigation for engineered antibody and protein therapeutics', *Nat Rev Drug Discov*, 23: 898-913.

Castilho, A., M. Windwarder, P. Gattinger, L. Mach, R. Strasser, F. Altmann, and H. Steinkellner. 2014. 'Proteolytic and N-glycan processing of human alpha1-antitrypsin expressed in Nicotiana benthamiana', *Plant Physiol*, 166: 1839-51.

Chaillan-Huntington, C. E., P. G. Gettins, J. A. Huntington, and P. A. Patston. 1997. 'The P6-P2 region of serpins is critical for proteinase inhibition and complex stability', *Biochemistry*, 36: 9562-70.

Chang, W. S., M. R. Wardell, D. A. Lomas, and R. W. Carrell. 1996. 'Probing serpin reactive-loop conformations by proteolytic cleavage', *Biochem J*, 314 (Pt 2): 647-53.

Chao, J., A. Schmaier, L. M. Chen, Z. Yang, and L. Chao. 1996. 'Kallistatin, a novel human tissue kallikrein inhibitor: levels in body fluids, blood cells, and tissues in health and disease', *J Lab Clin Med*, 127: 612-20.

Chapin, J. C., and K. A. Hajjar. 2015. 'Fibrinolysis and the control of blood coagulation', *Blood Rev*, 29: 17-24.

Charest-Morin, X., S. Betschel, R. Borici-Mazi, A. Kanani, G. Lacuesta, G. E. Rivard, E. Wagner, S. Wasserman, B. Yang, and C. Drouet. 2018. 'The diagnosis of hereditary angioedema with C1 inhibitor deficiency: a survey of Canadian physicians and laboratories', *Allergy Asthma Clin Immunol*, 14: 83.

Chaudhry, R., S. M. Usama, and H. M. Babiker. 2025. 'Physiology, Coagulation Pathways.' in, *StatPearls* (Treasure Island (FL)).

Chuang, Y. M., L. He, M. L. Pinn, Y. C. Tsai, M. A. Cheng, E. Farmer, P. C. Karakousis, and C. F. Hung. 2021. 'Albumin fusion with granulocyte-macrophage colony-stimulating factor acts as an immunotherapy against chronic tuberculosis', *Cell Mol Immunol*, 18: 2393-401.

Chung, D. W., K. Fujikawa, B. A. McMullen, and E. W. Davie. 1986. 'Human plasma prekallikrein, a zymogen to a serine protease that contains four tandem repeats', *Biochemistry*, 25: 2410-7.

Cicardi, M., and A. Agostoni. 1996. 'Hereditary angioedema', *N Engl J Med*, 334: 1666-7.

Cohn, D. M., P. Gurugama, M. Magerl, C. H. Katelaris, D. Launay, L. Bouillet, R. S. Petersen, K. Lindsay, E. Aygoren-Pursun, D. Maag, J. S. Butler, M. Y. Shah, A. Golden, Y. Xu, A. M. Abdelhady, D. Lebwohl, and H. J. Longhurst. 2025. 'CRISPR-Based Therapy for Hereditary Angioedema', *N Engl J Med*, 392: 458-67.

Colman, R. W., and A. H. Schmaier. 1997. 'Contact system: a vascular biology modulator with anticoagulant, profibrinolytic, antiadhesive, and proinflammatory attributes', *Blood*, 90: 3819-43.

Colman, R. W., Y. T. Wachtfogel, U. Kucich, G. Weinbaum, S. Hahn, R. A. Pixley, C. F. Scott, A. de Agostini, D. Burger, and M. Schapira. 1985. 'Effect of cleavage of the heavy chain of human plasma kallikrein on its functional properties', *Blood*, 65: 311-8.

Craig, T. J., H. H. Li, M. Riedl, J. A. Bernstein, W. R. Lumry, A. J. MacGinnitie, L. E. Stolz, J. Biedenkapp, and Y. Chyung. 2015. 'Characterization of anaphylaxis after ecallantide treatment of hereditary angioedema attacks', *J Allergy Clin Immunol Pract*, 3: 206-12 e4.

Craig, T. J., A. Reshef, H. H. Li, J. S. Jacobs, J. A. Bernstein, H. Farkas, W. H. Yang, E. S. G. Stroes, I. Ohsawa, R. Tachdjian, M. E. Manning, W. R. Lumry, I. M. Saguer, E. Aygoren-Pursun, B. Ritchie, G. L. Sussman, J. Anderson, K. Kawahata, Y. Suzuki, P. Staubach, R. Treudler, H. Feuersenger, F. Glassman, I. Jacobs, and M. Magerl. 2023. 'Efficacy and safety of garadacimab, a factor XIIa inhibitor for hereditary angioedema prevention (VANGUARD): a global, multicentre, randomised, double-blind, placebo-controlled, phase 3 trial', *Lancet*, 401: 1079-90.

Cruz, M. P. 2015. 'Conestat alfa (ruconest): first recombinant c1 esterase inhibitor for the treatment of acute attacks in patients with hereditary angioedema', *P T*, 40: 109-14.

Crystal, R. G. 1989. 'The alpha 1-antitrypsin gene and its deficiency states', *Trends Genet*, 5: 411-7.

Cugno, M., I. Bos, Y. Lubbers, C. E. Hack, and A. Agostoni. 2001. 'In vitro interaction of C1-inhibitor with thrombin', *Blood Coagul Fibrinolysis*, 12: 253-60.

Culica, M. E., A. L. Chibac-Scutaru, T. Mohan, and S. Coseri. 2021. 'Cellulose-based biogenic supports, remarkably friendly biomaterials for proteins and biomolecules', *Biosens Bioelectron*, 182: 113170.

Davis, A. E., 3rd. 1988. 'C1 inhibitor and hereditary angioneurotic edema', *Annu Rev Immunol*, 6: 595-628.

Davis, A. E., 3rd, P. Mejia, and F. Lu. 2008. 'Biological activities of C1 inhibitor', *Mol Immunol*, 45: 4057-63.

de Maat, S., C. C. Clark, M. Boertien, N. Parr, W. Sanrattana, Z. L. M. Hofman, and C. Maas. 2019. 'Factor XII truncation accelerates activation in solution', *J Thromb Haemost*, 17: 183-94.

de Maat, S., W. Sanrattana, R. K. Mailer, N. M. J. Parr, M. Hessing, R. M. Koetsier, J. C. M. Meijers, G. Pasterkamp, T. Renne, and C. Maas. 2019. 'Design and characterization of alpha1-antitrypsin variants for treatment of contact system-driven thromboinflammation', *Blood*, 134: 1658-69.

de Souza, L. R., B. M. Scott, V. Bhakta, D. A. Donkor, D. L. Perruzza, and W. P. Sheffield. 2018. 'Serpin Phage Display: The Use of a T7 System to Probe

Reactive Center Loop Libraries with Different Serine Proteinases', *Methods Mol Biol*, 1826: 41-64.
Dementiev, A., M. Simonovic, K. Volz, and P. G. Gettins. 2003. 'Canonical inhibitor-like interactions explain reactivity of alpha1-proteinase inhibitor Pittsburgh and antithrombin with proteinases', *J Biol Chem*, 278: 37881-7.
Deng, X., L. Wang, X. You, P. Dai, and Y. Zeng. 2018. 'Advances in the T7 phage display system (Review)', *Mol Med Rep*, 17: 714-20.
Dennis, M. S., A. Herzka, and R. A. Lazarus. 1995. 'Potent and selective Kunitz domain inhibitors of plasma kallikrein designed by phage display', *J Biol Chem*, 270: 25411-7.
Donaldson, V. H., and R. R. Evans. 1963. 'A Biochemical Abnormality in Herediatry Angioneurotic Edema: Absence of Serum Inhibitor of C' 1-Esterase', *Am J Med*, 35: 37-44.
Drouet, C., A. Lopez-Lera, A. Ghannam, M. Lopez-Trascasa, S. Cichon, D. Ponard, F. Parsopoulou, H. Grombirikova, T. Freiberger, M. Rijavec, C. L. Veronez, J. B. Pesquero, and A. E. Germenis. 2022. 'SERPING1 Variants and C1-INH Biological Function: A Close Relationship With C1-INH-HAE', *Front Allergy*, 3: 835503.
Dubois, E. A., and A. F. Cohen. 2010. 'Icatibant', *Br J Clin Pharmacol*, 69: 425-6.
Dunkelberger, J. R., and W. C. Song. 2010. 'Complement and its role in innate and adaptive immune responses', *Cell Res*, 20: 34-50.
Duran-Romana, R., B. Houben, M. De Vleeschouwer, N. Louros, M. P. Wilson, G. Matthijs, J. Schymkowitz, and F. Rousseau. 2024. 'N-glycosylation as a eukaryotic protective mechanism against protein aggregation', *Sci Adv*, 10: eadk8173.
Ebrahimizadeh, W., and M. Rajabibazl. 2014. 'Bacteriophage vehicles for phage display: biology, mechanism, and application', *Curr Microbiol*, 69: 109-20.
Eidelman, F. J. 2010. 'Hereditary angioedema: New therapeutic options for a potentially deadly disorder', *BMC Blood Disord*, 10: 3.
Eldering, E., C. C. Huijbregts, Y. T. Lubbers, C. Longstaff, and C. E. Hack. 1992. 'Characterization of recombinant C1 inhibitor P1 variants', *J Biol Chem*, 267: 7013-20.
Eldering, E., J. H. Nuijens, and C. E. Hack. 1988. 'Expression of functional human C1 inhibitor in COS cells', *J Biol Chem*, 263: 11776-9.
Elliott, P. R., D. A. Lomas, R. W. Carrell, and J. P. Abrahams. 1996. 'Inhibitory conformation of the reactive loop of alpha 1-antitrypsin', *Nat Struct Biol*, 3: 676-81.
Farkas, H., and L. Varga. 2011. 'Ecallantide is a novel treatment for attacks of hereditary angioedema due to C1 inhibitor deficiency', *Clin Cosmet Investig Dermatol*, 4: 61-8.
Farkas, H., L. Varga, D. Moldovan, K. Obtulowicz, T. Shirov, T. Machnig, H. Feuersenger, J. Edelman, D. Williams-Herman, and M. Rojavin. 2016. 'Assessment of inhibitory antibodies in patients with hereditary

angioedema treated with plasma-derived C1 inhibitor', *Ann Allergy Asthma Immunol*, 117: 508-13.

Fijen, L. M., and M. Levi. 2022. 'Prophylaxis with anti-activated factor XII for hereditary angioedema', *Lancet*, 399: 889-90.

Filion, M. L., V. Bhakta, L. H. Nguyen, P. S. Liaw, and W. P. Sheffield. 2004. 'Full or partial substitution of the reactive center loop of alpha-1-proteinase inhibitor by that of heparin cofactor II: P1 Arg is required for maximal thrombin inhibition', *Biochemistry*, 43: 14864-72.

Fujikawa, K., D. W. Chung, L. E. Hendrickson, and E. W. Davie. 1986. 'Amino acid sequence of human factor XI, a blood coagulation factor with four tandem repeats that are highly homologous with plasma prekallikrein', *Biochemistry*, 25: 2417-24.

Gettins, P. G. 2002. 'Serpin structure, mechanism, and function', *Chem Rev*, 102: 4751-804.

Ghannam, A., P. Sellier, O. Fain, L. Martin, D. Ponard, and C. Drouet. 2016. 'C1 Inhibitor as a glycoprotein: The influence of polysaccharides on its function and autoantibody target', *Mol Immunol*, 71: 161-65.

Gierczak, R. F., J. S. Sutherland, V. Bhakta, L. J. Toltl, P. C. Liaw, and W. P. Sheffield. 2011. 'Retention of thrombin inhibitory activity by recombinant serpins expressed as integral membrane proteins tethered to the surface of mammalian cells', *J Thromb Haemost*, 9: 2424-35.

Glassman, F., J. P. Lawo, M. A. Bica, A. Roberts, D. Pawaskar, H. Akama, M. Jain, and S. Goodson. 2025. 'Pharmacokinetics, Pharmacodynamics, and Safety of Subcutaneous and Intravenous Garadacimab Following Single-Dose Administration in Healthy Japanese and White Adults', *J Clin Pharmacol*, 65: 466-77.

Gonias, S. L., and W. M. Campana. 2014. 'LDL receptor-related protein-1: a regulator of inflammation in atherosclerosis, cancer, and injury to the nervous system', *Am J Pathol*, 184: 18-27.

Gosswein, T., A. Kocot, G. Emmert, W. Kreuz, I. Martinez-Saguer, E. Aygoren-Pursun, E. Rusicke, K. Bork, J. Oldenburg, and C. R. Muller. 2008. 'Mutational spectrum of the C1INH (SERPING1) gene in patients with hereditary angioedema', *Cytogenet Genome Res*, 121: 181-8.

Gower, R. G., P. J. Busse, E. Aygoren-Pursun, A. J. Barakat, T. Caballero, M. Davis-Lorton, H. Farkas, D. S. Hurewitz, J. S. Jacobs, D. T. Johnston, W. Lumry, and M. Maurer. 2011. 'Hereditary angioedema caused by c1-esterase inhibitor deficiency: a literature-based analysis and clinical commentary on prophylaxis treatment strategies', *World Allergy Organ J*, 4: S9-S21.

Gregorek, H., M. Kokai, T. Hidvegi, G. Fust, K. Sabbouh, and K. Madalinski. 1991. 'Concentration of C1 inhibitor in sera of healthy blood donors as studied by immunoenzymatic assay', *Complement Inflamm*, 8: 310-2.

Grevys, A., J. Nilsen, K. M. K. Sand, M. B. Daba, I. Oynebraten, M. Bern, M. B. McAdam, S. Foss, T. Schlothauer, T. E. Michaelsen, G. J. Christianson, D.

C. Roopenian, R. S. Blumberg, I. Sandlie, and J. T. Andersen. 2018. 'A human endothelial cell-based recycling assay for screening of FcRn targeted molecules', *Nat Commun*, 9: 621.

Grover, S. P., and N. Mackman. 2019. 'Intrinsic Pathway of Coagulation and Thrombosis', *Arterioscler Thromb Vasc Biol*, 39: 331-38.

———. 2022. 'Anticoagulant SERPINs: Endogenous Regulators of Hemostasis and Thrombosis', *Front Cardiovasc Med*, 9: 878199.

Gualtierotti, R., S. Pasca, A. Ciavarella, S. Arcudi, A. Giachi, I. Garagiola, C. Suffritti, S. M. Siboni, and F. Peyvandi. 2022. 'Updates on Novel Non-Replacement Drugs for Hemophilia', *Pharmaceuticals (Basel)*, 15.

Guo, R., W. Guo, L. Cao, H. Liu, J. Liu, H. Xu, W. Huang, F. Wang, and Z. Hong. 2016. 'Fusion of an albumin-binding domain extends the half-life of immunotoxins', *Int J Pharm*, 511: 538-49.

Guo, Y., H. Zhang, H. Lai, H. Wang, H. J. Chong-Neto, S. O. R. Valle, and R. Zhu. 2022. 'Long-term Prophylaxis with Androgens in the management of Hereditary Angioedema (HAE) in emerging countries', *Orphanet J Rare Dis*, 17: 399.

Han, E. D., R. C. MacFarlane, A. N. Mulligan, J. Scafidi, and A. E. Davis, 3rd. 2002. 'Increased vascular permeability in C1 inhibitor-deficient mice mediated by the bradykinin type 2 receptor', J Clin Invest, 109: 1057-63.

hang, G. D., C. J. Chen, C. Y. Lin, H. C. Chen, and H. Chen. 2003. 'Improvement of glycosylation in insect cells with mammalian glycosyltransferases', *J Biotechnol*, 102: 61-71.

Harris, C. T., and S. Cohen. 2024. 'Reducing Immunogenicity by Design: Approaches to Minimize Immunogenicity of Monoclonal Antibodies', *BioDrugs*, 38: 205-26.

Hayes, S., C. Farrell, A. Relan, and J. Anderson. 2021. 'Population pharmacokinetics of recombinant human C1 esterase inhibitor in children with hereditary angioedema', *Ann Allergy Asthma Immunol*, 126: 707-12.

He, Z., G. Wang, J. Wu, Z. Tang, and M. Luo. 2021. 'The molecular mechanism of LRP1 in physiological vascular homeostasis and signal transduction pathways', *Biomed Pharmacother*, 139: 111667.

Heit, C., B. C. Jackson, M. McAndrews, M. W. Wright, D. C. Thompson, G. A. Silverman, D. W. Nebert, and V. Vasiliou. 2013. 'Update of the human and mouse SERPIN gene superfamily', *Hum Genomics*, 7: 22.

Herz, J., and D. K. Strickland. 2001. 'LRP: a multifunctional scavenger and signaling receptor', *J Clin Invest*, 108: 779-84.

Hopkins, P. C., R. N. Pike, and S. R. Stone. 2000. 'Evolution of serpin specificity: cooperative interactions in the reactive-site loop sequence of antithrombin specifically restrict the inhibition of activated protein C', *J Mol Evol*, 51: 507-15.

Hor, L., J. Pan, J. C. Whisstock, R. N. Pike, and L. C. Wijeyewickrema. 2020. 'Mapping the binding site of C1-inhibitor for polyanion cofactors', *Mol Immunol*, 126: 8-13.

Huisman, L. G., J. M. van Griensven, and C. Kluft. 1995. 'On the role of C1-inhibitor as inhibitor of tissue-type plasminogen activator in human plasma', *Thromb Haemost*, 73: 466-71.

Huntington, J. A., R. J. Read, and R. W. Carrell. 2000. 'Structure of a serpin-protease complex shows inhibition by deformation', *Nature*, 407: 923-6.

Huntington, J. A., J. Reckless, S. G. I. Polderdijk, P. Hextall, and T. Baglin. 2025. 'The preclinical profile of SerpinPC- a potential new treatment for hemophilia', *Blood Adv*.

Idrovo-Hidalgo, T., M. F. Pignataro, L. M. Bredeston, F. Elias, M. G. Herrera, M. F. Pavan, S. Foscaldi, M. Suireszcz, N. B. Fernandez, D. E. Wetzler, C. H. Pavan, P. O. Craig, E. A. Roman, L. A. M. Ruberto, D. G. Noseda, L. I. Ibanez, C. Czibener, Consortium Argentinian AntiCovid, J. E. Ugalde, A. D. Nadra, J. Santos, and C. D'Alessio. 2024. 'Deglycosylated RBD produced in Pichia pastoris as a low-cost sera COVID-19 diagnosis tool and a vaccine candidate', *Glycobiology*, 34.

Im, H., M. S. Woo, K. Y. Hwang, and M. H. Yu. 2002. 'Interactions causing the kinetic trap in serpin protein folding', *J Biol Chem*, 277: 46347-54.

Irving, J. A., R. N. Pike, A. M. Lesk, and J. C. Whisstock. 2000. 'Phylogeny of the serpin superfamily: implications of patterns of amino acid conservation for structure and function', *Genome Res*, 10: 1845-64.

Ivanov, I., A. Matafonov, M. F. Sun, B. M. Mohammed, Q. Cheng, S. K. Dickeson, S. Kundu, I. M. Verhamme, A. Gruber, K. McCrae, and D. Gailani. 2019. 'A mechanism for hereditary angioedema with normal C1 inhibitor: an inhibitory regulatory role for the factor XII heavy chain', *Blood*, 133: 1152-63.

Izaguirre, G., and S. T. Olson. 2006. 'Residues Tyr253 and Glu255 in strand 3 of beta-sheet C of antithrombin are key determinants of an exosite made accessible by heparin activation to promote rapid inhibition of factors Xa and IXa', *J Biol Chem*, 281: 13424-32.

Izaguirre, G., A. R. Rezaie, and S. T. Olson. 2009. 'Engineering functional antithrombin exosites in alpha1-proteinase inhibitor that specifically promote the inhibition of factor Xa and factor IXa', *J Biol Chem*, 284: 1550-8.

Janciauskiene, S., S. Wrenger, S. Immenschuh, B. Olejnicka, T. Greulich, T. Welte, and J. Chorostowska-Wynimko. 2018. 'The Multifaceted Effects of Alpha1-Antitrypsin on Neutrophil Functions', *Front Pharmacol*, 9: 341.

Jedicke, N., N. Struever, N. Aggrawal, T. Welte, M. P. Manns, N. P. Malek, L. Zender, S. Janciauskiene, and T. Wuestefeld. 2014. 'alpha-1-antitrypsin inhibits acute liver failure in mice', *Hepatology*, 59: 2299-308.

Jeon, H., W. Meng, J. Takagi, M. J. Eck, T. A. Springer, and S. C. Blacklow. 2001. 'Implications for familial hypercholesterolemia from the structure of the LDL receptor YWTD-EGF domain pair', *Nat Struct Biol*, 8: 499-504.

Jia, H., Y. Guo, X. Song, C. Shao, J. Wu, J. Ma, M. Shi, Y. Miao, R. Li, D. Wang, Z. Tian, and W. Xiao. 2016. 'Elimination of N-glycosylation by site mutation

further prolongs the half-life of IFN-alpha/Fc fusion proteins expressed in Pichia pastoris', *Microb Cell Fact*, 15: 209.

Jia, L., L. Zhang, C. Shao, E. Song, W. Sun, M. Li, and Y. Gao. 2009. 'An attempt to understand kidney's protein handling function by comparing plasma and urine proteomes', *PLoS One*, 4: e5146.

Jiang, H., E. Wagner, H. Zhang, and M. M. Frank. 2001. 'Complement 1 inhibitor is a regulator of the alternative complement pathway', *J Exp Med*, 194: 1609-16.

Jin, L., J. P. Abrahams, R. Skinner, M. Petitou, R. N. Pike, and R. W. Carrell. 1997. 'The anticoagulant activation of antithrombin by heparin', *Proc Natl Acad Sci U S A*, 94: 14683-8.

Jung, Y. H., H. V. Wang, S. Ali, V. G. Corces, and I. Kremsky. 2023. 'Characterization of a strain-specific CD-1 reference genome reveals potential inter- and intra-strain functional variability', *BMC Genomics*, 24: 437.

Kalinska, M., U. Meyer-Hoffert, T. Kantyka, and J. Potempa. 2016. 'Kallikreins - The melting pot of activity and function', *Biochimie*, 122: 270-82.

Karbalaei, M., S. A. Rezaee, and H. Farsiani. 2020. 'Pichia pastoris: A highly successful expression system for optimal synthesis of heterologous proteins', *J Cell Physiol*, 235: 5867-81.

Kearney, K. J., J. Butler, O. M. Posada, C. Wilson, S. Heal, M. Ali, L. Hardy, J. Ahnstrom, D. Gailani, R. Foster, E. Hethershaw, C. Longstaff, and H. Philippou. 2021. 'Kallikrein directly interacts with and activates Factor IX, resulting in thrombin generation and fibrin formation independent of Factor XI', *Proc Natl Acad Sci U S A*, 118.

Kenniston, J. A., R. R. Faucette, D. Martik, S. R. Comeau, A. P. Lindberg, K. J. Kopacz, G. P. Conley, J. Chen, M. Viswanathan, N. Kastrapeli, J. Cosic, S. Mason, M. DiLeo, J. Abendroth, P. Kuzmic, R. C. Ladner, T. E. Edwards, C. TenHoor, B. A. Adelman, A. E. Nixon, and D. J. Sexton. 2014. 'Inhibition of plasma kallikrein by a highly specific active site blocking antibody', *J Biol Chem*, 289: 23596-608.

Khan, M. S., P. Singh, A. Azhar, A. Naseem, Q. Rashid, M. A. Kabir, and M. A. Jairajpuri. 2011. 'Serpin Inhibition Mechanism: A Delicate Balance between Native Metastable State and Polymerization', *J Amino Acids*, 2011: 606797.

Kim, J. K., M. Firan, C. G. Radu, C. H. Kim, V. Ghetie, and E. S. Ward. 1999. 'Mapping the site on human IgG for binding of the MHC class I-related receptor, FcRn', *Eur J Immunol*, 29: 2819-25.

Kluft, C., M. M. Trumpi-Kalshoven, A. F. Jie, and E. C. Veldhuyzen-Stolk. 1979. 'Factor XII-dependent fibrinolysis: a double function of plasma kallikrein and the occurrence of a previously undescribed factor XII- and kallikrein-dependent plasminogen proactivator', *Thromb Haemost*, 41: 756-73.

Knauer, D. J., D. Majumdar, P. C. Fong, and M. F. Knauer. 2000. 'SERPIN regulation of factor XIa. The novel observation that protease nexin 1 in the

presence of heparin is a more potent inhibitor of factor XIa than C1 inhibitor', *J Biol Chem*, 275: 37340-6.
Kolte, D., and Z. Shariat-Madar. 2016. 'Plasma Kallikrein Inhibitors in Cardiovascular Disease: An Innovative Therapeutic Approach', *Cardiol Rev*, 24: 99-109.
Konings, J., L. R. Hoving, R. S. Ariens, E. L. Hethershaw, M. Ninivaggi, L. J. Hardy, B. de Laat, H. Ten Cate, H. Philippou, and J. W. Govers-Riemslag. 2015. 'The role of activated coagulation factor XII in overall clot stability and fibrinolysis', *Thromb Res*, 136: 474-80.
Koumandou, V. L., and A. Scorilas. 2013. 'Evolution of the plasma and tissue kallikreins, and their alternative splicing isoforms', *PLoS One*, 8: e68074.
Kounnas, M. Z., F. C. Church, W. S. Argraves, and D. K. Strickland. 1996. 'Cellular internalization and degradation of antithrombin III-thrombin, heparin cofactor II-thrombin, and alpha 1-antitrypsin-trypsin complexes is mediated by the low density lipoprotein receptor-related protein', *J Biol Chem*, 271: 6523-9.
Krishnan, B., L. Hedstrom, D. N. Hebert, L. M. Gierasch, and A. Gershenson. 2017. 'Expression and Purification of Active Recombinant Human Alpha-1 Antitrypsin (AAT) from Escherichia coli', *Methods Mol Biol*, 1639: 195-209.
Kroeger, H., E. Miranda, I. MacLeod, J. Perez, D. C. Crowther, S. J. Marciniak, and D. A. Lomas. 2009. 'Endoplasmic reticulum-associated degradation (ERAD) and autophagy cooperate to degrade polymerogenic mutant serpins', *J Biol Chem*, 284: 22793-802.
Kuriakose, A., N. Chirmule, and P. Nair. 2016. 'Immunogenicity of Biotherapeutics: Causes and Association with Posttranslational Modifications', *J Immunol Res*, 2016: 1298473.
Lagrange, J., T. Lecompte, T. Knopp, P. Lacolley, and V. Regnault. 2022. 'Alpha-2-macroglobulin in hemostasis and thrombosis: An underestimated old double-edged sword', *J Thromb Haemost*, 20: 806-15.
Lamark, T., M. Ingebrigtsen, C. Bjornstad, T. Melkko, T. E. Mollnes, and E. W. Nielsen. 2001. 'Expression of active human C1 inhibitor serpin domain in Escherichia coli', *Protein Expr Purif*, 22: 349-58.
Lamb, Y. N. 2025. 'Marstacimab: First Approval', *Drugs*, 85: 263-69.
Landerman, N. S., M. E. Webster, E. L. Becker, and H. E. Ratcliffe. 1962. 'Hereditary angioneurotic edema. II. Deficiency of inhibitor for serum globulin permeability factor and/or plasma kallikrein', *J Allergy*, 33: 330-41.
Lathem, W. W., T. Bergsbaken, and R. A. Welch. 2004. 'Potentiation of C1 esterase inhibitor by StcE, a metalloprotease secreted by Escherichia coli O157:H7', *J Exp Med*, 199: 1077-87.
Law, R. H., Q. Zhang, S. McGowan, A. M. Buckle, G. A. Silverman, W. Wong, C. J. Rosado, C. G. Langendorf, R. N. Pike, P. I. Bird, and J. C. Whisstock. 2006. 'An overview of the serpin superfamily', *Genome Biol*, 7: 216.

Leach, J. K., K. Spencer, M. Mascelli, and T. G. McCauley. 2015. 'Pharmacokinetics of single and repeat doses of icatibant', *Clin Pharmacol Drug Dev*, 4: 105-11.

Lee, S. J., S. Evers, D. Roeder, A. F. Parlow, J. Risteli, L. Risteli, Y. C. Lee, T. Feizi, H. Langen, and M. C. Nussenzweig. 2002. 'Mannose receptor-mediated regulation of serum glycoprotein homeostasis', *Science*, 295: 1898-901.

Leeb-Lundberg, L. M., F. Marceau, W. Muller-Esterl, D. J. Pettibone, and B. L. Zuraw. 2005. 'International union of pharmacology. XLV. Classification of the kinin receptor family: from molecular mechanisms to pathophysiological consequences', *Pharmacol Rev*, 57: 27-77.

Lewis, J. H., R. M. Iammarino, J. A. Spero, and U. Hasiba. 1978. 'Antithrombin Pittsburgh: an alpha1-antitrypsin variant causing hemorrhagic disease', *Blood*, 51: 129-37.

Li, C., K. M. Voos, M. Pathak, G. Hall, K. R. McCrae, I. Dreveny, R. Li, and J. Emsley. 2019. 'Plasma kallikrein structure reveals apple domain disc rotated conformation compared to factor XI', *J Thromb Haemost*, 17: 759-70.

Li, Z., S. Alam, J. Wang, C. S. Sandstrom, S. Janciauskiene, and R. Mahadeva. 2009. 'Oxidized alpha1-antitrypsin stimulates the release of monocyte chemotactic protein-1 from lung epithelial cells: potential role in emphysema', *Am J Physiol Lung Cell Mol Physiol*, 297: L388-400.

Libretti, S., and Y. Puckett. 2025. 'Physiology, Homeostasis.' in, *StatPearls* (Treasure Island (FL)).

Lillis, A. P., L. B. Van Duyn, J. E. Murphy-Ullrich, and D. K. Strickland. 2008. 'LDL receptor-related protein 1: unique tissue-specific functions revealed by selective gene knockout studies', *Physiol Rev*, 88: 887-918.

Liu, C. P., T. I. Tsai, T. Cheng, V. S. Shivatare, C. Y. Wu, C. Y. Wu, and C. H. Wong. 2018. 'Glycoengineering of antibody (Herceptin) through yeast expression and in vitro enzymatic glycosylation', *Proc Natl Acad Sci U S A*, 115: 720-25.

Liu, D., S. Cai, X. Gu, J. Scafidi, X. Wu, and A. E. Davis, 3rd. 2003. 'C1 inhibitor prevents endotoxin shock via a direct interaction with lipopolysaccharide', *J Immunol*, 171: 2594-601.

Liu, D., C. C. Cramer, J. Scafidi, and A. E. Davis, 3rd. 2005. 'N-linked glycosylation at Asn3 and the positively charged residues within the amino-terminal domain of the c1 inhibitor are required for interaction of the C1 Inhibitor with Salmonella enterica serovar typhimurium lipopolysaccharide and lipid A', *Infect Immun*, 73: 4478-87.

Liu, L. 2018. 'Pharmacokinetics of monoclonal antibodies and Fc-fusion proteins', *Protein Cell*, 9: 15-32.

Liu, W., L. Li, J. Jiang, M. Wu, and P. Lin. 2021. 'Applications and challenges of CRISPR-Cas gene-editing to disease treatment in clinics', *Precis Clin Med*, 4: 179-91.

Lomas, D. A., and R. Mahadeva. 2002. 'Alpha1-antitrypsin polymerization and the serpinopathies: pathobiology and prospects for therapy', *J Clin Invest*, 110: 1585-90.

Long, A. T., E. Kenne, R. Jung, T. A. Fuchs, and T. Renne. 2016. 'Contact system revisited: an interface between inflammation, coagulation, and innate immunity', *J Thromb Haemost*, 14: 427-37.

Longhurst, H. J., K. Lindsay, R. S. Petersen, L. M. Fijen, P. Gurugama, D. Maag, J. S. Butler, M. Y. Shah, A. Golden, Y. Xu, C. Boiselle, J. D. Vogel, A. M. Abdelhady, M. L. Maitland, M. D. McKee, J. Seitzer, B. W. Han, S. Soukamneuth, J. Leonard, L. Sepp-Lorenzino, E. D. Clark, D. Lebwohl, and D. M. Cohn. 2024. 'CRISPR-Cas9 In Vivo Gene Editing of KLKB1 for Hereditary Angioedema', *N Engl J Med*, 390: 432-41.

Lunn, M., and E. Banta. 2011. 'Ecallantide for the treatment of hereditary angiodema in adults', *Clin Med Insights Cardiol*, 5: 49-54.

Lunn, M., C. Santos, and T. Craig. 2010. 'Cinryze as the first approved C1 inhibitor in the USA for the treatment of hereditary angioedema: approval, efficacy and safety', *J Blood Med*, 1: 163-70.

Maat, D. S., M. A. Prins, and C. P. D. Brussaard. 2019. 'Sediments from Arctic Tide-Water Glaciers Remove Coastal Marine Viruses and Delay Host Infection', *Viruses*, 11.

Mancuso, M. E., S. E. Croteau, and R. Klamroth. 2024. 'Benefits and risks of non-factor therapies: Redefining haemophilia treatment goals in the era of new technologies', *Haemophilia*, 30 Suppl 3: 39-44.

McCarthy, C., E. P. Reeves, and N. G. McElvaney. 2016. 'The Role of Neutrophils in Alpha-1 Antitrypsin Deficiency', *Ann Am Thorac Soc*, 13 Suppl 4: S297-304.

McMullen, B. A., K. Fujikawa, and E. W. Davie. 1991. 'Location of the disulfide bonds in human plasma prekallikrein: the presence of four novel apple domains in the amino-terminal portion of the molecule', *Biochemistry*, 30: 2050-6.

Melder, R. J., B. L. Osborn, T. Riccobene, P. Kanakaraj, P. Wei, G. Chen, D. Stolow, W. G. Halpern, T. S. Migone, Q. Wang, K. J. Grzegorzewski, and G. Gallant. 2005. 'Pharmacokinetics and in vitro and in vivo anti-tumor response of an interleukin-2-human serum albumin fusion protein in mice', *Cancer Immunol Immunother*, 54: 535-47.

Mikhailenko, I., F. D. Battey, M. Migliorini, J. F. Ruiz, K. Argraves, M. Moayeri, and D. K. Strickland. 2001. 'Recognition of alpha 2-macroglobulin by the low density lipoprotein receptor-related protein requires the cooperation of two ligand binding cluster regions', *J Biol Chem*, 276: 39484-91.

Miller, A., and W. W. Jedrzejczak. 2001. '[Albumin--biological functions and clinical significance]', *Postepy Hig Med Dosw*, 55: 17-36.

Miyata, T., and T. Horiuchi. 2023. 'Biochemistry, molecular genetics, and clinical aspects of hereditary angioedema with and without C1 inhibitor deficiency', *Allergol Int*, 72: 375-84.

Moestrup, S. K., T. L. Holtet, M. Etzerodt, H. C. Thogersen, A. Nykjaer, P. A. Andreasen, H. H. Rasmussen, L. Sottrup-Jensen, and J. Gliemann. 1993. 'Alpha 2-macroglobulin-proteinase complexes, plasminogen activator inhibitor type-1-plasminogen activator complexes, and receptor-associated protein bind to a region of the alpha 2-macroglobulin receptor containing a cluster of eight complement-type repeats', *J Biol Chem*, 268: 13691-6.

Mohammed, B. M., A. Matafonov, I. Ivanov, M. F. Sun, Q. Cheng, S. K. Dickeson, C. Li, D. Sun, I. M. Verhamme, J. Emsley, and D. Gailani. 2018. 'An update on factor XI structure and function', *Thromb Res*, 161: 94-105.

Motta, G., L. Juliano, and J. R. Chagas. 2023. 'Human plasma kallikrein: roles in coagulation, fibrinolysis, inflammation pathways, and beyond', *Front Physiol*, 14: 1188816.

Motta, G., and I. L. S. Tersariol. 2017. 'Modulation of the Plasma Kallikrein-Kinin System Proteins Performed by Heparan Sulfate Proteoglycans', *Front Physiol*, 8: 481.

Nilsen, J., M. Bern, K. M. K. Sand, A. Grevys, B. Dalhus, I. Sandlie, and J. T. Andersen. 2018. 'Human and mouse albumin bind their respective neonatal Fc receptors differently', *Sci Rep*, 8: 14648.

Nixon, A. E., D. J. Sexton, and R. C. Ladner. 2014. 'Drugs derived from phage display: from candidate identification to clinical practice', *MAbs*, 6: 73-85.

Nunez, A., I. Belmonte, E. Miranda, M. Barrecheguren, G. Farago, E. Loeb, M. Pons, F. Rodriguez-Frias, P. Gabriel-Medina, E. Rodriguez, J. Genesca, M. Miravitlles, and C. Esquinas. 2021. 'Association between circulating alpha-1 antitrypsin polymers and lung and liver disease', *Respir Res*, 22: 244.

Nussberger, J., M. Cugno, C. Amstutz, M. Cicardi, A. Pellacani, and A. Agostoni. 1998. 'Plasma bradykinin in angio-oedema', *Lancet*, 351: 1693-7.

Nussberger, J., M. Cugno, M. Cicardi, and A. Agostoni. 1999. 'Local bradykinin generation in hereditary angioedema', *J Allergy Clin Immunol*, 104: 1321-2.

O'Dwyer, C. A., M. E. O'Brien, M. R. Wormald, M. M. White, N. Banville, K. Hurley, C. McCarthy, N. G. McElvaney, and E. P. Reeves. 2015. 'The BLT1 Inhibitory Function of alpha-1 Antitrypsin Augmentation Therapy Disrupts Leukotriene B4 Neutrophil Signaling', *J Immunol*, 195: 3628-41.

Olson, S. T., R. Sheffer, and A. M. Francis. 1993. 'High molecular weight kininogen potentiates the heparin-accelerated inhibition of plasma kallikrein by antithrombin: role for antithrombin in the regulation of kallikrein', *Biochemistry*, 32: 12136-47.

Park, D. J., E. Duggan, K. Ho, R. A. Dorschner, M. Dobke, J. P. Nolan, and B. P. Eliceiri. 2022. 'Serpin-loaded extracellular vesicles promote tissue repair in a mouse model of impaired wound healing', *J Nanobiotechnology*, 20: 474.

Park, S., and J. K. Park. 2024. 'Back to basics: the coagulation pathway', *Blood Res*, 59: 35.

Pathak, M., S. S. Wong, I. Dreveny, and J. Emsley. 2013. 'Structure of plasma and tissue kallikreins', *Thromb Haemost*, 110: 423-33.

Pavlopoulou, A., G. Pampalakis, I. Michalopoulos, and G. Sotiropoulou. 2010. 'Evolutionary history of tissue kallikreins', *PLoS One*, 5: e13781.

Pawaskar, D., M. A. Tortorici, B. Zuraw, T. Craig, M. Cicardi, H. Longhurst, H. H. Li, W. R. Lumry, I. Martinez-Saguer, J. Jacobs, J. A. Bernstein, M. A. Riedl, C. H. Katelaris, P. K. Keith, A. Feussner, and J. Sidhu. 2018. 'Population pharmacokinetics of subcutaneous C1-inhibitor for prevention of attacks in patients with hereditary angioedema', *Clin Exp Allergy*, 48: 1325-32.

Petrache, I., I. Fijalkowska, T. R. Medler, J. Skirball, P. Cruz, L. Zhen, H. I. Petrache, T. R. Flotte, and R. M. Tuder. 2006. 'alpha-1 antitrypsin inhibits caspase-3 activity, preventing lung endothelial cell apoptosis', *Am J Pathol*, 169: 1155-66.

Pixley, R. A., R. G. Espinola, B. Ghebrehiwet, K. Joseph, A. Kao, K. Bdeir, D. B. Cines, and R. W. Colman. 2011. 'Interaction of high-molecular-weight kininogen with endothelial cell binding proteins suPAR, gC1qR and cytokeratin 1 determined by surface plasmon resonance (BiaCore)', *Thromb Haemost*, 105: 1053-9.

Polderdijk, S. G., T. E. Adams, L. Ivanciu, R. M. Camire, T. P. Baglin, and J. A. Huntington. 2017. 'Design and characterization of an APC-specific serpin for the treatment of hemophilia', *Blood*, 129: 105-13.

Powell, J. S., N. C. Josephson, D. Quon, M. V. Ragni, G. Cheng, E. Li, H. Jiang, L. Li, J. A. Dumont, J. Goyal, X. Zhang, J. Sommer, J. McCue, M. Barbetti, A. Luk, and G. F. Pierce. 2012. 'Safety and prolonged activity of recombinant factor VIII Fc fusion protein in hemophilia A patients', *Blood*, 119: 3031-7.

Prada, A. E., K. Zahedi, and A. E. Davis, 3rd. 1998. 'Regulation of C1 inhibitor synthesis', *Immunobiology*, 199: 377-88.

Prematta, M. J., T. Prematta, and T. J. Craig. 2008. 'Treatment of hereditary angioedema with plasma-derived C1 inhibitor', *Ther Clin Risk Manag*, 4: 975-82.

Proud, D., and A. P. Kaplan. 1988. 'Kinin formation: mechanisms and role in inflammatory disorders', *Annu Rev Immunol*, 6: 49-83.

Pyzik, M., T. Rath, W. I. Lencer, K. Baker, and R. S. Blumberg. 2015. 'FcRn: The Architect Behind the Immune and Nonimmune Functions of IgG and Albumin', *J Immunol*, 194: 4595-603.

Qi, J. H., and B. Anand-Apte. 2022. 'Deglycosylation Increases the Aggregation and Angiogenic Properties of Mutant Tissue Inhibitor of Metalloproteinase 3 Protein: Implications for Sorsby Fundus Dystrophy', *Int J Mol Sci*, 23.

Qureshi, O. S., T. F. Rowley, F. Junker, S. J. Peters, S. Crilly, J. Compson, A. Eddleston, H. Bjorkelund, K. Greenslade, M. Parkinson, N. L. Davies, R. Griffin, T. L. Pither, K. Cain, L. Christodoulou, L. Staelens, E. Ward, J. Tibbitts, A. Kiessling, B. Smith, F. R. Brennan, M. Malmqvist, F. Fallah-

Arani, and D. P. Humphreys. 2017. 'Multivalent Fcgamma-receptor engagement by a hexameric Fc-fusion protein triggers Fcgamma-receptor internalisation and modulation of Fcgamma-receptor functions', *Sci Rep*, 7: 17049.

Ravindran, S., T. E. Grys, R. A. Welch, M. Schapira, and P. A. Patston. 2004. 'Inhibition of plasma kallikrein by C1-inhibitor: role of endothelial cells and the amino-terminal domain of C1-inhibitor', *Thromb Haemost*, 92: 1277-83.

Rawlings, N. D., D. P. Tolle, and A. J. Barrett. 2004. 'MEROPS: the peptidase database', *Nucleic Acids Res*, 32: D160-4.

Reboul, A., M. H. Prandini, and M. G. Colomb. 1987. 'Proteolysis and deglycosylation of human C1 inhibitor. Effect on functional properties', *Biochem J*, 244: 117-21.

Ren, Z., S. Zhao, T. Li, H. J. Wedner, and J. P. Atkinson. 2023. 'Insights into the pathogenesis of hereditary angioedema using genetic sequencing and recombinant protein expression analyses', *J Allergy Clin Immunol*, 151: 1040-49 e5.

Reshef, A., C. Hsu, C. H. Katelaris, P. H. Li, M. Magerl, K. Yamagami, M. Guilarte, P. K. Keith, J. A. Bernstein, J. P. Lawo, H. Shetty, M. Pollen, L. Wieman, T. J. Craig, and Vanguard Study Group. 2025. 'Long-term safety and efficacy of garadacimab for preventing hereditary angioedema attacks: Phase 3 open-label extension study', *Allergy*, 80: 545-56.

Rhaleb, N. E., X. P. Yang, and O. A. Carretero. 2011. 'The kallikrein-kinin system as a regulator of cardiovascular and renal function', *Compr Physiol*, 1: 971-93.

Riedl, M. 2015. 'Recombinant human C1 esterase inhibitor in the management of hereditary angioedema', *Clin Drug Investig*, 35: 407-17.

Riedl, M. A., L. Bordone, A. Revenko, K. B. Newman, and D. M. Cohn. 2024. 'Clinical Progress in Hepatic Targeting for Novel Prophylactic Therapies in Hereditary Angioedema', *J Allergy Clin Immunol Pract*, 12: 911-18.

Riedl, M. A., M. Maurer, J. A. Bernstein, A. Banerji, H. J. Longhurst, H. H. Li, P. Lu, J. Hao, S. Juethner, W. R. Lumry, and Help Investigators. 2020. 'Lanadelumab demonstrates rapid and sustained prevention of hereditary angioedema attacks', *Allergy*, 75: 2879-87.

Ritchie, B. C. 2003. 'Protease inhibitors in the treatment of hereditary angioedema', *Transfus Apher Sci*, 29: 259-67.

Rocamora, F., S. Schoffelen, J. Arnsdorf, E. A. Toth, Y. Abdul, T. E. th Cleveland, S. P. Bjorn, M. Y. M. Wu, N. G. McElvaney, B. G. R. Voldborg, T. R. Fuerst, and N. E. Lewis. 2024. 'Glycoengineered recombinant alpha1-antitrypsin results in comparable in vitro and in vivo activities to human plasma-derived protein', *bioRxiv*.

Rosenberg, S., P. J. Barr, R. C. Najarian, and R. A. Hallewell. 1984. 'Synthesis in yeast of a functional oxidation-resistant mutant of human alpha-antitrypsin', *Nature*, 312: 77-80.

Rossi, V., I. Bally, S. Ancelet, Y. Xu, V. Fremeaux-Bacchi, R. R. Vives, R. Sadir, N. Thielens, and G. J. Arlaud. 2010. 'Functional characterization of the recombinant human C1 inhibitor serpin domain: insights into heparin binding', *J Immunol*, 184: 4982-9.

Rozevska, M., A. Kanepa, S. Purina, L. Gailite, I. Nartisa, H. Farkas, D. Rots, and N. Kurjane. 2024. 'Hereditary or acquired? Comprehensive genetic testing assists in stratifying angioedema patients', *Allergy Asthma Clin Immunol*, 20: 28.

Sanchez-Navarro, A., I. Gonzalez-Soria, R. Caldino-Bohn, and N. A. Bobadilla. 2021. 'An integrative view of serpins in health and disease: the contribution of SerpinA3', *Am J Physiol Cell Physiol*, 320: C106-C18.

Sand, K. M., M. Bern, J. Nilsen, B. Dalhus, K. S. Gunnarsen, J. Cameron, A. Grevys, K. Bunting, I. Sandlie, and J. T. Andersen. 2014. 'Interaction with both domain I and III of albumin is required for optimal pH-dependent binding to the neonatal Fc receptor (FcRn)', *J Biol Chem*, 289: 34583-94.

Sand, K. M., M. Bern, J. Nilsen, H. T. Noordzij, I. Sandlie, and J. T. Andersen. 2014. 'Unraveling the Interaction between FcRn and Albumin: Opportunities for Design of Albumin-Based Therapeutics', *Front Immunol*, 5: 682.

Sanrattana, W., C. Maas, and S. de Maat. 2019. 'SERPINs-From Trap to Treatment', *Front Med (Lausanne)*, 6: 25.

Santagostino, E., U. Martinowitz, T. Lissitchkov, B. Pan-Petesch, H. Hanabusa, J. Oldenburg, L. Boggio, C. Negrier, I. Pabinger, M. von Depka Prondzinski, C. Altisent, G. Castaman, K. Yamamoto, M. T. Alvarez-Roman, C. Voigt, N. Blackman, I. Jacobs, and Prolong-Fp Investigators Study Group. 2016. 'Long-acting recombinant coagulation factor IX albumin fusion protein (rIX-FP) in hemophilia B: results of a phase 3 trial', *Blood*, 127: 1761-9.

Sarkar, A., and P. L. Wintrode. 2011. 'Effects of glycosylation on the stability and flexibility of a metastable protein: the human serpin alpha(1)-antitrypsin', *Int J Mass Spectrom*, 302: 69-75.

Schapira, M., M. A. Ramus, B. Waeber, H. R. Brunner, S. Jallat, D. Carvallo, C. Roitsch, and M. Courtney. 1987. 'Protection by recombinant alpha 1-antitrypsin Ala357 Arg358 against arterial hypotension induced by factor XII fragment', *J Clin Invest*, 80: 582-5.

Schechter, I., and A. Berger. 1967. 'On the size of the active site in proteases. I. Papain', *Biochem Biophys Res Commun*, 27: 157-62.

Scheiner, S., D. A. Kleier, and W. N. Lipscomb. 1975. 'Molecular orbital studies of enzyme activity: I: Charge relay system and tetrahedral intermediate in acylation of serine proteinases', *Proc Natl Acad Sci U S A*, 72: 2606-10.

Schmaier, A. H., and K. R. McCrae. 2007. 'The plasma kallikrein-kinin system: its evolution from contact activation', *J Thromb Haemost*, 5: 2323-9.

Schmidt, A. E., and S. P. Bajaj. 2003. 'Structure-function relationships in factor IX and factor IXa', *Trends Cardiovasc Med*, 13: 39-45.

Scott, B. M., W. L. Matochko, R. F. Gierczak, V. Bhakta, R. Derda, and W. P. Sheffield. 2014. 'Phage display of the serpin alpha-1 proteinase inhibitor randomized at consecutive residues in the reactive centre loop and biopanned with or without thrombin', *PLoS One*, 9: e84491.

Scott, B. M., and W. P. Sheffield. 2020. 'Engineering the serpin alpha(1) - antitrypsin: A diversity of goals and techniques', *Protein Sci*, 29: 856-71.

Scott, C. F., R. W. Carrell, C. B. Glaser, F. Kueppers, J. H. Lewis, and R. W. Colman. 1986. 'Alpha-1-antitrypsin-Pittsburgh. A potent inhibitor of human plasma factor XIa, kallikrein, and factor XIIf', *J Clin Invest*, 77: 631-4.

Shah, C. H., N. Princic, K. A. Evans, and B. G. Schultz. 2023. 'Real-world changes in costs over time among patients in the United States with hereditary angioedema on long-term prophylaxis with lanadelumab', *J Med Econ*, 26: 871-77.

Shapiro, A. D., M. V. Ragni, L. A. Valentino, N. S. Key, N. C. Josephson, J. S. Powell, G. Cheng, A. R. Thompson, J. Goyal, K. L. Tubridy, R. T. Peters, J. A. Dumont, D. Euwart, L. Li, B. Hallen, P. Gozzi, A. J. Bitonti, H. Jiang, A. Luk, and G. F. Pierce. 2012. 'Recombinant factor IX-Fc fusion protein (rFIXFc) demonstrates safety and prolonged activity in a phase 1/2a study in hemophilia B patients', *Blood*, 119: 666-72.

Shariat-Madar, Z., F. Mahdi, and A. H. Schmaier. 2004. 'Recombinant prolylcarboxypeptidase activates plasma prekallikrein', *Blood*, 103: 4554-61.

Shariat-Madar, Z., and A. H. Schmaier. 2004. 'The plasma kallikrein/kinin and renin angiotensin systems in blood pressure regulation in sepsis', *J Endotoxin Res*, 10: 3-13.

Sheffield, W. P., L. J. Eltringham-Smith, and V. Bhakta. 2018. 'Fusion to Human Serum Albumin Extends the Circulatory Half-Life and Duration of Antithrombotic Action of the Kunitz Protease Inhibitor Domain of Protease Nexin 2', *Cell Physiol Biochem*, 45: 772-82.

Sheffield, W. P., A. Mamdani, G. Hortelano, S. Gataiance, L. Eltringham-Smith, M. E. Begbie, R. A. Leyva, P. S. Liaw, and F. A. Ofosu. 2004. 'Effects of genetic fusion of factor IX to albumin on in vivo clearance in mice and rabbits', *Br J Haematol*, 126: 565-73.

Sheikh, F., H. Alajlan, M. Albanyan, H. Alruwaili, F. Alawami, S. Sumayli, S. Al Gazlan, S. Abu Awwad, H. Al-Dhekri, B. Al-Saud, R. Arnaout, H. Alrayes, N. Sayes, M. H. Al-Hamed, H. Al-Mousa, S. AlShareef, and A. M. Alazami. 2023. 'Phenotypic and Genotypic Characterization of Hereditary Angioedema in Saudi Arabia', *J Clin Immunol*, 43: 479-84.

Sheng, J., Y. Wang, R. J. Turesky, K. Kluetzman, Q. Y. Zhang, and X. Ding. 2016. 'Novel Transgenic Mouse Model for Studying Human Serum Albumin as a Biomarker of Carcinogenic Exposure', *Chem Res Toxicol*, 29: 797-809.

Silverman, G. A., P. I. Bird, R. W. Carrell, F. C. Church, P. B. Coughlin, P. G. Gettins, J. A. Irving, D. A. Lomas, C. J. Luke, R. W. Moyer, P. A.

Pemberton, E. Remold-O'Donnell, G. S. Salvesen, J. Travis, and J. C. Whisstock. 2001. 'The serpins are an expanding superfamily of structurally similar but functionally diverse proteins. Evolution, mechanism of inhibition, novel functions, and a revised nomenclature', *J Biol Chem*, 276: 33293-6.

Simonovic, I., and P. A. Patston. 2000. 'The native metastable fold of C1-inhibitor is stabilized by disulfide bonds', *Biochim Biophys Acta*, 1481: 97-102.

Sinnathamby, E. S., P. P. Issa, L. Roberts, H. Norwood, K. Malone, H. Vemulapalli, S. Ahmadzadeh, E. M. Cornett, S. Shekoohi, and A. D. Kaye. 2023. 'Hereditary Angioedema: Diagnosis, Clinical Implications, and Pathophysiology', *Adv Ther*, 40: 814-27.

Sleep, D., J. Cameron, and L. R. Evans. 2013. 'Albumin as a versatile platform for drug half-life extension', *Biochim Biophys Acta*, 1830: 5526-34.

Smith, T. D., and M. A. Riedl. 2024. 'The future of therapeutic options for hereditary angioedema', *Ann Allergy Asthma Immunol*, 133: 380-90.

Song, S. 2018. 'Alpha-1 Antitrypsin Therapy for Autoimmune Disorders', *Chronic Obstr Pulm Dis*, 5: 289-301.

Stavenhagen, K., H. M. Kayili, S. Holst, C. A. M. Koeleman, R. Engel, D. Wouters, S. Zeerleder, B. Salih, and M. Wuhrer. 2018. 'N- and O-glycosylation Analysis of Human C1-inhibitor Reveals Extensive Mucin-type O-Glycosylation', *Mol Cell Proteomics*, 17: 1225-38.

Stockert, R. J. 1995. 'The asialoglycoprotein receptor: relationships between structure, function, and expression', *Physiol Rev*, 75: 591-609.

Stolz, L. E., and P. T. Horn. 2010. 'Ecallantide: a plasma kallikrein inhibitor for the treatment of acute attacks of hereditary angioedema', *Drugs Today (Barc)*, 46: 547-55.

Stratikos, E., and P. G. Gettins. 1998. 'Mapping the serpin-proteinase complex using single cysteine variants of alpha1-proteinase inhibitor Pittsburgh', *J Biol Chem*, 273: 15582-9.

Strickland, D. K., and L. Medved. 2006. 'Low-density lipoprotein receptor-related protein (LRP)-mediated clearance of activated blood coagulation co-factors and proteases: clearance mechanism or regulation?', *J Thromb Haemost*, 4: 1484-6.

Strickland, D. K., S. C. Muratoglu, and T. M. Antalis. 2011. 'Serpin-Enzyme Receptors LDL Receptor-Related Protein 1', *Methods Enzymol*, 499: 17-31.

Sulikowski, T., B. A. Bauer, and P. A. Patston. 2002. 'alpha(1)-Proteinase inhibitor mutants with specificity for plasma kallikrein and C1s but not C1', *Protein Sci*, 11: 2230-6.

Taggart, C., D. Cervantes-Laurean, G. Kim, N. G. McElvaney, N. Wehr, J. Moss, and R. L. Levine. 2000. 'Oxidation of either methionine 351 or methionine 358 in alpha 1-antitrypsin causes loss of anti-neutrophil elastase activity', *J Biol Chem*, 275: 27258-65.

Tait, J. F., and K. Fujikawa. 1987. 'Primary structure requirements for the binding of human high molecular weight kininogen to plasma prekallikrein and factor XI', *J Biol Chem*, 262: 11651-6.

Tankersley, D. L., and J. S. Finlayson. 1984. 'Kinetics of activation and autoactivation of human factor XII', *Biochemistry*, 23: 273-9.

Taylor, M. E., and K. Drickamer. 1993. 'Structural requirements for high affinity binding of complex ligands by the macrophage mannose receptor', *J Biol Chem*, 268: 399-404.

Teckman, J. H., and D. H. Perlmutter. 2000. 'Retention of mutant alpha(1)-antitrypsin Z in endoplasmic reticulum is associated with an autophagic response', *Am J Physiol Gastrointest Liver Physiol*, 279: G961-74.

Thangaraj, S. S., S. H. Christiansen, J. H. Graversen, J. J. Sidelmann, S. W. K. Hansen, A. Bygum, J. B. Gram, and Y. Palarasah. 2020. 'Contact activation-induced complex formation between complement factor H and coagulation factor XIIa', *J Thromb Haemost*, 18: 876-84.

Toldo, S., I. M. Seropian, E. Mezzaroma, B. W. Van Tassell, F. N. Salloum, E. C. Lewis, N. Voelkel, C. A. Dinarello, and A. Abbate. 2011. 'Alpha-1 antitrypsin inhibits caspase-1 and protects from acute myocardial ischemia-reperfusion injury', *J Mol Cell Cardiol*, 51: 244-51.

Travis, J., N. R. Matheson, P. M. George, and R. W. Carrell. 1986. 'Kinetic studies on the interaction of alpha 1-proteinase inhibitor (Pittsburgh) with trypsin-like serine proteinases', *Biol Chem Hoppe Seyler*, 367: 853-9.

Trimble, R. B., P. H. Atkinson, J. F. Tschopp, R. R. Townsend, and F. Maley. 1991. 'Structure of oligosaccharides on Saccharomyces SUC2 invertase secreted by the methylotrophic yeast Pichia pastoris', *J Biol Chem*, 266: 22807-17.

Turnier, J. L., H. I. Brunner, M. Bennett, A. Aleed, G. Gulati, W. D. Haffey, S. Thornton, M. Wagner, P. Devarajan, D. Witte, K. D. Greis, and B. Aronow. 2019. 'Discovery of SERPINA3 as a candidate urinary biomarker of lupus nephritis activity', *Rheumatology (Oxford)*, 58: 321-30.

Uddin, F., C. M. Rudin, and T. Sen. 2020. 'CRISPR Gene Therapy: Applications, Limitations, and Implications for the Future', *Front Oncol*, 10: 1387.

Valerieva, A., and H. J. Longhurst. 2022. 'Treatment of hereditary angioedema-single or multiple pathways to the rescue', *Front Allergy*, 3: 952233.

Valerieva, A., D. Nedeva, V. Yordanova, E. Petkova, and M. Staevska. 2021. 'Therapeutic management of hereditary angioedema: past, present, and future', *Balkan Med J*, 38: 89-103.

Van Deerlin, V. M., and D. M. Tollefsen. 1991. 'The N-terminal acidic domain of heparin cofactor II mediates the inhibition of alpha-thrombin in the presence of glycosaminoglycans', *J Biol Chem*, 266: 20223-31.

Varkoly, K., R. Beladi, M. Hamada, G. McFadden, J. Irving, and A. R. Lucas. 2023. 'Viral SERPINS-A Family of Highly Potent Immune-Modulating Therapeutic Proteins', *Biomolecules*, 13.

Veronez, C. L., D. Csuka, F. R. Sheikh, B. L. Zuraw, H. Farkas, and K. Bork. 2021. 'The Expanding Spectrum of Mutations in Hereditary Angioedema', *J Allergy Clin Immunol Pract*, 9: 2229-34.

Vidalino, L., A. Doria, S. Quarta, M. Zen, A. Gatta, and P. Pontisso. 2009. 'SERPINB3, apoptosis and autoimmunity', *Autoimmun Rev*, 9: 108-12.

Vodnik, M., U. Zager, B. Strukelj, and M. Lunder. 2011. 'Phage display: selecting straws instead of a needle from a haystack', *Molecules*, 16: 790-817.

Wagenaar-Bos, I. G., and C. E. Hack. 2006. 'Structure and function of C1-inhibitor', *Immunol Allergy Clin North Am*, 26: 615-32.

Wang, R., H. D. Li, Y. Cao, Z. Y. Wang, T. Yang, and J. H. Wang. 2023. 'M13 phage: a versatile building block for a highly specific analysis platform', *Anal Bioanal Chem*, 415: 3927-44.

Wang, X., S. Kumar, P. M. Buck, and S. K. Singh. 2013. 'Impact of deglycosylation and thermal stress on conformational stability of a full length murine IgG2a monoclonal antibody: observations from molecular dynamics simulations', *Proteins*, 81: 443-60.

Wang, Y., J. F. Marier, N. Kassir, C. Chang, and P. Martin. 2020. 'Pharmacokinetics, Pharmacodynamics, and Exposure-Response of Lanadelumab for Hereditary Angioedema', *Clin Transl Sci*, 13: 1208-16.

Wells, A. D., A. Woods, D. E. Hilleman, and M. A. Malesker. 2019. 'Alpha-1 Antitrypsin Replacement in Patients With COPD', *P T*, 44: 412-15.

Whisstock, J. C., and S. P. Bottomley. 2006. 'Molecular gymnastics: serpin structure, folding and misfolding', *Curr Opin Struct Biol*, 16: 761-8.

Whisstock, J. C., R. Skinner, R. W. Carrell, and A. M. Lesk. 2000. 'Conformational changes in serpins: I. The native and cleaved conformations of alpha(1)-antitrypsin', *J Mol Biol*, 296: 685-99.

Wilczynska, M., S. Lobov, P. I. Ohlsson, and T. Ny. 2003. 'A redox-sensitive loop regulates plasminogen activator inhibitor type 2 (PAI-2) polymerization', *EMBO J*, 22: 1753-61.

Wilkerson, R. G., and J. J. Moellman. 2022. 'Hereditary Angioedema', *Emerg Med Clin North Am*, 40: 99-118.

Wisniewski, P., T. Gangnus, and B. B. Burckhardt. 2024. 'Recent advances in the discovery and development of drugs targeting the kallikrein-kinin system', *J Transl Med*, 22: 388.

Wolf, B., M. Piksa, I. Beley, A. Patoux, T. Besson, V. Cordier, B. Voedisch, P. Schindler, D. Stollner, L. Perrot, S. von Gunten, D. Brees, and M. Kammuller. 2022. 'Therapeutic antibody glycosylation impacts antigen recognition and immunogenicity', *Immunology*, 166: 380-407.

Wolff, M. W., F. Zhang, J. J. Roberg, E. E. Caldwell, P. R. Kaul, J. N. Serrahn, D. W. Murhammer, R. J. Linhardt, and J. M. Weiler. 2001. 'Expression of C1 esterase inhibitor by the baculovirus expression vector system: preparation, purification, and characterization', *Protein Expr Purif*, 22: 414-21.

Wu, Y. 2015. 'Contact pathway of coagulation and inflammation', *Thromb J*, 13: 17.

Xie, Z., Z. Li, Y. Shao, and C. Liao. 2020. 'Discovery and development of plasma kallikrein inhibitors for multiple diseases', *Eur J Med Chem*, 190: 112137.

Yaron, J. R., L. Zhang, Q. Guo, S. E. Haydel, and A. R. Lucas. 2021. 'Fibrinolytic Serine Proteases, Therapeutic Serpins and Inflammation: Fire Dancers and Firestorms', *Front Cardiovasc Med*, 8: 648947.

Ye, S., A. L. Cech, R. Belmares, R. C. Bergstrom, Y. Tong, D. R. Corey, M. R. Kanost, and E. J. Goldsmith. 2001. 'The structure of a Michaelis serpin-protease complex', *Nat Struct Biol*, 8: 979-83.

Yousef, G. M., A. D. Kopolovic, M. B. Elliott, and E. P. Diamandis. 2003. 'Genomic overview of serine proteases', *Biochem Biophys Res Commun*, 305: 28-36.

Zahedi, K., A. E. Prada, and A. E. Davis, 3rd. 1993. 'Structure and regulation of the C1 inhibitor gene', *Behring Inst Mitt*: 115-9.

Zaman, R., R. A. Islam, N. Ibnat, I. Othman, A. Zaini, C. Y. Lee, and E. H. Chowdhury. 2019. 'Current strategies in extending half-lives of therapeutic proteins', *J Control Release*, 301: 176-89.

Zanichelli, A., R. Vacchini, M. Badini, V. Penna, and M. Cicardi. 2011. 'Standard care impact on angioedema because of hereditary C1 inhibitor deficiency: a 21-month prospective study in a cohort of 103 patients', *Allergy*, 66: 192-6.

Zeerleder, S., R. Engel, T. Zhang, D. Roem, G. van Mierlo, I. Wagenaar-Bos, S. M. van Ham, M. Wuhrer, D. Wouters, and I. Jongerius. 2021. 'Sugar Matters: Improving In Vivo Clearance Rate of Highly Glycosylated Recombinant Plasma Proteins for Therapeutic Use', *Pharmaceuticals (Basel)*, 14.

Zerbs, S., S. Giuliani, and F. Collart. 2014. 'Small-scale expression of proteins in E. coli', *Methods Enzymol*, 536: 117-31.

Zhang, G., D. J. Sexton, R. R. Faucette, Y. Qiu, and J. Wu. 2017. '2D-LC-MS/MS to measure cleaved high-molecular-weight kininogen in human plasma as a biomarker for C1-INH-HAE', *Bioanalysis*, 9: 1477-91.

Zhang, Q., R. H. Law, S. P. Bottomley, J. C. Whisstock, and A. M. Buckle. 2008. 'A structural basis for loop C-sheet polymerization in serpins', *J Mol Biol*, 376: 1348-59.

Zhao, M., T. Abdel-Razek, M. F. Sun, and D. Gailani. 1998. 'Characterization of a heparin binding site on the heavy chain of factor XI', *J Biol Chem*, 273: 31153-9.

Zheng, R., L. Zhang, R. Parvin, L. Su, J. Chi, K. Shi, F. Ye, and X. Huang. 2023. 'Progress and Perspective of CRISPR-Cas9 Technology in Translational Medicine', *Adv Sci (Weinh)*, 10: e2300195.

Zhou, A., R. W. Carrell, and J. A. Huntington. 2001. 'The serpin inhibitory mechanism is critically dependent on the length of the reactive center loop', *J Biol Chem*, 276: 27541-7.

Zhou, Q., and H. Qiu. 2019. 'The Mechanistic Impact of N-Glycosylation on Stability, Pharmacokinetics, and Immunogenicity of Therapeutic Proteins', *J Pharm Sci*, 108: 1366-77.

Zingale, L. C., L. Beltrami, A. Zanichelli, L. Maggioni, E. Pappalardo, B. Cicardi, and M. Cicardi. 2006. 'Angioedema without urticaria: a large clinical survey', *CMAJ*, 175: 1065-70.

Zubareva, E., M. Degterev, A. Kazarov, M. Zhiliaeva, K. Ulyanova, V. Simonov, I. Lyagoskin, M. Smolov, M. Iskakova, A. Azarova, and R. Shukurov. 2021. 'Physicochemical and Biological Characterization of rhC1INH Expressed in CHO Cells', *Pharmaceuticals (Basel)*, 14.

Zuraw, B. L. 2019. 'Cost-Effectiveness of Prophylactic Medications for the Treatment of Hereditary Angioedema Due to C1 Inhibitor Deficiency: A Real-World U.S. Perspective', *J Manag Care Spec Pharm*, 25: 148-51.